Design and Implementation
of
Linear Phase
Wave Digital Filters

By

A. P. S. Jones

A thesis submitted for the Degree of
Doctor of Philosophy

Department of Engineering
University of Warwick

October 1992

To my wife Sarah

..... patience and encouragement

Synopsis

A steady increase of research within the field of digital systems has resulted in a wide acceptance of the discrete approach to system design. Research has produced discrete techniques that complement those already in use in the analogue domain. A rapid improvement in the performance and availability of digital hardware has prompted a move from analogue to digital systems, especially within the field of signal processing.

This thesis considers the design of Wave Digital Filters (WDF's) to satisfy arbitrary magnitude and phase specifications with finite wordlength coefficients. It describes the structures and properties of ladder and lattice WDF's related to linear phase design through coefficient sensitivity and nonminimum-phase.

The initial part of this thesis concentrates upon the design and comparison of optimization techniques to satisfy magnitude-only and simultaneous lowpass frequency specifications upon ladder and lattice WDF's. Experiments confirm the unsuitability of the ladder WDF for simultaneous designs because of their minimum-phase characteristics. Successful simultaneous lowpass designs upon lattice WDF's were achieved through quasi-Newton algorithms using a dual line template scheme and a weighted L_p-metric error function.

The All Pass Sections(APS's) used to construct the lowpass lattice WDF were investigated and a range of APS's considered that would allow the lattice WDF structure to satisfy highpass, single bandpass and dual bandpass frequency specifications. Special case APS's for single and dual bandpass designs were generated by applying frequency transformations to the 1st and 2nd order lowpass APS's. Equations and characteristics for these APS's are detailed along with a number of examples of filter deigns.

The final area of this thesis concerns the design of finite wordlength solutions to magnitude-only and simultaneous frequency specifications, ranging from lowpass to dual bandpass type responses. Using the large wordlength solutions generated through the quasi-Newton optimization techniques as starting coefficients, a Hooke-Jeeves direct search algorithm was implemented to generate finite wordlength solutions.

Techniques detailed in this thesis provide a method for the generation of finite wordlength coefficients that satisfy arbitrary magnitude-only and simultaneous frequency specifications through optimization for the lattice WDF's.

Contents

Acknowledgements

The author would like to acknowledge the help and support of the following people;

Dr Stuart Lawson for ideas, discussion and encouragement as my supervisor on all aspects of my thesis.

Richard Green for research ideas and CASE award with Marconi.

Tony Wicks for TMS32010 coding of my lattice WDF structure and APS's.

The author would also like to acknowledge the financial support of the following bodies;

Scientific and Engineering Research Council

Marconi Underwater Systems Ltd

Warwick University

Declaration

The work in this thesis has been discussed in the following conference papers;

Lawson, S. S. and Jones, A. P. S., "Design of Wave Digital Filters with Prescribed Magnitude and Phase Requirements", Proc. ECCTD '89, No. 308, February 1989, pp1-5.

Jones, A. P. S. and Lawson, S. S., "An Approach to the design of Digital Filters with Prescribed Magnitude and Linear Phase Characteristics", 10th Saraga Colloquium 'Digital and Analogue Filters and Filters Systems', May 1990, pp3/1-4.

Jones, A. P. S., Lawson, S. S. and Wicks, A., "Design of Cascaded Allpass Structures with Magnitude and Delay Constraints using Simulated Annealing and Quasi-Newton Methods", Proc. ISCAS-91, Singapore, IEEE.

Lawson, S. S., Wicks, A. and Jones A. P. S., "Design and Implementation of Cascaded Allpass Digital Filter Structures with Magnitude and Delay Constraints", IEE Proc. 6th Int. Conf on DSP in Communications , Loughborough, 1991, pp31-35.

Within these conference papers the author would like to acknowledge the collaboration, ideas and discussions held with Dr. Lawson concerning the nature and characteristics of the Wave Digital Filter and A. Wicks involving Simulated Annealing optimization techniques.

Abbreviations

The following this abbreviations are used within this thesis

WDF	Wave Digital Filter
DSP	Digital Signal Processing
LTI	Linear Time Invarient
DFT	Discrete Fourier Tansform
FFT	Fast Fourier Transform
LBR	Lossless Bounded Real
MAP	Maximum Available Power
APS	All Pass Section
DTL	Doubly Terminated Lossless
FIR	Finite Impulse Response
IIR	Infinite Impulse Response

Chapter 1

Introduction

Digital filters may be found in a large range of digital systems, from domestic compact disc players to missile guidance systems. Although the principles of a digital filter are common across each application, the properties and performance of a specific digital filter will depend upon the operation and requirement of the overall system. A digital filter is designed to alter the frequency components of an input signal to a given specification. For a number of applications, this specification is only concerned with the magnitude characteristics of a signal. However, applications that also require the phase relationship between the frequency components of a signal to remain undistorted, are constrained to using digital filters that exhibit a linear phase characteristic.

1.1 Discrete System Properties

Any system may be defined as an operator or transformation, acting upon an input to produce a corresponding output. The nature of a transformation is determined by these inputs and outputs. A discrete system uses inputs and outputs that are a sequence of samples, representing a particular signal. Any discrete transform would therefore be constrained to produce a discrete output from a discrete input. An input sequence $\{\ldots, x(i), x(i+1), x(i+2), \ldots, x(j), \ldots\}$ may be considered as a vector, $\mathbf{x}$, of which the "n^{th} sample" is $x(n)$. This may be formally written as

$$\mathbf{x} = \{ x(n) \} \ , \quad -\infty < n < \infty$$

A digital system would represent these signals through a sequence built up from samples of the signal taken at a regular time interval. This time interval is known as the sampling period, T, and is related to the sampling frequency, F_s, by the equation $T = 1/F_s$. If a sequence represents a time varying signal then it is usual to define the sequences as having a finite number of elements, N, taken from when time equals zero. Under these definitions, a sequence can be written as,

$$\mathbf{x} = \{x(0), x(1), x(2), \ldots, x(n), \ldots, x(N-1)\} \ , \quad 0 \leq n \leq N-1$$

For every input sequence, $\mathbf{x}$, there will be a corresponding output sequence, $\mathbf{y}$. The operation of a discrete system is therefore to use a set of rules or transformations to convert an input sequence to the appropriate output sequence. A transformation can entail a large number of operations, either acting upon each element of a sequence in isolation or about previous input and/or output samples. Examples of these types of operations are given in Eq.(1.1), where Eq.(1.1a) shows a squaring function, Eq.(1.1b) generates an output element from a number of input elements and Eq.(1.1c) combines both input and output elements to calculate the next output element.

$$y(n) = (x(n))^2 , \qquad -\infty < n < \infty \qquad (1.1a)$$

So if $x = \{\ldots, x(i-1), x(i), x(i+1), \ldots\} \rightarrow y = \{\ldots, (x(i-1))^2, (x(i))^2, (x(i+1))^2, \ldots\}$

$$y(n) = x(n) + x(n-1) - x(n-2) , \qquad -\infty < n < \infty \qquad (1.1b)$$

So if $x = \{\ldots, x(i-3), x(i-2), x(i-1), x(i), \ldots\}$ then

$$y(i-1) = x(i-1) + x(i-2) - x(i-3) \quad \text{and} \quad y(i) = x(i) + x(i-1) - x(i-2)$$

$$y(n) = x(n+1) - 2\,x(n) + 4\,y(n-1) , \qquad -\infty < n < \infty \qquad (1.1c)$$

So if $x = \{\ldots, x(i-1), x(i), x(i+1), \ldots\}$ and $y = \{\ldots, y(i-1), y(i), y(i+1), \ldots\}$,

then $y(i) = x(i+1) - 2\,x(i) + 4\,y(i-1)$

If the input represents a sequence of samples separated in time, then the present output sample, y(i), must correspond in time to the present input sample, x(i). In this way, a transform is non-causal if the present output, y(i), requires an input value, x(i+1), that, as yet, does not exist. Therefore, the transform of Eq.(1.1c) is non-causal.

The basic structure of a discrete system is shown by Fig.(1.1), where the output sequence, y, Eq.(1.2), is related to the input sequence, x, and the transformation, $\Re$.

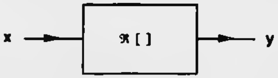

Figure 1.1 Discrete system with transformation, $\Re$.

$$y = \Re[\,x\,] \qquad (1.2)$$

A transformation can be characterised by a number of properties such as linearity, shift-invariance, stability and causality.

1.1.1 Linearity

This property describes the relationship between the input signal and the corresponding output signal. Linearity may be defined using the principles of superposition and scaling. A system is linear, if a linear combination of input sequences maps to a linear combination of output sequences. Therefore, if $y_1(n)$ and $y_2(n)$ are the responses to input samples $x_1(n)$ and $x_2(n)$, through a transformation, $\Re$, respectively, then a system will be linear if and only if

$$\Re[\, a\, x_1(n) + b\, x_2(n)] = a\, \Re[\, x_1(n)] + b\, \Re[\, x_2(n)] = a\, y_1(n) + b\, y_2(n)$$

for arbitrary constants a and b.

1.1.2 Shift-Invariance

This characteristic describes how the input/output relationship varies as the input sequence is shifted. A system is shift-invariant if the response to a shifted version of the input sequence, is identical to a shifted version of the response based upon the unshifted input. This can be described as, if $y(n) = \Re[x(n)]$ then $\Re$ is shift-invariant when $y(n - n_0) = \Re[x(n - n_0)]$ for all n_0. Where the index n is associated with time, then shift-invariance is described as time-invariance.

1.1.3 Stability

The stability of a transformation indicates how a system will behave to a given input. A transformation is stable if it produces a bounded output sequence for every bounded input sequence. This is referred to as bounded input bounded output (BIBO) stable.

1.1.4 Causality

Causality indicates whether a transformation can be realised. A causal transformation is one whose present output depends only on past inputs and outputs and the present input. Therefore the transformation of Eq.(1.3) is causal

$$\begin{aligned} y(m) = \{\, & a_1\, x(n) + a_2\, x(n-1) + a_3\, x(n-2) + \ldots. \\ & + b_1\, y(k) + b_2\, y(k-1) + b_3\, y(k-2) + \ldots.\} \end{aligned} \qquad (1.3)$$

if and only if $m \geq n$ and $m > k$, for arbitrary constants a_i and b_i, $i = 1, 2, ..$

Transformations that meet the linearity and time-invariance requirements, satisfy a broad class of Digital Signal Processing(DSP) operations. A digital filter is an example of a Linear Time-Invariant(LTI) structure and can be described by the transformation, $\Re$, of Fig.(1.1) and Eq.(1.2). A transformation can be completely characterised by its response to the unit impulse sequence, δ, defined as

$$\delta(n) = \begin{cases} 1 & n = 0 \\ 0 & \text{otherwise} \end{cases}$$

The unit impulse response, **h**, is the output sequence of a system when the input sequence is the unit impulse, δ. Therefore for a transformation, $\Re$, its unit impulse response is defined as

$$h(n) = \Re[\,\delta(n)] \qquad -\infty < n < \infty \qquad (1.4)$$

Any sequence can be described as a sequence of scaled unit impulses delayed by one sample period with respect to each other. Applying the properties of LTI structures, an output sequence, **y**, can be constructed by summing the system's scaled unit impulse responses for each element of the input sequence, **x**. This process is described in Eq.(1.5).

$$y(n) = \sum_{k=0}^{n} x(k)\, h(n-k), \qquad -\infty < n < \infty \qquad (1.5)$$

Eq.(1.5) represents the convolution of the input signal with the system's unit impulse response. Using the convolution operator, $*$, and the unit impulse response, **h**, then the output signal, **y**, of a system to an input sequence, **x**, can be expressed as

$$y(n) = x(n) * h(n) \qquad (1.6)$$

With the description of a LTI structure given by Eq.(1.6), the basic discrete structure of Fig.(1.1), can be redrawn for a LTI structure and is illustrated by Fig.(1.2).

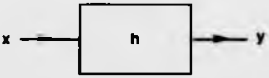

Figure 1.2 Discrete system in terms of the unit impulse response, **h**.

A continuous signal or waveform described in the time domain, may be redefined in the frequency domain though the Fourier transform. A time domain waveform and the corresponding frequency domain waveform, form a Fourier transform pair. The nature and properties of Fourier transform pairs are well known and can be extended to include discrete signals[3]. Using the Discrete Fourier Transform(DFT), a time domain sequence, **x**, may be defined as a series, **X**, in the frequency domain.

The discrete frequency domain is commonly known as the z domain, where z is a complex variable. Conversion of a time domain sequence, **x**, into a z domain sequence, **X**, is performed through the z transform. The general forms of the z transform and the inverse z transform are given by Eq.(1.7) and Eq.(1.8) respectively.

$$X(z) = \sum_{n=-\infty}^{\infty} x(n)\, z^{-n} \qquad (1.7)$$

$$x(n) = \frac{1}{2\pi j} \oint_c X(z)\, z^{n-1}\, dz \qquad (1.8)$$

where c represents a circular contour centred at the origin of the z domain, lying in the region of convergence of the function, X(z).

If the complex variable, z, is defined in its polar form as, $z = r\, e^{j\omega}$, then when $r = 1$ or $|z| = 1$, the z transformation is equal to the DFT. Using this idea, Eq.(1.8) can be modified to define the inverse z transform when $|z| = 1$, as

$$x(n) = \frac{1}{2\pi} \int_{-\pi}^{\pi} X(e^{j\omega})\, e^{j\omega n}\, d\omega \qquad (1.9)$$

The properties of the z transform can be used to describe the function of a discrete system in the discrete frequency domain. Fig.(1.3) shows a basic discrete system in terms of the z transforms of an input sequence, **x**, the output sequence, **y**, and the unit impulse response, **h**.

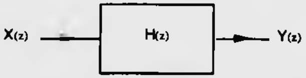

Figure 1.3 General discrete system in the z domain.

The z transform of the unit impulse response, **h**, is the transfer function, H(z). The relationship of the transfer function to the input and output sequences is given by Eq.(1.10).

$$Y(z) = X(z)\,H(z) \tag{1.10}$$

The system equation of Eq.(1.10) is the frequency domain equivalent of the time domain system equation given by Eq.(1.6). From these equations it can be seen that multiplication in the frequency domain is equivalent to convolution in the time domain.

The system equations of Eq.(1.6) and Eq.(1.10) can be rewritten in terms of the operations that occur within the functions of **h** and H(z), as Eq.(1.11) and Eq.(1.12) respectively.

$$y(n) = \sum_{i=0}^{n_1} a_i\, x(n-i) - \sum_{i=1}^{n_2} b_i\, y(n-i) \tag{1.11}$$

and

$$Y(z) \sum_{i=0}^{n_2} b_i\, z^{-i} = X(z) \sum_{i=0}^{n_1} a_i\, z^{-i} \tag{1.12}$$

where n_1 number of samples in **x**

n_2 number of samples in **y**

a_i arbitrary constants, $i = 0, 1, 2, \ldots, n_1$

b_i arbitrary constants, $i = 1, 2, \ldots, n_2$ and $b_0 = 1$

Equation(1.11) shows the general difference equation for a discrete system, while Eq.(1.12) is the equivalent general transfer function. Eq.(1.10) and Eq.(1.12) can be combined to express the transfer function, H(z), as,

$$H(z) = \frac{Y(z)}{X(z)} = \frac{\sum_{i=0}^{n_1} a_i\, z^{-i}}{1 + \sum_{i=1}^{n_2} b_i\, z^{-i}} \tag{1.13}$$

1.2 Phase and Group Delay

Functions defined within the z domain are complex in nature. Therefore any function, G(z), may be represented as

$$G(z) = \mathrm{Re}[\, G(z) \,] + j\,\mathrm{Im}[\, G(z) \,] \tag{1.14}$$

or in polar co-ordinates given in Eq.(1.15).

$$G(z) = |\, G(z) \,|\,(\cos\phi + j\sin\phi) \tag{1.15a}$$

$$G(z) = |\, G(z) \,|\, e^{j\phi} \tag{1.15b}$$

where

$$|G(z)| = \sqrt{\mathrm{Re}[G(z)]^2 + \mathrm{Im}[G(z)]^2} \quad \text{and} \quad \phi = \tan^{-1}\left(\frac{\mathrm{Im}[G(z)]}{\mathrm{Re}[G(z)]}\right)$$

The action of a digital filter is to accept or reject the frequency components of an input sequence by retaining or reducing the amplitude of each component. A digital filter will also effect the phase relationship between the frequency components of the input signal. A typical phase response of a lowpass filter is shown in Fig.(1.4).

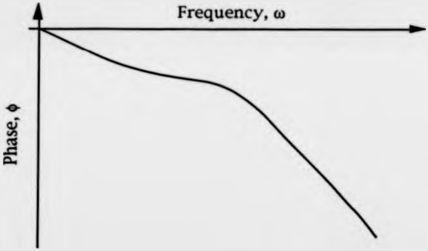

Figure 1.4 Typical lowpass phase response.

Each frequency component of a steady state input sequence passes through a system in an equal time period, t_{sys}. This system time delay, t_{sys}, will cause each frequency component of the input signal to experience a different phase change as it passes through the filter. It can be shown[12,36] that LTI structures do not effect the shape of a sinusoidal function, only its amplitude and phase.

Therefore, if an input function of the form

$$x(t) = C \sin(\omega\ t)$$

was applied to a LTI structure, then the output would be

$$y(t) = D \sin(\omega\ (t - t_{sys})) = D \sin(\omega t - \phi)$$

where the ratio of D to C indicates the change in amplitude of the sine function and ϕ, the phase difference between the input and output versions of the sine waveform. For a LTI structure to retain the phase information of an input signal, the phase relationship between the frequency components of that signal must be preserved. Consider the input function,

$$x(t) = C_1\ \sin(\omega_1\ t) + C_2\ \sin(\omega_2\ t) + C_3\ \sin(\omega_3\ t) \tag{1.16}$$

and the corresponding output function

$$y(t) = D_1\ \sin(\omega_1(t-t_{sys})) + D_2\ \sin(\omega_2(t-t_{sys})) + D_3\ \sin(\omega_3(t-t_{sys})) \tag{1.17}$$

Using the principles of superposition, the effect on each frequency component of the function in Eq.(1.16) can be considered in isolation and then recombined to produce Eq.(1.17). The individual input frequency components of Eq.(1.16), along with their corresponding output components from Eq.(1.17), are illustrated in Fig.(1.5). Each output frequency component has been delayed by an equal time delay, t_{sys}, due to the system.

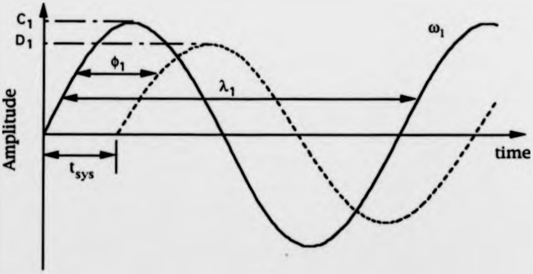

(a)

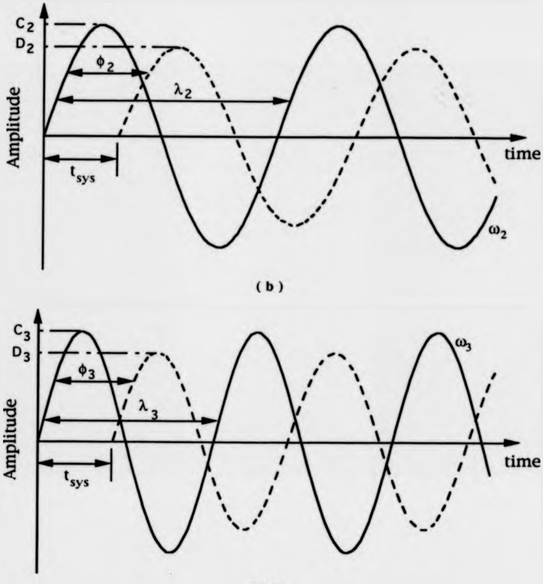

(b)

(c)

Figure 1.5 Frequency components (a) ω_1, (b) ω_2 and (c) ω_3 of the input and output functions given in Eq.(1.16) and (1.17).

From Fig.(1.5), it should be noted that all the frequency components of the input function are in phase. For the system to preserve this phase relationship, the frequency components of the output function are also required to be in phase. From Eq.(1.17), this will only occur when,

$$\omega_1 t_{sys} = \omega_2 t_{sys} = \omega_3 t_{sys} = \omega t_{sys}$$

Therefore, phase linearity will be preserved if a phase change, ϕ_i, at a frequency, ω_i, lies along the straight line, ωt_{sys}. This relationship is shown in Fig.(1.6).

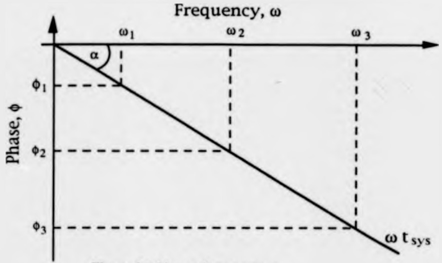

Figure 1.6 Linear phase response.

A linear phase LTI structure will therefore have the characteristic

$$\phi(\omega) = \omega\, t_{sys}$$

Linear phase can be defined in terms of the phase delay, $\alpha(\omega)$, or the group delay, $\tau(\omega)$. Phase delay is defined as,

$$\alpha(\omega) = -\frac{\phi(\omega)}{\omega} \qquad -\pi < \omega < \pi$$

A structure will therefore exhibit exactly linear phase if α is constant, illustrated in Fig.(1.6). Group delay is defined as the negative derivative of the phase with respect to the frequency, so

$$\tau(\omega) = -\frac{d\phi(\omega)}{d\omega} \tag{1.18}$$

Using Eq.(1.15b) and Eq.(1.18) the group delay can be expressed in terms of the transfer function, H(z).

$$\ln(\,H(z)\,) = \ln(\,|H(z)|\,) + j\,\phi(\omega)$$

$$\frac{1}{H(z)}\,\frac{dH(z)}{d\omega} = \frac{1}{|H(z)|}\,\frac{d|H(z)|}{d\omega} + j\,\frac{d\phi(\omega)}{d\omega}$$

$$\tau(\omega) = -\,\mathrm{Im}\left[\frac{1}{H(z)}\,\frac{dH(z)}{d\omega}\right] \tag{1.19}$$

Again, if $\tau(\omega)$ is constant, the system will exhibit an exactly linear phase response.

1.2.1 Characteristics of Linear Phase

For exactly linear phase,

$$\phi(\omega) = -\alpha\omega \qquad -\pi \le \omega \le \pi$$

where α is a constant phase delay. To determine the nature of a transfer function that satisfies this condition, H(z) needs to be expressed in terms of α. This can be achieved by combining Eq.(1.15a) and Eq.(1.7).

$$H(e^{j\omega}) = \sum_{n=1}^{N} h(n)\, e^{-j\omega n} = |\, H(e^{j\omega}) \,| \, (\cos(\alpha\omega) + j \sin(\alpha\omega)\,) \tag{1.20}$$

Taking the real and imaginary parts of Eq.(1.20),

$$\mathrm{Re}[\, H(e^{j\omega})\,] = |H(e^{j\omega})| \cos(\alpha\omega) = \sum_{n=1}^{N} h(n) \cos(\omega n)$$

$$\mathrm{Im}[\, H(e^{j\omega})\,] = |H(e^{j\omega})| \sin(\alpha\omega) = \sum_{n=1}^{N} h(n) \sin(\omega n)$$

then

$$\frac{\sin(\alpha\omega)}{\cos(\alpha\omega)} = \frac{\sum_{n=1}^{N} h(n) \sin(\omega n)}{\sum_{n=1}^{N} h(n) \cos(\omega n)}$$

and where $\alpha \ne 0$, then

$$\sum_{n=1}^{N} h(n) \sin[(\alpha - n)\, \omega] = 0 \tag{1.21}$$

Therefore, in order for a system described by h to possess a constant phase delay, or exactly linear phase, Eq.(1.21) must be satisfied for all of the sequence n = 1, N. A possible solution to this problem is,

$$\alpha = \frac{N+1}{2} \quad \text{and} \quad h(n) = h(N-n) \quad 1 \le n \le N \tag{1.22}$$

For the unit impulse response to satisfy Eq.(1.22), it must be symmetrical about the sample (N+1)/2 or α. The term, α, in Eq.(1.22) represents the constant angle of the phase response or the phase delay. Consider a typical impulse response, shown by Fig.(1.7), which has an odd number of samples, N, and which satisfies Eq.(1.22). The phase delay, α, will be an integer and the symmetry associated with linear phase, will occur around a sample point equal to the value of α.

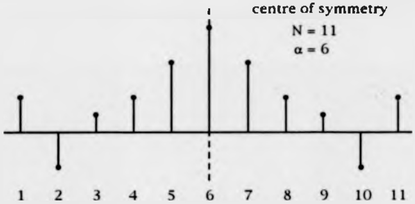

Figure 1.7 Symmetric impulse response with an odd number of samples.

If the number of samples of the unit impulse response is even, then α is no longer an integer and the symmetry point for a linear phase response will exist between two sample points. This is illustrated by Fig.(1.8).

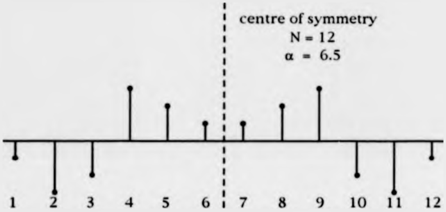

Figure 1.8 Symmetric impulse response with an even number of samples.

The impulse response symmetry, indicated by Fig.(1.7) and Fig.(1.8), relates to a condition when the function exhibits both constant phase delay and constant group delay. However, a full definition of the transfer function,

$$H(e^{j\omega}) = H^{*}(e^{j\omega})\, e^{j\phi(\omega)} \quad \text{or} \quad H(e^{j\omega}) = \pm\, |H(e^{j\omega})|\, e^{j\phi(\omega)}$$

shows that the impulse response will still possess linear phase if it exhibits either symmetry or anti-symmetry. The anti-symmetry case relates to a 'piece-wise linear' function, which has constant group delay but not constant phase delay. In most practical design cases, phase delay is of no interest. Where the filter's impulse response cannot be defined by a finite number of samples, exactly linear phase is impossible to obtain and the best that can be achieved is approximately linear phase.

Using the information about the unit impulse response symmetry, the position of the poles and zeros of a function exhibiting phase linearity can be determined. The position and relationship of the zeros of an exactly linear phase transfer function can be observed by considering a FIR filter. In order to exhibit linear phase a transfer function, H(z), must possess a symmetry or anti-symmetry of its unit impulse response, so

$$H(z) = \sum_{n=1}^{N} h(n)\ z^{-n} = h(1) + h(2)\ z^{-1} + h(3)\ z^{-2} + \ldots$$

$$\pm h(3)z^{-(N-2)} \pm h(2)z^{-(N-1)} \pm h(1)z^{-N}$$

The plus sign corresponds to a symmetric response, while the minus sign indicates anti-symmetry. Because of the symmetry of the unit impulse response, the transfer function, $H(z)$ and its inverse, $H(z^{-1})$ may be related by Eq.(1.23).

$$H(z^{-1}) = \pm z^{N} H(z) \qquad (1.23)$$

Eq.(1.23) shows that the functions $H(z)$ and $H(z^{-1})$ are identical, except for a delay of N samples and ± 1 factor. Under these conditions the two functions must posses identical zeros. Therefore to satisfy Eq.(1.23), the zeros of an exactly linear phase system must exist in sets that comprise a zero and its reciprocal about the unit circle, so $H(z^{-1})$ will possess the same set of zeros.

This property can be illustrated if $H(z)$ has a factor, $H_i(z)$, which is a complex conjugate zero pair at $r\ e^{\pm j\phi}$ when $r \neq 1$ and $\phi \neq 0$ or π, shown in Fig.(1.9) by points A and C. The function $H(z^{-1})$ will have a corresponding function $H_i(z^{-1})$, with a complex conjugate zero pair at $1/r\ e^{\pm j\phi}$, shown by points B and D in Fig.(1.9). To satisfy Eq.(1.23), $H(z)$ and $H(z^{-1})$ must possess the same zeros and so both functions must contain factors to produce the zeros at A, B, C and D of Fig.(1.9). If a factor $H_j(z)$ produces the zeros B and D, then $H_j(z^{-1})$ will generate the zeros A and C. Therefore Eq.(1.23) will only be satisfied if $H(z)$ contains both factors $H_i(z)$ and $H_j(z)$, where $H_i(z) = 1/H_j(z)$. An exactly linear transfer function must therefore contain zeros that exist in reciprocal complex conjugate groups.

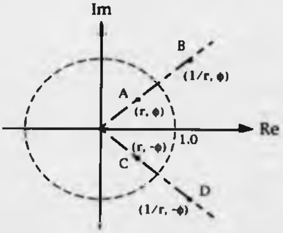

Figure 1.9 Reciprocal complex conjugate zero positions for linear phase.

Fig.(1.10) shows the typical zero positions of linear phase FIR filters for the four possible cases of linear phase design, odd or even filter order, N, with symmetrical or anti-symmetrical unit impulse responses.

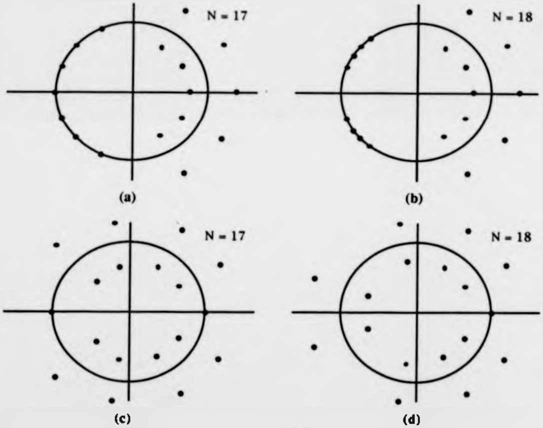

Figure 1.10 Zero positions for the four possible exactly linear phase FIR design cases; (a) odd symmetric, (b) even symmetric, (c) odd anti-symmetric and (d) even anti-symmetric.

1.2.2 Minimum- and Nonminimum-Phase

Fig.(1.10) indicates the relationship between zeros for exactly linear phase FIR structures. All linear phase systems should possess zeros in these types of positions, whether FIR or IIR in nature. IIR structures also possess poles within their transfer functions that constrain the possible positions for its zeros. For some IIR structures these constraints make it impossible to place zeros in reciprocal complex conjugate sets. The concept of minimum- and nonminimum-phase can be applied to a structure to determine if its zeros can be arranged into required positions. A formal definition of minimum-phase can be generated through the Hilbert Transform[29], or for discrete systems, the Discrete Hilbert Transform(DHT).

The DHT provides a method of relating the real part of a frequency response in the discrete domain to its imaginary part and vice versa. These two relationships form a DHT pair. If the z transform, $X(z)$, of a causal sequence $x(n)$, is described as

$$X(e^{j\omega}) = X_R(e^{j\omega}) + j\,X_I(e^{j\omega})$$

then it has the Hilbert transform pair

$$X_I(e^{j\omega}) = \frac{1}{2\pi}\,P\int_{-\pi}^{\pi} X_R(e^{j\phi})\cot\left(\frac{\phi-\omega}{2}\right)d\phi$$

and

$$X_R(e^{j\omega}) = x(0) - \frac{1}{2\pi}\,P\int_{-\pi}^{\pi} X_I(e^{j\phi})\cot\left(\frac{\phi-\omega}{2}\right)d\phi$$

where P denotes the Cauchy principle value of the integral[18].

For a system, $H(e^{j\omega})$, to exhibit minimum-phase then the components of its transfer functions, $\ln[|H(e^{j\omega})|]$ and $\arg[H(e^{j\omega})]$, must form a Hilbert transform pair. This may be re-expressed as

$$\ln[\,|H(e^{j\omega})|\,] = \hat{h}(0) - \frac{1}{2\pi}\,P\int_{-\pi}^{\pi} \arg[\,H(e^{j\phi})\,]\cot\left(\frac{\phi-\omega}{2}\right)d\phi$$

and

$$\arg[\ H(e^{j\omega})\ ] = \frac{1}{2\pi} P \int_{-\pi}^{\pi} \ln[\ |H(e^{j\phi})|\ ] \cot\left(\frac{\phi-\omega}{2}\right) d\phi$$

where $\hat{H}(z) = \ln(H(z))$ and $\hat{h}$ is the Fourier transform pair of $\hat{H}(z)$. Alternatively a system, $H(z)$, will exhibit minimum-phase if a causal stable inverse system, $H^{-1}(z)$, exists such that

$$H(z)\,H^{-1}(z) = 1.$$

Since $H^{-1}(z) = 1/H(z)$, the transfer function, $H(z)$, must have all its poles and zeros inside the unit circle in order for a stable and causal inverse system to exist.

The requirements for minimum-phase are contrary to those for linear phase and therefore, an exactly linear phase system requires an overall nonminimum-phase structure. This however does not eliminate minimum-phase structures from linear phase design as any rational function, $G(z)$, may be expressed in the form

$$G(z) = G_{min}(z)\,G_{ap}(z)$$

where $G_{min}(z)$ is a minimum-phase function and $G_{ap}(z)$ is an all-pass function for which has $|G_{ap}(e^{j\omega})| = 1$ for all ω.

The nature of $G_{ap}(z)$ is nonminimum-phase and the poles and zeros of this function can be used to produce an overall function that meets the linear phase requirements. A minimum-phase function can therefore be used in a linear phase design provided the overall phase response is modified by a phase equaliser, $G_{ap}(z)$. Linear phase designs through phase equalisation are discussed in Chapter 2.

1.3 Finite Wordlength Effects

A large amount of research has been directed at the effects of finite wordlength on digital systems, especially for digital filters. Initial work by Jackson[14] outlined a systematic approach to these finite wordlength effects by determining the relationship between roundoff noise and dynamic range. This approach of using uncorrelated noise sources to model rounding errors and other finite wordlength effects is detailed in a number of DSP text books[4,22,29,33].

Finite wordlength effects may be collected under four main headings;

(i) Conversion of an analogue signal to and from a digital equivalent.
This is usually known as conversion noise and will depend upon the quantization step, being the difference between consecutive representable numbers and the type of quantization used; rounding, value truncation or magnitude truncation.

(ii) Uncorrelated roundoff noise.
This is a generic term for the noise introduced to a signal within a filter due to arithmetic operations. The main calculation to cause this effect is multiplication. The bit length to accurately represent the product of two b bit numbers is 2b bits. This 2b bit number cannot be represented within a system limited to b bits so the number has to be reduced either through rounding or truncation. This introduces a certain amount of uncorrelated noise into the operation of the filter. The variance of this uncorrelated noise source will depend upon the type of arithmetic used, floating or fixed point, the signal limitation scheme and the type of number system used; 1's or 2's complement or signed-magnitude.

(iii) Inaccuracies in the filter response.
This noise source results from an inability to accurately reproduce a filter's frequency response using a finite number of bits for the filter coefficients. This results in a non-ideal transfer function. This effect can be offset if filter coefficients are designed to a finite wordlength, resulting in an acceptable finite wordlength transfer function.

(iv) Correlated roundoff noise (limit cycles).
Two types of correlated roundoff noise or parasitic oscillation exist, small scale (granular) and large scale (overflow). These effects are most apparent in fixed point recursive digital filters, where internal rounding errors for a constant input are highly correlated. Quantization causes the non-linear mapping of the lowest order bits of an internal signal under constant input. This generates limit cycles. For a recursive filter using rounding this means that there is no unique steady state output for a constant input. A so called deadband region exists containing a number of steady state outputs, the precise one being used depends on where the boundary of the dead band region was encountered.

Limit cycles are dependent upon a number of factors, mainly the filter realisation or structure and the quantization step. Signal quantization through rounding is most susceptible to limit cycle effects. Magnitude truncation provides a better alternative quantization procedure, however, it does not always eliminate deadband limit cycles.

Factors (ii)-(iv) are the only finite wordlength effects that relate directly to the digital filter's operation. In turn, each of these effects depends on the filter's structure and configuration. A great deal of work has been directed at ways to implement a given transfer function, $H(z)$. Each digital filter structure proposed corresponds to a different method of expressing the transfer function. A general function, $G(z)$, may be divided into smaller functions, $G_i(z)$ and $H_i(z)$, such the their combination equals $G(z)$. The general form for the combination of these functions, or a Lagrange structure, is shown in Fig.(1.11).

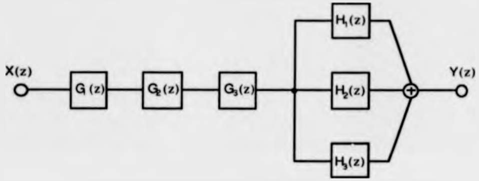

Figure 1.11 General Lagrange Structure.

The overall transfer function of the structure in Fig.(1.11) is,

$$G(z) = G_1(z)\, G_2(z)\, G_3(z) \Big(H_1(z) + H_2(z) + H_3(z) \Big)$$

The $G_i(z)$ functions of Fig.(1.11) are connected in cascade, while the $H_i(z)$ functions are connected in parallel. Each modification of the Lagrange structure will possess the same performance under large accuracy calculations. It is their finite wordlength performance, however, which is of interest. The form of the individual functions $G_i(z)$ and $H_i(z)$ is arbitrary, and a wide range of combinations exists for a given transfer function. A desire to analyse the overall structure for finite wordlength effects prompts to a break down of a response into small regular functions. These individual functions tend to be simple to analyse, having a first or second order nature.

A cascade structure may be represented as

$$H(z) = a_0 \left[\prod_{i=1}^{k_1} H_{1i}(z) \right] \left[\prod_{i=1}^{k_2} H_{2i}(z) \right]$$

where

$$H_{1i}(z) = \frac{1 + a_{1i}\, z^{-1}}{1 + b_{1i}\, z^{-1}} \quad \text{and} \quad H_{2i}(z) = \frac{1 + a_{1i}\, z^{-1} + a_{2i}\, z^{-2}}{1 + b_{1i}\, z^{-1} + b_{2i}\, z^{-2}}$$

The cascade of these sections also allows them to be defined in terms of functions which represent the numerators, $N_i(z)$ and denominators, $D_i(z)$, of each section, so that H(z) could be expressed as

$$H(z) = \frac{\prod_{i=1}^{k_1} N_i(z)}{\prod_{i=1}^{k_2} D_i(z)} \qquad (1.24)$$

Eq.(1.24) allows a cascaded structure to be constructed from first and second order sections with arbitrary numerator and denominator orderings and pairings.

A structure which has a parallel form, may be expressed as,

$$H(z) = \frac{a_n}{b_n} + \left[\sum_{i=1}^{k} H_i(z) \right]$$

where $H_i(z)$ is either a first or second order section of the form,

$$H_{1i}(z) = \frac{a_{0i}}{1 + b_{1i}\, z^{-1}} \quad \text{and} \quad H_{2i}(z) = \frac{a_{0i} + a_{1i}\, z^{-1}}{1 + b_{1i}\, z^{-1} + b_{2i}\, z^{-2}}$$

The noise properties of these 1st and 2nd order sections are relatively easy to analyse[29] and the overall performance of filter structures using these elements can be determined. An important observation from this analysis is that the order and pairing of cascaded second order sections can greatly effect the overall finite wordlength performance, because of overflow within the structure.

A large number of filter structures exist, each using a derivative of the general Lagrange structure, including the Direct forms that implement a transfer function without partitioning it into smaller functions. A large amount of research has been directed at analysing and comparing these various structures and their performance under finite wordlength conditions[23,16,5]. The main thrust of this research was to determine which properties of each structure improved the finite wordlength performance. A property suggested to measure finite wordlength performance concerned the sensitivity of the structure to changes in its parameters. Bode defined a sensitivity function, S, to determine this property by measuring how a function, F, changes with respect to one of its parameters, x. This property, defined in Eq.(1.25), is concerned with small parameter changes and as a result, small scale sensitivities.

$$S(F,x) = S_x^F = \frac{x}{F}\frac{\partial F}{\partial x} \tag{1.25}$$

Analogue structures known to possess low parameter sensitivity include Doubly Terminated Lossless(DTL) networks. These structures suffer only a small amount of distortion of their magnitude responses as the components' values are varied. This property is related to the ability of the DTL structure to deliver maximum power at points across its passband.

At these points of Maximum Available Power(MAP), the derivatives of the attenuation with respect to reactive components within the structure are zero. Therefore, at these MAP points the magnitude sensitivity to reactive components is zero and because the sensitivity is a smooth continuous function, the sensitivity in the region around these points is also likely to be low. This effect, together with a mathematical explanation, has been referred to as Orchard's argument[26,27,37,24,25].

In an attempt to reproduce the properties of the analogue DTL network in a digital circuit, Fettweis investigated a number of methods of converting a DTL structure into the discrete domain. The method adopted by Fettweis concentrated upon creating digital equivalents of analogue components such as an inductor, resistor, voltage source and transformer. First by describing the analogue components in terms of wave parameters and then converting them into the digital domain. A digital equivalent of the DTL structure was then constructed using these digital components.

The resulting Wave Digital Filters(WDF's) has been widely researched and have been shown to possess a superior roundoff noise performance compared to existing digital filter structures[17,38,13,8,42]. The sensitivities of WDF's and their reference analogue DTL filters have also been compared[43,28] and shown to bear a close correlation. Further work by Fettweis[7,6,10,2] and Jackson[15] has advanced a relationship between roundoff noise and attenuation coefficient sensitivity.

An alternative approach suggested by Vaidyanathan and Mitra[39,40,41] concerned deriving digital structures independent of analogue equivalents. The objective of this approach was to define a class of function based on the requirements for low coefficient sensitivity and then derive structures based upon these functions. The result consisted of two-port chain matrices which describing Lossless Bounded Real(LBR) functions. A WDF structure satisfies a LBR function and the results from the two design methods are similar in nature.

A comparison of various filter structures by Matharu[21] under a number of finite wordlength effects, has also been carried out. The structures under consideration were the ladder WDF, lattice WDF, unit element WDF, Gray-Markel lattice, direct form I and II, cascaded and parallel 2nd order sections. The results suggest that choice of filter structure is not clear cut and is dependant upon the filter arithmetic and numbering system. However, in all tests, the performance of WDF structures placed them at or near the top of each comparison list.

1.4 Wave Digital Filter (WDF)

1.4.1 Circuit Descriptions

Using a DTL analogue filter as a reference, Fettweis broke the filter into its constituent elements and modelled the circuit as a connection of one-port blocks. A digital equivalent of each analogue component was then generated and a structure constructed using these digital elements. Fettweis tried a number of different transforms to produce digital filters that retained the properties of their references. A successful transform adopted by Fettweis was to replace the voltage and current description of an element with an incident and reflected voltage wave notation. This notation is illustrated in Fig.(1.12) and their relationship is given by Eq.(1.26).

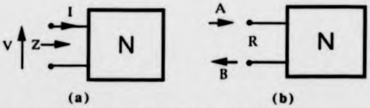

(a) (b)

Figure 1.12 General one-port circuit in terms of (a) voltage and current parameters and (b) voltage wave parameters.

$$\left.\begin{aligned} A &= V + I\,R \\ B &= V - I\,R \end{aligned}\right\} \qquad (1.26)$$

In the equations of Eq.(1.26), the parameter, A, represents the incident voltage wave, B the reflected voltage wave and R the port resistance of the circuit. Application of this wave notation allows analogue components to be described in terms of incident and reflected waves. Applying the z transform to analogue component described in terms of wave parameters, generates a set of digital elements that can be used to construct digital structures that possess the properties of their DTL reference networks.

Consider the one-port element in Fig.(1.13). Using Eq.(1.26) the reflected voltage wave, B, can be described in terms of the incident voltage wave, A, port resistance, R, and branch impedance, Z. This relationship is given in Eq.(1.27).

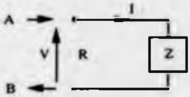

Figure 1.13 One-port circuit of impedance, Z, in terms of voltage and current and incident and reflected voltage waves.

$$V = I\,Z, \quad \begin{aligned} A &= I\,(Z + R) \\ B &= I\,(Z - R) \end{aligned} \quad \text{or} \quad B = A\left[\frac{(Z - R)}{(Z + R)}\right] \qquad (1.27)$$

If the one-port branch impedance, Z, represents a capacitor, C, then

$$Z = \frac{1}{s\,C} \quad \text{and} \quad B = A\left[\frac{(1/sC - R)}{(1/sC + R)}\right] \qquad (1.28)$$

The bilinear transform is defined as

$$s \rightarrow \frac{2}{T}\,\frac{\left(1 - z^{-1}\right)}{\left(1 + z^{-1}\right)} \qquad (1.29)$$

where T is the sampling period.

Combining Eq.(1.28) and (1.29) then

$$B = A\left[\frac{(T/2C - R) + z^{-1}(T/2C + R)}{(T/2C + R) + z^{-1}(T/2C - R)}\right]$$

The factor 2/T is a scalar that varies the value of the capacitor for different sampling frequencies.

If the capacitance value is redefined as

$$C' = \frac{2C}{T}$$

then

$$B = A\left[\frac{(1/C' - R) + z^{-1}(1/C' + R)}{(1/C' + R) + z^{-1}(1/C' - R)}\right]$$

If the port resistance, R, is set so $R = 1/C'$, then

$$B = A\,z^{-1}$$

Therefore the digital equivalent of a capacitor, C, under the wave parameter method suggested by Fettweis, is a unit delay, with a port resistance, T/2C. A list of digital building blocks and their equations is given in a review paper by Fettweis[11]. The port resistance places a constraint upon how the digital elements may be connected. To use an element within a circuit, the port resistance of connected one-ports must be identical. However, the port resistance is predefined by the modelled component value. To eliminate this problem, Fettweis also created adaptors to equalise the port resistance between two or more dissimilar one-port elements.

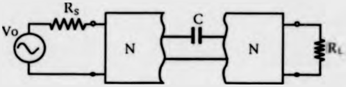

Figure 1.14 General DTL network with series capacitor, C.

Consider the series capacitor of the DTL network shown in Fig.(1.14). To model this component in a WDF, a simple delay is required. However, to use this element it needs to be connected to the rest of the network. To this end a 3-port series adapter is required and is shown in Fig.(1.15). The general equations describing a series connected capacitor, expressed in its wave chain matrix format, is given by Eq.(1.30).

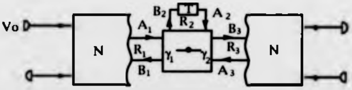

Figure 1.15 WDF including 3-port series adapter to model a capacitor, C.

$$\begin{bmatrix} A_1 \\ \\ B_1 \end{bmatrix} = \begin{bmatrix} \dfrac{(1 - z^{-1}(1-\gamma_2))}{(2-\gamma_1-\gamma_2)(1-z^{-1})} & \dfrac{(1-\gamma_1-\gamma_2 - z^{-1}(1-\gamma_1))}{(2-\gamma_1-\gamma_2)(1-z^{-1})} \\ \dfrac{(1-\gamma_1 - z^{-1}(1-\gamma_1-\gamma_2))}{(2-\gamma_1-\gamma_2)(1-z^{-1})} & \dfrac{(1-\gamma_2 - z^{-1})}{(2-\gamma_1-\gamma_2)(1-z^{-1})} \end{bmatrix} \cdot \begin{bmatrix} A_3 \\ \\ B_3 \end{bmatrix} \qquad (1.30)$$

It should be noted that the port resistance R_2, of Fig.(1.15), equals T/2C, while R_1 and R_3 will be set by the surrounding circuit. When the circuit is designed, however, the actual values of R_1 or R_3 may not be pre-set and could be chosen arbitrarily. In this case, these values may be used to eliminate γ_1 or γ_2. Three cases arise for this 3-port series adapter,

if $\gamma_1 \neq 1$, $\gamma_2 \neq 1$ and $R_2 = 1/C'$, then $\gamma_v = \dfrac{2R_v}{R_1 + R_3 + 1/C'}$, $v = 1,2$

or

if $\gamma_1 = 1$ and $R_2 = 1/C'$, then $R_1 = R_3 + 1/C'$, $\gamma_2 = \dfrac{R_3}{R_3 + 1/C'}$

or

if $\gamma_2 = 1$ and $R_2 = 1/C'$, then $R_3 = R_1 + 1/C'$, $\gamma_1 = \dfrac{R_1}{R_1 + 1/C'}$

where $C' = \dfrac{2C}{T}$

Using this technique, the overall complexity of a WDF circuit may be reduced. The chain matrices for the design cases when $\gamma_1 = 1$ or $\gamma_2 = 1$ can be determined by substitution into Eq.(1.30). A detailed explanation of these design procedures is given in the review paper by Fettweis. The final description of the one-port capacitor element and a 3-port series adapter, given by Eq.(1.30), was in the form of the wave chain matrix. Therefore, the original one-port approach was implemented within the circuit as a two-port element.

The necessity of using a separate adapter circuit can be avoided if a two-port approach is used from the start. This technique was described by Lawson[19]. An impedance, Z, illustrated by Fig.(1.16), is considered in terms of its chain matrix, shown by Eq.(1.31) and through the voltage wave notation, a digital equivalent can be derived and is given by Eq.(1.32).

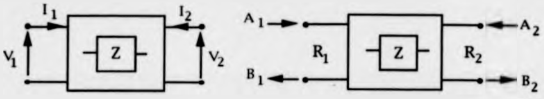

(a) (b)

Figure 1.16 Two-port circuit of series impedance, Z; (a) voltage and current parameters, (b) voltage wave parameters.

$$\begin{bmatrix} V_1 \\ I_1 \end{bmatrix} = \begin{bmatrix} A & B \\ C & D \end{bmatrix} \cdot \begin{bmatrix} V_2 \\ I_2 \end{bmatrix} \tag{1.31}$$

$$\begin{bmatrix} A_i \\ B_i \end{bmatrix} = \begin{bmatrix} 1 & R_i \\ 1 & -R_i \end{bmatrix} \cdot \begin{bmatrix} V_i \\ I_i \end{bmatrix} \qquad i = 1, 2$$

therefore

$$\begin{bmatrix} A_1 \\ B_1 \end{bmatrix} = \begin{bmatrix} 1 & R_1 \\ 1 & -R_1 \end{bmatrix} \cdot \begin{bmatrix} A & B \\ C & D \end{bmatrix} \cdot \begin{bmatrix} 1 & R_2 \\ 1 & -R_2 \end{bmatrix}^{-1} \cdot \begin{bmatrix} A_2 \\ B_2 \end{bmatrix} \tag{1.32}$$

Consider again, a series capacitor, C. The chain matrix for this analogue component in terms of s, is given by Eq.(1.33). It may be converted into a digital wave chain matrix equivalent, shown by Eq.(1.34), using the voltage wave descriptions and the bilinear transform of Eq.(1.29).

$$\begin{bmatrix} V_1 \\ I_1 \end{bmatrix} = \begin{bmatrix} 1 & -\frac{1}{s\,C} \\ 0 & -1 \end{bmatrix} \cdot \begin{bmatrix} V_2 \\ I_2 \end{bmatrix} \tag{1.33}$$

$$\begin{bmatrix} A_1 \\ \\ B_1 \end{bmatrix} = \begin{bmatrix} \frac{\beta_2 - (1 - \beta_1 + \beta_2)\, z^{-1}}{(1 + \beta_2)(1 - z^{-1})} & \frac{1 - \beta_1\, z^{-1}}{(1 + \beta_2)(1 - z^{-1})} \\ \frac{\beta_1 - z^{-1}}{(1 + \beta_2)(1 - z^{-1})} & \frac{(1 - \beta_1 + \beta_2) - \beta_2\, z^{-1}}{(1 + \beta_2)(1 - z^{-1})} \end{bmatrix} \cdot \begin{bmatrix} A_2 \\ \\ B_2 \end{bmatrix} \tag{1.34}$$

Again, as with the one-port and adapter method, the selection of R_1 or R_2 of Fig.(1.16), may not be pre-set by the surrounding circuit and either β_1 or β_2 may be eliminated.

This provides three design options.

if R_1 and R_2 are independent then $\beta_1 = \dfrac{R_2 + R1 - 1/C'}{R_2 + R_1 + 1/C'}$. $\beta_2 = \dfrac{R_2 - R_1 - 1/C'}{R_2 + R_1 + 1/C'}$

or

if $R_2 = R_1 + 1/C'$ then $\beta_1 = \dfrac{C'R_1}{1 + C'R_1}$. $\beta_2 = 0$

or

if $R_1 = R_2 + 1/C'$ then $\beta_1 = 1 + \beta_2$, $\beta_2 = \dfrac{C'R_2}{1 + C'R_2}$

where C' = 2C/T and T is the sampling period. A full description of these design procedures and their effects on realisation are discussed in Chapter 3.

Both the one-port and two-port design techniques rely upon the use of voltage wave notation and the bilinear transform. Although this method is widely used, it is not the only method to provide a viable solution. Other methods were investigated by Lawson, who proposed a general WDF concept using a chain matrix of the form

$$\begin{bmatrix} A_1 \\ B_1 \end{bmatrix} = [P] \cdot \begin{bmatrix} A & B \\ C & D \end{bmatrix} \cdot [Q]^{-1} \cdot \begin{bmatrix} A_2 \\ B_2 \end{bmatrix}$$

where P and Q are 2 by 2 matrices, that represent a number of different transformations[†], including voltage, current and power waves.

1.4.2 Structures

DTL networks, which form the reference filters for WDF designs, may be defined within two groups; ladder and lattice structures. The general DTL ladder network, shown by Fig.(1.17), is widely used in analogue circuits for radio and television as no element is more than one node away from the ground line and is therefore less susceptible to stray capacitance.

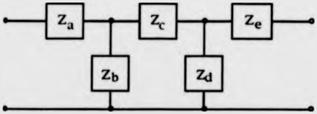

Figure 1.17 General Ladder Network.

[†] A comparison of a wide range of transforms is given by Lawson[20]

The single input-output path through a ladder circuit determines that the structure has a minimum-phase characteristic.

A general lattice circuit, shown by Fig.(1.18), possesses more than one input-output path, and may therefore be classed as having a nonminimum-phase characteristic. The lattice structure is more generally reduced to a balanced symmetric form, where $Z_a = Z_c$ and $Z_b = Z_d$.

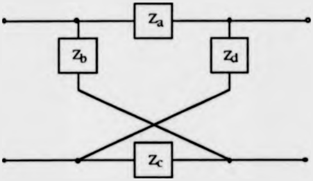

Figure 1.18 General Lattice Network.

Both ladder and lattice structures can be used as references for WDF's. These designs can be approached through the one or two-port techniques by reducing each impedance, Z_i, into a simple element, like a capacitor or an inductor, and then generating the appropriate WDF component. The symmetrical lattice structure, shown in Fig.(1.19), because of its nonminimum-phase characteristic, is ideal for implementing allpass functions and is widely used as phase equalisers in analogue designs. Lattice structures present practical design problems, however, because the pairs of branch impedances have to be matched within a high tolerance. This is a difficult task as analogue components are hard to adjust, and age and cycle with temperature. These effects are not evident in digital designs and the lattice WDF has been the subject of a great deal of research.

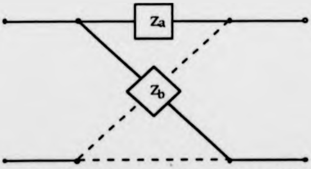

Figure 1.19 Balanced Symmetric Lattice Network.

The symmetrical lattice of Fig.(1.19), is given in terms of its canonic impedances, Z_a and Z_b. If the corresponding canonic reflectances for a symmetric WDF lattice are defined as S' and S", then

$$S' = \frac{Z_a - R}{Z_a + R} \quad \text{and} \quad S'' = \frac{Z_b - R}{Z_b - R}$$

where R, because the structure is symmetrical, represents the port resistance of each end of the lattice. Using these canonic reflectances, a general WDF lattice structure can be constructed and is shown by Fig.(1.20).

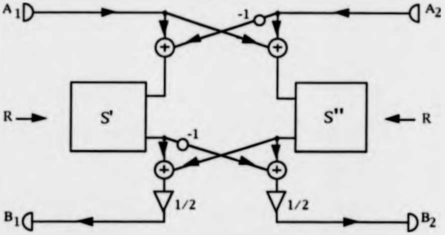

Figure 1.20 General discrete symmetrical lattice with canonic reflectances.

If the second input, A_2, is set to zero and B_1 or B_2 ignored, then this lattice structure can be simplified to produce a structure shown by Fig.(1.21). The transfer function of this structure will then be the sum or difference of the canonic reflectances.

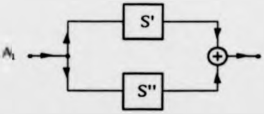

$$B_1 = \frac{S'' + S'}{2}$$

$$B_2 = \frac{S'' - S'}{2}$$

Figure 1.21 Simplified symmetrical lattice with canonic reflectances.

The actual implementation of S' and S" is a design parameter. Bartlett[12] devised a method of generating a lattice structure from a symmetric ladder network. The resulting lattice branches were cascade in structure, terminated by an open or short circuit. The functions S' and S" can be broken into a large number cascaded or parallel functions, typically first or second order sections. These sections may be designed through the one or two-port techniques.

All the structures considered have been derived from lumped element models. A WDF equivalent of distributed component structure has also been derived. The unit element is based upon a section of a transmission line of characteristic impedance, Z_0. Using the two-port approach, these unit element sections can be connected in cascade to produce a unit element WDF. One of the benefits of using distributed element models, is that the filter retains its analogue magnitude and phase relationships through an analogue to digital transformation. Thus, unit element filters designed to posses linear phase in the analogue domain also exhibits linear phase in the digital domain. This property allows the work by Rhodes[30,31,32], Scanlan[34,35] and Abele[1] into linear phase microwave filters to be applied to the design of linear phase unit element WDF's.

1.5 Research Objectives

The main purpose of this research was to investigate digital filters that could be used within a beamforming system. Any beamforming application, whether radar or sonar, consists of a fixed transmitter and receiver array. The phase of the signal transmitted from the array is varied so that the beam is swept over an angle about the array. Consequently, the range and bearing information of any signal received by the array will be contained within both the magnitude and phase frequency responses.

Therefore, any digital filter designed for this application must retain the phase information of the signal through any filtering. Current systems perform this function with an exactly linear phase FIR filter. The FIR filter requires a larger filter order to meet a magnitude-only specification than an IIR filter. In many practical design cases this difference in filter order, despite additions to an IIR filter order to achieve approximately linear phase, is still appreciable.

This large difference prompted the research to be concentrated on IIR filters which can be designed to have approximately linear phase to within a given specified tolerance. Beamforming application operate in real-time so speed is also an important factor. This narrowed the research to filter structures that exhibit an efficient use of hardware components, like multipliers and adders, as well as demonstrating small susceptibility to finite wordlength effects.

As mentioned in previous sections of this Chapter, the WDF offers a possible solution to this problem. At the start of the research project, no work had been published into the field of linear phase WDF's. The main objective of this thesis is to investigate approximately linear phase WDF's, their structures, designs and limitations.

The final stage of research is to generate finite wordlength linear phase WDF's to meet dual bandpass specifications and implement the resulting designs. This was to be either through existing DSP chips or some dedicated hardware design.

1.6 Summary

This Chapter has provided a brief introduction and review of the theory behind digital filter structures and the effects of finite wordlengths. Coefficient sensitivity has been introduced in relation to finite wordlength performance and the WDF. The characteristics of exactly linear phase have also been illustrated and related to the properties of nonminimum-phase structures.

The nature of FIR and IIR filter structures has been discussed in terms of linear phase. FIR filters possess a non-recursive structure and can therefore be designed to exhibit exactly linear phase. Recursive IIR filters, however, can only possess approximately linear phase. This thesis is concerned with WDF structures. WDF's are recursive in nature and can therefore only exhibit approximately linear phase. For the remainder of this thesis the term linear phase will represent approximately linear phase. If the phase response is exactly linear it will be stated as such.

Finally WDF structures and the design methodologies behind the one and two-port approaches, have been introduced. The purpose of this thesis is to examine the design options for linear phase WDF structures and procedures for their design.

Chapter 2 will develop and discuss a large number of these design options, while Chapter 3 and 4 will relate these design options to ladder and lattice WDF structures. Chapter 5 will outline the frequency translation techniques required to generate a dual bandpass response, while Chapter 6 discusses the design procedures and effects of finite wordlength lattice WDF's. A practical design example required to meet a linear phase dual bandpass filter specification under finite wordlength conditions is illustrated in Chapter 7. The discussion and conclusions of the thesis are provided in Chapter 8, along with a number of suggestions for further work.

References

1) Abele, T. A., "Transmission Line Filters Approximating a Constant Delay in a Maximally Flat Sense", IEEE Trans. Circuit Theory, Vol CT-14, No. 3, September 1967, pp298-306.

2) Bonzanigo, F., "Comment on 'Roundoff Noise and Attenuation Sensitivity in Digital Filters with Fixed-Point Arithmetic' ", IEEE Trans. Circuit and Systems, Vol CAS-21, No. 11, November 1974, pp809-810.

3) Brigham, E. O., *The Fast Fourier Transform*, Prentice-Hall, New Jersey, 1972.

4) DeFatta, D. J., Lucas, J. G. and Hodgkiss, W. S., *Digital Signal Processing: A System Design Approach*, Wiley, New York, 1988.

5) Ebert, P. M., Mazo, J. E. and Taylor, M. G., "Overflow Oscillations in Digital Filters", The Bell System Technical Journal, Vol 48, No. 11, November 1969, pp2999-3020.

6) Fettweis, A., "On Sensitivity and Roundoff Noise in Wave Digital Filters", IEEE Trans. Acoustics, Speech and Signal Processing, Vol ASSP-22, No. 5, October 1984, pp383-384.

7) Fettweis, A., "On the Connection Between Multiplier Word Length Limitation and Roundoff Noise in Digital Filters", IEEE Trans. Circuit Theory, Vol CT-19, No. 5, September 1972, pp486-491.

8) Fettweis, A., "Reduction of 'Roundoff Noise in Wave Digital Filters", IEEE Trans. Circuit and Systems, Vol CAS-21, No. 3, March 1974, pp305-310.

9) Fettweis, A., "Relay to F. Bonzanigo's 'Comment on "Roundoff Noise and Attenuation Sensitivity in Digital Filters with Fixed-Point Arithmetic"'", IEEE Trans. Circuit and Systems, Vol CAS-21, No. 11, November 1974, pp810-811.

10) Fettweis, A., "Roundoff Noise and Attenuation Sensitivity in Digital Filters with Fixed-Point Arithmetic", IEEE Trans. Circuit Theory, Vol CT-20, No. 3, March 1973, pp174-175.

11) Fettweis, A., "Wave Digital Filters: Theory and Practice", Proc IEEE, Vol 74, No. 2, February 1986, pp270-327.

12) Guillemin, E. A., *Synthesis of passive networks*, John Wiley and Sons, London, 1957.

13) Hwang, S. Y., "Comments on 'Reduction of 'Roundoff Noise in Wave Digital Filters'", IEEE Trans. Circuit and Systems, Vol CAS-22, No. 9, September 1975, pp764-764.

14) Jackson, L. B., "On the Interaction of Roundoff Noise and Dynamic Range in Digital Filters", The Bell System Technical Journal, Vol 49, No. 2, February 1970, pp159-184.

15) Jackson, L. B., "Roundoff Noise Bounds Derived from Coefficient Sensitivities for Digital Filters", IEEE Trans. Circuit and Systems, Vol CAS-23, No. 8, August 1976, pp481-485.

16) Knowles, J. B. and Olcayto, E. M., "Coefficient Accuracy and Digital Filter Response", IEEE Trans. Circuit Theory, Vol CT-15, No. 1, March 1968, pp31-41.

17) Ku, W. H. and Ng, S-M., "Floating-Point Coefficient Sensitivity and Roundoff Noise of Recursive Digital Filters Realized in Ladder Structures", IEEE Trans. Circuit and Systems, Vol CAS-22, No. 12, December 1975, pp927-936.

18) Lathi, B. P., Modern Digital and Analog Communication Systems, Holt-Saunders International, New York, 1983.

19) Lawson, S. S., "Digital filter structures from classical analogue networks", Ph. D. Thesis, University of London, 1975.

20) Lawson, S. S., "On a Generalization of the Wave Digital Filter Concept", Int. J. Circuit Theory Appl., Vol 6, No. 2, April 1978, pp107-120.

21) Matharu, P. S., "Architectures for the VLSI Implementation of Digital Filters", Ph. D. Thesis, The City University, 1988.

22) Oppenheim, A. V. and Schafer, R. W., Digital Signal Processing, Prentice-Hall International, London, 1975.

23) Oppenheim, A. V. and Weinstein, C. J., "Effects of Finite Register Length in Digital Filtering and the Fast Fourier Transform", Proc IEEE, Vol 60, No. 8, August 1972, pp957-976.

24) Orchard, H. J., "Computing the Envelope Delay of Ladder Networks", Electronics Letters, 21st July 1988, Vol 24, No. 15, pp976-977.

25) Orchard, H. J., "Filter Design by Iterated Analysis", IEEE Trans. Circuit and Systems, Vol CAS-32, No. 11, November 1985, pp1089-1096.

26) Orchard, H. J., "Loss Sensitivities in Singly and Doubly Terminated Filters", IEEE Trans. Circuit and Systems, Vol CAS-26, No. 5, May 1979, pp293-297.

27) Orchard, H. J., Temes, G. C. and Catalepe, T., "Sensitivity Formulas for Terminated Lossless Two-Ports", IEEE Trans. Circuit and Systems, Vol CAS-32, No. 5, May 1985, pp459-466.

28) Owenier, K-A., "A General Method for the Efficient Computation of Sensitivities in Wave Digital Filters", IEEE Trans. Circuit and Systems, Vol CAS-30, No. 10, October 1983, pp750-757.

29) Rabiner, L. R. and Gold, B., Theory and Application of Digital Signal Processing, Prentice-Hall, New Jersey, 1975.

30) Rhodes, J. D., "A Low-Pass Prototype Network for Microwave Linear Phase Filters", IEEE Trans. Microwave Theory and Techniques, Vol MTT-18, No. 6, June 1970, pp290-307.

31) Rhodes, J. D., "Filters Approximating Ideal Amplitude and Arbitrary Phase Characteristics", IEEE Trans. Circuit Theory, Vol CT-20, No. 2, March 1973, pp120-124.

32) Rhodes,J. D. and Ismail, M. Z., "In-Line Waveguide Selective Linear Phase Filters", IEEE Trans. Microwave Theory and Techniques, Vol MTT-22, No. 1, January 1974, pp1-5.

33) Roberts, R. A. and Mullis, C. T., Digital Signal Processing, Addison-Wesley, Massachusetts, 1987.

34) Scanlan, S. O. and Baher, H., "Filters with Maximally Flat Amplitude and Controlled Delay Responses", IEEE Trans. Circuits and Systems, Vol CAS-23, No. 5, May 1976, pp270-278.

35) Scanlan, S. O. and Rhodes, J. D., "Microwave Networks with Constant Delay", IEEE Trans. Circuit Theory, Vol CT-14, No. 3, September 1967, pp290-297.

36) Scott, R. E., *Linear Circuits*, Addison-Wesley, Massachusetts, 1960.

37) Temes, G. C. and Orchard, H. J., "First-Order Sensitivity and Worst Case Analysis of Doubly Terminated Reactance Two-Ports", IEEE Trans. Circuit Theory, Vol CT-20, No. 5, September 1973, pp567-571.

38) Ullrich, U., "Roundoff Noise and Dynamic Range of Wave Digital Filters", Signal Processing, Vol 1, pp45-64.

39) Vaidyanthan, P. P. and Mitra, S. K., "Low Passband Sensitivity Digital Filters: A Generalized Viewpoint and Synthesis Procedures", Proc IEEE, Vol 72, No. 4, April 1986, pp404-423.

40) Vaidyanthan, P. P., "A Unified Approach to Orthogonal Digital Filters and Wave Digital Filters, Based on LBR Two-Pair Extraction", IEEE Trans. Circuit and Systems, Vol CAS-32, No. 7, July 1985, pp673-686.

41) Vaidyanthan, P. P., Mitra, S. K. and Neuvo, Y., "A New Approach to the Realization of Low-Sensitivity IIR Digital Filters", IEEE Trans. Acoustics, Speech and Signal Processing, Vol ASSP-34, No. 2, April 1986, pp350-361.

42) Van Haften, D. and Chirlian, P. M., "An Analysis of Errors in Wave Digital Filters", IEEE Trans. Circuit and Systems, Vol CAS-28, No. 2, February 1981, pp154-160.

43) Yang, S. M., "On the Sensitivity of a Class of Wave Digital Filters", IEEE Trans. Circuit and Systems, Vol CAS-28, No. 12, December 1981, pp1158-1164.

Chapter 2

Design Approaches

2.1 Existing Methods

The first step in the design of a digital filter is to determine the specification, not just in terms of its frequency response, but also implementation and operational performance. These performance criteria become important when high sampling rates and short wordlength are required. WDF's, as mentioned in the previous Chapter, are considered to possess good operational performance under finite wordlength conditions. These filters are recursive in nature and cannot be designed to meet a magnitude and exactly linear phase specification simultaneously. FIR filters, although their non-recursive nature requires a larger filter order to fulfil a given magnitude specification than a recursive filter, can be designed to exhibit simultaneous magnitude and exactly linear phase responses.

Therefore the first design decision is based upon the tolerance placed upon the phase linearity. For a system requiring an exactly linear phase response, the FIR filter is the only solution. A more general phase linearity tolerance is usually expressed as a percentage deviation of the group delay about a nominal value. For wider linearity tolerances, recursive filter designs may be more efficient. However, as the tolerance becomes narrower, the difference in orders between these two filter types will decrease, until the required recursive filter order is higher than the non-recursive case. This places an upper limit on the efficiency and practically of recursive filters for simultaneous magnitude and linear phase designs.

There are three basic decisions in the design of a digital filter :-

(i) What filter structure ?

This decision concerns the nature of the filter, recursive or non-recursive and how the filter is to be constructed. For recursive filters, construction methods vary from the direct form, through cascaded or parallel second order sections, to WDF structures.

(ii) In which domain is the filter to be designed and simulated ?
Here the domain is a general description of a number of design approaches, such as design in frequency or time domains, or using discrete or continuous parameters. Modelling a filter could be fixed to finite wordlengths or allowed to use the full accuracy of the modelling system, producing an 'infinite' wordlength situation. Other factors in this domain decision concern how to represent the filter's response in each domain, as magnitude and phase frequency responses, pole/zero positions or as a time domain waveform.

(iii) How to calculate the filter parameters ?
For a digital filter, this decision concerns the filter's coefficient values. Methods include using analytical formulae based upon polynomials or through optimization techniques, such as the Remez exchange algorithm used for linear phase FIR filter designs.

It should be noted that each decision is related and dependant upon the filter specification. The elements of each of these decisions are discussed in the following sections.

2.2 Filter Structures

Classically, digital filter structures have been described as recursive or non-recursive. A better definition when dealing with linear phase designs is whether the structures exhibit minimum- or nonminimum-phase characteristics. This type of classification presents three options for the choice of structure for a filter to meet a simultaneous magnitude and phase specification :-

(i) Minimum-phase structure.
(ii) Connected minimum-phase and nonminimum-phase structures.
(iii) Nonminimum-phase structure.

Carlin[6,7] considered the use of a minimum-phase structure, being a DTL ladder network, to meet a simultaneous magnitude and phase specification. The conclusions of this work were that for minimum-phase structures the magnitude and phase requirements form reciprocal properties, such that one property had to be traded off against the other. Results showed a tight compromise between the two halves of the specification.

A great deal of work has been directed at the design of phase equalisers for analogue circuits. This technique, as mentioned in Chapter 1, consists of connecting a minimum-phase structure with a transfer function, $G_{min}(z)$, to a nonminimum-phase structure, which has a unity magnitude characteristic or an allpass nature. The phase of the nonminimum-phase circuit would be varied to linearize that of the minimum-phase structure. The overall transfer function, $G(z)$, given by

$$G(z) = G_{min}(z)\,G_{ap}(z)$$

has a magnitude characteristic provided by $G_{min}(z)$ and a linear phase frequency response produced through the allpass equaliser transfer function, $G_{ap}(z)$.

Deczky[13,14] and Vlach[48] extended this work into the digital domain to consider recursive cascaded second order sections. This type of section, through appropriate parameter values, can exhibit a minimum- or nonminimum-phase characteristic. Deczky grouped these ideas into a computer program to design digital filters based on cascaded second order sections to meet specifications simultaneous or through phase equalisation. Another structure that satisfies a simultaneous magnitude and phase specification is the FIR filter. The exactly linear phase FIR structure, shown by Fig.(2.1), has a non-recursive and nonminimum-phase characteristic.

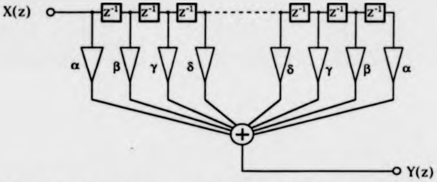

Figure 2.1 General structure of an exactly linear phase FIR filter.

The performance of this structure is determined by a large number of constraints that are imposed by the linear phase requirement. These constraints lead to a high order filter. The most notable constraint is that the structure exhibits exactly linear phase across all the frequency band. As a result, some of the degrees of freedom of the structure are used to enforce linear phase across the stopband of the filter.

If this constraint across the stopband can be removed, then the resulting FIR filter should have a lower order. This idea was proposed by Leeb and Henk[30]. The authors suggested that linear phase FIR filters and minimum-phase structures represent the extreme ends of possible solutions to a simultaneous magnitude and phase specification. The objective of their research was to produce a "nearly linear phase" FIR filter by moving the zeros from their reciprocal complex conjugate positions. The resulting filters would then exhibit linear phase across their pass bands only. As predicted, these filters required a lower order to meet the same specification than the exactly linear phase equivalents.

The next step in considering a filter structure is how to implement the various minimum- and nonminimum-phase circuits. For a digital filter the finite wordlength performance is of prime importance. To take advantage of structures known to posses good finite wordlength performance, filter designs should be based on WDF's. The main minimum-phase WDF structure is derived from an analogue DTL ladder network. The equivalent ladder WDF can be produced using the one or two port techniques discussed in Chapter 1. An example of a DTL ladder network is given in Fig.(2.2)(a), with the equivalent one-port WDF ladder circuit in Fig.(2.2)(b) and two-port model in Fig.(2.2)(c).

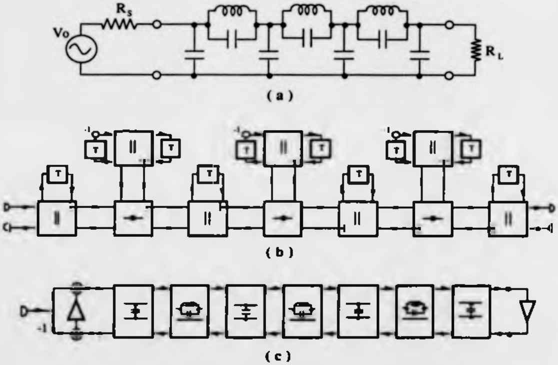

Figure 2.2 (a) 7th order DTL ladder network, with (b) one-port WDF equivalent and (c) two-port WDF model.

The main nonminimum-phase WDF structure is based upon a DTL lattice network. A digital lattice may be described in terms of its canonic impedances. The equivalent canonic reflectances for the WDF model may be derived through the one or two port techniques. This process can be illustrated by the DTL lattice structure of Fig.(2.3)(a) which acts as a reference for the one-port equivalent of Fig.(2.3)(b) and two-port circuit of Fig.(2.3)(c).

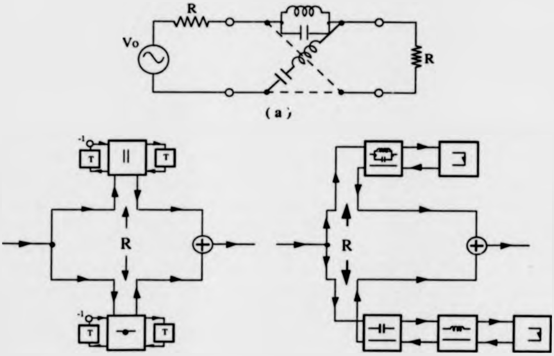

(a)

(b) (c)

Figure 2.3 (a) Symmetric DTL lattice structure showing canonic impedances, with (b) one-port equivalent WDF and (c) two-port equivalent WDF in terms of canonic reflectances.

The lattice structure represents a parallel connection of functions. These functions are allpass in nature and it is their combination which produces an overall transfer function that is not allpass. Although the lattice structure only contains two branches, more allpass functions can be added in parallel, to form the general polyphase systems[37,11,12,47] used for interpolation and decimation.

The more general description of a lattice WDF, shown by Fig.(2.4), is in terms of cascaded first and second order sections. A number of variations on this structure have also been suggested. One variation is to set one branch of the lattice as a pure delay, equal to the overall delay of the other branch. This circuit is given by Fig.(2.5).

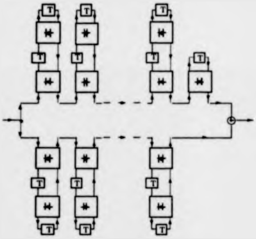

Figure 2.4 General lattice WDF using 1st and 2nd order sections.

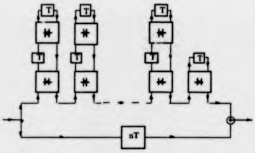

Figure 2.5 Lattice WDF with a pure delay branch.

The choice of filter structures that have good finite wordlength properties and minimum- or nonminimum-phase characteristics, can be reduced to the ladder or lattice WDF's. Simultaneous magnitude and phase design can then be approached on the minimum-phase ladder WDF and nonminimum-phase lattice WDF. Equaliser designs would consist of using both structures, the ladder for magnitude response and the lattice to perform the phase equalisation.

2.3 Domain Options

With the selection of a filter structure a transfer function can be generated. The form of this transfer function and what its parameters represent, will depend upon the filter structure and the design domain. For most applications a filter specification will be defined in terms of limits set upon its magnitude and phase frequency responses. The most common design technique is to start with a frequency response specification and then model and simulate the appropriate transfer function through the frequency domain.

This approach may not always be appropriate, especially for linear phase design, where the desired characteristics are defined as zero positions or unit impulse response symmetry. These linear phase characteristics may either be transferred into equivalent properties for the frequency response or the filter specification may be redefined into the same domain as these characteristics.

This possibility leads to a number of design options based upon which domain the filter specification is modelled and simulated. The time and frequency domain represent the two main possibilities, while within each domain a number of variations exist.

These domains may be characterised by the nature of the signal and how accurately it is represented. The main design domains are :-

(i) Time Domain;
  (a) Continuous signals to full accuracy
  (b) Discrete signals to full accuracy
  (c) Discrete signals with finite wordlength

(ii) Frequency Domain;
  (a) Continuous signals to full accuracy
  (b) Discrete signals to full accuracy
  (c) Discrete signals with finite wordlength

The filter specification, defined in the time domain, relates to a real signal, while the same specification in the frequency domain relates to a complex signal. A time domain signal can only be described in terms of amplitude. A frequency domain signal, however, can be described in a number of formats. Common format types include :-

(i) Complex signal
(ii) Magnitude and Phase (or Group Delay)
(iii) Real and Imaginary Components
(iv) Pole/Zero positions

Using a combination of these options, a large number of design domains exist. Selection of domain depends upon a number of parameters, most notably the frequency specification and filter performance. The output of a digital filter is a quantized discrete sequence of samples separated in time. The finite precision discrete time domain offers the most accurate modelling of the filter. This domain also allows a comparison of different rounding, overflow and scaling strategies for various wordlengths. Results from this domain should therefore bear a close correlation to the response of any actual hardware implementation.

The practicality of this and other time domain designs is limited by the availability of design equations and representation of a frequency domain specification. When the shape of the magnitude response is closely defined then an appropriate time domain waveform can be calculated. An example of this is the raised cosine filter, whose corresponding time domain waveform can be calculated through the

Fourier transform. Linear phase raised cosine filter design would consist of calculating the filter parameters to produce symmetry in the corresponding time domain function. Concerned with the design of linear phase raised cosine filters, Lind[32] proposed an optimization technique for these parameter calculations.

For the most common filter response specification, however, the shape of the magnitude is not defined, but given in terms of a tolerance upon its value at particular frequencies. This tolerance scheme is based upon the magnitude characteristics, using the concept of passbands and stopbands. A specification is expressed as limits or a tolerance upon the performance of the filter within these passbands and stopbands. For a magnitude specification, the tolerance scheme is defined as a maximum attenuation, α_p, in the passband and a minimum attenuation, α_s, in the stopband. A lowpass filter magnitude specification is shown in Fig.(2.6).

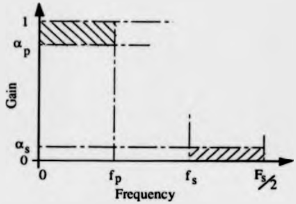

Figure 2.6 Tolerance scheme for a general digital lowpass filter

The magnitude specification of Fig.(2.6) can be expressed as,

$$1 \leq |G| \leq \alpha_p \quad \text{over the region} \quad 0 \leq f \leq f_p$$
$$\alpha_s \leq |G| \leq 0 \quad \text{over the region} \quad f_s \leq f \leq F_s/2$$

where the passband is the frequency region $0 \rightarrow f_p$ and the stopband is the frequency region $f_s \rightarrow F_s/2$, in which F_s is the sampling frequency.

Under this general type of specification, the actual value of the magnitude characteristic is not defined, only a tolerance upon its value at a particular frequency. It is very difficult to express this type of tolerance scheme in the time domain. An additional disadvantage of using the time domain is the lack of design equations, especially for linear phase. Extending Lind's ideas to general filter response designs is limited by an inability to define a general specification as a target function in the time domain.

These problems lead to a preference of the frequency domain for filter designs, despite the inability to accurately simulate finite wordlength effects. The major advantage of the frequency domain is the analytical formulae that exist for analogue magnitude-only designs. These formulae, based upon polynomials such as the Butterworth, Chebyshev and elliptic functions, can be extended to direct calculation of digital filter parameters for a discrete magnitude specification. The accuracy with which the magnitude response of a filter is modelled in the frequency domain, is dependant upon the filter structure and how close the filter parameters are to the ideal values. Differences between the ideal and actual values for the filter parameters are due to quantization when a digital filter is implement upon a finite wordlength system. The major result of this parameter quantization is to degrade the system's response characteristics from the ideal. The scale of this degradation will depend on the coefficient wordlength and filter structure. The effects of this process can be offset through optimization, producing finite wordlength coefficients that generate an acceptable filter response.

However, any finite wordlength optimization procedures based in the frequency domain cannot accurately model all the finite wordlength effects, such as overflow and quantization strategies. Any results are therefore only an approximation to the time domain performance. The accuracy of this approach will again depend upon the filter structure, the particular rounding and overflow strategies and system wordlengths. A more detailed discussion of these ideas is provided in Chapter 6.

When linear phase becomes a requirement of the frequency response, the number of design formulae becomes very limited. Linear phase analogue filter designs are most usually approached with phase equalisers[35]. A number of strategies for simultaneous design also exist. Ideas vary from a novel equaliser structure to explicit polynomial formulae.

Equaliser techniques range from embedding a bridged-T network within the analogue filter[28], to reducing the overall order of an equalised circuit through moving and cancelling the poles and zeros of the transfer function[19,39]. The polynomial approach starts from a number of objectives, either an all pole circuit[33,45], minimum-phase characteristics[21] or to calculate a polynomial to approximate the magnitude and phase response[40,15,44,46,25,38]. Each design method also has to compensate for the non-linear mapping of the phase response from the continuous to the discrete domain. Again, both equaliser and polynomial methods generate filter parameters that have an ideal value and so the discrete frequency responses will suffer distortion upon their quantization.

Complex signal and pole/zero position formats represent alternatives to the magnitude and phase descriptions for a filter's transfer function. Each format has advantages and disadvantages for filter design. Although the frequency response of a particular transfer function can be described as a complex signal, real and imaginary responses, magnitude and phase responses or as pole and zero positions, it is very difficult to describe a tolerance specification into each format from the general magnitude and phase definition. This is especially true for the complex and real and imaginary response formats.

The characteristics of linear phase, outlined in Chapter 1, were described in terms of unit impulse response symmetry or the position of the zeros of the transfer function. The pole and zero position format therefore offers the best method of describing the phase requirements in the frequency domain. The exact position of these zeros is not defined, only that they occur in reciprocal complex conjugate sets. The positions of the poles of the transfer function are determined by the magnitude response required from the filter's specification. Deczky[13] illustrated that a complex pole of the form $r\ e^{j\theta}$, exhibits magnitude and group delay responses with a resonance-type characteristic. The sharpness of the peak will depend upon the value of r and its position in the frequency response will be a function of θ. The effects of these resonance-type characteristics can be combined so that the turning points of the filter's responses can be adjusted by moving the appropriate poles and zeros. An example of a lowpass magnitude specification mapped onto a complex plane is illustrated by Fig.(2.7).

A zero on the unit circle indicates the position where the magnitude response approaches a value of zero. The magnitude response will also be determined by the position of the poles of the transfer function. The position of the poles for a given magnitude response, such as elliptic or Butterworth, is detailed in a number of analogue filter design text books[48,5].

The actual position of the poles and zeros of a transfer function will be derived from an ideal evaluation of a polynomial equation. The effect of quantizing these ideal coefficient values can readily be illustrated on pole/zero plots[34]. The main effect is to move the poles and zeros to a grid point next to their ideal positions.

Size and shape of the grid is determined by the structure of the filter and the quantizing step.

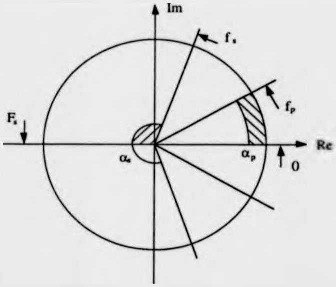

Figure 2.7 Tolerance scheme for a general digital lowpass filter given in the complex domain.

Techniques using pole and zero positions as design criteria, such as the program developed by Deczky, used structures in which the poles and zeros of the transfer function are independent of each other. This restriction makes this type of method unsuitable for the WDF structures considered.

Real and imaginary frequency responses are of little interest, as two templates are required to define the transfer function without the ability to accurately show the specification. When the transfer function is defined as a complex signal, as real and imaginary components, then although it is a single function, it becomes difficult to define the magnitude and phase targets.

In conclusion, for a digital filter specification with a magnitude response given as a tolerance scheme, the most appropriate design option is to use the discrete frequency domain. Finite wordlength effects are very difficult to model in the frequency domain except for coefficient quantization and as a result the finite wordlength coefficient responses calculated in the frequency domain should only be used as an estimate of the actual finite wordlength characteristics. Finally, the transfer function should be modelled and interpreted in terms of its magnitude and phase(or group delay) frequency responses.

2.4 Coefficient Generation

The coefficients form the heart of a digital filter and as such their calculation is a vital part of a digital filter design. Formulae exist which can be used to generate the filter coefficients to meet a prescribed magnitude specification. These formulae however, do not encompass a phase requirement directly. A polynomial can be constructed to possess high magnitude selectivity, like the elliptic function, or phase linearity, like the Bessel or synchronous functions[5]. The opposing nature of the amplitude selectivity and phase linearity in these polynomials makes them unsatisfactory for simultaneous magnitude and phase designs. This presents a number of design options :-

(i) derive formulae to describe and calculate the multipliers of a WDF for simultaneous or equaliser structure designs.

(ii) use optimization techniques to determine WDF multipliers for a given structure to meet some arbitrary specification.

(iii) use a combination of (i) and (ii) above.

Derivation of any design formulae would be based upon existing polynomials for the magnitude response and the pole/zero position required for linear phase[22,24]. These equations, if possible, would produce an accurate transfer function if its coefficients have infinite precision. The final step in generating a finite wordlength response would still require a certain amount of optimization to achieve acceptable response with finite wordlength coefficients.

An alternative is to use optimization for the whole design process. This is especially useful for showing relatively quickly, if design options are viable. Work towards the design of linear phase filters has been based upon the use of optimization techniques[41,8,3,2], both for equaliser and simultaneous approaches.

2.4.1 Optimization Considerations

In order to approach the design of digital filters through optimization three areas must be considered :-

(i) How to define the problem as a function to be minimised in relation to some arbitrary goal.

(ii) How to generate an error function which reflects the difference between the actual function and an ideal function.

(iii) Which type of optimization routine is appropriate to the problem and what information about the function it requires.

The first design area is concerned with how the problem is stated, both in terms of its parameters and goals. The final goals or targets of the problem will be determined by the design domain of the filter and what its parameters represent. For a general filter specification, the targets would be described by the magnitude and phase (or group delay) frequency responses. This is not the only method of describing the targets for this problem, as discussed in the previous section. However, magnitude and phase frequency responses are the most straightforward method for defining a general filter tolerance specification.

Describing the targets of the problem in terms of its magnitude and phase frequency responses, requires the simultaneous optimization of two functions. Both these functions are required to satisfy an ideal solution or target. For a linear phase specification, this target is a straight line of some angle, ϕ, while the magnitude target may have a number of forms based upon the same tolerance specification. These forms range from a brick wall target to defining an individual magnitude response at each frequency point, as with the raised cosine filter. General filters, however, have magnitude responses described with a maximum passband attenuation, α_p, and minimum stopband attenuation, α_s. Possible straight line targets for a lowpass filter specification are shown by Fig.(2.8).

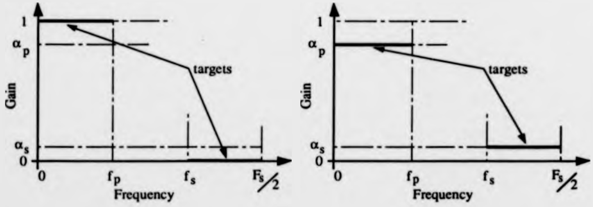

(a) (b)

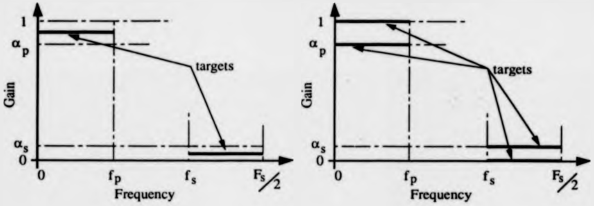

(c) (d)

Figure 2.8 Possible straight line magnitude targets. (a) brick wall of 1 and 0, (b) tolerance values of α_p and α_s, (c) mean value targets of $(1 + \alpha_p)/2$ and $\alpha_s/2$ and (d) dual line target scheme.

In Fig.(2.8), the diagrams (a)-(c) have a single target across the passband and stopband regions. Optimization would be required to minimise the deviation of the actual response from these straight lines. Although the filter specification allows a deviation in both the passband and stopbands, using these target ideas there would be no way to constrain the deviations to a prescribed limit. Fig.(2.8)(d) uses a dual target scheme, such that an optimization routine would only be required to minimise deviations outside the enclosed regions.

Although this type of dual target description is more accurate, it is computationally more expensive than the single line targets because, at each frequency point, the response has to be compared to the target and an error generated only if it lies outside the target band.

In all the target schemes of Fig.(2.8), the transition band has remained unspecified. This can affect the overall response and the ideas of single and dual line targets can be extended into the transition band. The practical implications of using these target designs for magnitude and phase responses are discussed in Chapter 3 and Chapter 4.

The final consideration within this area of problem definition is what the filter parameters represent and the limits upon their values. For digital filters these limits are due to stability constraints, forcing the filter coefficients to be limited to a prescribed range. For WDF structures a requirement to remain pseudopassive† also constrains the range of coefficient values.

---

† Pseudopassitivity[16] is the WDF equivalent of losslessness in analogue DTL networks.

Having defined the ideal response through the ideas of target templates, the next stage is to evaluate an error function that indicates the difference between the actual functions and the ideals. Error functions for filter design are usually based upon an approximation to the transfer function, generated by sampling the function at a number of frequency points. The larger the number of sample points, the greater the accuracy of the approximation but the higher the computational expense. Using this idea, the difference between the actual response and the appropriate target can be calculated at a number of frequency points. An overall error function can then use these individual differences in a number of ways. Existing error functions use the maximum individual difference as the overall error, a sum of the differences or a sum of the squares of the differences. Each method can be derived from a general form of the L_p-norm, given in Eq.(2.1).

$$\| v \|_p = \left[\sum_{i=1}^{n} |v_i|^p \right]^{1/p} \qquad p \in \{1,2,3,\ldots\} \cup \{\infty\} \tag{2.1}$$

The L_p-norm of a vector v can be generated from Eq.(2.1). This equation can be extended to the difference between two functions, defined as Lp-metrics. This function in given by Eq.(2.2), for two vectors x and y.

$$\| x - y \|_p = \left[\sum_{i=1}^{n} |x_i - y_i|^p \right]^{1/p} \qquad p \in \{1,2,3,\ldots\} \cup \{\infty\} \tag{2.2}$$

The error function based upon the largest difference is associated with the L_∞-metric, given by Eq.(2.3), while the sum of differences is the L_1-norm of Eq.(2.4). The sum of squares of individual errors is related to the L_2-norm of Eq.(2.5)

$$L_\infty = \| x - y \|_\infty = \max_{i=1,2,\ldots,n} \left\{ |x_i - y_i| \right\} \tag{2.3}$$

$$L_1 = \| x - y \|_1 = \sum_{i=1}^{n} |x_i - y_i| \tag{2.4}$$

$$L_2 = \| x - y \|_2 = \sqrt{\sum_{i=1}^{n} |x_i - y_i|^2} \tag{2.5}$$

An error function using n points to approximate the transfer function, may need to emphasise the error at some frequency points, especially when the passband performance is more important than the stopband performance. The L_p-metrics can be modified to include a weighting vector, λ, which contains a weight for each frequency point. The weighted L_p-metric is given by Eq.(2.6)

$$\| x - y \|_p^{\lambda} = \left[\sum_{i=1}^{n} \left(\lambda_i \, | x_i - y_i | \right)^p \right]^{1/p} \qquad p \in \{1,2,3,\ldots\} \cup \{\infty\} \qquad (2.6)$$

As mentioned earlier this design technique must simultaneously optimize a transfer function against two targets, representing the magnitude and phase frequency responses. To do this any error function must include both target errors. A method used by Deczky entailed the weighted L_p-metrics of each target and a ratio factor to combine these two errors. The general form of this equation in given by Eq.(2.7).

$$\text{Error} = \beta \left[\sum_{i=1}^{n} \left(W_i^g \, | \hat{G}_i - G_i | \right)^p \right]^{\frac{1}{p}} + (1 - \beta) \left[\sum_{i=1}^{m} \left(W_i^d \, | \hat{D}_i - D_i | \right)^p \right]^{\frac{1}{p}} \qquad (2.7)$$

where β is a factor $0 \le \beta \le 1$

n	points in gain response	m	points in phase response
W^g	gain weight vector	W^d	phase weight vector
$\hat{G}$	ideal gain target vector	$\hat{D}$	ideal phase target vector
G	actual gain vector	D	actual phase vector

If Eq.(2.7) is used as the basis of an error function, there are a number of modifications that can be introduced to increase the versatility of the function. The major element of these possible changes is the total number, distribution and spacing of the frequency points at which the actual response is sampled. The nature and value of these options provide the designer with a finer control over the error function and consequently the optimization procedure. The range and implications of these modifications to the error function of Eq.(2.7) are discussed for practical design examples in Chapter 3 and Chapter 4.

The final area of concern within this design decision is the actual optimization routine itself. A large number of techniques and procedures have been developed and the performance of each one is dependant upon the nature of the problem and information available. Each optimization algorithm is created to exploit a particular property of a function or its constraints.

The heart of any optimization procedure is its search direction and the information used to generate it. An optimization routine may therefore be classified in terms of the information required to calculate its search direction, using first derivatives (Jacobian) or second derivatives (Hessian) and the limits it places upon the search direction from parameter constraints. The three main optimization categories are : -

(i) Newton-type Methods.
These algorithms use the Hessian matrix, or a finite difference approximation to the Hessian, to define the search direction. These types of algorithms are among the most powerful for general problems.

(ii) Quasi-Newton Method.
Algorithms of this type approximate the Hessian matrix with a matrix that is modified at each iteration, to include information obtained about the curvature of the function along with the latest search direction. Although not as robust as Newton-type methods, they are computationally more efficient.

(iii) Conjugate-Gradient Methods.
These methods calculate the search direction without storing the information within Hessian or Jacobian matrices. These algorithms are ideally suited to large problems but are not usually as reliable or efficient as Newton-type or Quasi-Newton methods.

A more detailed explanation and comparison of optimization algorithms can be found in text books[1,18,20]. A large number of refinements of these procedures have been developed including Hooke-Jeeves[23], Fletcher-Powell[17] and Simulated Annealing[9,26] and then applied to the field of digital filter design. Examples include the finite wordlength program developed by Steiglitz[42], a program by Deczky using the Fletcher-Powell algorithm and Benvenuto[4] with simulated annealing techniques.

A more formal method of combining simultaneous magnitude and phase frequency responses into a single function is through the ideas of Multiple Criteria Optimization(MCO). Using this technique, the problem is not considered as two combined functions, but as a large single function, each element of which corresponds to a frequency point of either response. The ideas behind MCO are discussed by Steuer[43] and Osyczka[36], while their application to simultaneous magnitude and phase filters is considered by Lightner[10,31].

Overall selection of an optimization routine is based upon the properties of the problem and the information available. An error function based upon L_p-metrics using single line targets will be smooth, with continuous first and second order derivatives. If the filter multipliers are calculated to the full possible accuracy, then the bounds on the optimization routine will be simple, being bounds on the range of multiplier values. If finite wordlength constraints are imposed, then the optimization algorithm will be required to accept non-linear constraints. If the error function is based upon dual line targets then the first and second order derivatives become discontinuous. In conclusion, the choice of optimization routine will vary depending on how the problem is specified and what information is available.

2.5 Design Choice - Summary

The purpose of this Chapter was to illustrate and discuss the options available for the design of linear phase digital filters. These options centre upon selecting a filter structure, a design domain and a method of generating the filter coefficients.

The low coefficient sensitivity and as a consequence good finite wordlength performance of WDF structures, implies that they are the most suitable structure for filter designs. Two of the basic WDF structures are the lattice and the ladder. Overall the ladder network has a better performance than the lattice.

This is mainly due to the superior stopband properties of the ladder network, shown by the lower gain coefficient sensitivities in the stopband. Linear phase requirements indicate structures that have nonminimum-phase characteristics. This constraint suggests the lattice structure over the ladder network. Both structures were investigated for linear phase performance, concerning the tradeoff between amplitude selectivity and phase linearity for ladder networks and the stopband coefficient sensitivity in lattice structures.

The design and simulation of a digital filter can be approached through a number of domains, such as the time and frequency domains. Although this offers a greater design flexibility, the practicality of each approach is limited by an ability to define a general tolerance specification in that particular domain. This constraint limits general filter designs to the continuous or discrete frequency domains, describing the responses in terms of magnitude and phase. Non-linear mapping from the continuous to discrete frequency domain, due to the bilinear transform further limits the practical choice to the discrete frequency domain.

The final output of a digital filter design will be a set of quantized filter coefficients. A number of methods may be used to generate the infinite precision coefficient values but to produce an acceptable performance, the final step of finite wordlength coefficient design must involve some amount of optimization. Due to the lack of analytical formulae for the design of linear phase digital filters, the whole design process should be approached through optimization. Optimization techniques could then be applied to both ladder and lattice WDF linear phase designs under simultaneous or equaliser procedures.

References

1) Adby, P. R. and Dempster, M. A. H., Introduction to Optimization Methods, Chapman and Hall, London, 1974.

2) Baher, H. and O'Malley, M., "On the Design of Selective Linear Phase Wave Digital Filters", IEEE Pacific Rim Conf. Comm., Comp and Signal Processing, June 1987, pp228-230.

3) Bel Bachir, M. F. and Caelen, J., "Recursive Digital Filter Design with Linear Phase", IEEE Pacific Rim Conf. Comm., Comp and Signal Processing, June 1987, pp243-247.

4) Benvenuto, N. and Marchesi, M., "Digital Filter Design by Simulated Annealing", IEEE Trans. Circuit and Systems, Vol CAS-36, No. 3, March 1989, pp459-460.

5) Blinchikoff, H. J. and Zverev, A. I., Filtering in the Time and Frequency Domains, J. Wiley and Sons, New York, 1976.

6) Carlin, H. J. and Wu, J-L. C., "Amplitude Selectivity Versus Constant Delay in Minimum-Phase Lossless Filters", IEEE Trans. Circuits and Systems, Vol CAS-23, No. 7, July 1976, pp447-455.

7) Carlin, H. J. and Wu, J-L. C., "Linear Phase Commensurate Line Networks with Amplitude Selectivity", IEEE Proc. Int. Conf. Circuits and Systems, 1976, pp536-539.

8) Chottera, A. T. and Jullien, G. A., "A Linear Programming Approach to Recursive Digital Filter Design with Linear Phase", IEEE Trans. Circuits and Systems, Vol CAS-29, No. 3, March 1982, pp139-149.

9) Corana, A., Marchesi, M., Martini, C. and Ridella, S., "Minimizing Multimodal Functions of Continuous Variables with the 'Simulated Annealing' Algorithm", ACM Trans. Math. Software, Vol 13, No. 3, September 1978, pp262-280.

10) Cortelazzo, G. and Lightner, M. R., "Simultaneous Design in both Magnitude and Group-Delay of IIR and FIR Filters based on Multiple Criterion Optimization", IEEE Trans. Acoustics, Speech and Signal Processing, Vol ASSP-32, No. 5, October 1984, pp949-967.

11) Crochiere, R. E. and Rabiner, L. R., "Further Considerations in the Design of Decimators and Interpolators", IEEE Trans. Acoustics, Speech and Signal Processing, Vol ASSP-24, No. 4, August 1976, pp296-311.

12) Crochiere, R. E. and Rabiner, L. R., "Interpolation and Decimation of Digital Signals - A Tutorial Review", Proc. IEEE, Vol 69, No. 3, March 1981, pp300-331.

13) Deczky, A. G., "Recursive Digital Filters Having Equiripple Group Delay", IEEE Trans. Circuits and Systems, Vol CAS-21, No. 1, January 1974, pp131-1349.

14) Deczky, A. G., "Synthesis of Recursive Digital Filters Using the Minimum p-Error Criterion", IEEE Trans. Audio Electroacoustic., Vol AU-20, October 1972, pp257-263.

15) Fettweis, A., "A Simple Design of Maximally Flat Delay Digital Filters", IEEE Trans. Audio Electroacoustic., Vol AU-20, June 1972, pp112-114.

16) Fettweis, A., "Pseudopassivity, Sensitivity and Stability of Wave Digital Filters", IEEE Trans. Circuit Theory, Vol CT-19, No. 11, November 1972, pp668-673.

17) Fletcher, R. and Powell, M. J. D., "A Rapid Convergent Descent Method for Minimization", Computer Journal, Vol 6, No. 2, July 1963, pp163-168.

18) Fletcher, R., *Practical Methods of Optimization*, Wiley, New York, 1987.

19) Foldvári-Oros, J., Henk, T. and Simonyi, E., "Simultaneous Amplitude and Phase Approximation for Lumped and IIR-Filters", IEEE Int. Conf. Circuits and Systems 1988, pp2501-2504.

20) Gill, P. E., Murray, W. and Wright, M. H., *Practical Optimization*, Academic Press, London, 1981.

21) Haykin, S. S., "Gain-Phase Analysis of Digital Filters with Applications", Int J. Cir. Theory and Applications, Vol 1, 1973, pp305-311.

22) Henk, T., "The Generation of Arbitrary Phase Polynomials by Recurrence Formulae", Int J. Cir. Theory and Applications, Vol 9, 1981, pp461-478.

23) Hooke, R. and Jeeves, T. A., "'Direct Search' Solution of Numerical and Statistical Problems", Jour. Assoc. Comput. Mach., Vol 8, No. 2, April 1961, pp212-229.

24) Jarry, P., Garault, Y. and Clapeau, M., "Generalized Linear Phase Polynomials - Application in Filter Synthesis", Int J. Cir. Theory and Applications, Vol 4, 1976, pp381-398.

25) Johnson, T. J. "Simultaneous Magnitude and Phase Equalization using Digital Filters", IEEE Trans. Circuit and Systems, Vol CAS-25, No. 5, May 1978, pp319-321.

26) Kirkpatrick, S., Gelatt, C. D. and Vechi, M. P., "Optimization by Simulated Annealing", Science, Vol 220, No. 4598, 13th May 1983, pp671-680.

27) Kunold, I., "Linear Phase Realization of Wave Digital Lattice Filters", IEEE Trans. Circuits and Systems, Vol CAS-34, No. 4, March 1986, pp131-1349.

28) Kwan, R. K. and Bach, G. G., "Simultaneous Approximations in Filter Design", IEEE Trans. Circuit Theory, Vol CT-16, No. 1, March 1969, pp117-121.

29) Leeb, F. and Henk, T., "Simultaneous Amplitude and Phase Approximation for FIR Filters", Int J. Cir. Theory and Applications, Vol 17, 1989, pp363-374.

30) Leeb, F. and Henk, T., "Simultaneous Approximation for Bireciprocal Lattice Wave Digital Filters", IEE Euro. Conf. Cir. Theory and Design, 5-8 September 1989, pp472-476.

31) Lightner, M. R. and Director, S. W., "Multiple Criterion Optimization for the Design of Electronic Circuits", IEEE Trans. Circuits and Systems, Vol CAS-28, No. 3, March 1981, pp169-179.

32) Lind, L. F., "Linear Phase Filter Design in the Time Domain", IEE Tenth Saraga Colloquium on 'Digital and Analogue Filters and Filtering Systems', 25th May 1990, pp1/1-1/4.

33) Maria, G. A. and Fahmy, M. M., "A New Design Technique for Recursive Digital Filters", IEEE Trans. Circuit and Systems, Vol CAS-23, No. 5, May 1976, pp323-325.

34) Mitra, S. K. and Sherwood, R. J., "Estimation of Pole-Zero Displacements of a Digital Filter due to Coefficient Quantization", IEEE Trans. Circuit and Systems, Vol CAS-21, No. 1, January 1974, pp116-124.

35) Nedunuri, R. "Synthesis of Recursive Digital Filters with Prescribed Attenuation and Group-Delay Characteristics", IEEE Trans. Circuit and Systems, Vol CAS-23, No. 11, November 1976, pp686-688.

36) Osyczka, A., `Multicriterion Optimization in Engineering with Fortran Programs`, J. Wiley and Sons, New York, 1984.

37) Renfors, M. and Saramäki, T., "Recursive Nth-Band Digital Filters - Part I: Design and Properties, Part II: Design of Multistage Decimators and Interpolators", IEEE Trans. Circuit and Systems, Vol CAS-34, No. 1, January 1987, pp24-39/pp40-51.

38) Rhodes, J. D. and Fahmy, M. I. F., "Digital Filters with Maximally Flat Amplitude and Delay Characteristics", Int J. Cir. Theory and Applications, Vol 2, 1974, pp3-11.

39) Sadughi, S. and Kim, H. K., "An Approximation Procedure for Selective Linear Phase Filters", IEEE Trans. Circuit and Systems, Vol CAS-34, No. 8, August 1987, pp967-969.

40) Saramäki, T. and Neuvo, Y., "An Implicit Solution for IIR Filters with Equiripple Group Delay", IEEE Trans. Circuit and Systems, Vol CAS-32, No. 5, May 1985, pp476-478.

41) Saramäki, T. and Neuvo, Y., "Digital Filters with Equiripple Magnitude and Group Delay", IEEE Trans. Acoustics, Speech and Signal Processing, Vol ASSP-32, No. 6, December 1984, pp1194-1200.

42) Steiglitz, K., "Designing Short-Word Recursive Digital Filters", Proc. 9th Annual Allerton Conf. Cir. and System Theory, October 1971, pp778-788.

43) Steuer, R. E., `Multiple Criteria Optimization: Theory, Computation and Application`, Wiley, New York, 1986.

44) Thajchayapong, P. and Lomtong, P., "A Maximally Flat Group Delay Recursive Digital Filter with Controllable Magnitude", IEEE Trans. Circuit and Systems, Vol CAS-25, No. 1, January 1978, pp51-53.

45) Thiran, J-P., "Equal-Ripple Delay Recursive Digital Filters", IEEE Trans. Circuit Theory, Vol CT-18, No. 3, November 1971, pp664-669.

46) Unbehauen, R. "Recursive Digital Low-Pass Filters with Predetermined Phase or Group Delay and Chebyshev Stopband Attenuation", IEEE Trans. Circuit and Systems, Vol CAS-28, No. 9, September 1981, pp905-912.

47) Valenzuela, R. A. and Constantinides, A. G., "Digital Signal Processing Schemes for Efficient Interpolation and Decimation", Proc. IEE, Vol 130, Pt. G, No. 6, December 1983, pp225-235.

48) Vlach, J., Computerized Approximation and Synthesis of Linear Networks, Wiley, New York, 1969.

Chapter 3

Ladder WDF's

A large number of modifications have been proposed for the ladder WDF since Fettweis first developed it in 1971[4,5]. Each modification was directed at improving the performance and efficiency of the structure. Sedlmeyer extended Fettweis' ideas to a structure with a true ladder configuration[13,3], while other research concerned overflow stability criteria and design techniques. For practical considerations, the design and analysis of a ladder WDF needs to be automated through a computer program. The efficiency and speed of any program will depend upon the possible design approaches.

This Chapter considers the design of linear phase ladder WDF's. The research outlined ranges from the choice of circuit configuration and components to design procedures. The Chapter discusses the ladder WDF design approach suggested by Lawson and provides system equations for the ladder structure along with two-port chain matrices of a number of possible circuit elements. The operation of a computer program, called WAVE, written to implement this design approach, is also explained. Simultaneous magnitude and phase ladder WDF specifications were approached with optimization using the WAVE program. The optimization techniques follow the ideas discussed in Chapter 2. Finally the Chapter details a number of experimental results from the use of the program and the performance of various optimization strategies. The Chapter concludes with a number of observations about the compromise between magnitude and phase requirements in minimum-phase structures and the efficiency of quasi-Newton optimization techniques.

3.1 Design Choices

Following the conclusions of Chapter 2, the designs for linear phase ladder WDF were based upon the simultaneous solution of a magnitude and phase specification through optimization. Within this approach a large number of design options exist, each of which can be used to enhance this procedure.

3.1.1 Reference circuit options

Design options for ladder WDF structures are very limited, only allowing the combination of lossless elements. These elements may include a series capacitor, a parallel inductor, a tuned circuit or a unit element. Within these options, the most obvious choice is to construct a ladder WDF based solely on lumped elements or a circuit built from a cascade of distributed components. An additional option would be to mix the types of components within a single structure.

The ladder WDF structure, based upon lumped components, can have a wide variety of combinations, each well known to analogue design theory. A number of possible ladder WDF reference circuits are illustrated in Fig.(3.1).

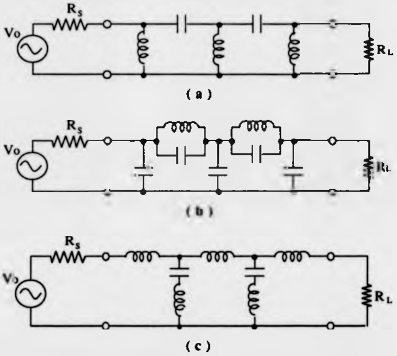

(c)

Figure 3.1 General DTL analogue circuits.

The DTL circuits of Fig.(3.1) may all be used as reference structures for the design of a ladder WDF. Although these circuits have the same order, the tuned circuits of Fig.(3.1)(b) and (c) can be designed to possess higher magnitude selectivity. Consequently, the circuits of Fig.(3.1)(b) and (c) are used to implement elliptic functions, while the circuit of Fig.(3.1)(a) can be used to produce Butterworth or Chebyshev type responses.

A typical analogue circuit constructed from distributed elements is shown by Fig.(3.2)(a), along with equivalent digital circuit based upon the unit element.

Design of this unit element may be approached through the techniques suggested by Fettweis or Lawson. The Unit Element Wave Digital Filter(UEWDF) derived through the Fettweis procedure from the analogue circuit of Fig.(3.2)(a) is illustrated by Fig.(3.2)(b), while the appropriate Lawson circuit is shown by Fig.(3.2)(c).

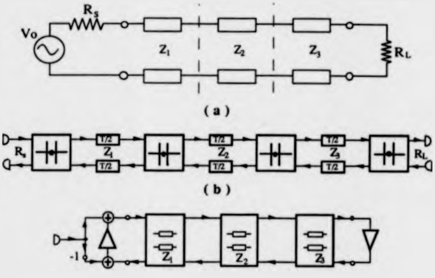

(a)

(b)

(c)

Figure 3.2 (a) DTL network using distributed elements with equivalent (b) Fettweis circuit and (c) Lawson model.

Although the structures of Fig.(3.2)(b) and (c) are generated through different design techniques, they have a similar performance. The circuit of Fig.(3.2)(b) was used by Renner[12] and Hyder[8] to illustrate the principles and properties of the unit element WDF.

Authors who have used the unit element within WDF designs include Thiran[14], Denton[15] and Reekie et al.[11]. These designs were based upon reference filters which contained both distributed and lumped elements. An example of a mixed component reference circuit is shown by Fig.(3.3), along with the equivalent WDF's constructed through the Fettweis and Lawson design approaches.

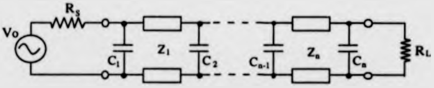

(a)

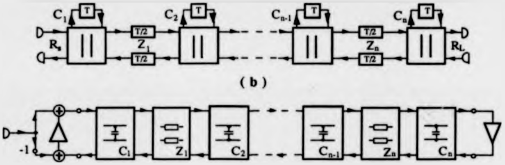

(b)

(c)

Figure 3.3 (a) Mixed component DTL network with (b) equivalent Fettweis WDF and (c) Lawson WDF equivalent.

The work by Thiran was directed at developing structures with the unit element that would require a lower number of multipliers than an equivalent circuit with a true ladder configuration, such as those of Fig.(3.1). The objective of Denton and Carlin was to apply existing microwave theory to the design of selective, constant group delay WDF's based upon the reference circuit of Fig.(3.3)(a). Although these WDF's could be designed to achieve a constant group delay within a given limit, the frequency selectivity and stop band attenuation was poor. The poor stopband performance is also a limitation of the pure unit element WDF of Fig.(3.2).

One of the main research objectives of this project concerned designing WDF's that have linear phase and good frequency selectivity. Under this direction the research was concentrated upon reference structures known to possess high frequency selectivity, such as the circuits of Fig.(3.1)(b) and (c).

3.1.2 Optimization considerations

As outlined in Chapter 2, there are a large number of parameters that have to be considered when optimization is applied to filter design. The conclusions of Chapter 2 suggested that optimization should be carried out in the discrete frequency domain. The selection of an optimization algorithm would depend upon the nature of the error function and what information about this error function was available. The error function would, in turn, depend upon how the filter specification was defined and how any differences between the actual and desired responses were measured.

Following the suggestions of Chapter 2, the filter specification can be expressed as a set of straight line targets. These target lines could indicate the mean values of the function or define limits for an acceptable response. These ideas relate to the simple single and dual line templates, shown for a lowpass filter specification by Fig.(3.4).

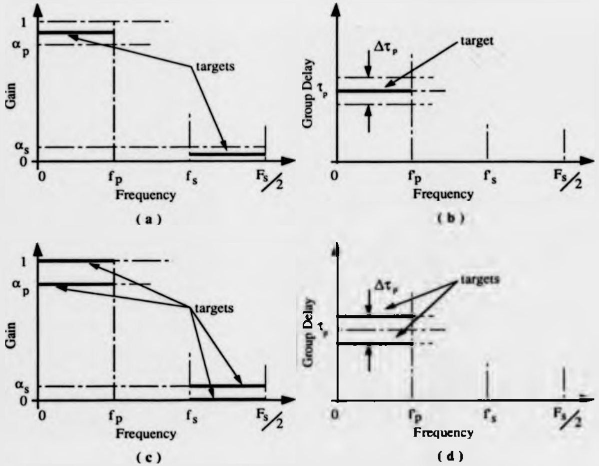

Figure 3.4 Target templates based upon single line (a) gain and (b) group delay values and dual line (c) gain and (d) group delay values.

The error function derived in Chapter 2 is based upon a weighted L_p-metric, being the sum of the weighted differences between two vectors. For an error function, one of these vectors would represent the actual frequency response, either the gain or group delay, while the other would contain the ideal values. These vectors would be described as a set of frequencies points within a target template. For lowpass templates, such as those illustrate by Fig.(3.4), the gain error vector could consist of n_1 points in the region $0 \le f \le f_p$, n_2 points for $f_p \le f \le f_s$ and n_3 points across $f_s \le f \le F_s/2$. A group delay error vector may consist of m_1 points within the region $0 \le f \le f_p'$. For the templates of Fig.(3.4), the frequency specification for the gain and group delay responses are not identical. This represents a general design situation, where the width of a particular frequency band may differ for gain and group delay specifications.

The number and relative position of the points within each error template can be used to alter the overall error function and therefore possible solutions. The relative spacing of these points can be arbitrary, but it is more usual to arrange them according to some analytical expression. Possible spacing formulae include linear, sine, cosine and double cosine. These spacing types are illustrated in Fig.(3.5).

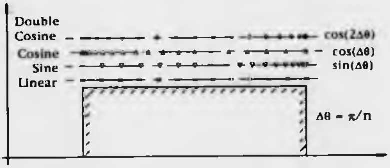

Figure 3.5 Possible template point spacing.

The point spacing is usually chosen so that more points are clustered around the regions of the function that change the most. Therefore in filter designs, points tend to be clustered around the transition band edges. In this way, for the lowpass filter specification shown by Fig.(3.4), the sine spacing would be used for the passband region and the cosine spacing for the stopband. The double cosine spacing would be appropriate for bandpass or bandstop designs.

Other factors that effect the choice of an optimization routine are its efficiency and convergence rate. Algorithms that offer a high convergence rate require a large amount of information about the function, such as first and second order derivatives. This information can be very computationally expensive, especially if the filter order is high. Although algorithms that require less information about the function, converge slower, they may operate faster because of the removal of derivative calculations.

Computational expense is not only a function of the filter's structure but also the parameters that the optimization routine is acting upon. If the final value of these parameters is to conform to a finite wordlength specification, then the optimization routine would be required to satisfy non-linear constraints upon the multiplier coefficients. Filter designs that do not specify finite wordlength conditions may use basic algorithms with simple bounds upon the optimized parameters. These bounds are determined by stability conditions and will vary depending upon what the parameters represent. The parameters could be the reference filter component values or the ladder WDF multiplier values. Both methods, each with the same number of variables, introduce a certain amount of extra calculation into the process of determining the transfer function of the ladder WDF and consequently the error function. Optimization on the reference filter component values requires calculating the equivalent ladder WDF multiplier values for each iteration. The extra calculation introduced by optimizing the multipliers directly is due to the dependent nature of some of multipliers. To ensure the structure retains its WDF properties, dependant multiplier values must be determined at each iteration of the optimization process.

To increase the efficiency and versatility of this simultaneous magnitude and phase ladder WDF approach, all design options must be considered. A comparison of these options will then provide an indication of their contributions to the overall design problem.

3.2 Ladder WDF equations

The ladder WDF consists of a cascade connection of blocks, which represent equivalent analogue components. For an automated design process, the nature and ease with which these blocks can be calculated and interconnected plays a vital role. The most obvious design method is to describe each block in terms of its two-port chain matrix, so that the overall ladder WDF is the product of the appropriate chain matrices. These chain matrices can be derived from analogue components, either through the one-port and adaptor techniques proposed by Fettweis, or the two-port approach suggested by Lawson.

3.2.1 Interconnection

A major constraint on the use of digital blocks to describe a ladder WDF, is their interconnection. For the reference analogue DTL network, all connections must obey Kirchhoff's laws, so for Fig.(3.6), $V_i = V_j$, $I_i = I_j$ and $Z_i = Z_j = Z$.

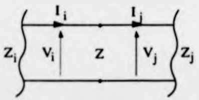

Figure 3.6 A voltage/current node within a circuit.

The equivalent connection using voltage wave notation of Fig.(3.6), is shown by Fig.(3.7). For a direct connection of the two blocks in Fig.(3.7), $A_j = B_i$ and $A_i = B_j$. To ensure that Kirchhoff's laws are still satisfied, $R_i = R_j = R$. A wave notation of Kirchhoff's laws may be expressed by stating that connected ports must have the same wave parameter orientation and equal port resistances.

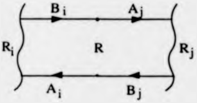

Figure 3.7 An incident/reflected wave node within a circuit.

The other major constraint for the design of a digital system is the existence of delay free loops. These limit the realization of a design, as the filter cannot reach a stable state at the end of each sampling period. This problem can be illustrated by the signal flow graph of Fig.(3.8), which shows the interconnection of three two-port elements given in terms of their scattering matrices, $\sigma(z)$, $\delta(z)$ and $\lambda(z)$.

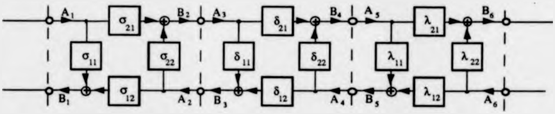

Figure 3.8 Interconnection of three two-port sections.

A delay free path will only exist if the equation of a loop contains a constant term. Therefore, the first interconnection of Fig.(3.8), will only contain a delay free path if both σ_{22} and δ_{11} have constant terms. For the second interconnection, a delay free loop will only exist if δ_{22} and λ_{11} both contain constant terms. To eliminate these possible delay free paths, it is only necessary to ensure that one element of a loop does not contain a constant term, not both. This condition presents three main design options for Fig.(3.8) :-

(i) Remove constant terms from σ_{11}, δ_{11} and λ_{11} elements.
(ii) Remove constant terms from σ_{22}, δ_{22} and λ_{22} elements.
(iii) Remove the constant terms from σ_{22} and λ_{11} elements

The ladder WDF is derived from a DTL ladder network, an example of which is shown by Fig.(3.9). To accurately model this structure, digital equivalents for the voltage source and the load and source resistances are also required.

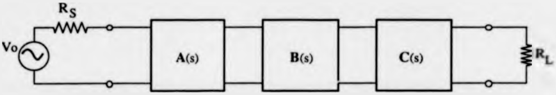

Figure 3.9 General ladder DTL network of two-port sections.

The resistive source and resistive load of Fig.(3.9) are illustrated in Fig.(3.10). Using the relationship between voltage and current to incident and reflected waves, the source voltage V_0 can be expressed with voltage waves, A_i and B_i and the port resistance, R_i. The load resistance can also be defined in voltage wave notation.

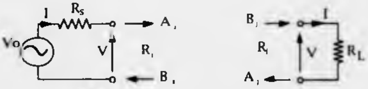

(a) (b)

Figure 3.10 Source and load circuits of a DTL network.

$$V = V_0 - I R_s , \begin{bmatrix} A_i \\ B_i \end{bmatrix} = \begin{bmatrix} 1 & R_i \\ 1 & -R_i \end{bmatrix} \cdot \begin{bmatrix} V \\ I \end{bmatrix} \qquad V = I R_L , \begin{bmatrix} A_j \\ B_j \end{bmatrix} = \begin{bmatrix} 1 & R_j \\ 1 & -R_j \end{bmatrix} \cdot \begin{bmatrix} V \\ I \end{bmatrix}$$

therefore

$$A_i = \frac{2R_i}{R_s + R_i} V_0 + \frac{R_s - R_i}{R_s + R_i} B_i \qquad B_j = \frac{R_L - R_j}{R_L + R_j} A_j$$

or

$$A_i = (1 - \alpha) V_0 + \alpha B_i \qquad B_j = \beta A_j$$

The complete digital equivalent structure of the analogue circuit of Fig.(3.9) is given by Fig.(3.11). The action of the external multipliers is to modify the port resistance values R_A and R_B. Interconnection constraints require that for Fig.(3.11), $R_A = R_1$, $R_2 = R_3$, $R_4 = R_5$ and $R_6 = R_B$. However, the actual values of these port resistances are not set and this allows a degree of freedom in the design of the ladder structure.

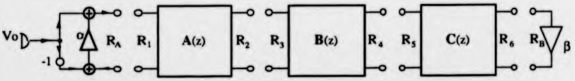

Figure 3.11 Equivalent general ladder WDF using two-port sections.

Having ensured that connected ports have equal port resistances, the next design criterion requires the removal of any delay free loops. For Fig.(3.11), if the sections A, B and C have the scattering matrices σ, δ and λ respectively, then four possible delay free loops exist, between $\alpha \Leftrightarrow \sigma_{11}$, $\sigma_{22} \Leftrightarrow \delta_{11}$, $\delta_{22} \Leftrightarrow \lambda_{11}$ and $\lambda_{22} \Leftrightarrow \beta$. The process for removing these delay free paths follows the ideas outlined for Fig.(3.8). The first procedure concerns removing any constant terms from a circuit connected to the input port of an element and is known as *source design*, as the design process moves from the source of the structure. The second process removes any constant terms from a circuit connected to the output port of an element. This is called *load design*, again because the design process moves from the load. The final design approach removes delay free loops, moving simultaneously from the source and the load, to reach the middle of the circuit. This design approach is known as *middle design*.

Applying the source design procedure to the circuit in Fig.(3.11), the first step is to remove the constant term in the loop connected to the input port of A. This entails setting the multiplier α to zero, so

$$\alpha = \frac{R_s - R_A}{R_s + R_A} = 0$$

$$\therefore \qquad R_A = R_s$$

and because of the connectivity constraints, then $R_1 = R_s$. The next step is to remove any constant terms of the circuit connected to the input of port B. This involves the removal of any constant terms from σ_{22}. The action of this step reduces the complexity of the overall chain matrix by making the values of the port resistances, previously independent, related to each other. Within this relationship between the port resistances and the modelled component values, the only free parameter for this design method is the output port, R_2. The value of this resistance is adjusted to remove any constant terms within the σ_{22} element. This value of R_2 is passed to R_3, because they are directly connected. Using this new value for R_3 and the modelled component within section B, the port resistance R_4 is made dependent upon R_3 and R_4 is adjusted then to remove any constant terms in the δ_{22} element. This process continues until the final port resistance value, R_B, is determined and the external multiplier, β, can be calculated.

The operation of the source design method may be summarized as moving from the source of the structure, using the undefined values of a section's output port resistance to remove any delay free loops. Through this process the output port resistance of a section is made dependent upon the input port resistance and the modelled components within that section.

Conversely, the load design procedure starts at the load of the structure and works toward the source. If this process is applied to Fig.(3.11), then the first step is to remove any constant terms in the path connected to the output port of the last section, C. To do this, the load multiplier, β, must equal zero, so,

$$\beta = \frac{R_L - R_B}{R_L + R_B} = 0$$

$$\therefore \qquad R_B = R_L$$

The value for the port resistance R_B is passed to R_6 because they are directly connected. Elimination of any delay free paths between C and B with this design procedure entails the removal of any constant terms from λ_{11}. This process makes the two-port resistances dependent upon each other and then adjusts the value of R_5 to remove any constant terms in λ_{11}. This value for R_5 in turn determines the value for R_4. The design process continues removing constant terms from the δ_{11} and σ_{11} elements of the circuit's scattering matrices by defining an appropriate value for the input port resistance of each section, until the source multiplier is reached. The calculated value of R_A can then be used to determine α.

The middle design procedure uses the ideas of both source and load design processes. This procedure moves simultaneously from the source and load ends of the structure to meet at some arbitrary point within the network. If the middle design procedure is applied to Fig.(3.11) and section B is chosen as its arbitrary point, the first step is to follow the source design procedure until section B is reached. This requires the removal of α and eliminating constant terms from σ_{22}. The next is to move from the load of the circuit, removing β and any constant terms from λ_{11}. This design procedure leaves the scattering matrix of B unaffected and may possess constant terms in both its δ_{11} and δ_{22} elements.

Although the middle design procedure removes both external multipliers, the resulting circuit requires the same number of multipliers as the source and load design cases. This is due to the nature of the section chosen as the arbitrary point for the design procedure. This section has both port resistance values set by the surrounding circuit and therefore cannot be simplified by making the port resistances dependent. Under this criterion, the section contains an extra multiplier compared to an equivalent section modified for the load or source design procedures. Although the middle design procedure could be implemented around sections A, B or C, Fettweis[6] noted that the dynamic range of the ladder WDF structure was improved if this arbitrary point was near the centre of the circuit.

3.2.2 Overall system equations

The general ladder WDF, illustrated by Fig.(3.12), has the chain matrix of Eq.(3.1) and the transfer function, H(z), given by Eq.(3.2).

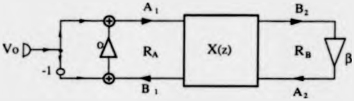

Figure 3.12 Overall ladder WDF two-port structure.

$$\begin{bmatrix} A_1 \\ B_1 \end{bmatrix} = \begin{bmatrix} x_{11} & x_{12} \\ x_{21} & x_{22} \end{bmatrix} \cdot \begin{bmatrix} A_2 \\ B_2 \end{bmatrix} \qquad (3.1)$$

$$H(z) = \frac{A_2 + B_2}{2V_o} = \frac{1 - \alpha}{\left(x_{12} - \alpha\, x_{22} + \beta\left(x_{11} - \alpha\, x_{21}\right)\right)} \qquad (3.2)$$

with

$$\alpha = \frac{R_s - R_A}{R_s + R_A} \quad \text{and} \quad \beta = \frac{R_L - R_B}{R_L + R_B}$$

where R_s and R_L represent the source and load resistance values of the reference analogue DTL circuit respectively. Each of the three design procedures modifies the overall transfer function of the general ladder WDF circuit of Fig.(3.12) by removing α or β or both. This in turn alters Eq.(3.2) to give a different transfer function for each design method.

Source design :

$\alpha = 0$, so $R_A = R_s$ and using Eq.(3.2) then

$$H_s(z) = \frac{1}{x_{12} + \beta\, x_{11}}, \qquad \text{where} \quad \beta = \frac{R_L - R_B}{R_L + R_B} \qquad (3.3)$$

Load design :

$\beta = 0$, so $R_B = R_L$ and using Eq.(3.2) then

$$H_L(z) = \frac{1 - \alpha}{x_{12} - \alpha\, x_{22}} \qquad \text{where} \quad \alpha = \frac{R_s - R_A}{R_s + R_A} \qquad (3.4)$$

Middle design :

$\alpha = 0$ and $\beta = 0$, so $R_A = R_s$ and $R_B = R_L$ and using Eq.(3.2) then

$$H_m(z) = \frac{1}{x_{12}} \tag{3.5}$$

Each design method simplifies the structure of Fig.(3.12) and by using the appropriate transfer function, the performance of a filter under each design method can be determined. The performance can be measured in terms of the magnitude, phase and group delay frequency responses and coefficient sensitivities. All of these calculations depend on the overall system chain matrix, **X**, given by Eq.(3.1). This chain matrix is the product of the chain matrices of each digital component within the circuit. It is these components that determine the coefficient sensitivities of the overall structure. The equations to calculate **X** and its derivatives are therefore required in terms of individual component's chain matrices.

Consider Fig.(3.13), and the individual chain matrices, given in Eq.(3.6), for its elements.

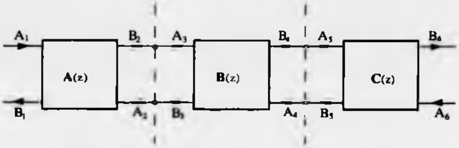

Figure 3.13 Ladder WDF two-port structure.

$$\begin{bmatrix} A_1 \\ B_1 \end{bmatrix} = \begin{bmatrix} a_{11} & a_{12} \\ a_{21} & a_{22} \end{bmatrix} \cdot \begin{bmatrix} A_2 \\ B_2 \end{bmatrix}, \qquad \begin{bmatrix} A_3 \\ B_3 \end{bmatrix} = \begin{bmatrix} b_{11} & b_{12} \\ b_{21} & b_{22} \end{bmatrix} \cdot \begin{bmatrix} A_4 \\ B_4 \end{bmatrix}$$

$$\begin{bmatrix} A_5 \\ B_5 \end{bmatrix} = \begin{bmatrix} c_{11} & c_{12} \\ c_{21} & c_{22} \end{bmatrix} \cdot \begin{bmatrix} A_6 \\ B_6 \end{bmatrix} \tag{3.6}$$

To calculate the overall transfer function of this structure under the three design procedures detailed by Eq.(3.3-5), the product of the individual chain matrices to determine **X**, must be found. The direct connection of these blocks means that $A_2 = B_3$, $A_3 = B_2$, $A_4 = B_5$ and $A_5 = B_4$. Therefore, the overall transfer function is not simply the product of chain matrices themselves, but modified chain matrices, which have their columns swapped. The overall chain matrix of the structure of Fig.(3.13), in terms of the modified chain matrices, is given by Eq.(3.7).

$$\begin{bmatrix} A_1 \\ B_1 \end{bmatrix} = [A'] \cdot [B'] \cdot [C'] \cdot \begin{bmatrix} B_6 \\ A_6 \end{bmatrix} \tag{3.7}$$

where $[A'] = \begin{bmatrix} a_{12} & a_{11} \\ a_{22} & a_{21} \end{bmatrix}$

Using these ideas, the properties of the overall ladder structure may be described in terms of the individual components through their chain matrices. The product of the modified individual chain matrices to generate the overall modified chain matrix, **X'**, of the structure may be defined as,

$$\mathbf{X}' = \prod_{i=1}^{n} \mathbf{X}'_i \tag{3.8}$$

where n is the number of chain matrices within the structure. The gain and phase response of the appropriate ladder WDF circuit can therefore be calculated from the transfer functions given by Eq.(3.3-5).

The group delay response of a circuit may be defined as,

$$\tau(\omega) = -\operatorname{Im}\left[\frac{1}{H(z)}\,\frac{dH(z)}{d\omega}\right]$$

To calculate this function for the ladder structure, the derivative of H(z) with respect to the frequency, ω, is required. For the source, load and middle design cases mentioned, this results in three equations for the group delay, derived from Eq.(3.3-5) respectively.

Source design ;

$$\tau_s(\omega) = \operatorname{Im}\left[\frac{1}{\left(x_{12} + \beta\, x_{11}\right)} \cdot \left(\frac{d(x_{12})}{d\omega} + \beta\,\frac{d(x_{11})}{d\omega}\right)\right] \tag{3.9}$$

Load design ;

$$\tau_L(\omega) = \operatorname{Im}\left[\frac{1}{\left(x_{12} - \alpha\, x_{22}\right)} \cdot \left(\frac{d(x_{12})}{d\omega} - \alpha\,\frac{d(x_{22})}{d\omega}\right)\right] \tag{3.10}$$

Middle design ;

$$\tau_m(\omega) = \operatorname{Im}\left[\frac{1}{\left(x_{12}\right)} \cdot \left(\frac{d(x_{12})}{d\omega}\right)\right] \tag{3.11}$$

To calculate the derivative of the overall chain matrix with respect to ω, it is necessary to differentiate each chain matrix in turn. However, because matrices are not commutative, i.e. $\mathbf{A} \cdot \mathbf{B} \neq \mathbf{B} \cdot \mathbf{A}$, then if

$$\mathbf{X}' = \mathbf{A}' \cdot \mathbf{B}' \cdot \mathbf{C}' \tag{3.12}$$

the derivatives will be

$$\frac{d\mathbf{X}'}{d\omega} = \frac{d\mathbf{A}'}{d\omega} \cdot \mathbf{B} \cdot \mathbf{C} + \mathbf{A} \cdot \frac{d\mathbf{B}'}{d\omega} \cdot \mathbf{C} + \mathbf{A} \cdot \mathbf{B} \cdot \frac{d\mathbf{C}'}{d\omega}$$

The derivative of an overall chain matrix can therefore be defined as,

$$\frac{d\mathbf{X}'}{d\omega} = \sum_{i=1}^{n} \left[\prod_{k=0}^{i-1} X_k \cdot \frac{dX'_i}{d\omega} \cdot \prod_{k=i+1}^{n+1} X_k \right] \tag{3.13}$$

where $\mathbf{X}'_0$ and $\mathbf{X}'_{n+1}$ are equal to the identity matrix, $\mathbf{I}$.

Eq.(3.13) may be simplified if natural logs of Eq.(3.12) are taken before it is differentiated. If this technique is applied to Eq.(3.12), the derivative with respect to ω is,

$$\frac{1}{\mathbf{X}'} \cdot \frac{d\mathbf{X}'}{d\omega} = \frac{1}{\mathbf{A}'} \cdot \frac{d\mathbf{A}'}{d\omega} + \frac{1}{\mathbf{B}'} \cdot \frac{d\mathbf{B}'}{d\omega} + \frac{1}{\mathbf{C}'} \cdot \frac{d\mathbf{C}'}{d\omega} \tag{3.14}$$

Using the form of Eq.(3.14), the differential of a general chain matrix, $\mathbf{X}'$, with respect to the frequency, ω, may be defined as,

$$\frac{1}{\mathbf{X}'} \cdot \frac{d\mathbf{X}'}{d\omega} = \sum_{i=1}^{n} \frac{1}{\mathbf{X}'_i} \cdot \frac{d\mathbf{X}'_i}{d\omega} \tag{3.15}$$

Coefficient sensitivity frequency responses are a function of the filter's multipliers, particular to each element's chain matrix, and the property being calculated, such as gain, phase or group delay. The sensitivities of the gain, $|H|$, with respect to a multiplier value, α_k, is defined as

$$S_{\alpha_k}^{|H|} = \frac{\alpha_k}{|H|} \cdot \frac{d|H|}{d\alpha_k} \tag{3.16}$$

while the group delay sensitivities are,

$$S_{\alpha_k}^{\tau} = \frac{\alpha_k}{\tau} \cdot \frac{d\tau}{d\alpha_k} \tag{3.17}$$

If the transfer function, H(z), is expressed in its polar form, the gain coefficient sensitivities may be expressed as,

$$S_{\alpha_k}^{|H|} = \alpha_k \cdot \mathrm{Re}\left[\frac{1}{H} \cdot \frac{dH}{d\alpha_k} \right] \tag{3.18}$$

Using Eq.(3.18), equations for the gain coefficient sensitivities of each ladder design procedure can be generated from Eq.(3.3-5).

Source design :

$$S_{s_{\alpha_k}}^{|H|} = \alpha_k \,.\, \mathrm{Re}\left[\frac{-1}{(x_{12} + \beta\ x_{11})} \cdot \left(\frac{d(x_{12})}{d\alpha_k} + \beta\, \frac{d(x_{11})}{d\alpha_k} \right) \right]$$

Load design :

$$S_{L_{\alpha_k}}^{|H|} = \alpha_k \cdot \mathrm{Re}\left[\frac{-1}{(x_{12} - \alpha\ x_{22})} \cdot \left(\frac{d(x_{12})}{d\alpha_k} - \alpha\, \frac{d(x_{22})}{d\alpha_k} \right) \right]$$

Middle design :

$$S_{m_{\alpha_k}}^{|H|} = \alpha_k \cdot \mathrm{Re}\left[\frac{-1}{(x_{12})} \cdot \left(\frac{d(x_{12})}{d\alpha_k} \right) \right]$$

Following the same procedure used for the differential with respect to ω, expressed by Eq.(3.15), then differentiated with respect to the multiplier, α_k, can be written as,

$$\frac{1}{X'} \cdot \frac{dX'}{d\alpha_k} = \sum_{i=1}^{n} \frac{1}{X_i'} \cdot \frac{dX_i'}{d\alpha_k} \tag{3.19}$$

However, the multiplier α_k, will only exist in one element matrix and will be unrelated to any multipliers in another element. Therefore, if the multiplier α_k only exists in the matrix X_m', then the derivatives of the other matrices will be zero and Eq.(3.19) will reduce to,

$$\frac{1}{X'} \cdot \frac{dX'}{d\alpha_k} = \frac{1}{X_m'} \cdot \frac{dX_m'}{d\alpha_k} \tag{3.20}$$

The group delay coefficient sensitivity equation of Eq.(3.17) may be expressed as,

$$S_{\alpha_k}^{\tau} = \frac{\alpha_k}{\tau} \cdot \mathrm{Im}\left[\frac{1}{H} \cdot \frac{dH}{d\alpha_k} \cdot \frac{1}{H} \cdot \frac{d\,H}{d\omega} - \frac{1}{H} \cdot \frac{d\left(\frac{dH}{d\omega}\right)}{d\alpha_k} \right] \tag{3.21}$$

Again, for each of the design procedures the group delay coefficient sensitivities can be derived in terms of the overall chain matrix. Using Eq.(3.21), Eq.(3.3-5) and Eq.(3.9-11), the equations for the group delay coefficient sensitivities can be determined for each of the design procedures.

Source design :

$$S_{s\alpha_k}^{\tau} = \frac{\alpha_k}{\tau} \cdot \operatorname{Im}\left[\frac{1}{(x_{12} + \beta\, x_{11})} \cdot \left(\frac{d\left(\frac{d(x_{12})}{d\omega}\right)}{d\alpha_k} + \beta\, \frac{d\left(\frac{d(x_{11})}{d\omega}\right)}{d\alpha_k} \right) - \frac{1}{(x_{12} + \beta\, x_{11})^2} \cdot \left(\frac{d(x_{12})}{d\alpha_k} + \beta\, \frac{d(x_{11})}{d\alpha_k} \right) \cdot \left(\frac{d(x_{12})}{d\omega} + \beta\, \frac{d(x_{11})}{d\omega} \right) \right]$$

Load design :

$$S_{L\alpha_k}^{\tau} = \frac{\alpha_k}{\tau} \cdot \operatorname{Im}\left[\frac{1}{(x_{12} - \alpha\, x_{22})} \cdot \left(\frac{d\left(\frac{d(x_{12})}{d\omega}\right)}{d\alpha_k} - \alpha\, \frac{d\left(\frac{d(x_{22})}{d\omega}\right)}{d\alpha_k} \right) - \frac{1}{(x_{12} - \alpha\, x_{22})^2} \cdot \left(\frac{d(x_{12})}{d\alpha_k} - \alpha\, \frac{d(x_{22})}{d\alpha_k} \right) \cdot \left(\frac{d(x_{12})}{d\omega} - \alpha\, \frac{d(x_{22})}{d\omega} \right) \right]$$

Middle design :

$$S_{m\alpha_k}^{\tau} = \frac{\alpha_k}{\tau} \cdot \operatorname{Im}\left[\frac{1}{(x_{12})} \cdot \left(\frac{d\left(\frac{d(x_{12})}{d\omega}\right)}{d\alpha_k} \right) - \frac{1}{(x_{12})^2} \cdot \left(\frac{d(x_{12})}{d\alpha_k} \right) \cdot \left(\frac{d(x_{12})}{d\omega} \right) \right]$$

The derivatives of an overall chain matrix, $\mathbf{X}'$, with respect to ω and then a multiplier α_k, can be expressed as,

$$\frac{1}{\mathbf{X}'} \cdot \frac{d\left(\frac{d\mathbf{X}'}{d\omega}\right)}{d\alpha_k} = \frac{1}{\mathbf{X}'_m} \cdot \left[\frac{d\left(\frac{d\mathbf{X}'_m}{d\omega}\right)}{d\alpha_k} - \frac{d\mathbf{X}'_m}{d\alpha_k} \cdot \left(\frac{1}{\mathbf{X}'_m} \cdot \frac{d\mathbf{X}'_m}{d\omega} - \sum_{i=1}^{n} \frac{1}{\mathbf{X}'_i} \cdot \frac{d\mathbf{X}'_i}{d\omega} \right) \right]$$

where α_k only exist in $\mathbf{X}'_m$ and n is the number of elements in the ladder structure.

3.2.3 Building Blocks

Digital circuits that model equivalent analogue components can be considered as building block with which a ladder WDF can be constructed. Following the design methods proposed by Lawson, these building blocks would be two-port sections that model various analogue elements. For general ladder WDF designs, the only elements that are required are the basic lumped components of the inductor and capacitor and a distributed component based upon a section of transmission line, also known as a unit element. Using these lumped and distributed components, seven primitive building blocks can be designed to cover most filter requirements.

These primitives are :-

(i) Series Elements : (a) inductor.
(b) capacitor.
(c) tuned LC circuit.

(ii) Parallel Elements : (a) inductor.
(b) capacitor.
(c) tuned LC circuit.

(iii) Unit Element.

Using the generalised WDF design technique suggested by Lawson, a wave chain matrix of an analogue component can be derived from its voltage and current chain matrix, **C**, and a set of transformations defined by **P** and **Q**. The equation to produce the wave chain matrix is given by Eq.(3.22).

$$\begin{bmatrix} A_1 \\ B_1 \end{bmatrix} = [P] \cdot [C] \cdot [Q]^{-1} \cdot \begin{bmatrix} A_2 \\ B_2 \end{bmatrix} \qquad (3.22)$$

The two-port series lumped element of impedance, Z_s, shown by Fig.(3.14), it well known in two-port theory[1] and has a voltage and current chain matrix, C_s, given by Eq.(3.23).

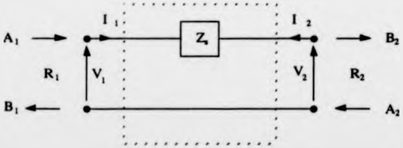

Figure 3.14 General series two-port element of impedance Z_s.

$$\begin{bmatrix} V_1 \\ I_1 \end{bmatrix} = [C_s] \cdot \begin{bmatrix} V_2 \\ I_2 \end{bmatrix} \tag{3.23}$$

where

$$C_s = \begin{bmatrix} 1 & -Z_s \\ 0 & -1 \end{bmatrix}$$

If the matrices **P** and **Q** are the voltage wave transformations, then

$$\mathbf{P} = \begin{bmatrix} 1 & R_1 \\ 1 & -R_1 \end{bmatrix} \qquad \mathbf{Q} = \begin{bmatrix} 1 & R_2 \\ 1 & -R_2 \end{bmatrix} \tag{3.24}$$

and the wave chain matrix of a series impedance, Z_s, using Eq.(3.22-24) is given by

$$\begin{bmatrix} A_1 \\ \\ B_1 \end{bmatrix} = \begin{bmatrix} \dfrac{R_2 - R_1 - Z_s}{2R_2} & \dfrac{R_2 + R_1 + Z_s}{2R_2} \\ \dfrac{R_2 + R_1 - Z_s}{2R_2} & \dfrac{R_2 - R_1 + Z_s}{2R_2} \end{bmatrix} \cdot \begin{bmatrix} A_2 \\ \\ B_2 \end{bmatrix} \tag{3.25}$$

Applying these ideas to the parallel lumped element of Fig.(3.15), which has a voltage/current chain matrix, C_p, given by Eq.(3.26), then the wave chain matrix for this element is given by Eq.(3.27).

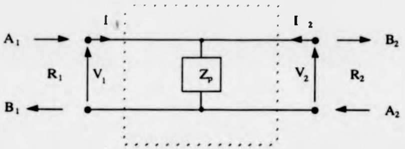

Figure 3.15 General parallel two-port element of impedance Z_p.

$$\begin{bmatrix} V_1 \\ I_1 \end{bmatrix} = [C_p] \cdot \begin{bmatrix} V_2 \\ I_2 \end{bmatrix} \tag{3.26}$$

where

$$C_p = \begin{bmatrix} 1 & 0 \\ 1/Z_p & -1 \end{bmatrix}$$

$$\begin{bmatrix} A_1 \\ \\ B_1 \end{bmatrix} = \begin{bmatrix} \dfrac{R_2 - R_1 + (R_1 R_2/Z_p)}{2R_2} & \dfrac{R_2 + R_1 + (R_1 R_2/Z_p)}{2R_2} \\ \dfrac{R_2 + R_1 - (R_1 R_2/Z_p)}{2R_2} & \dfrac{R_2 - R_1 - (R_1 R_2/Z_p)}{2R_2} \end{bmatrix} \cdot \begin{bmatrix} A_2 \\ \\ B_2 \end{bmatrix} \tag{3.27}$$

The lumped impedances Z_s and Z_p are functions of the continuous frequency variable, s. To convert s-domain chain matrices into the z-domain, the bilinear transform is used. If the series impedance, Z_s, represents a capacitor, C, then

$$Z_s = \frac{1}{s\,C} \tag{3.28}$$

Combining Eq.(3.25), Eq.(3.28) and the bilinear transform, then the chain matrix of a series capacitor can be expressed as,

$$\begin{bmatrix} A_1 \\ \\ B_1 \end{bmatrix} = \begin{bmatrix} \dfrac{\beta_2 - (1 - \beta_1 + \beta_2)\, z^{-1}}{(1 + \beta_2)(1 - z^{-1})} & \dfrac{1 - \beta_1\, z^{-1}}{(1 + \beta_2)(1 - z^{-1})} \\ \\ \dfrac{\beta_1 - z^{-1}}{(1 + \beta_2)(1 - z^{-1})} & \dfrac{(1 - \beta_1 + \beta_2) - \beta_2\, z^{-1}}{(1 + \beta_2)(1 - z^{-1})} \end{bmatrix} \cdot \begin{bmatrix} A_2 \\ \\ B_2 \end{bmatrix} \tag{3.29}$$

with

$$\beta_1 = \frac{R_2 + R_1 - 1/C'}{R_2 + R_1 + 1/C'} \quad \text{and} \quad \beta_2 = \frac{R_2 - R_1 - 1/C'}{R_2 + R_1 + 1/C'} \quad \text{and} \quad C' = \frac{2\,C}{T}$$

If the scattering matrix of the series capacitor is σ, then delay free loops can be eliminated if constant terms from σ_{11} or σ_{22} are removed. The scattering matrix, σ, of a series capacitor element generated from the chain matrix of Eq.(3.29), is given by Eq.(3.30).

$$\begin{bmatrix} B_x \\ \\ B_y \end{bmatrix} = \begin{bmatrix} \dfrac{(1 - \beta_1 + \beta_2) - \beta_2\, z^{-1}}{(1 - \beta_1\, z^{-1})} & \dfrac{(\beta_1 - \beta_2)(1 - z^{-1})}{(1 - \beta_1\, z^{-1})} \\ \\ \dfrac{(1 + \beta_2)(1 - z^{-1})}{(1 - \beta_1\, z^{-1})} & -\left(\dfrac{\beta_2 - (1 - \beta_1 + \beta_2)\, z^{-1}}{(1 - \beta_1\, z^{-1})}\right) \end{bmatrix} \cdot \begin{bmatrix} A_x \\ \\ A_y \end{bmatrix} \tag{3.30}$$

with

$$\beta_1 = \frac{R_2 + R_1 - 1/C'}{R_2 + R_1 + 1/C'} \quad \text{and} \quad \beta_2 = \frac{R_2 - R_1 - 1/C'}{R_2 + R_1 + 1/C'} \quad \text{and} \quad C' = \frac{2\,C}{T}$$

The chain matrix of Eq.(3.29) relates to the middle design approach. For this design technique, constant terms exist in both the σ_{11} and σ_{22} elements of its scattering matrix. Delay free loops are eliminated by ensuring that the appropriate constant terms of connected elements are removed.

To use a series capacitor within a circuit generated through the source design procedure, its chain matrix of Eq.(3.29) must be modified so that constant terms in the σ_{22} element of its scattering matrix, given by Eq.(3.30) are removed. Referring to the scattering matrix of Eq.(3.30), the constant term in the σ_{22} element can be removed if $\beta_2 \Rightarrow 0$. For $\beta_2 = 0$, then

$$R_2 - R_1 - \frac{1}{C'} = 0 \tag{3.31}$$

Through the condition $\beta_2 = 0$, the two port resistances, previously independent, are now related to each other by the Eq.(3.31). The value of C is defined by the reference circuit and using the source design approach, the input port resistance is determined by the previous section. Therefore, the only free parameter is R_2. Expressing Eq.(3.31) in terms of R_2 and substituting it into Eq.(3.29), the source design chain matrix for a series capacitor is shown by Eq.(3.32).

$$\begin{bmatrix} A_1 \\ \\ B_1 \end{bmatrix} = \begin{bmatrix} -\left(\frac{(1-\beta_3)\, z^{-1}}{1 - z^{-1}}\right) & \frac{1 - \beta_3\, z^{-1}}{1 - z^{-1}} \\ \frac{\beta_3 - z^{-1}}{1 - z^{-1}} & \frac{1 - \beta_3}{1 - z^{-1}} \end{bmatrix} \cdot \begin{bmatrix} A_2 \\ \\ B_2 \end{bmatrix} \tag{3.32}$$

where

$$\beta_3 = \frac{C'\, R_1}{1 + C'\, R_1} \quad \text{and} \quad R_2 = R_1 + \frac{1}{C'}$$

Although the design process reduces the complexity of the section, from Eq.(3.29) to Eq.(3.32), the port resistance values are made dependent upon each other. Under the source design procedure, the value of the input port resistance of the first section is set equal to the source resistor of the reference circuit. A dependence between the input and output port resistances, similar to Eq.(3.31), determines the value of the output resistance and consequently the input port resistance value of the next section.

The load design procedure uses elements that have the constant terms removed from the σ_{11} elements of their scattering matrices. Applying this rule to the series capacitor scattering matrix of Eq.(3.30), requires that $1 + \beta_1 - \beta_2 \Rightarrow 0$. In order to allow this condition then $1 + \beta_1 - \beta_2 = 0$ and therefore

$$R_1 - R_2 - \frac{1}{C'} = 0 \tag{3.33}$$

For the load design procedure, the only free parameter in Eq.(3.33), is R_1. Rearranging Eq(3.33) in terms of R_1 and substituting it into Eq.(3.29), results in the chain matrix for a series capacitor, Eq.(3.34).

$$\begin{bmatrix} A_1 \\ \\ B_1 \end{bmatrix} = \begin{bmatrix} -\left(\frac{1 - \beta_4}{\beta_4 (1 - z^{-1})}\right) & \frac{1 - \beta_4 z^{-1}}{\beta_4 (1 - z^{-1})} \\ \frac{\beta_4 - z^{-1}}{\beta_4 (1 - z^{-1})} & \frac{(1 - \beta_4) z^{-1}}{\beta_4 (1 - z^{-1})} \end{bmatrix} \cdot \begin{bmatrix} A_2 \\ \\ B_2 \end{bmatrix} \qquad (3.34)$$

where

$$\beta_4 = \frac{C' R_2}{1 + C' R_2} \quad \text{and} \quad R_1 = R_2 + \frac{1}{C'}$$

Again the complexity of the chain matrix is reduced but the port resistances are made dependent upon each other. With the load design procedure, the value of the output port resistance of the last section is set equal to the load resistor of the reference circuit. Using equations similar to Eq.(3.33), the input port resistance value of a section may be determined to remove any delay free paths and passed back to the output port resistance of the previous section.

To evaluate the overall system equations the derivatives of the chain matrix for each component are required. The derivatives required are with respect to the frequency, ω, the section's multipliers and the double derivative of the chain matrices with respect to the frequency and then the section's multipliers.

The chain matrices for each of the six lumped elements considered, calculated for each of the three design procedures, are detailed in Appendix A1-A6. Included in these equations are the matrices required to calculate the group delay and the coefficient sensitivities for gain and group delay responses. The unit element chain matrix is derived from the equations describing the commensurate transmission lines[2] with characteristic impedance, Z_0. The equations for this section are illustrated in Appendix A7. Appendix A8 provides design examples using lumped component filters for each of the three design techniques discussed.

3.3 WAVE : two-port WDF design program

This is a menu driven program written in C upon a UNIX based Sun Workstation, which uses the GHOST[7] routines to generate a graphical output and the NAG[10] routines to provide the optimization algorithms. The program is based upon the two-port approach to WDF designs. It is capable of simulating and analysing a ladder or lattice structure using the two-port building blocks illustrated in Appendix A1-7.

The operation of the program may be divided into the three areas of design, analysis and coefficient generation. The first area concerns the generation and storage of filter designs in data files. These designs may have a ladder or lattice structure and through the program the user may alter the type and value of the elements within these structures. The filter designs are constructed as cascaded two-port sections. As each building block is added, the modelled component value is recorded, along with its position in the chain. For a lattice filter there are two branches, terminated by an open or short circuit, and therefore two cascaded two-port circuits. Modification of these structures can be approached by alteration of the position or type of the two-port section, or the modelled component values.

Design of a highpass or bandpass filters is achieved with an appropriate selection and combination of elements within a structure. The theory and design of filter structures to achieve various frequency transformations is covered in standard analogue design books[15]. The main principle of a lowpass to highpass or bandpass to bandstop frequency transformation is to replace a capacitor with an inductor and vice versa. The objective of a lowpass to bandpass frequency transformation is to increase the degrees of freedom of an element by converting it into a tuned circuit. These procedures are illustrated in Fig.(3.16), where the lowpass structure of Fig.(3.16)(a) has an equivalent highpass circuit given by Fig.(3.16)(b) and an equivalent bandpass structure illustrated by Fig.(3.16)(c).

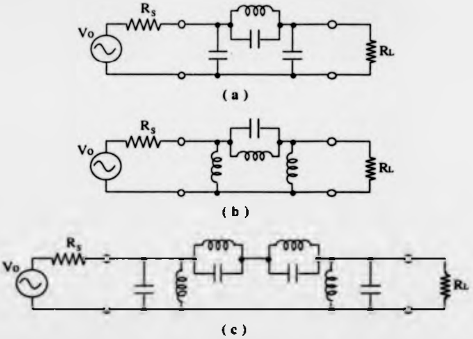

(a)

(b)

(c)

Figure 3.16 (a) Lowpass ladder structure with (b) equivalent highpass and (c) bandpass circuits.

The design of single bandstop and dual band structures can be approached using similar ideas.

Having completed the design of a reference DTL network, the digital multipliers for the structure can be calculated. This calculation may follow one of the three design techniques outlined in the previous section. Each process selects the appropriate elements' chain matrices and multiplier equations for that design procedure. The final step of the design process is to enter the frequency response specification for the filter. This specification may cover lowpass, highpass, single and dual bandpass and bandstop filter types. Having selected a filter response type, cut-off frequencies are entered for both magnitude and group delay specifications. The magnitude tolerances are entered as limits in dBs over the passband(s) and stopband(s), while the group delay is specified as a maximum deviation only over the passband(s). All of this information about the structure, filter specification and its parameter values can then be saved to a data file for subsequent use. This information can also be displayed in a textual form and printed.

The analysis side of the program is responsible for calculation of the various frequency responses of the ladder and lattice structures. The program calculates each response at 1024 points. This number produces a high degree of resolution within each response and allows the FFT to be used to generate a time domain response if required. Using an old or new data file, a menu within the program allows the user to specify the frequency range required. The program will then calculate the gain, magnitude, phase and group delay responses at 1024 points over the specified frequency region. Another menu provides for the calculation of the gain coefficient sensitivities, again allowing the frequency range to be specified. The sensitivity response for each multiplier coefficient can then be displayed individually or as a set.

Each of these responses is displayed on the screen through the use of a GHOST routine. Users have the option to record these graphs for later output to a printer.

The final area of the program is the coefficient generation. This process is approached through the use of optimization and the ideas discussed in Chapter 2. The main elements within this part of the program are the optimization algorithms and the error function with its target templates. The optimization process is based upon the error function discussed in Chapter 2, using a weighted L_p-metric. The error function implemented in the program is given by Eq.(3.35).

$$\text{Error} = \beta \left[\sum_{i=1}^{n} \left(W_i^g \, |\hat{G}_i - G_i| \right)^p \right]^{\frac{1}{p}} + (1 - \beta) \left[\sum_{i=1}^{m} \left(W_i^d \, |\hat{D}_i - D_i| \right)^p \right]^{\frac{1}{p}} \quad (3.35)$$

where β is a factor $0 \leq \beta \leq 1$

n	points in gain response	m	points in delay response
W^g	gain weight vector	W^d	delay weight vector
$\hat{G}$	ideal gain target vector	$\hat{D}$	ideal delay target vector
G	actual gain vector	D	actual delay vector

The program has a menu devoted to defining various parameters within this error function, the target templates and possible optimization routines. The target templates are generated as a pair of vectors that describe the gain and group delay responses. The filter's magnitude response is described in terms of its gain as this limits the response to the range 1 and 0 which in turn simplifies the design of the template. The phase linearity requirement is specified in terms of a constant group delay because the phase response is a discontinuous signal varying between $-\pi$ and π. Using the group delay response also allows a simplification of the target templates. Each element within the target template vectors contains a frequency value, a target response value and a weighting. The target values themselves can be based upon a straight line approximation using a single line to specify the mean value required or two lines to define the limits of an acceptable response. An alternative to the straight line approximation is to specify the actual response required at each particular frequency. This would represent an "ideal" template situation, where the magnitude response would be based upon an elliptic or Chebyshev type function and the group delay would be based on some equiripple shape.

The final area of consideration within the target template definitions, are the transition band(s). If the concept of ideal target values is used, then the transition band(s) will be directly determined by the desired magnitude response. However, if straight line approximations are used, then a number of options exist about how the transition band should be specified. Fig.(3.17) illustrates a number of possibilities for both single and dual line template definitions.

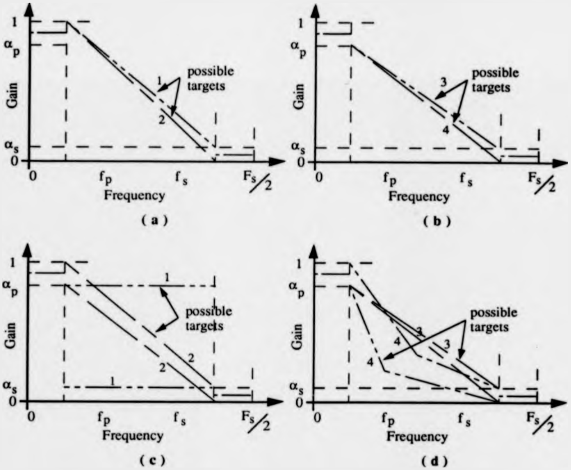

Figure 3.17 Lowpass transition band targets for (a)-(b) single line templates and (c)-(d) dual line templates.

The number and position of the elements within the target vectors can be altered directly through a program menu, along with the weighting factors for each frequency region. The value of the ratio that determines the contribution of the gain and group delay errors to the overall error may also be directly set through the program. Using this parameter, the optimization routines can be applied to gain only, group delay only or simultaneous gain and group delay design problems.

The program offers a number of optimization routines, although their suitability to a filter design problem will depend upon the type of target definitions used. The optimization routines implemented in this program are quasi-Newton functions that can operate with or without derivatives and with simple bounds upon the coefficient values. The routines EO4JAF and EO4KCF are linked from the NAG library. The optimization routine EO4JAF does not require derivatives while EO4KCF expects continuous first order derivatives which makes it unsuitable for designs specified using dual line target templates.

3.4 Experimental Results

The objective of the experimental part of the research was to determine the performance of the ladder WDF for simultaneous magnitude and phase specification and various optimization strategies. The initial area of this work was concerned with testing the optimization techniques against problems with known solutions. This involved designs of magnitude-only specifications, where the phase linearity was ignored. Using information gained about the optimization strategies, the design examples were expanded to include phase linearity.

3.4.1 Magnitude-only design

The magnitude-only filter design tests were based upon a suite of lowpass specifications. These specifications were chosen to include a wide variation of attenuations, cut-off frequencies and filter orders. The equivalent ladder WDF for each specification was constructed through both the source and load design techniques. The example specifications, which are just satisfied by an elliptic function, are given by Table(3.1). Data files for each specification of Table(3.1) were generated using values from the appropriate reference table entries[15].

The optimization techniques discussed in Chapter 2 were implemented within the computer program and applied to the various specifications of Table(3.1). The first optimization strategy to be investigated was the template structures. Three basic template types were tried, the single and dual straight line approximations and the ideal line templates. The error function was based upon measuring the difference between the actual and ideal values of the magnitude responses at certain frequencies. The number and distribution of the points at which the response was measured was also an optimization parameter and will be discussed later in this section. Because the error function only requires the magnitude response at certain frequencies, the target templates need only to be defined at these points.

Spec number	filter order	passband att (dB)	stopband att (dB)	passband freq (Hz)	stopband freq (Hz)	sampling freq (Hz)
1	3	0.2	30	0.1	0.2	1
2	5	0.01	70	0.1	0.26	1
3	5	0.01	50	0.2	0.32	1
4	5	0.1	100	0.15	0.39	1
5	7	0.002	60	0.05	0.08	1
6	7	0.05	90	0.3	0.39	1
7	7	0.0005	40	0.1	0.13	1

Table 3.1 Lowpass filter specification examples.

The straight line templates were generated from the filter specification where each frequency point in the same filter band, would have identical template values. The ideal line template was produced by calculating the magnitude response of a filter that had component values taken from tables, recording it at the required frequency points and then using these values as the ideal line template.

For an equal number of frequency points, with a linear spacing, a typical set of passband template values for the single line, dual line and ideal line approaches are shown by Fig.(3.18).

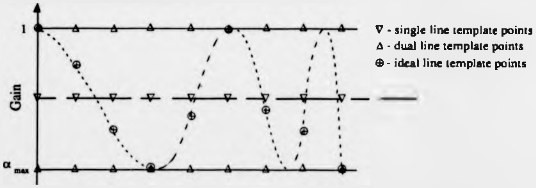

Figure 3.18 Typical passband template values for the three template approaches.

The ideal line template provides the greatest amount of control over the final solution. The final magnitude response can be directed toward an equiripple Chebyshev/elliptic shape or a monotonic Butterworth type shape. The dual line templates provide slightly more control than the single line templates, as the response can be encouraged to exist with a specific tolerance region. However, it is not as versatile as the ideal line scheme, as it cannot define the required shape of the response, only its limits.

For the design examples considered, the specification can only just be met by an elliptic function of the given order and therefore, the elliptic function represents a goal for the optimization process. The basic quasi-Newton optimization routine E04JAF was applied to a number of filter specifications of Table(3.1) using each of the template types. An elliptic function with the reference table component values represents a global solution for a particular problem and therefore template schemes that most closely described that function should cause the quickest convergence.

To demonstrate this hypothesis, the filter's parameters were optimized under each template type and the convergence rates, using the same optimization algorithm, compared. The initial position for the filter's parameter values was varied, starting with the goal solution values, then varying each parameter individually about its viable limits and finally varying the parameters as sets, moving them from their lower bound values to their upper limit. For the ladder WDF multiplier values these bounds are $-1 < x < 1$, while for the component of the reference DTL network, the bounds are $0 < y < \infty$.

In all filter specifications tried the optimization procedure based upon the ideal line templates always converged to the solution and invariably managed to do so with a number of iterations less than 200 times the order of the filter. Under the straight line template systems, the dual line scheme converged more frequently than the single line scheme. Convergence, however, was very slow and some times failed to reduce the error to an acceptable value. This may have been due to the optimization routine being stuck in a local minimum because of a poor set of weights or frequency points. It was noticed that using the straight line schemes, if a multiplier value was started or was moved to a boundary value it tended to remain there. This resulted in a non-optimum solution.

An additional factor that seemed to limit the convergence of examples based upon the straight line templates, was how the transition band was specified. The previous section has already mentioned a number of possible schemes for both the single and dual line template systems. The effect on convergence of a wide variety of transition band schemes was compared for a number of filter specifications using identical weightings and error points. Schemes that proved to be the most successful where those that encouraged a sharper cut-off rate than a direct line between the passband edge and stopband edge. This was especially true for filter specification that had wide transition bands. These sharp cut-off schemes were constructed from two 'hinged' lines. Examples of this type of line for the two straight line template schemes are shown in Fig.(3.19).

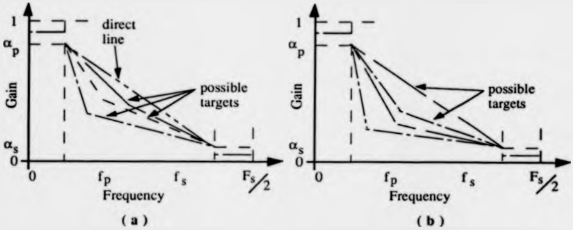

Figure 3.19 Examples of transition band specifications for (a) single and (b) dual line templates.

Because of the nature of the dual line template system, the overall error can become zero if the response lies within the region defined by the template. Using this fact the position of the transition band templates, shown by Fig.(3.19), can be determined by applying the ideal response to the template. When the initial error function is zero then the transition band targets have the correct settings. When the optimization routine is applied to an error function based upon dual line templates set up this way, the convergence rate was much quicker than using alternative transition band schemes. The performance of the optimization routine using the hinged single line transition band targets of Fig.(3.19)(a) was also greater than other straight line possibilities.

In all transition band target schemes of Fig.(3.19), the lines are defined from the lower passband tolerance edge to the upper stopband tolerance edge. The targets are constructed in this way to ensure that the overall transition band width is not narrower than the specification and the template most closely reflect the ideal solution.

Having determined the best type of shaped transition band targets, the effects of the number and position of the error frequency points were investigated. As mentioned in Section 3.1.2, the number and distribution of the error points can be arbitrary but usually follow some analytical formulae. These formulae are structured so that it groups the error points around a transition edge of the filter's specification. From Fig.(3.5), it can be seen that a sine function congregates points to its right hand end, while the cosine function groups points about its left hand end. If points are specified in the transition band, then under what distribution should they be arranged. The effects of different distribution upon the convergence rate of an optimization routine are difficult to quantify, but the linear or double cosine functions appear to be the most appropriate.

More important than the distribution of the error points, is their actual number. An obvious initial rule would be to use an equal number of points in each band of the specification. The total number of points presents a compromise between the accuracy with which the response is measured and the time taken to generate the error function at each iteration. From a large number of tests this compromise settled into a range of 15 - 40 error points per band. Tests in which no error points were specified in the transition band tended not to converge to an acceptable solution when the transition band was wide compared to the passband width and using straight line templates.

The next optimization parameter to be considered for the magnitude-only design involved the error function weights and how they should be defined. A number of possibilities exist, from defining an individual weight for each error point, using the same weight for a specification band, to equal weights for every error point. Each error point can also be associated with an upper and lower weight, so that if the difference between the actual and target responses is positive then one weight value is applied and another if the difference is negative.

For ideal line templates the error at a particular point has an equal significance whether it is positive or negative and whether it is in the pass, stop or transition band. For a problem defined using the ideal line template system, the most appropriate weighting scheme uses an equal weight value for each error point. However, under this template system, weights have a limited affect on the convergence rate of the optimization routine due to the efficiency of the template system itself.

For the straight line templates, the weights play a vital role in ensuring that the filter response meets the specification. This is especially true for the stopband performance when the templates are defined in terms of gain. Here a percentage deviation of the actual response from the targets in the stopband has a lower value than the same percentage deviation in the passband. Therefore, if no weights are used, the error due to the passband will contribute disproportionately to the overall error function. This results in filter responses that have a poor stopband performance, especially when single line templates are used. A weighting scheme that would provide the best results is one that ensures that a percentage deviation in each band generates the same error. Using this rule, if a lowpass filter has a passband width of 0.1 (approximately 1 dB) and a stopband width of 0.001 (approximately 40 dB), then the weight ratio of passband to stopband should be 1:100.

The final parameter within the error function implemented, is the L_p-metric that is calculated. The range of possible value for p is $1 \leq p \leq \infty$. A general error function was written into the computer program, allowing any integer value of p to be used. A special function was included to determine the L_∞-metric situation. A wide variation of values for p was investigated on a number of lowpass filter specifications under a dual line template system using the weighting rule outlined earlier. For most tests the examples using high p values failed to converge, while lower values, especially $p = 2$, proved to be the most successful.

The last variable to be tested within the optimization process was the optimization algorithms themselves. Using the derivatives generated to determine the coefficient sensitivities for the ladder structure, the Jacobian matrix can be calculated. With this information, algorithms that require derivative could be applied to the problem, such as E04KCF from the NAG library. This algorithm is a quasi-Newton function similar to E04JAF. Quasi-Newton algorithms were chosen because of the quicker speed of operation than Newton type methods and a higher stability and accuracy than conjugate-gradient based algorithms.

Applying E04KCF to a number of lowpass specifications with error functions based upon L_2-metrics and the three template types, a number of properties became apparent. One of the main feature was its inability to work with the discontinuous derivatives of the dual line templates. The other main feature was the time taken to converge compared to the simple E04JAF algorithms which does not require derivatives. In most cases for problems based upon the ideal line templates, although the algorithm converged in fewer iterations, the overall time taken to solve the problem was about the same, especially for higher order structures. This may be due to the efficiency of the ideal line template scheme. This type of algorithm could not be applied to the dual line template system and although the performance of the single line scheme improved, the actual solutions produced using this template system were always poor.

The experience and knowledge gained of the optimization routines through the magnitude only design of the filter specifications of Table(3.1), was extended to higher order filters. This however highlighted an advantage of the dual line system over the ideal line template scheme. The ideal line scheme requires the target optimization parameters to generate the template targets. Therefore when design tables do not include the desired passband attenuations or filter order, then the ideal line templates cannot be used. The main part of the experimentation was based upon 13th and 15th order structures using the dual line template scheme with the E04JAF optimization routine. These tests confirmed earlier observations about the selection of weighting schemes and the number and distribution of error points.

3.4.2 Simultaneous designs

This area of the experimental work forms the heart of the two-port ladder WDF research. No previous work had been published about the design of simultaneous magnitude and phase ladder WDF's based purely upon lumped elements. This initial part of this research was to construct ladder WDF's from DTL reference networks that are known to possess low coefficient sensitivity and high frequency selectivity. Using these filters and the optimization techniques developed for the magnitude only designs, the simultaneous specifications were addressed. The goal of the research was to produce a set of guidelines for both the optimization techniques involved and the filter order required for a given simultaneous specification.

The design approach adopted involved selecting one of the lowpass filter specifications of Table(3.1), constructing the appropriate target templates and then introducing a wide group delay tolerance. The filter's parameters were then optimized, starting from different initial values, until a solution was found. If no solution could be found, then the overall filter order would be increased and the process repeated.

The error function variables were set based upon the knowledge gained from the magnitude only designs. Each of the target template types was also applied to the problem. For the ideal line templates, the magnitude template was determined from a filter satisfying the magnitude only specification, while the group delay template was constructed from a raised sine function. The amplitude and number of cycles of the sine function over the width of the template was determined from the specification. The amplitude of the function was defined by the group delay tolerance, as a percentage of the mean group delay value, while the number of cycles of the function was the overall order of the filter minus the order required to meet the magnitude specification. The straight line templates were constructed from the filter specification and based upon the ideas illustrated in Fig.(3.4) and Fig.(3.18).

Following the idea suggested by Lightner[9], the number of optimization parameters was increased for the simultaneous designs to include the group delay value about which the template was defined. With filter designs, the actual value of the group delay is not too important only that its value is not too large. Using this mean group delay value as an optimization parameter, the group delay tolerance template can be moved up or down to reduce the error function.

The ratio factor, β, of the error function given in Eq.(3.35), which determines the contributions of the gain and group delay errors to the overall error, are the only variable not considered so far. The valid range of values for β is $0 \leq \beta \leq 1$. The condition $\beta = 0$ relates to a group delay only design, while $\beta = 1$ produces a magnitude-only design. The true effect of β can be masked by the weightings used on the gain and group delay error points. To remove these possible effects, the weighting scheme of the group delay error points should follow that suggested for the gain error points. With this rule a percentage deviation in each band of a template would generate an equal error. Under this scheme, if a lowpass specification has a gain passband width of 0.1, a gain stopband width of 0.001 and a group delay passband width of 0.1 (this is a 1% tolerance at a group delay value of 10 seconds) then the total error is 0.201. The weights for the gain passband, gain stopband and group delay passband would then be 2.01 : 201 : 2.01 or 1 : 100 : 1 respectively. However, because the group delay only contributes an error from one band as opposed to the gain template which has two, or three if the transition band is defined, then the weightings should be adjusted. In the case considered, the new weighting ratio would be 1 : 100 : 2.

Using a weighting scheme that ensures that equal deviations in the gain and group delay templates contribute equal errors to the overall error function, then a β value of 0.5 should balance the two responses. However, the requirements for constant group delay are contrary to sharp changes in the gain response. In this case it is very difficult to obtain constant group delay around the region of the transition band. Therefore if too much emphasis is placed upon the group delay response, then the gain will fail to achieve the required stopband performance and the design solutions will not represent useful filter solutions. For a number of design examples the values of β that caused this effect to occur are around 0.5. In these cases values of β between 0.6 and 0.9 were required to force the optimization routine to approach acceptable simultaneous gain and group delay responses.

The effect of the variation of β can be seen in Fig.(3.20), where the value of β for the same lowpass specification is varied from 0.1 to 0.9. It can be seen that the gain and group delay responses do not form an acceptable filter shape until the value of β is greater than 0.6. Another observation of the filter responses, produced using a number of different optimization settings, is a tendency to place poles within the transition and stopbands of the gain response. This can be seen in Fig.(3.20)(b) and (c).

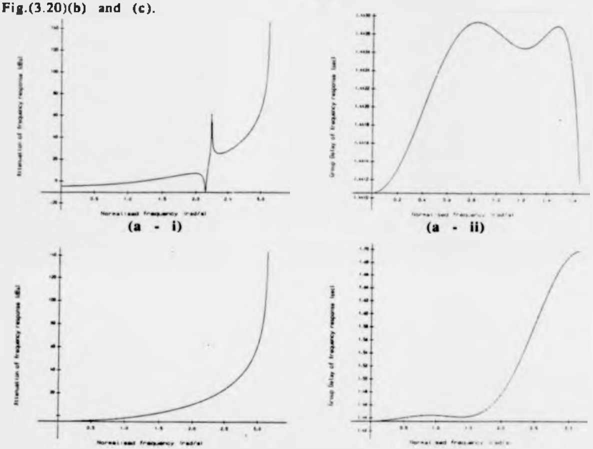

(a - i) (a - ii)

(b - i) (b - ii)

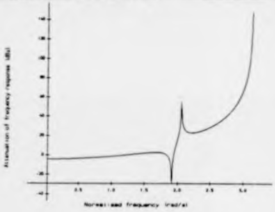

(c - i)

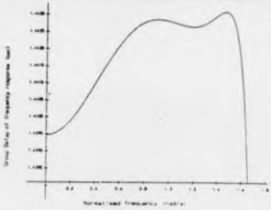

(c - ii)

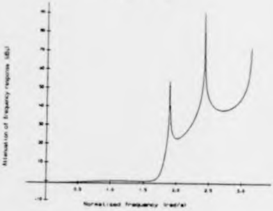

(d - i)

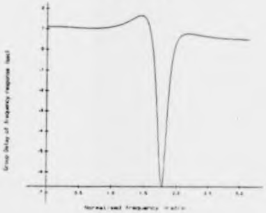

(d - ii)

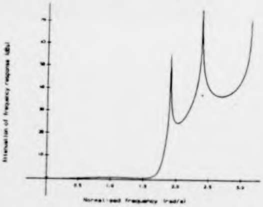

(e - i)

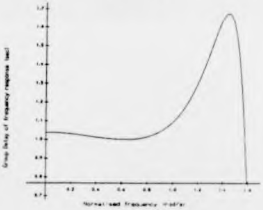

(e - ii)

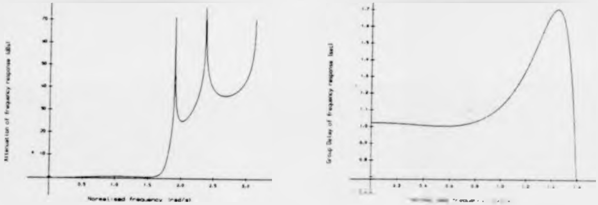

(f - i) (f - ii)

Figure 3.20 Simultaneous design solutions showing (i) gain and (ii) group delay responses for ; (a) $\beta = 0.1$, (b) $\beta = 0.3$, (c) $\beta = 0.5$, (d) $\beta = 0.6$, (e) $\beta = 0.8$, (f) $\beta = 0.9$.

A wide variation of error function parameters was tried for the optimization of a simultaneous magnitude and phase specification. All the tests followed the procedures outlined for the magnitude only designs. However, despite increasing the order of the filter a number of times, the optimization routine failed to find solutions to the given problems. These results tend to support the theory that for minimum-phase structures, the gain and group delay requirements form a reciprocal pair. In this way, a move to improve the gain performance of a filter causes the group delay response to be degraded. All the examples tried indicate that the compromise between the gain and group delay performance is so tight that no simultaneous designs are possible using this structure.

The relationship between the gain and group delay responses can be illustrated by a number of simultaneous design examples. For these filter designs, the value of β was varied to enhance either the gain or group delay side of the specification. The examples shown have the lowpass specifications given in Table(3.2) and solutions for various β values shown by Fig.(3.21), Fig.(3.22) and Fig.(3.23).

Figure number	filter order	passband att (dB)	stopband att (dB)	passband freq (Hz)	stopband freq (Hz)	F_s (Hz)	g. delay dev (%)
3.21	7	1	40	0.1	0.3	1	0.7
3.22	9	1	60	0.1	0.3	1	0.8
3.23	9	1	40	0.1	0.3	1	0.8

Table 3.2 Lowpass gain and group delay specification examples.

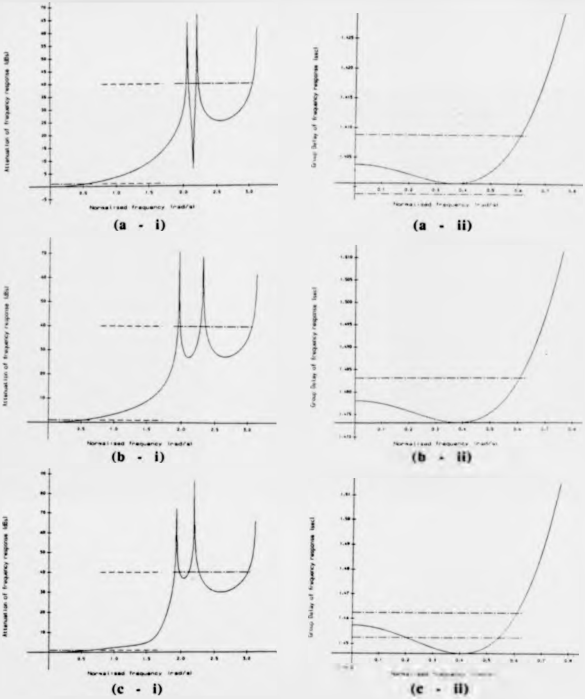

(a - i) (a - ii)

(b - i) (b - ii)

(c - i) (c - ii)

Figure 3.21 Simultaneous design solutions showing (i) gain and (ii) group delay responses for ; (a) $\beta = 0.4$, (b) $\beta = 0.5$, (c) $\beta = 0.6$.

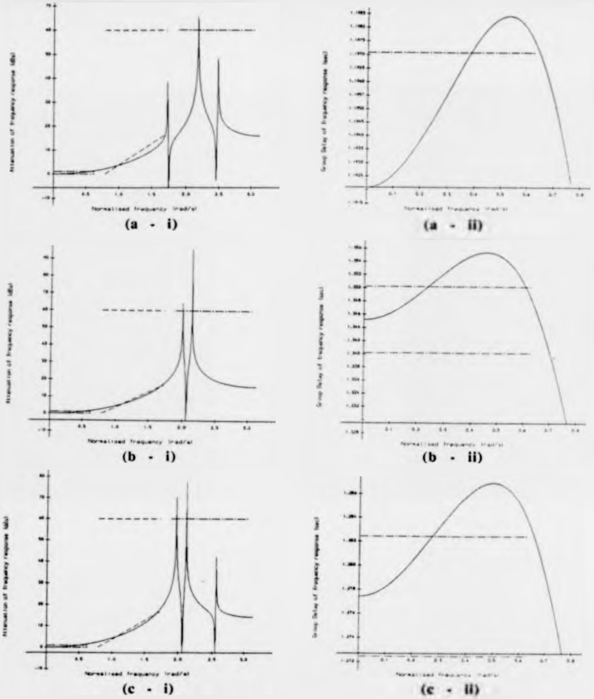

(a - i) (a - ii)

(b - i) (b - ii)

(c - i) (c - ii)

Figure 3.22 Simultaneous design solutions showing (i) gain and (ii) group delay responses for ; (a) $\beta = 0.4$, (b) $\beta = 0.5$, (c) $\beta = 0.6$.

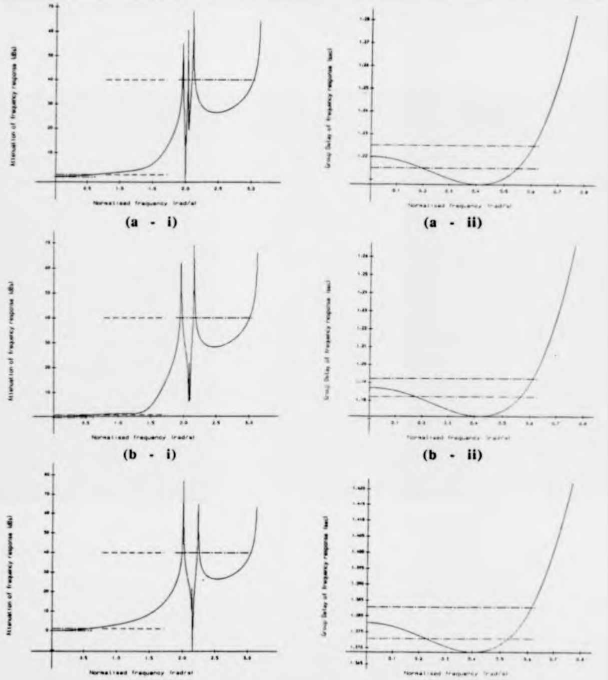

(a - i) (a - ii)

(b - i) (b - ii)

(c - i) (c - ii)

Figure 3.23 Simultaneous design solutions showing (i) gain and (ii) group delay responses for ; (a) $\beta = 0.4$, (b) $\beta = 0.5$, (c) $\beta = 0.6$.

In each of these design examples the optimization used the dual line template scheme, with a total of 56 error points distributed according to the sine/cosine functions. These examples also use a dual weighting scheme so that errors above the top template line and below the bottom template line, were subject to different weights. Each test was performed using the E04JAF routine and the multiplier values were started at their upper boundary conditions.

The compromise between the gain and group delay specifications is best shown by Fig.(3.21). With β = 0.4, the responses of Fig.(3.21)(a) satisfy the group delay template, just fail the gain passband specification but badly violate the gain stopband criteria. As the β value is increased to 0.5, the passband gain and group delay responses, shown by Fig.(3.21)(b), just fails specification, while the gain stopband performance has improved. Finally with β = 0.6, shown in Fig.(3.21)(c), the gain passband response lies within the template, while the gain stopband performance just fails specification. The group delay passband response, however, lies well outside the targets. Although the responses of Fig.(3.21)(b), where β = 0.5, represent the best solution to the problem, none of these solutions actually satisfy the simultaneous specification.

3.5 Two-port design conclusions

The objective of this Chapter has been to detail the design approaches for simultaneous magnitude and phase ladder WDF's. The design approach of using two-port blocks to simulate circuit elements and construct ladder WDF's has been shown to be effective and straight forward. However, a wide variety of optimization tests have shown that a ladder WDF based upon a purely lumped component reference network is incapable of satisfying a simultaneous magnitude and phase specification. This work confirms the idea that minimum-phase structures suffer a tight compromise between their gain and group delay responses. As such, simultaneous ladder WDF designs are very difficult to achieve, if not impossible for severe filter specifications.

Other ladder WDF circuits, based on reference networks using distributed or a mixture of distributed and lumped elements, were also considered. These filters, despite the possibility of selective gain and group delay designs, are limited by poor frequency selectivity. This results in designs requiring a higher filter order to achieve a magnitude specification than ladder WDF's based upon lumped elements only.

Despite the lack of success in designing simultaneous magnitude and phase ladder WDF's, a great deal of practical knowledge was gained in the use of optimization techniques for filter designs. These optimization strategies cover a range of target template schemes, error functions, their parameter settings and the performance of various optimization algorithms.

Of the target templates considered, the ideal line scheme provides the most accurate representation of the desired response and ensures a relatively quick convergence rate for magnitude only designs. The main disadvantage of this template system is the necessity of defining an individual value for each error point of the target. A more convenient template scheme is the dual line system. Although the desired response cannot be modelled as accurately as with the ideal line system, the dual line templates are very easy to construct from a general filter specification. Finally the single line templates proved the least successful target scheme for these filter design problems. Despite their ease of construction, their inability to represent a tolerance region proved to make any filter solutions unsuitable.

A sampling error function based upon a weighted L_p-metric and quasi-Newton optimization algorithms seemed well suited to the design problem. Each parameter of the error function was considered and their most efficient values determined. The weighting scheme followed a rule that an equal deviation in each band of a template generates an equal contribution to the overall error. The error points should number 15 - 40 per band of a template and be distributed under a scheme that clusters points around a transition edge. Finally the value of p used for the L_p-metric in the error function, which proved to be the most successful was around 2.

The results of this Chapter have shown that minimum-phase structures are unsuitable for simultaneous magnitude and phase designs. Although programs written to simulate and design ladder WDF's cannot achieve simultaneous specifications, they can still be used for magnitude-only or group delay only specifications. An alternative would be to investigate nonminimum-phase structures, such as the lattice WDF. Although all the optimization strategies developed could be applied to a lattice structure constructed from two-port elements, this option was not followed. This was for a number of reasons, of which the main one concerned the complexity and variety of element blocks. From hardware design considerations, the preferred filter structure would be constructed from a small number of simple and regular blocks. A lattice WDF can be designed from one-port first and second order allpass sections. These blocks are very simple in structure and are based upon the two-port adaptor developed by Fettweis. Because of the large differences in design approaches and structure requirements, research was turned to a new program devoted to lattice WDF's. The theory and results from this work are outlined in Chapter 4.

References

1) Adby, P. R., *Applied Circuit Theory - Matrix and Computer Methods*, Ellis Horwood, J. Wiley and Sons, New York, 1980.

2) Denton, G. and Carlin, H. J., "Selective, Constant Delay Wave Digital Filters", Int J. Cir. Theory and Applications, Vol 7, 1979, pp171-178.

3) Fettweis, A., "Canonic Realization of Ladder Wave Digital Filters", Int J. Cir. Theory and Applications, Vol 3, 1975, pp321-332.

4) Fettweis, A., "Digital Filter Structures Related to Classical Filter Network", Arch. Elek. Übertrag., Vol 25, 1971, pp79-89.

5) Fettweis, A., "Some Principles of Designing Digital Filters Imitating Classical Filter Structures", IEEE Trans. Circuit Theory, Vol CT-18, No. 1, March 1971, pp314-316.

6) Fettweis, A., "Wave Digital Filters: Theory and Practice", Proc IEEE, Vol 74, No. 2, February 1986, pp270-327.

7) GHOST-80, Graphic routines, UKAEA Culham Laboratory, Oxon 1985.

8) Hyder Ali, M. and Yarlagadda, R., "A note on the Unit Element Synthesis", IEEE Trans. Circuits and Systems, Vol CAS-25, No. 3, March 1978, pp172-174.

9) Lightner, M. R. and Director, S. W., "Multiple Criterion Optimization for the Design of Electronic Circuits", IEEE Trans. Circuits and Systems, Vol CAS-28, No. 3, March 1981, pp169-179.

10) Numerical Algorithms Group, *E04 - Minimizing or Maximizing a Function*, Mark 11, Vol 3, January 1984.

11) Reekie, H. M., Petrie, N., Mavor, J., Denyer, P. B. and Lau, C. H., "Design and Implementation of Digital Wave Filters using Universal Adaptor Structures", Proc. IEE, Vol 131, Pt. F, No. 6, October 1984, pp615-622.

12) Renner, K. and Gupta, S. C., "On the Design of Wave Digital Filters with a Minimal Number of Multipliers", IEEE Trans. Circuit and Systems, Vol CAS-21, No. 1, January 1974, pp137-145.

13) Sedlmeyer, A. and Fettweis, A., "Digital Filters with True Ladder Configuration", Int J. Cir. Theory and Applications, Vol 1, 1973, pp5-10.

14) Thiran, J.-P., "On Unit Element Structures for Wave Digital Filters", IEEE Trans. Circuit and Systems, Vol CAS-24, No. 1, January 1977, pp20-28.

15) Zverev, A. I., *Handbook of Filter Synthesis*, J. Wiley and Sons, New York, 1967.

Chapter 4

Lattice WDF's

This Chapter outlines the design of lattice WDF's and a discussion of their application to simultaneous magnitude and phase specifications. The Chapter starts with a comparison of various lattice WDF structures and a detailed description of a simplified lattice WDF. This lattice structure is constructed from first and second order All Pass Sections(APS's) and the equations for this structure and the APS's are provided. Computer programs written to design and analyse the lattice WDF structure are outlined, along with simultaneous filter designs generated with these programs. The Chapter concludes with a discussion of optimization techniques developed to approach this design problem and the suitability of the lattice WDF for simultaneous filter specifications.

4.1 Design Options

Design of a lattice WDF may be considered within two main areas. The first area entails the form of the lattice structure, its elements and how it is implemented. The other concerns the generation of the multiplier coefficients for a particular lattice structure. Each design area involves a number of options that are discussed within this section.

4.1.1 Lattice WDF structures

The reference structure of a lattice WDF is based upon the symmetric DTL circuit of Fig.(4.1) using canonic impedances, Z_a and Z_b. Canonic impedances can be determined directly from a lattice DTL network or from a symmetric ladder DTL circuit through Bartlett's bisection theorem[5]. Design of a lattice WDF from a symmetric ladder DTL network using this bisection method was illustrated by Fettweis et al.[2].

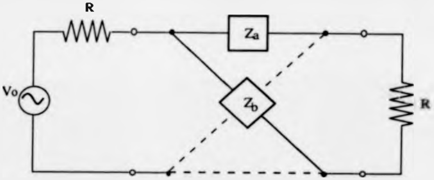

Figure 4.1 Lattice DTL networks with canonic impedances, Z_a and Z_b.

The canonic impedances of the reference lattice circuit of Fig.(4.1) can be modelled in the discrete frequency domain by canonic reflectances, S' and S". The first step of this procedure is to describe the lattice DTL network in terms of its voltage wave scattering matrix and canonic impedances. This scattering matrix is then converted into the discrete frequency domain through the bilinear transform to produce a discrete wave scattering matrix, S. Symmetry of the lattice structure results in $S_{11} = S_{22}$ and $S_{12} = S_{21}$. The canonic reflectances, S' and S", of the lattice WDF can be determined from the scattering matrix, S, using Eq.(4.1) and Eq.(4.2) respectively.

$$S' = S_{11} - S_{12} \tag{4.1}$$

$$S'' = S_{11} + S_{12} \tag{4.2}$$

With the canonic reflectances, a general lattice WDF can be constructed and is illustrated by Fig.(4.2).

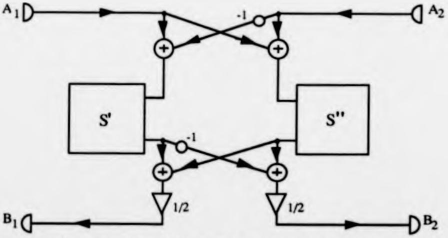

Figure 4.2 General lattice WDF with canonic reflectances, S' and S".

A more usual description of the general lattice WDF of Fig.(4.2) is to set the second input parameter, A_2, to zero and then ignore either B_1 or B_2. The resulting structure is shown by Fig.(4.3), with its two system equations given by Eq.(4.3) and Eq.(4.4).

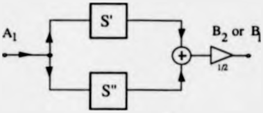

Figure 4.3 Simplified lattice WDF structure.

$$\frac{B_2}{A_1} = \frac{S'' - S'}{2} \tag{4.3}$$

$$\frac{B_1}{A_1} = \frac{S'' + S'}{2} \tag{4.4}$$

The primary design consideration for the lattice structure is the construction of the canonic reflectances, S' and S". These circuits can be implemented using the one- or two-port techniques outlined in Chapter 1. Two-port designs use the ideas and models discussed in Chapter 3, where S' and S" would be constructed as a cascade of two-port elements and terminated by an open or short circuit. The resulting circuits would have a one-port nature and could be implemented as the branches of the lattice WDF structure of Fig.(4.3). An example of a symmetric lattice DTL network is illustrated in Fig.(4.4), along with an equivalent lattice WDF circuit designed through the two-port design approach.

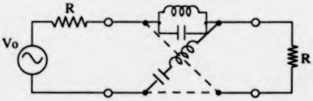

(a)

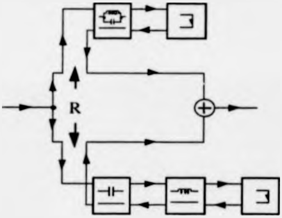

(b)

Figure 4.4 (a) Lattice DTL network with (b) equivalent two-port design lattice WDF circuit.

The main disadvantage of this design approach is the large number of different sections required to model a lattice arm. Following the two-port design techniques of Chapter 3, a lattice arm may involve, typically, two or three of the six primitive lumped building block elements considered. A hardware implementation of this design approach would therefore require physical models for each of the two-port building blocks. This is a large drawback for any VLSI implementation where a circuit should consist of a small number of simple and regular elements.

The one-port lattice design approach follows that applied to general IIR filter designs, where a function is simulated by a cascade of first and second order sections. For the lattice WDF structure, its canonic reflectances would be designed from allpass one-port sections. This design technique is preferred from a VLSI point of view as the overall filter has a regular structure and the APS's are simple elements, making them ideal building blocks.

First and second order APS's may have a number of forms, such as the direct form, a WDF basis or the Mitra-Hirano[10] structures. A comparison of the performance of these APS's was provided by Renfors and Zigouris[12] for roundoff noise, dynamic range and scaling. The conclusions of this work demonstrated that although the WDF structures operated at a lower maximum sampling rate than the direct forms, they had superior roundoff performance for very wide-band and very narrow-band filter specifications and good stability properties.

The WDF APS's are based upon the two-port adaptor developed by Fettweis[1,3]. The two-port adaptor has the symbol illustrated by Fig.(4.5) and a possible circuit diagram shown in Fig.(4.6). The scattering matrix of the two-port adaptor is given by Eq.(4.5).

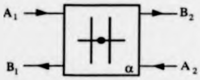

Figure 4.5 Two-port adaptor symbol.

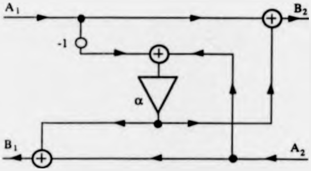

Figure 4.6 Possible circuit diagram for a two-port adaptor.

$$\begin{bmatrix} B_1 \\ B_2 \end{bmatrix} = \begin{bmatrix} -\alpha & 1+\alpha \\ 1-\alpha & \alpha \end{bmatrix} \cdot \begin{bmatrix} A_1 \\ A_2 \end{bmatrix} \qquad -1 < \alpha < 1 \qquad (4.5)$$

Limits for the value of α within the two-port adaptor ensure that the structure is stable and retains the WDF properties of the overall network. The circuit of Fig.(4.6) is not the only interpretation of the scattering matrix of Eq.(4.5). Gazsi[4] investigated a number of different circuits to describe the two-port adaptor against a range of performance criteria, such as dynamic range and scaling for sinusoidal excitation. Conclusions from this work indicated that the optimum selection of a two-port adaptor circuit depended upon the value of the multiplier within that section. Different circuits were developed for multiplier values in the ranges $-1 < \alpha < -1/2$, $-1/2 < \alpha < 0$, $0 < \alpha < 1/2$ and $1/2 < \alpha < 1$.

A first order APS, constructed using the two-port adaptor, is illustrated in Fig.(4.7), while examples of second order APS's are given in Fig.(4.8). Each of these second order sections has the same transfer function under infinite precision calculations and therefore the selection of a particular model as a reference, is arbitrary.

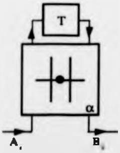

Figure 4.7 First order APS using two-port adaptor.

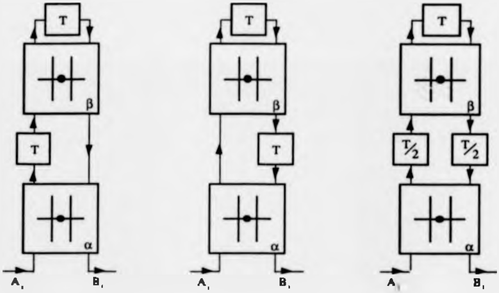

(a) (b) (c)

Figure 4.8 Examples of second order APS's using two-port adaptors.

An implementation of the simplified lattice WDF structure of Fig.(4.3) using the first order APS of Fig.(4.7) and the second order APS of Fig.(4.8)(a), is illustrated in Fig.(4.9). In this structure the position of the single first order section, at the start or end of a lattice arm and in the upper or lower arm, is again arbitrary. Practical hardware designs may however impose scaling problems that require an appropriate ordering of the first and second order APS's dependent upon their multiplier values.

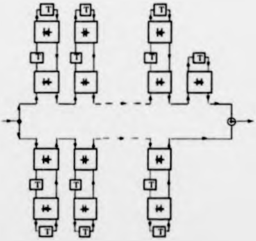

Figure 4.9 Lattice WDF structure using cascaded first and second order APS's.

An alternative structure to that shown by Fig.(4.9), is to replace one of the lattice arms by a pure delay. The value of the delay used would equal the overall delay of the other arm. This structure, shown by Fig.(4.10), was proposed by Kunold[6] for simultaneous magnitude and phase designs. A limitation of this type of lattice WDF circuit is that the degrees of freedom and efficiency of the network have been reduced by using one of the lattice arms as a pure delay. It is therefore less likely to satisfy an arbitrary magnitude and phase specification than the type of circuit shown by Fig.(4.9).

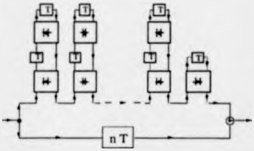

Figure 4.10 Lattice WDF structure with a pure delay arm.

Another possibility is the bireciprocal structure, where the delays within the first and second order sections are doubled. This structure would have the same form as the circuit of Fig.(4.9), but use the first and second order APS's illustrated by Fig.(4.11).

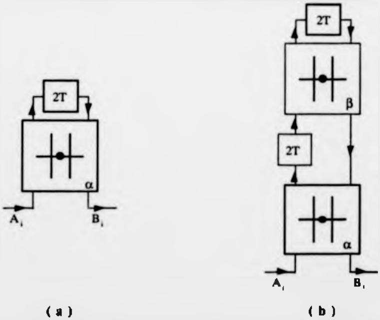

Figure 4.11 Bireciprocal (a) first and (b) second order APS's.

The main feature of this bireciprocal structure is that the magnitude response is constrained to a cut-off frequency of half the sampling frequency. Recent work by Leeb and Henk[7] has shown that through a Remez type optimization algorithm, simultaneous bireciprocal magnitude and linear phase designs are possible using this type of structure. Their work also considered linear phase design with phase equalizers. These equalizer circuits were based upon the lattice WDF of Fig.(4.10) with a pure delay lattice branch. Magnitude and phase designs approached through phase equalization use a separate circuit to satisfy the magnitude response and a lattice structure to ensure the overall network meets the phase requirements. The magnitude circuit may be a lattice WDF itself or a ladder WDF. Equalization techniques, however, require an overall filter order that is higher than that needed for simultaneous designs.

Of the structures considered, the lattice WDF of Fig.(4.9) represents the most efficient network. It is this circuit, therefore, upon which arbitrary simultaneous magnitude and phase designs were initiated. Definition of this structure placed the single first order section, when required, at the end of the upper lattice arm. The form of the second order APS's followed that illustrated by Fig.(4.8)(a) and where arranged so that the overall order of the branches of the lattice did not differ by more than two.

4.1.2 Optimization considerations

The objective of this research was to determine the multiplier coefficients of a WDF structure that satisfied an arbitrary magnitude and phase specification. Following the design ideas discussed in Chapter 2, conclusions suggested optimization for the coefficient generation. Optimization techniques outlined in Chapter 2 and implemented on ladder WDF designs, were based upon target templates and a weighted L_p-metric error function. The target templates were constructed from the filter specification using the gain and/or group delay frequency responses. Because the goal of the optimization process was determined from these templates, the optimization procedure was independent of the filter structure and its elements. These optimization techniques may therefore be applied to both the ladder and lattice WDF structures, as well as other filter types.

With optimization procedures based upon target templates the only elements that are filter dependent are the frequency responses for a given set of multiplier values and the valid range for these multiplier values. To determine a set of coefficients for a lattice WDF through optimization, the frequency response for a given lattice structure must be calculated. The transfer function for the lattice WDF structure illustrated by Fig.(4.9) is detailed in Section 4.2.1, along with equations to determine the group delay response and the coefficient sensitivity functions. The structure of Fig.(4.9) is based upon first and second order APS's and therefore the overall equations for this structure are dependent upon the formulae of these sections. All the required design equations for these first and second order APS's are provided in Section 4.2.2.

Following the experience gained from applying the template based optimization procedures to the ladder WDF structure, the most effective techniques and parameter settings were applied to lattice WDF designs. These optimization techniques included the three template types, the error function of Eq.(2.7) and the number and distribution of the error points.

The target templates provide a method of describing the desired response. These descriptions may entail an approximation by a single straight line, a set of boundary conditions defined by a dual set of straight lines or an ideal line that exactly specifies the desired response at each frequency point. The versatility and convenience of the ideal line template schemes for use on the lattice WDF's was improved due to the explicit formulae developed by Gazsi[4]. With these equations the ideal line magnitude templates for Butterworth, Chebyshev and elliptic type responses could be generated for any lowpass specifications. These equations avoid a limitation encountered for ladder WDF designs based upon the ideal line templates of only having a restricted number of responses defined in reference tables. Definition of the ideal line group delay templates followed the sine function procedures detailed for the ladder WDF designs. The convergence rates achieved for magnitude-only designs with the ideal line template schemes on ladder designs proved the importance of accurately representing the target function. Following this observation, modifications to the optimization techniques applied to the lattice WDF were centered upon the accuracy with which the desired responses were modelled.

The high degree of accuracy achieved with the ideal line template scheme is not possible using the straight line templates. In an attempt to improve the accuracy of the straight line templates, the positions of the last error points of a template band were adjusted. A frequency specification defines a maximum attenuation across the passband and a minimum attenuation across a stopband. A response that just meets a specification should therefore leave the passband with a value of the maximum attenuation and enter the stopband with the minimum attenuation value. To encourage the optimization routine to adjust the frequency response to pass through these points, the error points at the edge of a template were moved to these positions. This procedure is illustrated in Fig.(4.12) for the single and dual line template schemes.

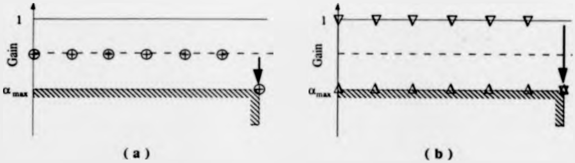

Figure 4.12 Examples of passband error point movement for (a) single and (b) dual line template schemes.

Another step to improve the performance of the straight line template schemes concerned the transition band descriptions. Ladder WDF magnitude specifications approached through the straight line templates when the transition band was not defined, invariably failed to provide an acceptable solution. Experimentation with various transition band schemes showed methods with a steep initial cut-off rate followed by a shallower cut-off rate were most successful. The principle behind this idea is that two asymptotic lines can more accurately model the typical gain response over the transition band than a single straight line. The method implemented in the ladder WDF designs involved a 'hinged' line. The start and finish of a template line was fixed to the edges of the passband and stopband and the hinge of the line moved around the transition band. This idea was discussed in Section 3.4.1 of Chapter 3.

The hinged line transition band technique requires vertical and horizontal displacement information to determine the position of each hinge, increasing the complexity of the template and its definition. An alternative to this method was to replace the hinged line by an angled line. For a dual line template scheme each transition band would require two angled lines, shown by Fig.(4.13). Using this type of transition band definition scheme, the gain response can be encouraged to cut-off at a quicker rate by increasing the angle of the template line. With a dual line template scheme this type of angled line definition can cause problems if the angle is very steep. In this situation the upper template line can move below the lower template line. To avoid this, when the upper template line passes below the highest value of the lower template line, the angle of the upper line from that point is altered so that it meets the edge of the next template band. This process is illustrated by Fig.(4.13)(b) and (d).

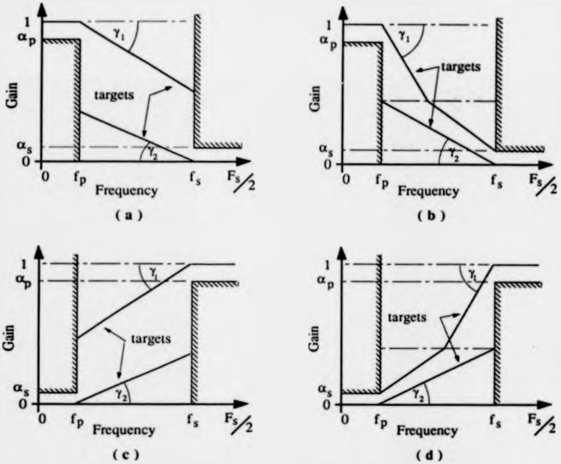

Figure 4.13 Modified transition band definitions for the dual line template scheme.

The efficiency of the modifications to the straight line templates and the repositioning of the edge error points was considered with reference to the convergence rate of the optimization routine and the shape of any filter solutions.

4.2 Lattice WDF equations

The design and analysis of the lattice structure requires equations to determine the gain, phase and group delay frequency responses as well as the derivatives of these responses for the coefficient sensitivity calculations. The sensitivity properties of the lattice structure are a function of its components, being the first and second order APS's. The system equations are therefore required in terms of these building blocks and their derivatives.

4.2.1 Overall system equations

Using the circuit illustrated in Fig.(4.3) as a basis for the lattice structure and the relationship defined by Eq(4.4), the transfer function of the simplified lattice structure can be written as

$$H(z) = \frac{S'' + S'}{2} \qquad (4.6)$$

The general form of the canonic reflectances, S' and S", is in terms of a cascade of first and second order APS's. If $H_1(z)$ represents the transfer function of a first order section and $H_2(z)$ the transfer function of a second order section, then the canonic reflectances, S' and S", can be expressed by Eq.(4.7).

$$S_i = \prod_{k=1}^{n_i} H_{1k}(z) \quad \prod_{k=1}^{m_i} H_{2k}(z) \qquad i = 1 \text{ and } 2 \qquad (4.7)$$

where

S_1	upper branch, S'	S_2	lower branch, S"
n_1	1st order sections in S'	n_2	1st order sections in S"
m_1	2nd order sections in S'	m_2	2nd order sections in S"

However, the order of the lattice arms should not differ by more than two. Under this rule only one first order APS would exist in one arm of the lattice structure. If the overall filter order is odd and the first order section occurs in the upper branch S', then Eq(4.6) and Eq(4.7) can be combined to define the transfer function of an odd order lattice WDF as

$$H(z) = \frac{\prod_{i=1}^{m_2} H_{2i}(z) + H_1(z) \cdot \prod_{i=1}^{m_1} H_{2i}(z)}{2} \qquad (4.8)$$

where

m_1	2nd order sections in S' branch	m_2	2nd order sections in S" branch
$H_1(z)$	1st order APS transfer function	$H_2(z)$	2nd order APS transfer function

If the filter order is even, then the transfer function of Eq.(4.8) simplifies to Eq.(4.9).

$$H(z) = \frac{\prod_{i=1}^{m_2} H_{2i}(z) + \prod_{i=1}^{m_1} H_{2i}(z)}{2} \qquad (4.9)$$

Using the principle of first and second order sections, values for m_1 and m_2 of Eq.(4.8) and Eq.(4.9) can be determined very easily for any filter order, N. Equations to evaluate m_1 and m_2 are given by Eq.(4.10) and Eq.(4.11) respectively.

$$m_1 = \mathrm{Int}\left(\frac{N}{4}\right) \tag{4.10}$$

$$m_2 = \mathrm{Int}\left(\frac{N+2}{4}\right) \tag{4.11}$$

If the filter order, N = 11, then $m_1 = 2$ and $m_2 = 3$. For this example, the upper lattice arm would contain two second order sections, while the lower arm would possess three. Because the filter order is odd, a first order section is required. This would be placed in the upper arm so that the order of each lattice arm did not differ by more than two. With values for m_1 and m_2, the gain and phase frequency responses for any filter order can be determined through either Eq.(4.8) or Eq.(4.9) and expressions for the transfer functions, $H_1(z)$ and $H_2(z)$. Equations for the transfer functions of the first and second order APS's are detailed in Section 4.2.2.

To determine the performance of the lattice WDF, the group delay and coefficient sensitivity responses are also required. These calculations follow the techniques outlined for the ladder WDF circuit in Section 3.3.2 of Chapter 3 of using natural logs. The group delay can be defined as

$$\tau(\omega) = -\,\mathrm{Im}\left[\frac{1}{H(z)}\cdot\frac{dH(z)}{d\omega}\right]$$

Using the definition of the transfer function, H(z), given by Eq.(4.6) the group delay for the lattice structure can be written as

$$\tau(\omega) = -\,\mathrm{Im}\left[\frac{1}{S'' + S'}\cdot\left(\frac{dS''}{d\omega} + \frac{dS'}{d\omega}\right)\right] \tag{4.12}$$

Group delay evaluation requires the derivatives of the canonic reflectances with respect to the frequency, ω. If one of the canonic reflectances is described as

$$S_i = A(z)\,.\,B(z)\,.\,C(z)\,.\,D(z) \tag{4.13}$$

then taking natural logs of Eq.(4.13), the derivative of S_i with respect to ω can be expressed as

$$\frac{1}{S_i}\cdot\frac{dS_i}{d\omega} = \frac{1}{A(z)}\cdot\frac{dA(z)}{d\omega} + \frac{1}{B(z)}\cdot\frac{dB(z)}{d\omega} + \frac{1}{C(z)}\cdot\frac{dC(z)}{d\omega} + \frac{1}{D(z)}\cdot\frac{dD(z)}{d\omega}$$

Using the general form of the transfer function of a lattice arm given by Eq.(4.7), the derivative of a lattice arm, S_i, with respect to the frequency, ω, can be determined from Eq.(4.14).

$$\frac{1}{S_i} \cdot \frac{dS_i}{d\omega} = \sum_{k=1}^{n_i} \frac{1}{H_{1k}(z)} \cdot \frac{dH_{1k}(z)}{d\omega} + \sum_{k=1}^{m_i} \frac{1}{H_{2k}(z)} \cdot \frac{dH_{2k}(z)}{d\omega} \qquad i = 1, 2 \qquad (4.14)$$

where

S_1	lattice branch S'	S_2	lattice branch S"
n_1	1st order APS's in S' branch	n_2	1st order APS's in S" branch
m_1	2nd order APS's in S' branch	m_2	2nd order APS's in S" branch
$H_1(z)$	1st order APS transfer function	$H_2(z)$	2nd order APS transfer function

The group delay response of the lattice WDF can be determined from Eq.(4.12) and the appropriate evaluation of Eq.(4.14) for each branch of the lattice structure. Eq.(4.14) is a sum of the terms that represent the derivative of a section's transfer function with respect to ω divided by its transfer function. Therefore in order to determine a value for Eq.(4.14) and in turn Eq.(4.12), the parameter

$$\frac{1}{G(z)} \cdot \frac{dG(z)}{d\omega}$$

is required, where $G(z)$ is the transfer function of a first or second order APS. Expressions for this parameter for both first and second order APS's are provided in Section 4.2.2.

The gain and phase coefficient sensitivities for the lattice structure require the derivatives of each first and section order section with respect to the filter's multipliers. The group delay coefficient sensitivity requires the derivatives of each section, first with respect to ω and then with respect to the multiplier coefficients. The gain, phase and group delay coefficient sensitivities for a multiplier, α_k, are given by Eq.(4.15), Eq.(4.16) and Eq.(4.17) respectively.

$$S_{\alpha_k}^{|H|} = \frac{\alpha_k}{|H|} \cdot \frac{\partial |H|}{\partial \alpha_k} \qquad (4.15)$$

$$S_{\alpha_k}^{\theta} = \frac{\alpha_k}{\theta} \cdot \frac{\partial \theta}{\partial \alpha_k} \qquad (4.16)$$

$$S_{\alpha_k}^{\tau} = \frac{\alpha_k}{\tau} \cdot \frac{\partial \tau}{\partial \alpha_k} \qquad (4.17)$$

If the overall transfer function is expressed in its polar form then

$$H(z) = |H(z)|\, e^{j\theta} \tag{4.18}$$

Taking natural logs of Eq.(4.18) and differentiating with respect to a multiplier, α_k, produces Eq.(4.19).

$$\frac{1}{H(z)} \cdot \frac{dH(z)}{d\alpha_k} = \frac{1}{|H(z)|} \cdot \frac{d|H(z)|}{d\alpha_k} + j\,\frac{d\theta}{d\alpha_k} \tag{4.19}$$

where $j = \sqrt{-1}$

From Eq.(4.19), the gain and phase coefficient sensitivities of Eq.(4.15) and Eq.(4.16) can be redefined to give Eq.(4.20) and Eq.(4.21) respectively.

$$S^{|H|}_{\alpha_k} = \alpha_k \cdot \mathrm{Re}\left[\frac{1}{H(z)} \cdot \frac{dH(z)}{d\alpha_k} \right] \tag{4.20}$$

$$S^{\theta}_{\alpha_k} = \frac{\alpha_k}{\theta} \cdot \mathrm{Im}\left[\frac{1}{H(z)} \cdot \frac{dH(z)}{d\alpha_k} \right] \tag{4.21}$$

Both Eq.(4.20) and Eq.(4.21) require the derivatives of the overall transfer function with respect to the structure's individual multipliers. These multipliers only exist in one section of the structure and are independent of each other. Therefore, differentiating the overall transfer function of Eq.(4.6) with respect to a multiplier will produce two different results, depending upon in which branch of the lattice that particular multiplier is contained. The differentiation of each lattice arm with respect to single multiplier also simplifies because the derivatives of the sections that do not contain a particular multiplier will also be zero. This information can be used to simplify the gain and phase coefficient sensitivity equations. Differentiating Eq.(4.6) with respect to a multiplier α_k, produces

$$\frac{dH(z)}{d\alpha_k} = \frac{1}{2} \cdot \left(\frac{dS''}{d\alpha_k} + \frac{dS'}{d\alpha_k} \right)$$

and because α_k will only exist in S' or S'', then

$$\frac{dH(z)}{d\alpha_k} = \frac{1}{2} \cdot \frac{dS_i}{d\alpha_k} \tag{4.22}$$

where

$i = 1$ or 2 , $S_1 = S'$ and $S_2 = S''$.

A general transfer function of a branch of a lattice is given in Eq.(4.23)

$$S_i = \prod_{k=1}^{L_i} X_k \tag{4.23}$$

where

i 1 or 2 for each lattice arm (with S_1 = S' and S_2 = S").
L_i 1st and 2nd order APS's in branch S_i.
X_k transfer function of kth section of the branch.
(X_k being a 1st or 2nd order APS transfer function)

Taking natural logs of Eq.(4.23) and differentiating it with respect to a multiplier, α_k, which is contained within that branch, gives

$$\frac{1}{S_i} \cdot \frac{dS_i}{d\alpha_k} = \sum_{k=1}^{L_i} \frac{1}{X_k} \cdot \frac{dX_k}{d\alpha_k}$$

If all the multipliers are independent and α_k only exists in the section X_m, then the derivative of a branch, S_i, with respect to a multiplier, α_k, is given in Eq.(4.24).

$$\frac{1}{S_i} \cdot \frac{dS_i}{d\alpha_k} = \frac{1}{X_m} \cdot \frac{dX_m}{d\alpha_k} \tag{4.24}$$

Combining Eq.(4.22) and Eq.(4.24), the differential of the overall transfer function with respect to a multiplier, α_k, can be expressed as

$$\frac{dH(z)}{d\alpha_k} = \frac{1}{2} \cdot S_i \cdot \frac{1}{X_m} \cdot \frac{X_m}{d\alpha_k} \tag{4.25}$$

where i = 1 or 2 for the relevant lattice branch that contains the section X_m which possess the multiplier, α_k. Using the derivative of the overall transfer function with respect to α_k, Eq.(4.25), the gain and phase coefficient sensitivities of Eq.(4.20) and Eq.(4.21) can be written as Eq.(4.26) and Eq.(4.27) respectively.

$$S_{\alpha_k}^{|H(z)|} = \alpha_k \cdot \mathrm{Re}\left[\frac{S_i}{S'' + S'} \cdot \frac{1}{X_m} \cdot \frac{dX_m}{d\alpha_k} \right] \tag{4.26}$$

$$S_{\alpha_k}^{\theta} = \frac{\alpha_k}{\theta} \cdot \mathrm{Im}\left[\frac{S_i}{S'' + S'} \cdot \frac{1}{X_m} \cdot \frac{dX_m}{d\alpha_k} \right] \tag{4.27}$$

Evaluation of the gain and phase coefficient sensitivities requires the term shown by Eq.(4.28) for each multiplier within the lattice, where $G_m(z)$ is the transfer function of the section that contains α_k.

$$\frac{1}{G_m(z)} \cdot \frac{dG_m(z)}{d\alpha_k} \qquad (4.28)$$

Calculation of the factor of Eq.(4.28) can be approached as an evaluation of the inverse of $G_m(z)$ multiplied by the derivative of $G_m(z)$ with respect to α_k or as an analytical expression for the first and second order APS's. Because the explicit value of the derivative of each section is not required, the second approach is a more efficient calculation process. Formulae to determine the parameter given by Eq.(4.28) for first and second order APS's are provided in Section 4.2.2.

The final system performance equation to be evaluated is the group delay coefficient sensitivities. Differentiating the group delay, given by Eq.(4.12), with respect to a multiplier, α_k, modifies the group delay coefficient sensitivity equation of Eq.(4.17) so that it can be written as

$$S^{\tau}_{\alpha_k} = \frac{\alpha_k}{\tau} \cdot \mathrm{Im}\left[\frac{1}{(S'' + S')^2} \cdot \left(\frac{dS''}{d\alpha_k} + \frac{dS'}{d\alpha_k}\right) \cdot \left(\frac{dS''}{d\omega} + \frac{dS'}{d\omega}\right) - \frac{1}{S'' + S'} \cdot \left(\frac{d\left(\frac{dS''}{d\omega}\right)}{d\alpha_k} + \frac{d\left(\frac{dS'}{d\omega}\right)}{d\alpha_k} \right) \right] \qquad (4.29)$$

However, α_k only exists in one section of one branch of the lattice structure. Therefore, the derivatives of the lattice arm and sections with respect to α_k that do not containing that particular multiplier, will be zero. Using this property, the group delay sensitivity equation of Eq.(4.29) reduces to

$$S^{\tau}_{\alpha_k} = \frac{\alpha_k}{\tau} \cdot \mathrm{Im}\left[\frac{1}{(S'' + S')^2} \cdot S_i \cdot \left(\frac{1}{X_m} \cdot \frac{dX_m}{d\alpha_k}\right) \cdot \left(\frac{dS''}{d\omega} + \frac{dS'}{d\omega}\right) - \frac{1}{S'' + S'} \cdot \left(\frac{d\left(\frac{dS_i}{d\omega}\right)}{d\alpha_k} \right) \right] \quad \text{where } i = 1 \text{ or } 2 \qquad (4.30)$$

with

$$d\alpha_k = S_i \cdot \left[\left(\frac{1}{X_m} \cdot \frac{dX_m}{d\alpha_k}\right) \cdot \left(\frac{1}{S_i} \cdot \frac{dS_i}{d\omega}\right) + \frac{d\left(\frac{1}{X_m} \cdot \frac{dX_m}{d\omega}\right)}{d\alpha_k} \right]$$

where X_m is the transfer function of the only section of lattice arm, S_i, that contains the multiplier, α_k. For Eq.(4.30), the parameter given by Eq.(4.31) can be evaluated directly or expanded to the form shown by Eq.(4.32).

$$\frac{d\left(\frac{1}{X_m} \cdot \frac{dX_m}{d\omega}\right)}{d\alpha_k} \qquad (4.31)$$

$$\frac{1}{X_m}\cdot\frac{d\left(\frac{dX_m}{d\omega}\right)}{d\alpha_k} - \left(\frac{1}{X_m}\cdot\frac{dX_m}{d\omega}\right)\cdot\left(\frac{1}{X_m}\cdot\frac{dX_m}{d\alpha_k}\right) \tag{4.32}$$

Calculation of this term would be more efficient if an analytical expression of Eq.(4.31) was derived for the first and second order section rather than the combination of the terms of Eq.(4.32). Equations to determine Eq.(4.31) for the first and second order APS's are provided in Section 4.2.2.

4.2.2 Building Blocks

To determine the properties of the lattice WDF using the equations derived for the frequency and sensitivity responses, the transfer functions and derivatives for the first and second order APS's are required. The transfer function of the first order APS, illustrated by Fig.(4.14), can be determined from the scattering matrix for the two-port adaptor and the relationship between the wave parameters given in Eq.(4.33).

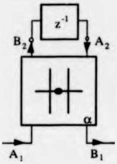

Figure 4.14 First order APS with wave parameters.

$$\begin{bmatrix} B_1 \\ B_2 \end{bmatrix} = \begin{bmatrix} -\alpha & 1+\alpha \\ 1-\alpha & \alpha \end{bmatrix} \cdot \begin{bmatrix} A_1 \\ A_2 \end{bmatrix} \qquad A_2 = z^{-1} \, . \, B_2 \tag{4.33}$$

Combining the equations of Eq.(4.33), the transfer function of the first order section can be derived and is given by Eq.(4.34).

$$H_1(z) = \frac{B_1}{A_1} = \frac{-\alpha + z^{-1}}{1 - \alpha\, z^{-1}} \tag{4.34}$$

The allpass nature of this first order section can be seen from its transfer function, where if the numerator is $G(z)$ then the denominator has the function $G(z^{-1})$ and $H_1(z)$ has a pole at α and a zero at $1/\alpha$. The stability of this transfer function is dependent upon the position of its pole within the unit circle in the z domain. To ensure that the pole lies within the unit circle, then the section's multiplier must be limited to the range $-1 < \alpha < 1$.

Evaluation of the group delay is based upon an expression for the derivative of the transfer function with respect to ω, divided by that transfer function. This parameter for the first order section is given by Eq.(4.35).

$$\frac{1}{H_1(z)} \cdot \frac{dH_1(z)}{d\omega} = j\frac{z^{-1}(\alpha^2 - 1)}{(-\alpha + z^{-1})(1 - \alpha z^{-1})} \tag{4.35}$$

The gain and phase coefficient sensitivities of Eq.(4.26) and Eq.(4.27) are based upon an expression for the differential of each section with respect to its multiplier(s). This term for the first order APS of Fig.(4.14), which has a multiplier α, is given by Eq.(4.36).

$$\frac{1}{H_1(z)} \cdot \frac{dH_1(z)}{d\alpha} = \frac{z^{-2} - 1}{(-\alpha + z^{-1})(1 - \alpha z^{-1})} \tag{4.36}$$

The final expression for the first order section is the one required to evaluate the group delay coefficient sensitivities. This parameter can be determined from Eq.(4.37).

$$\frac{d\left(\frac{1}{H_1(z)} \cdot \frac{dH_1(z)}{d\omega}\right)}{d\alpha} = j\frac{z^{-1}\left(4\alpha z^{-1} - (1 + \alpha^2)(1 + z^{-2})\right)}{\left(-\alpha + z^{-1}\right)^2\left(1 - \alpha z^{-1}\right)^2} \tag{4.37}$$

The transfer function, $H_2(z)$, of the second order APS illustrated by Fig.(4.15), can be determined from the relationship between the equations of Eq.(4.38) and is given by Eq.(4.39).

$$\begin{bmatrix} B_1 \\ B_2 \end{bmatrix} = \begin{bmatrix} -\alpha & 1 + \alpha \\ 1 - \alpha & \alpha \end{bmatrix} \cdot \begin{bmatrix} A_1 \\ A_2 \end{bmatrix} \qquad \begin{bmatrix} B_3 \\ B_4 \end{bmatrix} = \begin{bmatrix} -\beta & 1 + \beta \\ 1 - \beta & \beta \end{bmatrix} \cdot \begin{bmatrix} A_3 \\ A_4 \end{bmatrix}$$

$$A_4 = z^{-1} . B_4 \;,\; A_3 = z^{-1} . B_2 \text{ and } A_2 = B_3 \tag{4.38}$$

$$H_2(z) = \frac{B_1}{A_1} = \frac{\alpha + (1 - \alpha)\beta z^{-1} - z^{-2}}{-1 + (1 - \alpha)\beta z^{-1} + \alpha z^{-2}} \tag{4.39}$$

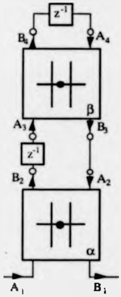

Figure 4.15 Second order APS with wave parameters.

The stability of this allpass function is determined by the position of its complex conjugate poles. The stability criteria of this second order APS can be determined by comparing its denominator to the denominator of a standard second order section, given by Eq.(4.40).

$$z^2 + 2\,r\cos(\theta)\,z + r^2 \tag{4.40}$$

For the standard second order section it is known[11] stability requires $|r| < 1$. Applying this limit to the appropriate parameters of Eq.(3.39) results in the stability conditions $-1 < \alpha < 0$ and $-1 < \beta < 1$ for the second order APS of Fig.(4.15).

The equation of the second order section required to determine the group delay response is shown by Eq.(4.41).

$$\frac{1}{H_2(z)} \cdot \frac{dH_2(z)}{d\omega} = j\,\frac{z^{-1}(1-\alpha^2)(\beta - 2z^{-1} + \beta z^{-2})}{(\alpha + (1-\alpha)\beta z^{-1} - z^{-2})(-1 + (1-\alpha)\beta z^{-1} + \alpha z^{-2})} \tag{4.41}$$

The terms required for the calculation of the gain and phase coefficient sensitivities, provided for the two multipliers α and β, are given by Eq.(4.42) and Eq.(4.43) respectively.

$$\frac{1}{H_2(z)} \cdot \frac{dH_2(z)}{d\alpha} = \frac{(z^{-2} - 1)(1 - 2\beta z^{-1} + z^{-2})}{(\alpha + (1-\alpha)\beta z^{-1} - z^{-2})(-1 + (1-\alpha)\beta z^{-1} + \alpha z^{-2})} \tag{4.42}$$

$$\frac{1}{H_2(z)} \cdot \frac{dH_2(z)}{d\beta} = \frac{z^{-1}(1 - \alpha^2)(z^{-2} - 1)}{(\alpha + (1-\alpha)\beta z^{-1} - z^{-2})(-1 + (1-\alpha)\beta z^{-1} + \alpha z^{-2})} \tag{4.43}$$

The final expressions for this section are those required to determine the group delay coefficient sensitivities. These terms for the multipliers α and β, are given by Eq.(4.44) and Eq.(4.45) respectively.

$$\frac{d\left(\frac{1}{H_2(z)}\cdot\frac{dH_2(z)}{d\omega}\right)}{d\alpha} = j\, z^{-1}\left(\beta - 2z^{-1} + \beta z^{-2}\right)\left(\alpha + (1-\alpha)\beta z^{-1} - z^{-2}\right)^{-2}$$

$$\Big(2z^{-2}((1-\alpha)^2\beta^2 - 2\alpha) - 2\beta z^{-1}(1-\alpha)^2(1+z^{-2})$$

$$+ (1+\alpha^2)(1+z^{-4})\Big)\left(-1 + (1-\alpha)\beta z^{-1} + \alpha z^{-2}\right)^{-2} \quad (4.44)$$

$$\frac{d\left(\frac{1}{H_2(z)}\cdot\frac{dH_2(z)}{d\omega}\right)}{d\beta} = j\, z^{-1}\left(\alpha^2 - 1\right)\left(\alpha + (1-\alpha)\beta z^{-1} - z^{-2}\right)^{-2}$$

$$\Big(\alpha(1+z^{-6}) + z^{-2}(1+z^{-2})(1 + \alpha(\alpha - 3) + \beta^2(1-\alpha)^2)$$

$$- 4\beta z^{-3}(1-\alpha)^2\Big)\left(-1 + (1-\alpha)\beta z^{-1} + \alpha z^{-2}\right)^{-2} \quad (4.45)$$

4.3 Lattice WDF design and analysis software

Software written to implement simultaneous magnitude and phase designs on the lattice WDF structure falls into the two areas of design and analysis. The design side of the software is provided through a menu driven program called "WDF". This program is based upon the optimization techniques and algorithms discussed for the ladder WDF program. A menu within this program allows the user to enter the order of the lattice, its initial multiplier values and frequency specification. The position and number of first and second order APS's are calculated automatically from the filter order. Frequency specifications are entered as a set of vectors that contain the frequency edge and attenuation values. Under this vector scheme any filter type can be defined from a lowpass to a dual bandpass specification. Frequency specifications can also be defined with different frequency edges for the gain and group delay responses. The information about the lattice structure, its parameters and frequency specification can then be recorded into a data file.

All optimization parameters of this lattice WDF program are contained within a single menu. This menu allows one of the single, dual or ideal line template schemes to be selected, along with the number and position of the error points at which the templates are defined. The weights for the gain and group delay templates may be set individually or calculated automatically through an option within the menu that ensures that an equal deviation in each template contributes an equal error to the overall function. Other options in this menu allow the value of the angled line for transition band definitions to be altered, the optimization algorithm to be changed and variation of the ratio that determines the relative contributions of the gain and group delay errors to the overall function. A menu walk-through of this program is provided in Appendix B1, along with an example to illustrate the design procedure and optimization options.

A limitation of the ladder WDF program was imposed by the GHOST routines used for graphical output. The GHOST routines required an environment which could support a window system, typically a graphics window within Suntools. This meant that the ladder WDF program could not be run on different systems even when graphics were not required. For this reason the analytical and graphical elements of the lattice WDF software were not included within the "WDF" design program. A more versatile graphical system than the GHOST approach was provided through a program called MatLab[9]. Within MatLab a wide range of analytical and graphical procedures can be achieved through built-in functions. A program called "mltwdf" was written in the MatLab procedural language to provide an analysis of any lattice WDF solutions generated from the "WDF" program.

The program "mltwdf" has three elements. The first concerns the entry of data files. These data files are stored in the MatLab format and are created by the design program "WDF". These data files may be loaded into "mltwdf" either individually or as a set. This allows the performance of lattice WDF solutions under slightly different optimization parameters to be compared directly. The other two elements of this program relate directly to the analysis and display of a lattice WDF in the frequency and time domains. The frequency domain side of the program calculates the magnitude, gain, phase and group delay responses over an arbitrary frequency range. Gain, phase and group delay coefficient sensitivities can be evaluated for individual or sets of multipliers within the lattice structure, again over an arbitrary frequency range. The final element within the frequency domain part of the program is concerned with the calculation of the poles and zeros of the structure. The program highlights the poles of each lattice arm along with the zeros of the overall structure. The poles and zeros of the lattice WDF structure can be determined from the overall transfer function given by Eq.(4.6).

Expressing the transfer function of each branch of the lattice in terms of a numerator and denominator polynomial, Eq.(4.6) can be expressed as

$$H(z) = \frac{\left(\frac{N''(z)}{D''(z)} + \frac{N'(z)}{D'(z)}\right)}{2} = \frac{N''(z)\,D'(z) + N'(z)\,D''(z)}{2\,D'(z)\,D''(z)} \qquad (4.46)$$

The poles of Eq.(4.46) are the roots of the two denominator polynomials D'(z) and D''(z). The zeros can be determined from the roots of the numerator of Eq.(4.46). This means that the zeros of the structure cannot be associated with a single lattice arm in the way the poles of the lattice can.

Each of the responses calculated is displayed to the screen through MatLab and the user is given the option of printing the graphs to a file or laser printer.

While the frequency domain side of the software program calculates the filter responses to the full accuracy of the system, the time domain calculations are performed to finite wordlength criterion. The impulse response of the lattice structure can be determined with arbitrary wordlengths for the input, output and internal signals and for the multiplier coefficients. A finite wordlength impulse response can then be converted into the frequency domain with a FFT routine provided by MatLab. This process allows the user to analyse the response of a lattice structure to different rounding, finite wordlength and overflow strategies. The time domain side of the program also allows a user to determine the time domain response of a lattice filter to a number of different input functions such as the step, ramp and square wave. Again all responses generated by this part of the program are displayed to the screen and can be recorded for output to a laser printer. A menu walk through for this program is provided in Appendix B2 along with a frequency and time domain analysis of the example considered in Appendix B1.

Ancillary software written to aid in the investigation of the lattice WDF included an implementation of the Gazsi formulae called "ellip" and a linear phase FIR program called "linfir". The program "ellip" was written in C++ and allows a user to define an arbitrary lowpass magnitude specification. From this specification the order of a lattice WDF required to satisfy a Butterworth, Chebyshev and elliptic response can be calculated along with the appropriate multiplier values. A demonstration of the "ellip" program is provided in Appendix B1 where it is used to generate the lattice multiplier coefficients for the lowpass design example. The linear phase FIR program was written to implement a Remez exchange algorithm routine provided within MatLab. With this software the order of a FIR filter to satisfy an arbitrary magnitude and exactly linear phase specification could be determined and compared with the filter orders of simultaneous lattice WDF solutions.

4.4 Experimental Results

The experimental work for the designs of lattice WDF's followed the procedures laid down for the ladder WDF designs. These procedures entailed the investigation of various optimization techniques and strategies on magnitude-only specifications with known solutions. With these specifications the convergence rates and the shapes of filter solutions for a wide combination of different target templates, transition band definitions, error points and optimization algorithms were compared. With the experience gained from magnitude-only designs, the research was extended to include simultaneous magnitude and phase specifications.

4.4.1 Magnitude-only design

As with the ladder WDF research, the lattice magnitude-only investigations were based upon a suite of lowpass specifications with a range of filter orders and attenuations. These specifications, which were just satisfied by an elliptic function, are given in Table(4.1).

Spec number	Filter order	Gain passband		Gain stopband		Samp freq (Hz)
		att (dB)	freq (Hz)	att (dB)	freq (Hz)	
1	5	1	0.05	50	0.07	1
2	7	1	0.1	50	0.11	1
3	9	0.1	0.02	100	0.04	1
4	11	0.5	0.075	100	0.09	1

Table 4.1 Lowpass filter specification examples.

Each of the lowpass specifications of Table(4.1) was investigated using the three target templates, the two quasi-Newton algorithms and different starting positions for the multiplier values. Results supported the theories outlined for the ladder WDF designs, in that the more accurately the target function can be modelled, the quicker the convergence rate. For identical specifications and the same optimization settings, the convergence rate of tests based upon the ideal, dual and single line template schemes fell roughly into a ratio of $4n^2 : 2n^{2.5} : n^3$ respectively, where n was the number of variables. This shows that as the number of variables to be optimized increases, target templates that do not accurately model the magnitude response required an increasing number of iterations to converge. This imposes a severe limitation upon the use of the single line template scheme for high filter orders.

Another observation with the use of the single line template scheme is the shape of the final solutions, especially across the passband. These solutions tend to ripple from the unity gain line to just below the template line. A typical example of this type of response across a passband is shown by Fig.(4.16).

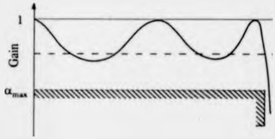

Figure 4.16 Typical gain passband response with single line template.

The single line templates are calculated to pass along the centre of the tolerance specification for each band in an attempt to encourage the function to equiripple about these template lines. The gain is prevented from achieving a value greater than one by limiting the valid range of the multiplier values so that the structure remains pseudopassive and retains its WDF properties. The nature of the lattice structure forces some turning points of the function to move to the zero or unity gain limits. With reference to Fig.(4.16), the optimization routine cannot minimize the response above the template line as the turning points on the unity gain line cannot be moved down. The optimization routine can however minimize the response below the template line. The response of Fig.(4.16) is typical of a single line template solution where the weighting values were too high.

This effect was noticed in both the passband and stopband regions of the gain response and highlights a disadvantage of the single line template scheme because of their reliance upon correct weighting values. These weighting values, which were the same across a template band, do not follow the equal deviation/equal error rule derived for ladder WDF designs and a trial and error process is required to determine the correct values. The speed penalty this introduces into the design process can be offset by optimization algorithms that use derivatives. Switching from the NAG quasi-Newton algorithm E04JAF to E04KCF decrease the number of iterations required by a factor of ten. Despite the extra derivative calculations required at each iteration, in most cases the actual time taken for a problem to converge was noticeably quicker. Overall the single line templates, while being very simple, are limited by their susceptibility to weights and a slow convergence rate for higher order filter specifications.

The dual line templates, although unsuitable for use with the E04KCF algorithm, are not as susceptible to weighting values and the equal deviation/equal error weighting rule appears to be satisfactory. This is partly due to the nature of the template scheme because the error function can approach zero when the response lies within the template limits. Therefore even if a very large weighting value is applied to a region of the dual line template, its effects will be eliminated when the response lies within the bounds of that region. Using this property the passband or stopband regions of a filter can be emphasized with large weight values.

Other results from the lattice magnitude-only designs confirmed earlier observations from ladder designs. These included the number and distribution of error points and starting position for the multiplier values. The number of error points to balance the criteria of accuracy and speed fell into the range of 20-40 points per band with an equal number of points in each band. Equal numbers of error points were used in order not to offset the overall effects of the weighting values. The magnitude-only designs converged quicker when more error points were clustered about the transition edges of the template. This follows the sine/cosine spacing ideas discussed in Chapter 3. The idea of moving error points to the boundary positions of a template, illustrated by Fig.(4.12), also improved the convergence rate and shape of the magnitude-only responses. Each of the optimization tests was performed with the multiplier values starting at different points within their valid bounds. Positions were varied from the ideal values, first by moving a single multiplier to its boundary values and then by moving all the multiplier values to their lower, middle and upper boundary limits. Results tended to show that convergence rates were improved if the multiplier values were started in the middle of their boundary limits, nominally at a value of zero. This placed each multiplier within the bounds of any solution and avoided them being stuck at local minima around the edges of the function.

4.4.2 Simultaneous designs

The objective of this area of research was to optimize lattice coefficient values to satisfy an arbitrary magnitude and phase specifications. The optimization process centered upon starting with a lattice filter order that satisfied an elliptic lowpass magnitude specification and then increasing the width of the group delay tolerance until a simultaneous solution was found for that filter order. From this solution, the group delay tolerance was halved and the filter order increased until a new solution was generated. Under this method a family of solutions could be tabulated for filter order and passband group delay deviation.

This design procedure was implemented on the three template schemes with the optimization techniques and settings developed for the lattice magnitude-only designs. Each test was performed with 31 error points in each band of the lowpass specification using a sine spacing for the passband, linear spacing for the transition band and cosine spacing for the stopband. The optimization variables for each test contained the lattice WDF multipliers and a parameter that represented the value about which the group delay passband template was generated. Errors between the actual and template values were combined under the weighted L_p-metric error function of Eq.(2.7). Although the error function implemented in the "WDF" program could determine any integer norm value, tests were performed with low norm values typically, p=2. This followed experience from the simultaneous ladder WDF tests.

The initial simultaneous design investigations were carried out on single line templates with the NAG E04JAF optimization routine. Difficulties in determining the appropriate weighting values and an inability to impose different group delay tolerances soon lead to this template type being eliminated from the investigation.

The next area of interest concentrated upon the ideal line templates. The gain templates were determined by calculating the filter coefficient values to satisfy a particular lowpass specification from the Gazsi formulae and then equating the ideal line gain templates to the lattice's frequency response with these coefficient values. The group delay ideal line templates were based upon a sine function with an amplitude determined by the group delay tolerance and whose period was an optimization parameter. The general nature of the optimization routine considered allowed the gain and group delay responses to possess different frequency edges. This generality meant that the error points in the passband of the gain and group delay templates could differ in number and distribution. Initial tests used a sine spacing for the error points across the group delay passband template, although this was later switched to a linear spacing. The gain within the passband of a WDF filter cannot move above unity and so the only concern for the gain template was that the response did not move below the maximum attenuation specification. This was most likely to occur at a transition edge and so more points were clustered around these regions. This reasoning was not true for the group delay response and it was as equally likely to ripple above or below its templates. To compensate for this fact, the error point spacing was altered from a sine spacing to a linear format.

Research using optimization techniques based upon the ideal line templates investigated a number of parameters and their values. The main optimization parameter for simultaneous designs is the β factor within the error function that determines the relative contributions of the gain and group delay errors. From ladder WDF designs a range for this parameter to ensure an acceptable filter response fell within the range $0.6 < \beta < 0.9$. This range of values for β was also true for the lattice WDF designs. However, despite a wide combination of error point numbers, weights and β values, optimization through the ideal line templates failed to satisfy a magnitude and phase specification completely. This, in part, may be due to the shape of the ideal targets. For the examples considered the target magnitude response had an elliptic form while the group delay target was an equi-spaced, equi-ripple function. The characteristics of wide and rapid changes in gain are contrary to phase linearity for a filter's response and it may therefore be impossible to achieve an elliptic type magnitude response with an equi-spaced, equi-ripple group delay.

Research into the implications of this theory is limited with the ideal line templates and outlines a major disadvantage of the ideal line templates compared to dual line schemes. The ideal line templates cannot be generated unless the desired responses are known at each frequency point. However, no research has produced a polynomial that can exhibit arbitrary magnitude and phase properties. Therefore, the shape of a magnitude response that permits phase linearity is very difficult to define. As a consequence, the ideal line gain templates cannot be defined. This problem is also true for the group delay templates, where an equi-spaced and equi-ripple response may be detrimental to a desired gain response. To determine the nature and shape of filter responses that can possess an arbitrary magnitude and phase characteristic, research was altered to designs based upon the dual line template schemes.

The dual line template scheme proved to be the most successful design technique for simultaneous magnitude and phase designs. A large range and combination of optimization parameters were investigated from weights to the angles of the transition band templates. Experimental results showed that the most successful optimization settings had β values in the range $0.7 < \beta < 0.8$ and weights that followed the equal deviation/equal error rule. For a lowpass specification the gain error points followed the sine/linear/cosine spacing, while the group delay error point spacing was linear over the passband. An equal number of error points, in the range of 25 - 45 for each template region, was also found to provide solutions relatively accurately and quickly.

A design example can be used to illustrate how the overall order of a filter and its frequency responses were modified to meet an identical gain specification with various group delay tolerances. The orders of this suite of solutions can then be compared to the order of an elliptic function that satisfies the magnitude specification and the order of a FIR filter satisfying the same magnitude specification but with exactly linear phase.

Consider the lowpass filter specification shown in Table(4.2).

Gain passband		Gain stopband		Delay passband		Samp
att (dB)	edge (Hz)	att (dB)	edge (Hz)	dev (%)	edge (Hz)	freq (Hz)
0.1	0.08	34	0.16	10 - 0.005	0.09	1

Table 4.2 Lowpass filter specification.

Using the "ellip" program the order of Butterworth, Chebyshev and elliptic functions to satisfy the magnitude specification of Table(4.2) can be determined. Through the program "linfir", the order of a FIR filter required to satisfy the same magnitude specification and exactly linear phase can also be evaluated. These filter orders are detailed in Table(4.3).

Filter	Lattice WDF			Linear
type	Butterworth	Chebyshev	Elliptic	Phase FIR
Filter order	9	5	5	26

Table 4.3 Filter orders to satisfy the magnitude part of the specification from Table(4.2).

Under the design procedure outlined at the start of this section, the initial optimization was performed on a lattice WDF with the order of an elliptic function that satisfied the magnitude specification. For the example considered, this order was five. The frequency responses of a 5^{th} order lattice WDF that satisfies the magnitude part of the specification of Table(4.2) using the elliptic function are shown by Fig.(4.17).

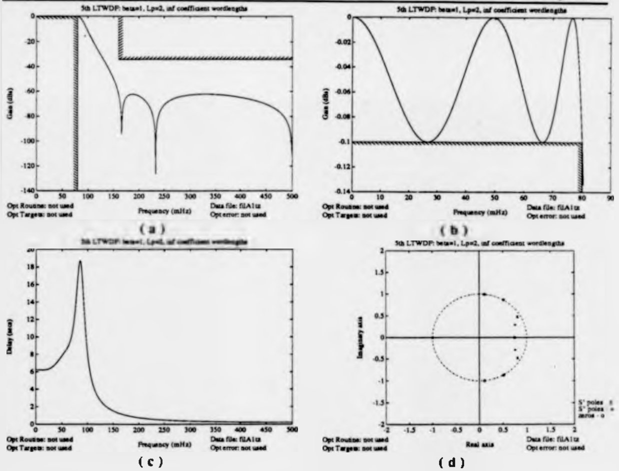

Figure 4.17 Frequency responses of a 5th order lattice WDF. (a) overall magnitude, (b) passband magnitude, (c) overall group delay and (d) pole/zero plot.

Characteristic of the elliptic function, shown in Fig.(4.17), is an equal number of turning points in both the passband and stopband, an equi-ripple gain format and a high frequency selectivity. The elliptic function also exhibits a very poor phase linearity or non-constant group delay response. A Bessel polynomial, on the other hand, is constructed to possess good phase linearity. Its linear phase is achieved at the expense of frequency selectivity. Both these polynomials and the others considered within filter designs were constructed to possess a minimum-phase characteristic. The tradeoff between frequency selectively and phase linearity was clearly highlighted by designs on the minimum-phase ladder WDF structure in Chapter 3.

The nonminimum-phase lattice structure can also implement the classic minimum-phase polynomials, demonstrated in Fig.(4.17). However a more efficient procedure would be to consider nonminimum-phase polynomials. If a lattice WDF is to satisfy an arbitrary magnitude and linear phase specification then it must follow a nonminimum-phase polynomial that contains the characteristics of high frequency selectivity and phase linearity. These would include a ripple in both gain passbands and stopbands, similar to the elliptic polynomial and zeros that exist in reciprocal complex conjugate sets.

The specification of Table(4.2) requires a group delay tolerance between 10% and 0.005%. From a simultaneous solution for the 5th order lattice WDF with a very wide group delay tolerance, the order of the filter was increased until a solution with a 10% group delay deviation was produced. The order of a lattice WDF to satisfy this specification was seven and its frequency responses are illustrated by Fig.(4.18). The frequency responses of filter solutions that satisfied the 0.1% and 0.005% group delay tolerances are illustrated by Fig.(4.19) and Fig.(4.20) respectively.

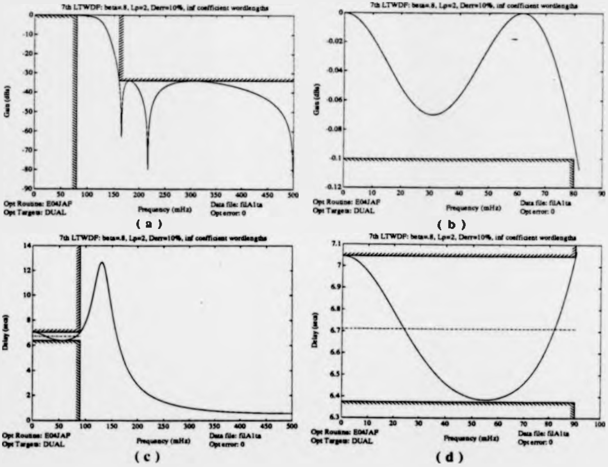

(a) (b)

(c) (d)

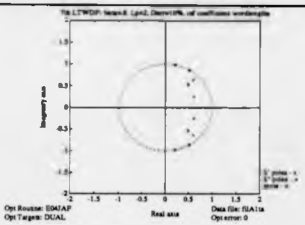

(e)

Figure 4.18 7th order lattice WDF with 10% group delay tolerance showing, (a) overall and (b) passband magnitude and (c) overall and (d) passband delay frequency responses and (e) pole/zero plot.

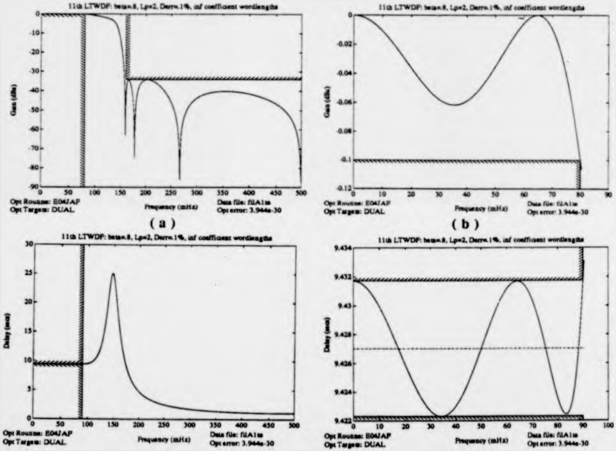

(a) (b)

(c) (d)

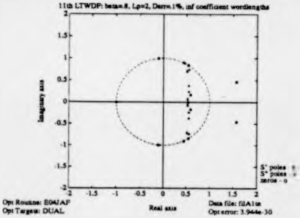

(e)

Figure 4.19 11th order lattice WDF with 0.1% group delay tolerance showing, (a) overall and (b) passband magnitude and (c) overall and (d) passband delay frequency responses and (e) pole/zero plot.

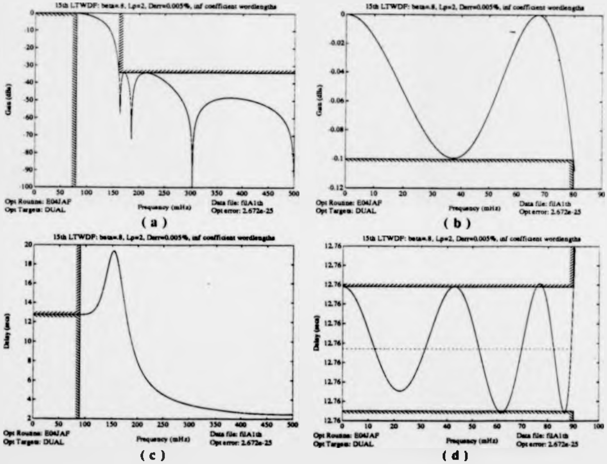

(a)

(b)

(c)

(d)

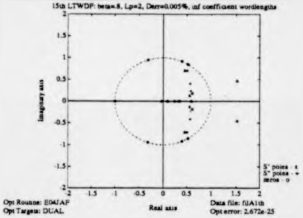

(e)

Figure 4.20 15^{th} order lattice WDF with 0.005% group delay tolerance showing, (a) overall and (b) passband magnitude and (c) overall and (d) passband delay frequency responses and (e) pole/zero plot.

The filter orders of the design solutions to the specification given in Table(4.2) are detailed in Table(4.5), along with the order of the elliptic function that satisfies the magnitude part of the specification and the order of the equivalent exactly linear phase FIR filter.

	Lattice WDF									FIR
	Elliptic	Group delay deviation (%)								linear
	function	10	5	1	0.5	0.1	0.05	0.01	0.005	phase
filter order	5	7	7	7	9	11	11	15	15	26

Table 4.5 Filter order of solutions satisfying the specification of Table(4.2).

A number of properties from various solutions can be observed when the filter responses are compared. These properties concern the increasing filter order required to satisfy a narrowing group delay tolerance and how these extra degrees of freedom are distributed within the gain and group delay responses. From Table(4.5) it can be seen that halving the group delay tolerance requires approximately an increase of two in the overall filter order. This increase in filter order does not increase the turning points across the passband of the gain response but instead places more turning points in the gain stopband and the group delay passband. The distribution of these turning point across the various group delay tolerance solutions is detailed in Table(4.6).

		Group delay deviation (%)							
		10	5	1	0.5	0.1	0.05	0.01	0.005
filter order		7	7	7	9	11	11	15	15
turning points	gain passband	1.5	1.5	1.5	1.5	1.5	1.5	1.5	1.5
	gain stopband	2	2	2	2	3	3	4	3
	delay passband	1	1	2	2	2	2.5	2.5	3

Table 4.6 Turning points of solutions satisfying the specification of Table(4.2).

The characteristic of the optimization routine of using the extra filter orders within the gain stopband and delay passband responses can also be demonstrated through a second lowpass filter example. The specification of this example uses the same group delay tolerance range as the first example and is detailed in Table(4.7). The orders of the solutions to this specification are given by Table(4.8), along with the orders of the appropriate Butterworth, Chebyshev and elliptic functions and the equivalent exactly linear phase FIR filter.

Gain passband		Gain stopband		Delay passband		Samp
att (dB)	edge (Hz)	att (dB)	edge (Hz)	% dev	edge (Hz)	freq (Hz)
0.17	500	40	750	10 - 0.005	550	2500

Table 4.7 Specification of second lowpass filter example.

	Lattice WDF											Linear phase FIR
	Butt fun	Cheb fun	Ellip fun	Group delay deviation (%)								
				10	5	1	0.5	0.1	0.05	0.01	0.005	
filter order	11	7	5	11	13	13	13	15	15	17	17	22

Table 4.8 Filter orders satisfying the specification of Table(4.7).

The turning points of these filter solutions across the gain and group delay responses are illustrated by Table(4.9).

		Group delay deviation (%)							
		10	5	1	0.5	0.1	0.05	0.01	0.005
filter order		11	13	13	13	15	15	17	17
turning points	gain passband	1.5	1.5	1.5	1.5	2.5	1.5	1.5	1.5
	gain stopband	3	2	2	3	3	3	2	2
	delay passband	1.5	2	3	3	4	4	5.5	5.5

Table 4.9 Turning points of solutions satisfying the specification of Table(4.7).

Frequency responses of the solutions to the design example of Table(4.7) with the 10%, 1% and 0.01% group delay tolerances are shown by Fig.(4.21), Fig.(4.22) and Fig.(4.23) respectively.

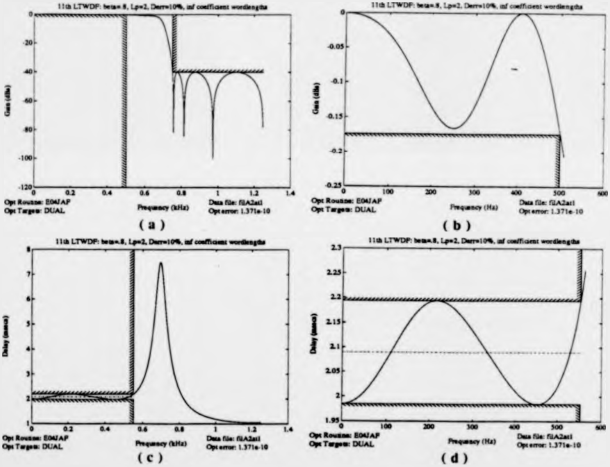

(a) (b)

(c) (d)

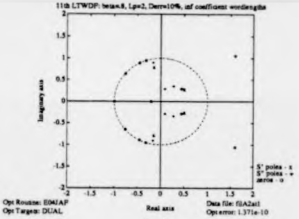

(e)

Figure 4.21 11th order lattice WDF with 10% group delay tolerance showing, (a) overall and (b) passband magnitude and (c) overall and (d) passband delay frequency responses and (e) pole/zero plot.

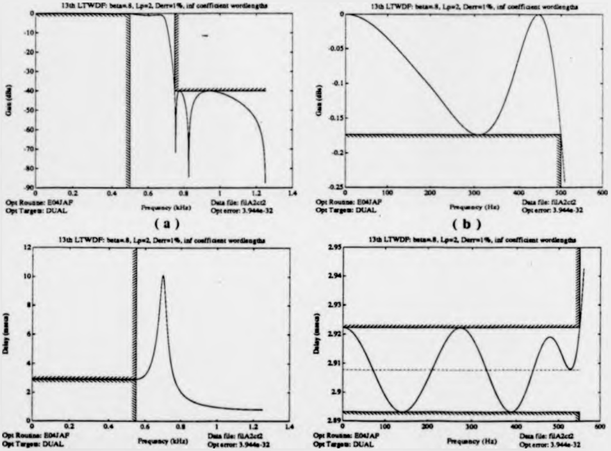

(a)

(b)

(c)

(d)

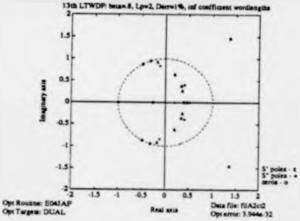

(e)

Figure 4.22 13^{th} order lattice WDF with 1% group delay tolerance showing, (a) overall and (b) passband magnitude and (c) overall and (d) passband delay frequency responses and (e) pole/zero plot.

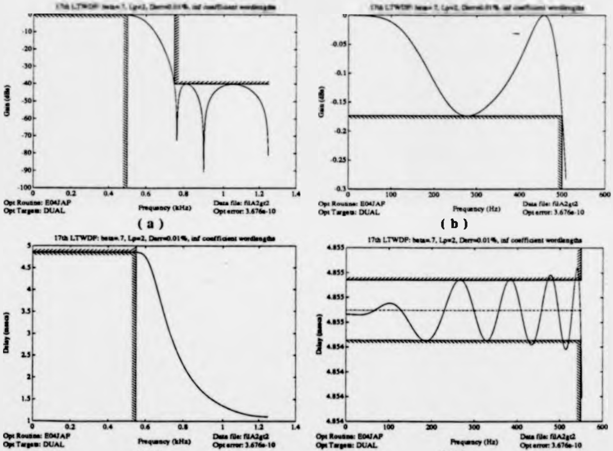

(c)

(d)

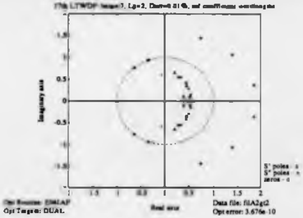

(e)

Figure 4.23 17th order lattice WDF with 0.01% group delay tolerance showing, (a) overall and (b) passband magnitude and (c) overall and (d) passband delay frequency responses and (e) pole/zero plot.

The frequency responses of the simultaneous design solutions shown by Fig.(4.18) to Fig.(4.23) indicate the nature of the function required to satisfy an arbitrary magnitude and linear phase specification. Gain responses ripple in both the passband and the stopband. The gain response should therefore possess the frequency selectivity of an elliptic type function. The group delay response also ripples across the passband. Narrowing the width of the group delay tolerance increases the order of filter required and results in a larger number of ripples over its group delay passband region. The zeros of the lattice structure for these solutions lie in reciprocal complex conjugate sets while the poles of the two lattice arms are interlaced upon an arc within the unit circle. The position of the zeros follows the patterns predicted for linear phase requirements within Chapter 1. The interlacing of the poles from each lattice arm is consistent with the ideas outlined by Gazsi[4] for the canonic polynomials of the lattice structure.

Other features of the simultaneous solutions that can be seen from the frequency responses include the distribution of turning points or degrees of freedom of the structure. For the range of design examples investigated, an increase of the filter order and therefore its degrees of freedom were not used to increase the number of turning points in the gain passband region. This feature is not necessarily a prerequisite for a simultaneous solution but a property of the optimization procedure and the dual line template scheme. This was shown through magnitude-only designs based on the dual line templates. Solutions were achieved with the same filter order as the elliptic function but which did not possess the same number of turning points in the passband and stopband. Optimization tended to limit the number of turning points within the passband in favour of the transition band and stopband.

The distribution of the turning points within the frequency responses of the solutions of the two design examples considered are listed by Table(4.6) and Table(4.9). Calculating the possible number of turning points for a given filter order and those listed in the two tables reveals a discrepancy. The turning points that make up the difference between these two values have been placed in the transition band by the optimization routine. Their presents cannot usually be noticed unless the angles of the transition band templates are not set correctly. The magnitude response of Fig.(4.22)(a) illustrates the effect of an inappropriate template definition and shows a turning point in the transition band.

The use of turning points in a transition band is typical of filter specifications with unequal gain and group delay passband widths. The transition band is a region of rapid change for the gain response. However, rapid changes in gain are detrimental to phase linearity. If the group delay passband is wider than the gain passband then the optimization routine will find it very difficult to remain within the template bounds at the edge of the group delay passband when the gain starts to drop off from a frequency point within that region. To avoid this difficulty the optimization routine tends to move the gain cut-off point into the transition band past the group delay passband edge. This is achieved by placing some of the available turning points of the structure in the transition band. This process was hindered by the error point repositioning ideas illustrated in Fig.(4.12). With unequal gain and group delay passband widths, the gain will not necessarily have the maximum attenuation at the edge of its passband. Therefore this modification to the optimization templates was no longer applied for simultaneous design tests.

The final area of research within the lowpass simultaneous design stage involved a comparison with linear phase FIR filters and equalized elliptic IIR filters. Work by Rabiner and Gold[11] tabulated the filter order, mean group delay value and the number of multiplication per sample for a wide range of lowpass specifications for linear phase FIR filters and IIR filters with an elliptic magnitude response and equalizer. Each table listed the results for lowpass specifications with identical attenuation characteristics and different cut-off frequencies. The equalizer method was tabulated for a number of group delay tolerances over a passband that had the same width as the gain passband.

Conclusions from this work indicate that to equalize an elliptic function to a group delay deviation of about 3% requires an increase of approximately 30% in the number of multiplications per sample compared to FIR filter design. It was also noticed that the mean passband group delay value of the equalized circuit was always higher than the FIR cases. The authors make a number of observations about the use of a cascaded second order section IIR filter for simultaneous designs. They suggest that the extra multipliers required to implement the second order section as nonminimum-phase elements for simultaneous designs offsets a reduction in the overall filter order required. From this assumption they found it unlikely that any advantage could be gained from the use of simultaneous designs compared to an equalizer approach.

Results from optimization tests of the lattice WDF to satisfy a number of the Rabiner and Gold lowpass specifications, given in Table(4.10), are tabulated in Table(4.11) along with the equivalent FIR and equalized elliptic parameters.

Spec	Gain passband		Gain stopband		Samp
No.	att (dB)	edge (Hz)	att (dB)	edge (Hz)	freq (Hz)
1	0.1746	0.0502	80	0.20273	1
2	0.1746	0.09846	80	0.25119	1
3	0.3546	0.25	60	0.34153	1
4	0.3546	0.25	60	0.30689	1

Table 4.10 Specifications for comparisons of simultaneous designs with linear phase FIR and equalized elliptic solutions.

In Table(4.11), N represent the order of each filter (in the equalizer case N' is the order of the elliptic filter and N" the equalizer order), M is the number of multiplications required per sample and τ_g is the group delay value. The term τ% indicates group delay tolerance across the passband for that specification.

From the results shown in Table(4.11), it can be seen that the simultaneous lattice WDF solutions have a lower group delay value than the equivalent FIR and equalized filter solutions. The order and number of multiplications per sample of the simultaneous designs are also lower than the FIR cases. This however does not appear to be true for the performance of the simultaneous designs against the equalizer solutions. Although the method of defining the group delay error as a percentage deviation can compensate for different sampling frequencies, it does not accurately reflect the actual width of the group delay error in itself.

Spec No.	FIR filter			Equalized filter					Lattice WDF			
	N	M	τ_g	τ%	N'	N"	M	τ_g	τ%	N	M	τ_g
1	21	11	10	12.1	5	2	11	28.7	12.1	9	9	9.03
				3.4	5	4	13	42.7	3.4	9	9	13.29
2	21	11	10	11.6	5	2	11	14.5	11.6	9	9	8.14
				4.1	5	4	13	22.2	4.1	11	11	6.69
				0.8	5	6	15	29.4	0.8	11	11	9.51
3	29	15	14	37.4	5	2	11	8.4	37.4	9	9	5.47
				21.6	5	4	13	10.6	21.6	11	11	5.37
				11.6	5	6	15	13.7	11.6	11	11	4.78
				5.6	5	8	17	16.9	5.6	13	13	4.51
				2.4	5	10	19	20.3	2.4	13	13	7.85
4	45	23	22	34.7	6	4	14	13.8	34.7	11	11	5.84
				25.0	6	6	16	16.0	25.0	13	13	5.37
				16.9	6	8	18	18.7	16.9	15	15	7.28
				11.7	6	10	20	22.0	11.7	15	15	6.99
				7.9	6	12	22	25.5	7.9	17	17	8.86
				5.2	6	14	24	29.4	5.2	17	17	8.71
				3.2	6	16	26	32.8	3.2	19	19	12.16
				1.8	6	18	28	36.3	1.8	19	19	11.98

Table 4.11 Performance parameters of equivalent simultaneous lattice WDF, linear phase FIR and equalized elliptic structures.

To accurately compare the simultaneous and equalizer design results of Table(4.11) the actual group delay errors need to be determined. All the equalizer solutions possess mean passband group delay values that are approximately three times larger than the equivalent simultaneous values. Therefore despite achieving identical group delay percentage deviations, the performance of the simultaneous solutions is better because they have narrower group delay error widths. Under these conditions the filter orders of Table(4.11) cannot be directly compared but in most cases the simultaneous solutions require a lower filter order than the equalizer designs despite of more stringent group delay tolerances.

Although Table(4.11) does not allow a direct comparison of simultaneous and equalizer designs, it does highlight the differences in group delay values produced under each design approach. In most design examples the mean passband group delay value under the simultaneous approach was lower than the FIR solutions. This feature was especially true for narrow passband widths since the lattice WDF is only concerned with the linearity of the group delay across the passband, while the FIR filter exhibits exactly linear phase over the whole frequency range. The efficiency of the lattice WDF over the FIR filter design reduces as the passband width is increased or the group delay tolerance is very narrow.

Another feature that varied the performance of the simultaneous lattice WDF over the FIR filter was the width of the transition band. Specifications with narrow transition bands required high order FIR filters because of their poor frequency selectivity and exactly linear phase over the whole frequency range. This feature can be seen in Table(4.11), where the relative performance of the lattice WDF increases compared to the FIR filter approach when the width of the transition band of a frequency specification is decreases.

4.5 Lattice WDF design conclusions

The conclusions of this part of the research fall into two areas. The performance of various optimization techniques directed at lattice WDF designs and the suitability of the lattice WDF for simultaneous magnitude and phase designs.

Through computer programs written to design and analyse the lattice WDF a wide range and combination of optimization techniques were investigated. These techniques included different target definitions, weighting procedures, number and distributed of error points, multiplier starting positions and optimization algorithms. Results from both magnitude-only and simultaneous specifications have shown that the more accurately the desired function can be described, the faster the problem will converge. In this way, magnitude-only designs optimized with the ideal line templates converged very quickly. These templates can only be used when the form of the solution is already known and are of little practical use for magnitude-only designs. For simultaneous specifications they offer the best approach of generating the magnitude and group delay responses to a desired shape. However, simultaneous tests using an elliptic function for the ideal gain target and an equi-ripple, equi-spaced group delay target, failed to find any acceptable solutions. These results lead to a conclusion that the characteristics of the elliptic polynomial are contrary to an equi-ripple, equi-spaced group delay response for the lattice structure.

Lack of information about minimum- and nonminimum-phase functions capable of satisfying an arbitrary magnitude and phase specification meant that no ideal line templates could be defined. This reason prompted a more detailed investigation with the straight line templates. Although the single line template scheme proved to be of little practical use for simultaneous designs, the dual line templates performed very well under most filter specifications. With the dual line templates as a basis for further tests, optimization procedures and their parameter values were compared. Of the optimization procedures considered, the most effective for simultaneous designs concerned the introduction of a variable that represented the mean value of a group delay passband template. Optimizing this parameter along with the lattice multiplier values allowed the optimization routines to move the group delay template up and down to find a solution.

Other optimization parameter settings that contributed to an improved convergence rate and filter response shape involve a weighting scheme that worked on an equal deviation/equal error rule, a technique that clustered error points around the region of the template with the most activity, an error function based upon a weighted L_p-metric and quasi-Newton optimization algorithms. From a large number of tests, the importance of defining the transition band accurately also became apparent, even with very narrow transition band widths.

The suitability of the lattice WDF for simultaneous magnitude and phase designs depends on a number of factors. The most important factor is that the structure can be designed to meet an arbitrary simultaneous specification. From the theory outlined in Chapter 1, linear phase can only be achieved with a structure that has a nonminimum-phase characteristic and can place its zeros in reciprocal complex conjugate sets. The results of Section 4.4.2 have shown that this is possible with the lattice WDF structure. The other suitability criteria concern practical design and hardware implementation properties. Other structures, notably the cascaded section order section IIR filter can be designed to satisfy a simultaneous specification. It is therefore the finite wordlength performance and physical hardware models that are of interest in selecting the lattice WDF over any other filter structure.

The lattice WDF considered in this research is constructed from first and second order APS's. These sections, detailed in Section 4.2, are very simple in structure and possess good dynamic range and scaling properties. The regular nature of the lattice structure means that any hardware implementation need only construct a single section and then data and multiplier values multiplexed into it. A more detailed discussion of these hardware ideas and the VLSI implications for the lattice WDF was provided by Matharu[8]. Conclusions of this research indicate that the lattice WDF is a very efficient structure from a hardware implementation point of view.

The final consideration with the use of the lattice WDF is that simultaneous designs represent the most efficient method of satisfying a magnitude and phase specification. Designs requiring exactly linear phase can only be satisfied by FIR filters. However, a small tolerance in the phase linearity can allow a large reduction in the filter order and its operation speed. Use of a WDF structure ensures a good finite wordlength performance and results have confirmed that a simultaneous design approach requires a lower order than with equalizer techniques.

From all the properties considered, simultaneous designs on the lattice WDF structure based upon first and second order APS's does represent the most effective method of satisfying an arbitrary magnitude and phase specification. Research up to this point has been directed at generating lowpass filter lattice coefficient values that have a large accuracy. Work detailed in Chapter 5 concerns the methods of achieving highpass, bandpass and bandstop versions of the lattice WDF, while Chapter 6 details the optimization procedures and performance of lattice WDF's satisfying finite wordlength constraints.

References

1) Fettweis, A., "Digital Filter Structures Related to Classical Filter Network", Arch. Elek. Übertrag., Vol 25, 1971, pp79-89.

2) Fettweis, A., Levin, H. and Sedlmeyer, A., "Wave Digital Lattice Filters", Int J. Cir. Theory and Applications, Vol 2, 1974, pp203-211.

3) Fettweis, A., "Wave Digital Filters: Theory and Practice", Proc IEEE, Vol 74, No. 2, February 1986, pp270-327.

4) Gazsi, L., "Explicit Formulas for Lattice Wave Digital Filters", IEEE Trans. Circuits and Systems, Vol CAS-32, No. 1, January 1985, pp68-88.

5) Guillemin, E. A., `Synthesis of passive networks`, John Wiley and Sons, London, 1957.

6) Kunold, I., "Linear Phase Realization of Wave Digital Lattice Filters", Proc. Euro. Conf. Circuit Theory and Design, No. 308, September 1989, pp512-516.

7) Leeb, F. and Henk, T., "Simultaneous Approximation for Bireciprocal Lattice Wave Digital Filters", Proc. Euro. Conf. Circuit Theory and Design, No. 308, September 1989, pp473-476.

8) Matharu, P. S., "Architectures for the VLSI Implementation of Digital Filters", Ph. D. Thesis, The City University, 1988.

9) `MatLab`, MathWorks Inc, Portola Valley, California, 1985.

10) Mitra, S. K. and Hirano, K., "Digital All-Pass Networks", IEEE Trans. Circuits and Systems, Vol CAS-21, No. 9, September 1974, pp688-700.

11) Rabiner, L. R. and Gold, B., Theory and Application of Digital Signal Processing, Prentice-Hall, New Jersey, 1975.

12) Renfors, M. and Zigouris, E., "Signal Processor Implementation of Digital All-Pass Filters", IEEE Trans. Acoustics, Speech and Signal Processing, Vol ASSP-36, No. 5, May 1988, pp714-729.

Chapter 5

WDF Frequency Transformations

The object of this Chapter is to outline the theory and design procedures behind WDF frequency transformations and lattice WDF structures that can exhibit highpass, bandpass, bandstop, dual bandpass and dual bandstop type responses. The equations and models for these transformed WDF structures are developed and related to the original lowpass structure. The characteristics of the various frequency transforms are detailed through a design example that converts a lowpass solution into the various filter types considered. The Chapter ends with a discussion of the design and optimization considerations for these transformed lattice WDF structures in satisfying magnitude-only and simultaneous specifications. The implications of these design and optimization considerations are highlighted through a number of examples.

5.1 Frequency Transforms

The purpose of a frequency transform is to alter the transfer function of a lowpass filter to produce a circuit with a highpass, bandpass or bandstop type response. The principle of a frequency transform is to shift and/or scale the frequency axis of a filter's response. The action of modifying the frequency axis of a lowpass response can be seen through Fig.(5.1) and Fig.(5.2).

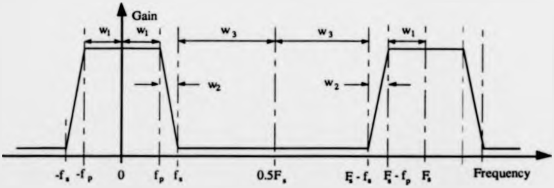

Figure 5.1 General digital lowpass gain response.

A shift of half the sampling frequency, F_s, transforms the lowpass response of Fig.(5.1) into the highpass response shown in Fig.(5.2)(a). The bandstop response, shown by Fig.(5.2)(b), is achieved by doubling the sampling frequency of the lowpass response, while the bandpass response of Fig.(5.2)(c) is produced through a frequency shift and scaling.

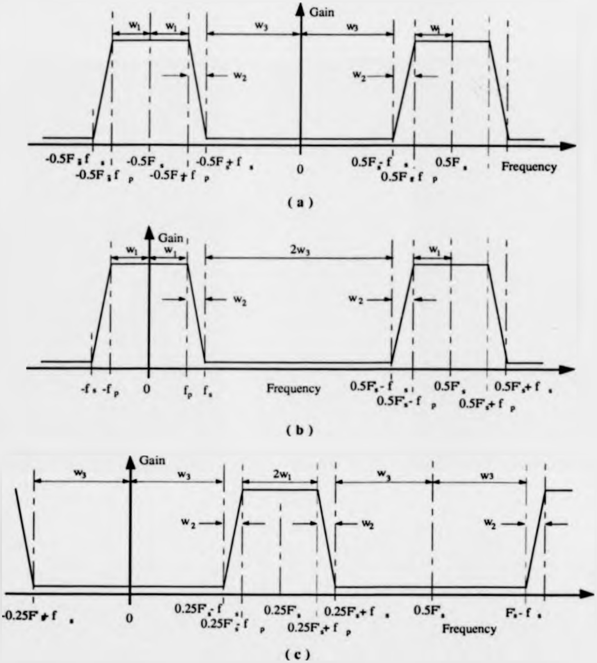

Figure 5.2 Frequency transformations applied to a lowpass response to produce equivalent (a) highpass, (b) bandstop and (c) bandpass responses.

A frequency transform is applied to the transfer function of a filter by replacing each frequency dependent variable with a new frequency dependent function. The frequency shift of $0.5F_s$ that produces a lowpass-highpass transformation corresponds to the substitution shown by Eq.(5.1).

$$z^{-1} \Rightarrow -z^{-1} \tag{5.1}$$

The lowpass-bandstop transform can be described as

$$z^{-1} \Rightarrow z^{-2} \tag{5.2}$$

while the lowpass-bandpass transform can be expressed as

$$z^{-1} \Rightarrow -z^{-2} \tag{5.3}$$

All the transforms described by Eq.(5.1) - Eq.(5.3) are very simple functions that do not alter the relative passband and stopband widths and generate symmetric bandpass and bandstop type responses. Modifying the width and cut-off frequencies of a filter's response requires a more complicated set of frequency transformations.

The general specification for a lowpass-highpass transform is illustrated by Fig.(5.3).

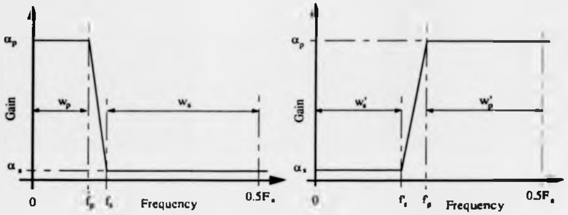

(a) (b)

Figure 5.3 General lowpass-highpass transform specification.

The equation of a lowpass-highpass transformation able to achieve the conversion shown by Fig.(5.3), is well known in analogue filter designs[6] and has been adapted to digital designs by Constantinides[2]. This transform is given in Eq.(5.4).

$$z^{-1} \Rightarrow -\left(\frac{z^{-1} + \alpha}{1 + \alpha z^{-1}}\right) \tag{5.4}$$

where

$$\alpha = -\left(\frac{\cos(\pi(f_p - f'_p)T)}{\cos(\pi(f_p + f'_p)T)}\right)$$

If the desired highpass response has the same passband width as the reference lowpass response, such that for Fig.(5.3) $w_p = w'_p$, then $\alpha \Rightarrow 0$ and Eq.(5.4) reduces to the simple transform of Eq.(5.1).

The general lowpass-bandpass transformation specification is illustrated by Fig.(5.4) and can be produced through the transform shown in Eq.(5.5).

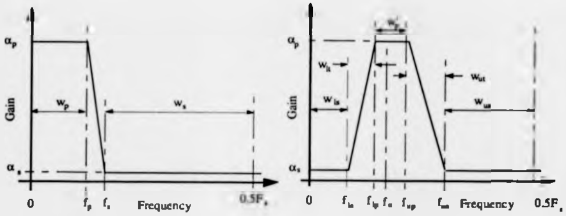

(a) (b)

Figure 5.4 General lowpass-bandpass transform specification.

$$z^{-1} \Rightarrow -\left(\frac{z^{-2} - \left(\frac{2\alpha k}{k+1}\right) z^{-1} + \left(\frac{k-1}{k+1}\right)}{\left(\frac{k-1}{k+1}\right) z^{-2} - \left(\frac{2\alpha k}{k+1}\right) z^{-1} + 1} \right) \tag{5.5}$$

where

$$\alpha = \left(\frac{\cos(\pi(f_{up} - f_{lp})T)}{\cos(\pi(f_{up} + f_{lp})T)} \right) \text{ and } k = \cot\left(\pi(f_{up} - f_{lp})T\right) \tan\left(\pi f_p T\right)$$

Within the transform of Eq.(5.5), the parameter α is responsible for moving the centre of the passband, shown by the frequency point f_o in Fig.(5.4)(b), while k varies the width of the passband, w'_p. If the required passband width for the bandpass response, w'_p, is equal to the passband width of the lowpass prototype, w_p, then $k \Rightarrow 1$ and Eq.(5.5) reduces to Eq.(5.6).

$$z^{-1} \Rightarrow -z^{-1}\left(\frac{z^{-1} - \alpha}{1 - \alpha z^{-1}}\right) \tag{5.6}$$

where

$$\alpha = \cos\left(2 \pi f_o T\right) = \left(\frac{\cos(\pi(f_{up} - f_{lp})T)}{\cos(\pi(f_{up} + f_{lp})T)} \right)$$

If a symmetric bandpass response is required, the centre frequency $f_o = 1/4T$ so $\alpha \Rightarrow 0$ and Eq.(5.6) will simplify to the frequency transform of Eq.(5.3).

The general lowpass-bandstop frequency transformation, shown by Fig.(5.5), has equations that are detailed in Eq.(5.7) and Eq.(5.8).

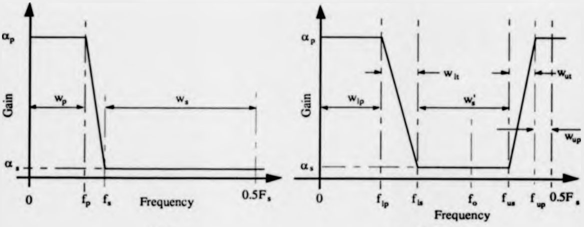

(a) (b)

Figure 5.5 General lowpass-bandstop transform specification.

$$z^{-1} \Rightarrow \left(\frac{z^{-2} - \left(\frac{2\alpha k}{k+1}\right) z^{-1} + \left(\frac{k-1}{k+1}\right)}{\left(\frac{k-1}{k+1}\right) z^{-2} - \left(\frac{2\alpha k}{k+1}\right) z^{-1} + 1} \right) \tag{5.7}$$

where

$$\alpha = \left(\frac{\cos(\pi(f_{up} - f_{lp})T)}{\cos(\pi(f_{up} + f_{lp})T)} \right) \text{ and } k = \tan\big(\pi(f_{up} - f_{lp})T\big) \tan\big(\pi f_p T\big)$$

Within Fig.(5.5), when $w_{lp} + w_{up} = w_p$ then $k \Rightarrow 1$ and the transform of Eq.(5.7) reduces to Eq.(5.8).

$$z^{-1} \Rightarrow z^{-1} \left(\frac{z^{-1} - \alpha}{1 - \alpha z^{-1}} \right) \tag{5.8}$$

where

$$\alpha = \cos\big(2 \pi f_o T\big) = \left(\frac{\cos(\pi(f_{up} - f_{lp})T)}{\cos(\pi(f_{up} + f_{lp})T)} \right)$$

Again when the centre frequency of the bandstop response is such that $f_o = 1/4T$, then $\alpha \Rightarrow 0$ and the frequency transform of Eq.(5.8) simplifies to Eq.(5.2).

The objective of this area of research was to derive WDF structures that can exhibit various filter response types. Authors have approached WDF frequency transformations from a number of different angles. These methods may be grouped into three main approaches. The first method starts with an analogue lowpass DTL network, generates an equivalent highpass, bandpass or bandstop analogue DTL circuit and then derives a WDF circuit from this reference structure.

This approach was discussed in Chapter 3 for highpass and bandpass ladder WDF designs. The next method also starts with an analogue lowpass DTL network but applies the appropriate frequency transformation in conjunction with the WDF equations to the elements of the circuit to produce a transformed WDF component. With these elements a transformed WDF structure could be constructed. This technique was outlined by Ali[1] and Swamy and Thyagarajan[7].

The final design method entails describing freuuency transformations in terms of WDF elements. This approach, followed by Lawson[4] and Güllüoglu[3], is possible because of the form of the frequency transforms given in Eq.(5.1), Eq.(5.6) and Eq.(5.8). With this design technique a lowpass WDF structure can be converted into a highpass WDF structure by adding a -1 multiplier to each delay unit because the transform of Eq.(5.1) replaces z^{-1} with $-z^{-1}$. The frequency transforms of Eq.(5.6) and Eq.(5.8) represent the transfer function of a two-port adaptor connected to a single delay element. Therefore bandpass and bandstop designs are possible by replacing every unit delay of the lowpass prototype with a first order APS and a unit delay. The difference between the bandpass and bandstop transforms of Eq.(5.6) and Eq.(5.8) means that all bandpass modifications would also have to include a -1 multiplier.

Of the frequency transformation method considered, the one proposed by Lawson offers the most versatile approach as it removes the need for the design of a reference DTL circuit. With this technique it is also very easy to generate the components for multiple band filter specifications, especially the APS's required for lattice WDF structures.

5.2 Frequency transformed lattice WDF elements.

The research into frequency transforms and finite wordlength effects was based upon the lattice WDF structure. This structure, shown by Fig.(5.6), has its canonic reflectances constructed as a cascade of first and second order APS's.

The lowpass lattice WDF structure considered in Chapter 4 used the first and second order APS's that were detailed in Section 4.2.2. Lattice WDF structures that would be capable of exhibiting highpass, bandpass or bandstop type responses would have the same structure as that shown in Fig.(5.6) but would be constructed from APS's that were the appropriate frequency transformed versions of the first and second order APS's of the lowpass circuit.

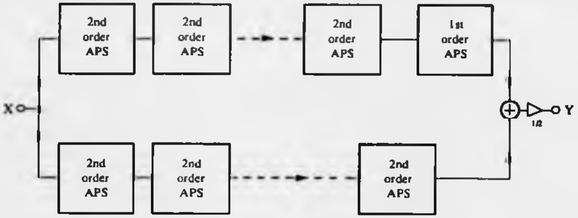

Figure 5.6 Lattice WDF structure.

Any lattice WDF structures derived would have their multiplier values determined through optimization. The optimization targets used to generate these values would be defined by the cut-off frequencies and passband widths of the filter's response. Therefore because the passband widths for a particular specification would be calculated directly, frequency transformations that alter passband widths would not be required. Under this condition Eq.(5.1) is sufficient for lowpass-highpass transformations, while Eq.(5.6) and Eq.(5.8) are adequate for bandpass and bandstop transforms as they move the centre frequency point but do not alter the passband widths.

Using the lowpass-highpass transform of Eq.(5.1) it is easy to develop the first and second order APS's of a highpass lattice WDF structure. The lowpass APS's are shown by Fig.(5.7), while the equivalent highpass APS's are illustrated by Fig.(5.8).

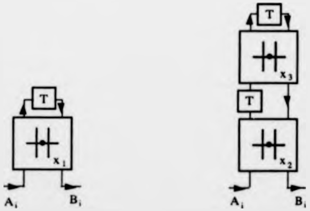

(a) (b)

Figure 5.7 Lowpass (a) first and (b) second order APS's.

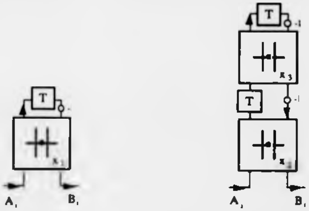

(a) (b)

Figure 5.8 Highpass (a) first and (b) second order APS's.

The lowpass-bandpass transform of Eq.(5.6) and lowpass-bandstop transform of Eq.(5.8) only differ by a minus sign and therefore the equivalent first and second order APS's will only differ by the inclusion or exclusion of a -1 multiplier. The action of the two frequency transforms of Eq.(5.6) and Eq.(5.8) is to replace each unit delay of an APS with a two-port adaptor and a unit delay. Applying this procedure to the first and second order APS's of Fig.(5.7) results in the bandpass and bandstop APS's shown by Fig.(5.9). For these APS's, the bandpass models require the extra -1 multipliers while the bandstop elements do not.

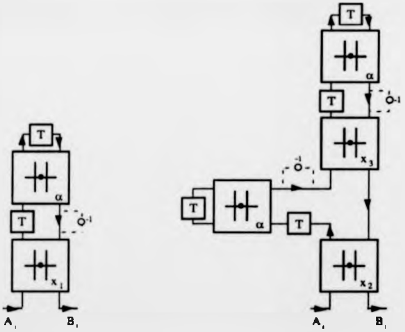

(a) (b)

Figure 5.9 Bandpass and bandstop (a) 2nd and (b) 4th order APS's.

The APS's of Fig.(5.9) are second and fourth order elements where parameters x_1, x_2 and x_3 represent the section's multipliers and α an element that moves the centre point of the bandpass or bandstop response. This factor, defined in Eq.(5.6) and Eq.(5.8), would be determined for a given frequency specification and then the same value applied to each APS of a circuit.

The frequency transformation ideas of Eq.(5.6) and Eq.(5.8) can be used to extend the lattice WDF structure to multiple band type responses. Therefore if Eq.(5.6) and Eq.(5.8) were applied to the bandpass and bandstop APS's of Fig.(5.9), then dual bandpass and dual bandstop APS's could be designed. These dual bandpass and dual bandstop APS's will, again, only differ by the inclusion or exclusion of -1 multipliers. The transformed APS's for these dual band lattice WDF structures are shown by Fig.(5.10), where the parameters α and β are calculated to independently shift the position of the two bands of the response.

Dual bandpass lattice WDF structures will be based upon the fourth and eighth order APS's of Fig.(5.10) which include the -1 multipliers, while the dual bandstop circuit will use the APS's of Fig.(5.10) without these extra multipliers.

In all design cases the lattice WDF structure is based upon the circuit of Fig.(5.6) with the appropriate transformed first and second order APS's. Because of this, each circuit can be described by the overall lattice WDF equations derived in Section 4.2.1 of the Chapter 4. The only parameters that will differ are the transfer functions and derivatives of the various APS's. To evaluate the gain, phase and group delay responses of the highpass, bandpass and bandstop structures, the parameters derived for the lowpass first and second order APS's in Section 4.2.2 must be determined for the APS's of Fig.(5.8), Fig.(5.9) and Fig.(5.10).

The transfer function of the various APS's can be derived from the scattering matrix of the two-port adaptor and wave parameter relationships. An alternative to this design approach is to use the transforms of Eq.(5.1), Eq.(5.6) and Eq.(5.8) on the transfer functions of the APS of the lowpass structure. Both methods produce identical results.

The design equations of the APS's for the highpass and single and dual bandpass and bandstop lattice WDF structures were determined through a symbolic mathematical computer program called Mathematica[5]. These equations are detailed in Appendix C1 - C5.

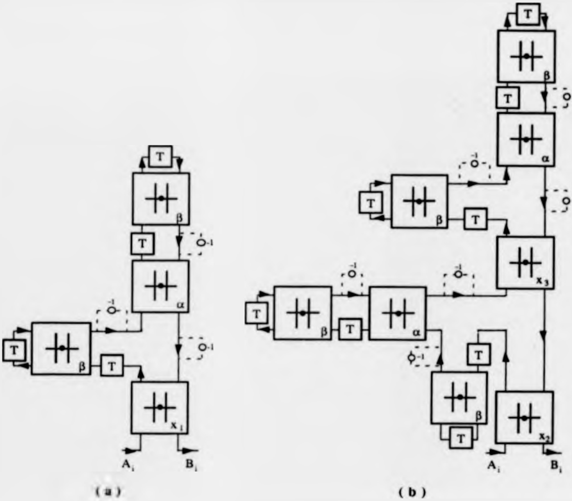

Figure 5.10 Dual bandpass and bandstop (a) 4th and (b) 8th order APS's.

5.3 Characteristics of frequency transformations

To investigate the behaviour and properties of the various transformed lattice WDF structures, their equations were included within the design program, "WDF". This design program automatically calls the appropriate APS's for a given frequency specification, allowing highpass, single and dual bandpass and bandstop filters to be created and analysed.

To illustrate the characteristics of the various frequency transforms, the multiplier values of a lowpass filter, Fig.(5.11), that satisfied the simultaneous specification of Table(5.1), were applied to equivalent highpass and single and dual bandpass and bandstop lattice WDF structures. This set of multipliers is given in Table(5.2).

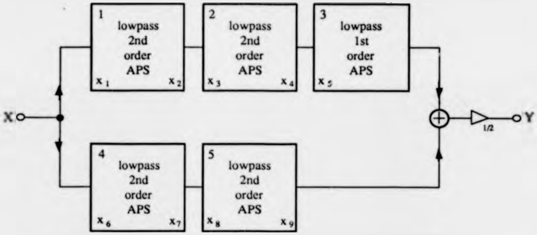

Figure 5.11 9th order lowpass lattice WDF structure.

Gain passband		Gain stopband		Delay passband		Samp.
att (dB)	edge (Hz)	att (dB)	edge (Hz)	dev (%)	edge (Hz)	freq (Hz)
0.1	0.08	34	0.16	0.5	0.09	1

Table 5.1 Simultaneous lowpass filter specification.

Upper lattice arm			Lower lattice arm		
APS No.	APS type	multiplier values	APS No.	APS type	multiplier values
1	2nd	$x_1 =$ -0.8828314045 $x_2 =$ 0.6172207384	4	2nd	$x_6 =$ -0.7152976626 $x_7 =$ 0.6370727390
2	2nd	$x_3 =$ -0.5456894656 $x_4 =$ 0.8245115507	5	2nd	$x_8 =$ -0.4759607014 $x_9 =$ 0.9079765957
3	1st	$x_5 =$ 0.6571687539			

Table 5.2 Lowpass lattice WDF multiplier values
that satisfy the specification of Table(5.1).

The first step of the investigation concerned the simple frequency transforms shown in Table(5.3). The magnitude response of the 9th order lowpass lattice WDF, using the multiplier values from Table(5.2), is shown in Fig.(5.12)(a). Fig.(5.12) also shows the magnitude response of the equivalent filter structures that were generated with the transforms of Table(5.3) and using the multipliers of Table(5.2).

Lowpass response to	Simple frequency transform
Highpass	$z^{-1} \Rightarrow -z^{-1}$
Bandpass (single)	$z^{-1} \Rightarrow -z^{-2}$
Bandstop (single)	$z^{-1} \Rightarrow z^{-2}$
Bandpass (dual)	$z^{-1} \Rightarrow -z^{-4}$
Bandstop (dual)	$z^{-1} \Rightarrow z^{-4}$

Table 5.3 Simple frequency transforms.

From Fig.(5.12) it can be seen that the frequency transformations of Table(5.3) retain the amplitude characteristics of the original lowpass response, exhibiting identical passband and stopband widths and attenuations. The phase linearity of these frequency transformations can be observed through the group delay responses. The group delay responses for the original lowpass lattice WDF and the five structures constructed through the transforms of Table(5.3) are illustrated in Fig.(5.13). The poles and zeros of these WDF structures are shown in Fig.(5.14).

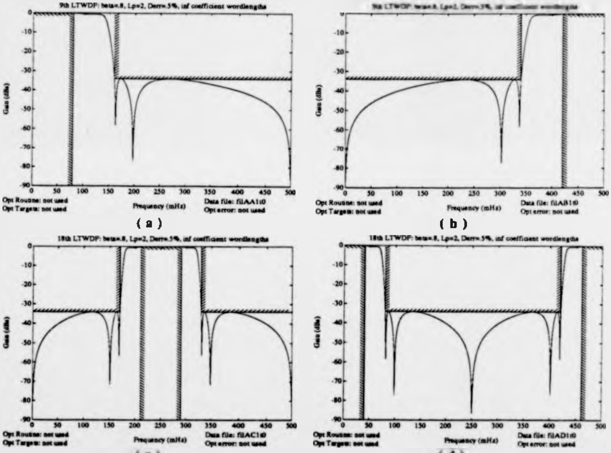

(a) (b)

(c) (d)

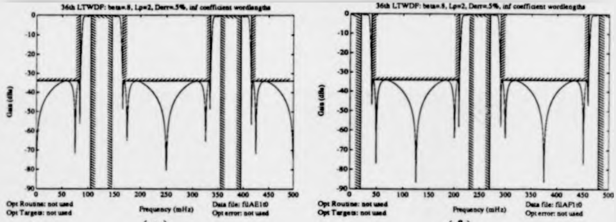

(e) (f)

Figure 5.12 Magnitude responses of equivalent (a) lowpass, (b) highpass, (c) bandpass, (d) bandstop, (e) dual bandpass and (f) dual bandstop filters.

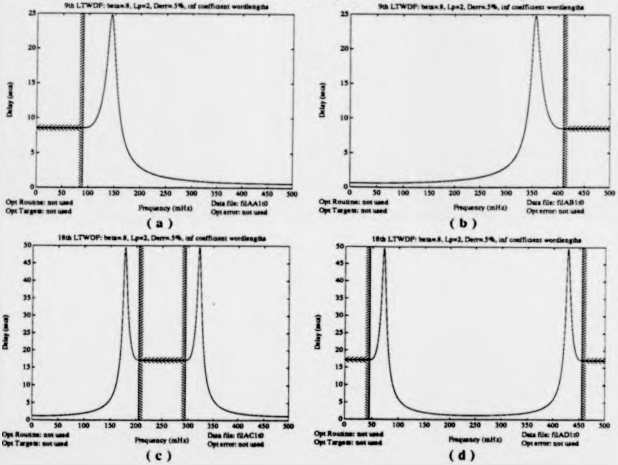

(a) (b)

(c) (d)

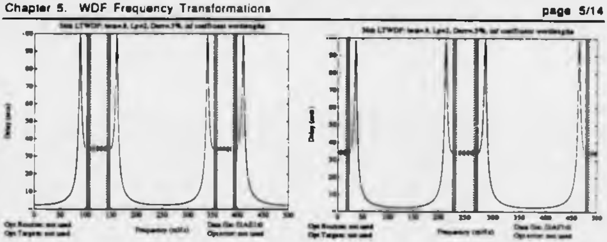

(e) (f)

Figure 5.13 Group delay responses of equivalent (a) lowpass, (b) highpass, (c) bandpass, (d) bandstop, (e) dual bandpass and (f) dual bandstop filters.

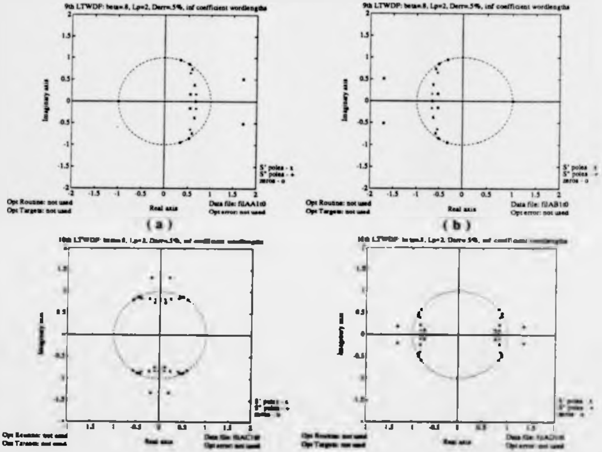

(a) (b)

(c) (d)

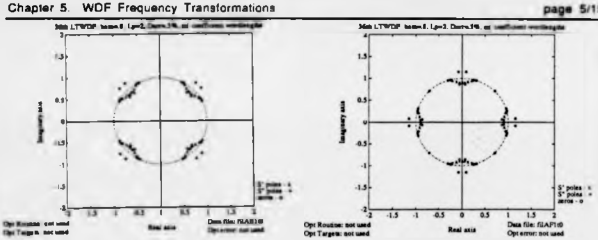

(e) (f)

Figure 5.14 Pole/zero plots of equivalent (a) lowpass, (b) highpass, (c) bandpass, (d) bandstop, (e) dual bandpass and (f) dual bandstop filters.

From the responses shown in Fig.(5.13) and Fig.(5.14), it can be seen that the frequency transforms of Table(5.3) are linear in their effect upon the phase of the structure. Therefore a lattice WDF derived from a linear phase lowpass prototype through the transforms of Table(5.3), will also exhibit linear phase.

The next stage of the investigation involved frequency transformations that moved the centre point of a bandpass or bandstop type response. Using the lowpass prototype of Fig.(5.11), equivalent single and dual band lattice WDF structures were constructed from the various APS's described in Section 5.2. Each lattice structure was then implemented with the multiplier values contained in Table(5.2). Along with the asymmetric frequency transformations, Table(5.4) contains the transformation values applied to the example structures and the Figure numbers associated with the frequency responses of these examples.

Lowpass to	Frequency transforms	α value	β value	Fig No.
Bandpass (single)	$z^{-1} \Rightarrow \quad -z^{-1}\left(\frac{-\alpha + z^{-1}}{1 - \alpha z^{-1}}\right)$	0.8090	/	5.17
Bandstop (single)	$z^{-1} \Rightarrow \quad z^{-1}\left(\frac{-\alpha + z^{-1}}{1 - \alpha z^{-1}}\right)$	-0.1874	/	5.18
Bandpass (dual)	$z^{-1} \Rightarrow \quad -z^{-1}\left(\frac{-\alpha\beta+(\alpha+\beta^2(1+\alpha))z^{-1}-\beta(2+\alpha)z^{-2}+z^{-3}}{1-\beta(2+\alpha)z^{-1}+(\alpha+\beta^2(1+\alpha))z^{-2}-\alpha\beta z^{-3}}\right)$	0.8090	-0.5878	5.19
Bandstop (dual)	$z^{-1} \Rightarrow \quad z^{-1}\left(\frac{\alpha\beta-(\alpha-\beta^2(1-\alpha))z^{-1}-\beta(2-\alpha)z^{-2}+z^{-3}}{1-\beta(2-\alpha)z^{-1}-(\alpha-\beta^2(1-\alpha))z^{-2}+\alpha\beta z^{-3}}\right)$	0.3090	-0.3090	5.20

Table 5.4 Single and multiple band frequency transforms.

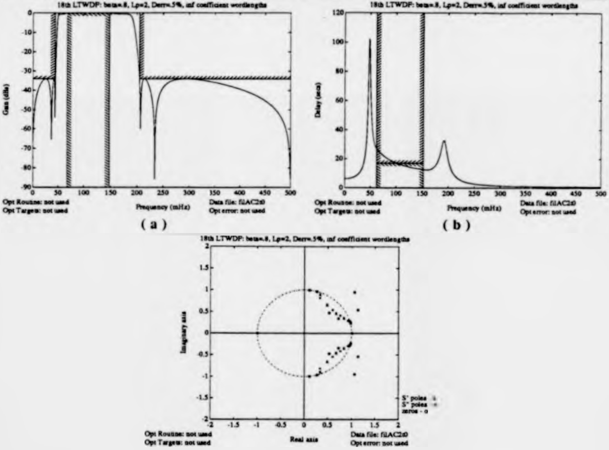

(a) (b)

(c)

Figure 5.15 Asymmetric single bandpass (a) magnitude and (b) group delay responses with (c) pole/zero plot.

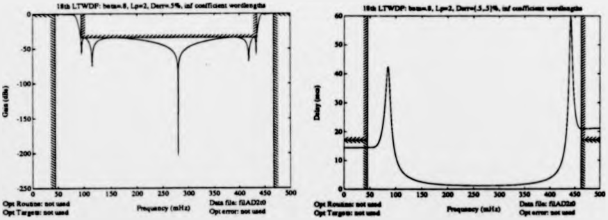

(a) (b)

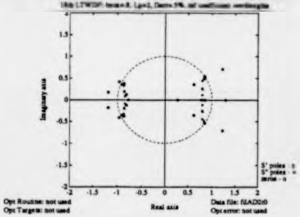

(c)

Figure 5.16 Asymmetric single bandstop (a) magnitude and (b) group delay responses with (c) pole/zero plot.

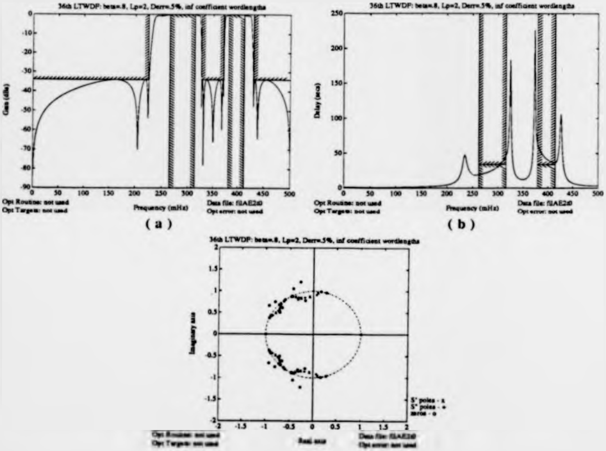

(a) (b)

(c)

Figure 5.17 Asymmetric dual bandpass (a) magnitude and (b) group delay responses with (c) pole/zero plot.

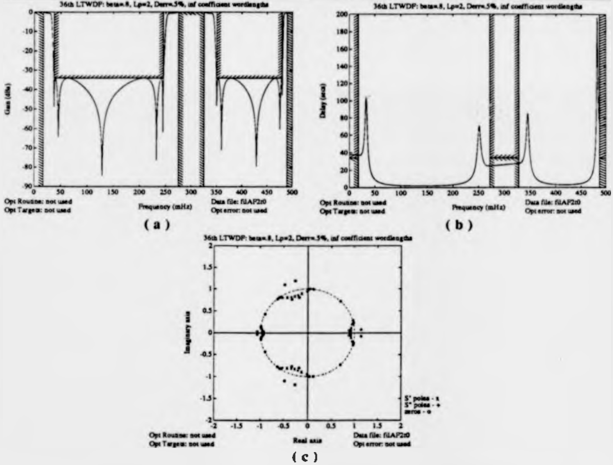

Figure 5.18 Asymmetric dual bandstop (a) magnitude and (b) group delay responses with (c) pole/zero plot.

Comparing the magnitude response of the symmetric bandpass filter of Fig.(5.12)(c) with the asymmetric response of Fig.(5.15)(a), then it can be seen that the frequency transformation of Table(5.4) retains the passband width and attenuation levels of the response but alters the widths of the transition bands and stopbands. This effect is also noticeable in the magnitude responses of the other asymmetric filters, shown by Fig.(5.16)(a), Fig.(5.17)(a) and Fig.(5.18)(a).

Comparing the frequency responses of the symmetric and asymmetric bandpass and bandstop examples, it can be observed that the transforms of Table(5.4) also distort the group delay responses. The main effect of this distortion can be observed by comparing the single bandpass symmetric and asymmetric group delay responses, shown by Fig.(5.13)(c) and Fig.(5.17)(b) respectively. In these group delay responses, the asymmetric frequency transformations have introduced an incline to the passband region of the response. The angle of this incline increases as the centre of the passband is moved away from the centre of the responses. Therefore the more asymmetric the response, the larger the group delay distortion due to the frequency transformation.

The effects of the asymmetric frequency transformations can also be observed in the position of a filter's poles and zeros. To illustrate these effects the pole/zero plots of the single bandpass WDF under the symmetric and asymmetric frequency transformations are shown in Fig.(5.19) with their frequency specifications. Both examples were implemented with identical multiplier values and exhibit equivalent frequency responses except that the centre of the asymmetric bandpass response has been shifted to a frequency of 0.1 Hz.

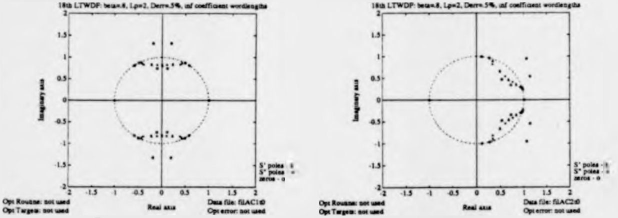

Figure 5.19 Pole/zero plot of equivalent asymmetric and symmetric bandpass filters.

The zeros of the linear phase symmetric bandpass filter, shown by Fig.(5.19)(a), exist in reciprocal complex conjugate sets. This feature was expected from lowpass linear phase designs. The zeros also possess a symmetry about the centre of the passband, which is the imaginary axis for the symmetric bandpass response. Observations of the non-linear phase asymmetric bandpass filter, Fig.(5.19)(b), revealed that the zeros also exist in reciprocal complex conjugate sets. This feature is contrary to expectation as the structure does not exhibit linear phase. Another observation about the zeros of Fig.(5.19)(b) is that they were no longer symmetric about the centre of the passband.

From these observations the requirements for linear phase bandpass filters cannot be expressed in terms of ensuring zeros exist in reciprocal complex conjugate sets but as reciprocal sets that are symmetric about the centre of the passband(s) of the response. This lack of zero symmetry and phase non-linearity can also be seen in the pole/zero plots of the other asymmetric filter examples, shown by Fig.(5.16)(c), Fig.(5.17)(c) and Fig.(5.18)(c).

The final stage of the asymmetric frequency transformation investigation was to characterise the movement of frequency points under the transforms. Fig.(5.20) shows the passband magnitude response of the symmetric and asymmetric single bandpass filter considered previously.

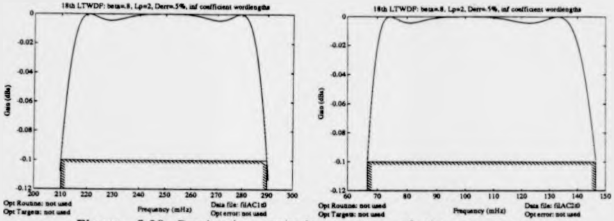

Figure 5.20 Passband magnitude response of the asymmetric and symmetric bandpass filters.

The action of the asymmetric transforms of Table(5.4) is not to shift a response along the frequency axis but to compress one half the response and expand the other half. The effect of this compression and expansion can be seen in Fig.(5.20) and between Fig.(5.12)(c) and Fig.(5.15)(a). For the asymmetric bandpass example considered, the centre of the response is moved to a frequency of 0.1 Hz, while the centre of the symmetric response is at 0.25 Hz. From the passband magnitude responses of Fig.(5.20)(b) it can be seen that the distances from the centre of the response to the edges of the passband are unequal. This is the result of compressing the 0 - 0.25 Hz region of the symmetric bandpass response into the 0 - 0.1 Hz range and expanding the 0.25 - 0.5 Hz region to fit the 0.1 - 0.5 Hz area of the asymmetric bandpass response.

The nature of the asymmetric lowpass-bandpass frequency transformation can be determined if the frequency mapping is described analytically. This can be achieved by expressing the transform in terms of a lowpass frequency variable and an equivalent bandpass frequency variable. This procedure is illustrated in Eq.(5.9), where the z transform within the lowpass-bandpass transform of Table(5.4), is represented in terms of its complex exponential.

$$e^{-j\omega} = -e^{-j\omega'}\left(\frac{-\alpha + e^{-j\omega'}}{1 - \alpha e^{-j\omega'}}\right) \tag{5.9}$$

where

$\alpha = \cos\left(\omega_0 T\right)$ ω_0 centre frequency value

ω lowpass prototype frequency ω' asymmetric bandpass frequency

Eq.(5.9) cannot be solved analytically for ω' but simplifying it to Eq.(5.10) allows ω' to be found iteratively for a particular value of ω and transformation value, α.

$$\cos(\omega T) = \frac{2 \sin^2(\omega' T)}{1 - 2\alpha\cos(\omega' T) + \alpha^2} - 1 \tag{5.10}$$

Using Eq.(5.10) the equivalent frequency specification for the asymmetric bandpass filter can be determined along with the symmetric specification by setting $\alpha = 0$. The filter specifications for the symmetric and asymmetric bandpass examples considered are detailed in Table(5.5), together with the original lowpass specification.

filter type	Atten (dB)		α value	Frequency edges (Hz)	f_0 (Hz)
	pass	stop			
lowpass	0.1	34	/	0 → 0.08 → 0.16 → 0.5	/
bandpass (symmetric)	0.1	34	0	0 → 0.17 → 0.21 → 0.29 → 0.33 → 0.5	0.25
bandpass (asymmetric)	0.1	34	0.809	0 → 0.044 → 0.066 → 0.146 → 0.203 → 0.5	0.1

Table 5.5 Filter specification for a lowpass filter with symmetric and asymmetric bandpass equivalents.

The frequency mapping of the other asymmetric frequency transformations of Table(5.4) can be determined in a similar manner as the bandpass transform by expressing the lowpass frequency variable in terms of the transformed frequency variable.

The characteristics of the frequency transformations considered can be grouped by their effects on the magnitude and phase responses. The simple transforms of Table(5.3) are linear in their modification of the magnitude and phase responses. The transformed magnitude responses retain their passband and stopband attenuations and maintain the widths of the various passbands, stopbands and transition bands. The linearity of these simple transforms also ensures that a linear phase lowpass response will produce a transformed filter with linear phase.

The frequency transformations of Table(5.4), which allow asymmetric filter responses, produce non-linear effects on both the magnitude and group delay responses. Under the asymmetric frequency transformations the magnitude response retains their passband and stopband attenuations and passband widths but experience distortion of the width of each transition band. The most severe effect of the asymmetric frequency transforms is the distortion introduced to the group delay response. Therefore a linear phase lowpass response will not transform into a linear phase asymmetric band type response.

The non-linear characteristics of the asymmetric frequency transformations of Table(5.4) impose a design limitation upon arbitrary magnitude and linear phase specifications. Due to these limitations an asymmetric band type response that requires equal transition band widths and linear phase cannot be derived from a lowpass prototype. Two design methods can be implemented to counteract the non-linear effects of the frequency transforms. The first design method would be based upon a lowpass prototype optimized to satisfy the magnitude and a pre-distorted group delay response. To ensure the gain response possessed equal transition band widths the transformation value for each section would also be optimized. The alternative method would be to optimize the multiplier and transformation values directly on the appropriate filter structure. The implications of these two design approaches are discussed in Section 5.4.

5.4 Design considerations with frequency transforms

The initial part of this research investigated the design options involved in satisfying arbitrary magnitude and phase specifications. Conclusions of this work suggested a lattice WDF structure whose multiplier values were determined through optimization. The optimization techniques developed for this problem were based upon dual line templates, a weighted L_p-metric error function and quasi-Newton algorithms. The general nature of the dual line templates and the error function allowed them to be extended from lowpass specifications to cover highpass, bandpass and bandstop type responses. It was therefore upon the lattice WDF structure and the dual line optimization techniques that the design of frequency transformed structures was approached.

5.4.1 Design approaches

Using the dual line templates and a weighted L_p-metric error function meant that the only design parameter that needed to be addressed was the use of the frequency transformations. Of main concern was the non-linearity of the general frequency transformations and a method under which they should be applied. Two methods exist, either incorporate the non-linearities of a particular transform into a lowpass specification and then convert the lowpass solution into the appropriate response, or design the required frequency specification directly on the transformed lattice structure.

The direct design approach is a more efficient technique as it eliminates the need to determine the distortion effects of each possible frequency transformation. This method also allows the effects of finite wordlength criteria to be measured directly, a factor that will become important when finite wordlength designs are considered.

The final design consideration with the frequency transformations is the actual values applied to the APS's of the lattice structure. The APS's and frequency transformations considered use the same transformation value for each APS within the lattice structure. Applying a different transformation value to each APS may improve the versatility of the structure. This procedure would allow the cut-off point of each APS of a transformed structure to be adjusted to satisfy an asymmetric frequency specification with equal transition band widths. Following this idea a transformed bandpass structure would contain a number of independent multipliers equal to the order of the equivalent lowpass structure plus an extra multiplier per APS. Therefore the single bandpass 2^{nd} order APS, shown by Fig.(2.21)(a) would contain two independent multipliers while the fourth order APS of Fig.(2.21)(b) would possess three independent multipliers.

If a 7^{th} order lowpass lattice WDF was transformed into a single bandpass structure then its order would be 14^{th} with three 4^{th} order APS's and one 2^{nd} order APS. When the same frequency transformation value is used within the bandpass structure, there would only be seven independent multipliers. If a different transformation value was applied to each APS then the number of independent multipliers would increase to eleven since there are four APS's within the structure.

Extending this idea from single band to dual band structures, then an 8^{th} order APS would only contain four independent multipliers, two coefficient values, x_2 and x_3 and two frequency transforms, α and β, shown in Fig.(5.10). Transforming a 7^{th} order lowpass filter into a 28^{th} order dual bandpass/bandstop structure would only require seven independent multipliers if the same frequency transformation value was applied to each APS. However when different transformation values were applied to each APS, the total number of independent multipliers would increase to fifteen.

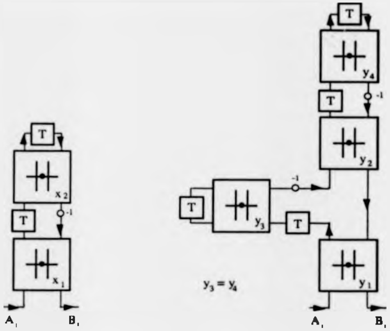

(a) (b)

Figure 5.21 General bandpass (a) 2^{nd} and (b) 4^{th} order APS's.

5.4.2 Optimization considerations

The lowpass optimization techniques based upon a weighted L_p-metric and dual line templates were very easy to extend to an arbitrary frequency response type. The only extra parameters required for these optimization procedures involved the transformed lattice WDF structures, the transformation values for these structures and the valid bounds for these values. The frequency responses and derivatives for the transformed structures can be determined from the design equations detailed in Section 4.2.1 and the properties of the various APS's are outlined in Appendix C1-C5. The limits on the multiplier values to ensure the stability and pseudopassivity of these transformed structures are also detailed in Appendix C1-C5.

Other optimization considerations concern filter responses that have multiple bands. If this type of filter response is required to possess constant group delay across each of its passbands, then a general design specification should allow different group delay deviations across each passband. A very effective optimization technique introduced into the simultaneous lowpass solutions involved a parameter that represented the position about which the group delay passband templates were generated. The value of this parameter could be varied by the optimization routine to alter the position of the group delay template dynamically. Extending this idea to multiple band type response could involve applying the same group delay template position to each passband of the response or the use of a separate variable for each delay passband template. Allowing each delay passband template to move independently increases the degrees of freedom available to the optimization routine and the possibility of producing a solution.

The final optimization consideration entails the performance of the optimization techniques and the various transformed lattice structures. The first part of this concern involved the effectiveness of the dual line templates, error function settings and optimization algorithms on the frequency transformed lattice structures. To discover the most effective optimization settings for these transformed lattice WDF structures a number of magnitude-only and simultaneous specifications were investigated.

The other area of concern entailed the introduction of extra optimization parameters in the form of different transformation values and individual group delay passband template variables. The introduction of a separate variable for each group delay passband template was minor in comparison to the use of independent frequency transformation values. Under the most basic design approach the value(s) of the frequency transformations would be determined analytically for a filter specification and the value(s) applied to each APS of the structure. Although this approach limits the frequency responses achievable, it reduces the number of optimization variables required to that required by an equivalent lowpass specification.

The other approach entailed a different frequency transformation value for each APS of a structure. With this approach the performance of the frequency response of the structure would be increased at the expense of extra optimization variables, one for each APS of the structure.

The increased frequency response performance of each of these design techniques needs to be measured against extra computational cost. Implementing the APS design equations within the computer program "WDF", the properties of these design techniques were compared through an appropriate selection of frequency transformation values. Tests to determine the relative merits of these design procedures were carried out in conjunction with investigations into the most efficient optimization routine settings. The main features of these investigations are highlighted through a number of design examples in the next section.

5.5 Design examples

A wide combination of settings was investigated to determine the 'best' values of the optimization parameters for various lattice WDF filter types using identical frequency transformation values for each APS. Tests were then extended to structures with different transformation values for each APS. These tests were performed using magnitude-only and simultaneous specifications on bandpass and bandstop type lattice WDF structures.

5.5.1 Magnitude-only design

The objective of the magnitude-only designs was to confirm the optimization techniques developed for lowpass structures would work under any filter type and magnitude specification. The first step of this research concerned bandpass and bandstop specifications that could be transformed from a lowpass solution with a single transformation value. This transformation value was determined analytically for a specification and not included as an optimization variable.

Testing under this procedure required the definition of a lowpass filter specification and calculation of the order of an elliptic function that could satisfy that specification. From this lowpass specification an equivalent symmetric and two asymmetric bandpass specifications were constructed and the appropriate frequency transformation values calculated. The multiplier values of the bandpass structure were then optimized to satisfy the frequency specifications. These bandpass multiplier values should then converge to a similar set of values as the equivalent lowpass solution.

To illustrate this process consider the lowpass filter and equivalent symmetric and asymmetric bandpass filter specifications shown in Table(5.6). A 7th order elliptic function was found to satisfy the lowpass specification of Table(5.6) and the multiplier values for this function are given in Table(5.7). The frequency responses of a lowpass lattice WDF structure using the multipliers of Table(5.7) are shown in Fig.(5.22).

Filter type	Atten (dB)		α value	Frequency edges (Hz)	f_o (Hz)
	pass	stop			
Lowpass	0.1	50	/	0 → 0.1 → 0.15 → 0.5	/
Bandpass (symmetric)	0.1	50	0	0 → 0.175 → 0.2 → 0.3 → 0.325 → 0.5	0.25
Bandpass (asymmetric)	0.1	50	0.618	0 → 0.082 → 0.1 → 0.2 → 0.232 → 0.5	0.144
Bandpass (asymmetric)	0.1	50	-0.326	0 → 0.222 → 0.25 → 0.35 → 0.372 → 0.5	0.303

Table 5.6 Filter specification.for lowpass filter with symmetric and asymmetric bandpass equivalents.

Upper lattice arm			Lower lattice arm		
APS No.	APS type	multiplier values	APS No.	APS type	multipliers value
1	2nd	$x_1 =$ -0.783992 $x_2 =$ 0.840820	3	2nd	$x_4 =$ -0.635752 $x_5 =$ 0.916427
2	1st	$x_3 =$ 0.751907	4	2nd	$x_6 =$ -0.930190 $x_7 =$ 0.796660

Table 5.7 Lowpass lattice WDF multiplier values that satisfy the lowpass specification of Table(5.6) with an elliptic function.

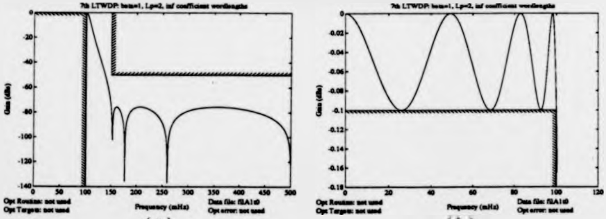

(a) (b)

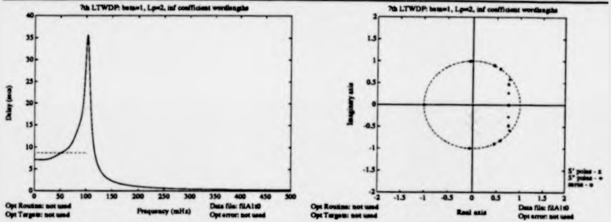

(c) (d)

Figure 5.22 Lowpass 7th order lattice responses; (a) overall and (b) passband magnitudes, (c) overall group delay and (d) pole/zero responses.

Zeroing the initial multiplier values, optimizing with the dual line templates set to the lowpass frequency specification of Table(5.6) and the optimization procedures discussed in Chapter 4, resulted in the multipliers of Table(5.8). With these multipliers, the 7th order lowpass lattice filter possessed the frequency responses shown in Fig.(5.23).

Upper lattice arm			Lower lattice arm		
APS No.	APS type	multiplier values	APS No.	APS type	multiplier values
1	2^{nd}	$x_1 =$ -0.553318 $x_2 =$ 0.827318	3	2^{nd}	$x_4 =$ -0.868729 $x_5 =$ 0.780335
2	1^{st}	$x_3 =$ -0.028986	4	2^{nd}	$x_6 =$ -0.001459 $x_7 -$ 0.556476

Table 5.8 Lowpass lattice WDF multiplier values that satisfy the lowpass specification of Table(5.6) under optimization.

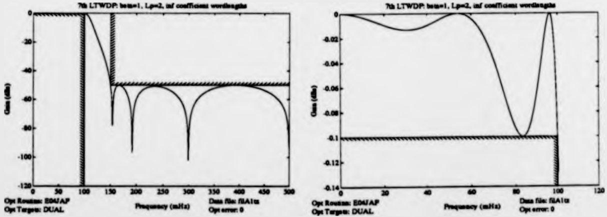

(a) (b)

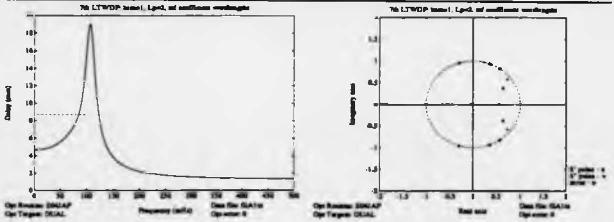

(c) (d)

Figure 5.23 Lowpass 7th order frequency; (a) overall and (b) passband magnitude, (c) overall group delay and (d) pole/zero responses.

With the optimization settings for weights, error points and transition band template angles determined from the lowpass design, the bandpass specifications of Table(5.6) were approached with a 14th order bandpass structure. The multiplier values designed to satisfy the symmetric bandpass specification are given in Table(5.9) along with frequency responses that are detailed in Fig.(5.24).

lattice arm	APS Nos	APS type	APS multipliers			
Upper	1	4th	$x_1 =$ -0.49493	$x_2 =$ 0.77795	$x_3 =$ 0.0	$x_4 =$ 0.0
	2	2nd	$x_5 =$ 0.26279	$x_6 =$ 0.0		
Lower	3	4th	$x_7 =$ -0.85634	$x_8 =$ 0.77329	$x_9 =$ 0.0	$x_{10} =$ 0.0
	4	4th	$x_{11} =$ -0.17252	$x_{12} =$ 0.63186	$x_{13} =$ 0.0	$x_{14} =$ 0.0

Table 5.9 Bandpass lattice WDF multiplier values that satisfy the symmetric specification of Table(5.6) under optimization.

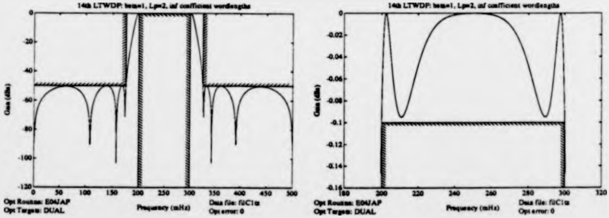

(a) (b)

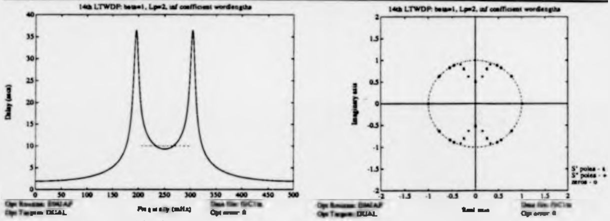

(c) (d)

Figure 5.24 Symmetric bandpass frequency; (a) overall and (b) passband magnitude, (c) overall group delay and (d) pole/zero responses.

The multiplier values for the 14th order bandpass filter that satisfied the first and second asymmetric bandpass specifications of Table(5.6) are listed in Table(5.10) and Table(5.11) respectively. The frequency responses of these two asymmetric examples are given by Fig.(5.25) and Fig.(5.26).

lattice arm	APS Nos	APS type	APS multipliers			
Upper	1	4th	$x_1 =$ -0.49612	$x_2 =$ 0.77376	$x_3 =$ 0.618	$x_4 =$ 0.618
	2	2nd	$x_5 =$ 0.30323	$x_6 =$ 0.618		
Lower	3	4th	$x_7 =$ -0.85689	$x_8 =$ 0.77359	$x_9 =$ 0.618	$x_{10} =$ 0.618
	4	4th	$x_{11} =$ -0.19585	$x_{12} =$ 0.64808	$x_{13} =$ 0.618	$x_{14} =$ 0.618

Table 5.10 Bandpass lattice WDF multiplier values that satisfy the first asymmetric specification of Table(5.6) under optimization.

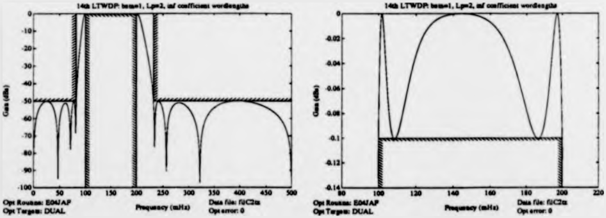

(a) (b)

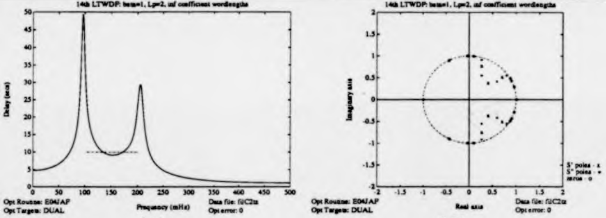

(c) (d)

Figure 5.25 First asymmetric bandpass specification; (a) overall and (b) passband magnitude, (c) overall group delay and (d) pole/zero responses.

lattice arm	APS Nos.	APS type	APS multipliers			
Upper	1	4th	$x_1 =$ -0.50159	$x_2 =$ 0.77789	$x_3 =$ -0.326	$x_4 =$ -0.326
	2	2nd	$x_5 =$ 0.28259	$x_6 =$ -0.326		
Lower	3	4th	$x_7 =$ -0.18526	$x_8 =$ 0.64554	$x_9 =$ -0.326	$x_{10} =$ -0.326
	4	4th	$x_{11} =$ -0.85835	$x_{12} =$ 0.77240	$x_{13} =$ -0.326	$x_{14} =$ -0.326

Table 5.11 Bandpass lattice WDF multiplier values that satisfy the second asymmetric specification of Table(5.6) under optimization.

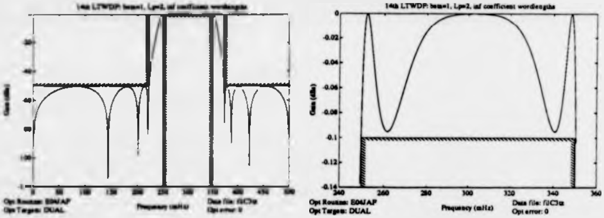

(a) (b)

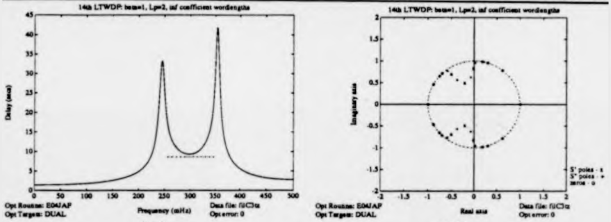

(c) (d)

Figure 5.26 Second asymmetric bandpass specification; (a) overall and (b) passband magnitude, (c) overall group delay and (d) pole/zero responses.

The frequency responses shown in Fig.(5.24), Fig(5.25) and Fig(5.26) illustrate that the optimization techniques have produced solutions to the frequency specifications of Table(5.6). Comparing the multiplier values of Table(5.9-11) with the equivalent lowpass values of Table(5.8) indicates that the bandpass responses are similar to a transformed lowpass solution.

The next part in this area of research entailed bandpass and bandstop specifications that could not be satisfied by a transformed lowpass solution, such as asymmetric responses that had equal transition band widths and different attenuation levels for passband(s) or stopband(s). This procedure involved applying a different transformation value to each APS of the structure, where the values for these individual transformations were determined by optimization. With this technique the total number of multipliers that required optimization was less than the order of the filter. This is due to the nature of the bandpass and bandstop fourth order APS's. Although these sections contain four multipliers, two of them are constrained to be equal and so only three values needed to be optimized.

The first step in the use of different frequency transformation values as optimization variables was to ensure that the optimization routines would find solutions to the bandpass filter specifications of Table(5.6). For these specifications the optimized value for the frequency transformation within each APS should all be equal.

Optimization with independent frequency transformation values to satisfy the bandpass specifications of Table(5.6) produced the multiplier sets shown in

Table(5.12). The overall and passband magnitude frequency responses for these three solutions are detailed by Fig.(5.27).

lattice arm	APS Nos	APS type	APS multipliers			
Solution for symmetric bandpass specification from Table(5.6)						
Upper	1	4^{th}	$x_1 = -0.56349$	$x_2 = 0.82848$	$x_3 = 0.00029$	$x_4 = 0.00029$
	2	2^{nd}	$x_5 = -0.02835$	$x_6 = 0.00769$		
Lower	3	4^{th}	$x_7 = -0.87043$	$x_8 = 0.77751$	$x_9 = -0.00171$	$x_{10} = -0.00171$
	4	4^{th}	$x_{11} = -0.00001$	$x_{12} = 0.57016$	$x_{13} = 0.00515$	$x_{14} = 0.00515$
Solution for first asymmetric bandpass specification from Table(5.6)						
Upper	1	4^{th}	$x_1 = -0.60435$	$x_2 = 0.81773$	$x_3 = 0.61574$	$x_4 = 0.61574$
	2	2^{nd}	$x_5 = 0.41679$	$x_6 = 0.65283$		
Lower	3	4^{th}	$x_7 = -0.28928$	$x_8 = 0.80159$	$x_9 = 0.63673$	$x_{10} = 0.63673$
	4	4^{th}	$x_{11} = -0.87891$	$x_{12} = 0.77316$	$x_{13} = 0.61361$	$x_{14} = 0.61361$
Solution for second asymmetric bandpass specification from Table(5.6)						
Upper	1	4^{th}	$x_1 = -0.56351$	$x_2 = 0.77078$	$x_3 = -0.33805$	$x_4 = -.033805$
	2	2^{nd}	$x_5 = 0.48690$	$x_6 = -0.38872$		
Lower	3	4^{th}	$x_7 = -0.86453$	$x_8 = 0.76334$	$x_9 = -0.33000$	$x_{10} = -0.33000$
	4	4^{th}	$x_{11} = -0.32571$	$x_{12} = 0.76399$	$x_{13} = -0.36426$	$x_{14} = -0.36426$

Table 5.12 Bandpass lattice WDF multiplier values that satisfy the specifications of Table(5.6) with different transformation values.

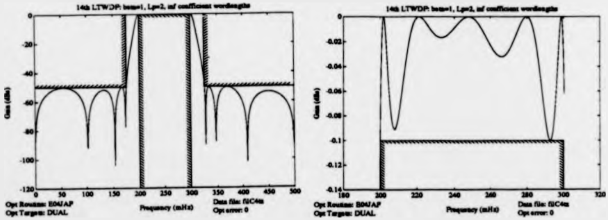

(a) (b)

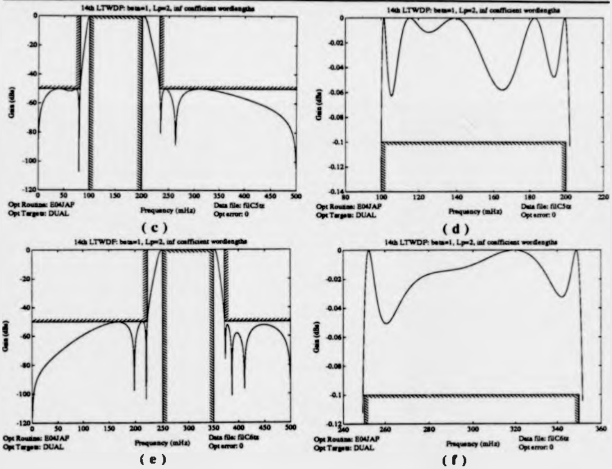

(c) (d)

(e) (f)

Figure 5.27 Magnitude responses of bandpass filters that satisfy Table(5.6) specifications; symmetric (a) overall and (b) passband, 1st asymmetric (c) overall and (d) passband and 2nd asymmetric (e) overall and (f) passband.

Having confirmed that this independent frequency transformation technique was capable of solving specifications that have lowpass equivalents, the next step was to consider specifications that have no lowpass equivalent. Two asymmetrical bandpass specifications considered are shown in Table(5.13). Frequency specifications that cannot be satisfied by a transformed lowpass solution are characterised by asymmetric responses with equal transition band widths and different passband and stopband attenuations.

Example	Spec.	lower stopband	passband	upper stopband
1	Att (dB)	50	0.1	50
	Freq (Hz)	0 → 0.075	0.1 → 0.2	0.225 → 0.5
2	Att (dB)	50	0.5	40
	Freq (dB)	0 → 0.22	0.26 → 0.34	0.38 → 0.5

Table 5.13 Asymmetric bandpass lattice WDF frequency specifications.

The multiplier values for the bandpass structures that satisfy the frequency specifications of Table(5.13) are given in Table(5.14), while the overall and passband magnitude frequency responses of these solutions are shown by Fig.(5.28).

The design procedure applied to the single bandpass and bandstop filter structures was then implemented upon the dual bandpass and bandstop specifications.

lattice arm	APS Nos.	APS type	APS multipliers			
Solution for first asymmetric bandpass specification from Table(5.13)						
Upper	1	4th	$x_1 =$ -0.43929	$x_2 =$ 0.89926	$x_3 =$ 0.30252	$x_4 =$ 0.30252
	2	2nd	$x_5 =$ 0.83177	$x_6 =$ 0.77833		
Lower	3	4th	$x_7 =$ -0.42034	$x_8 =$ 0.78190	$x_9 =$ 0.44439	$x_{10} =$ 0.44439
	4	4th	$x_{11} =$ -0.87554	$x_{12} =$ 0.78063	$x_{13} =$ 0.61582	$x_{14} =$ 0.61582
Solution for second asymmetric bandpass specification from Table(5.13)						
Upper	1	4th	$x_1 =$ -0.12300	$x_2 =$ 0.75314	$x_3 =$ -0.29057	$x_4 =$ -0.29057
	2	2nd	$x_5 =$ -0.08425	$x_6 =$ -0.38170		
Lower	3	4th	$x_7 =$ -0.05054	$x_8 =$ 0.90045	$x_9 =$ -0.54704	$x_{10} =$ -0.54704
	4	4th	$x_{11} =$ -0.03810	$x_{12} =$ 0.90682	$x_{13} =$ -0.05533	$x_{14} =$ -0.05533

Table 5.14 Bandpass lattice WDF multiplier values that satisfy the specifications of Table(5.13).

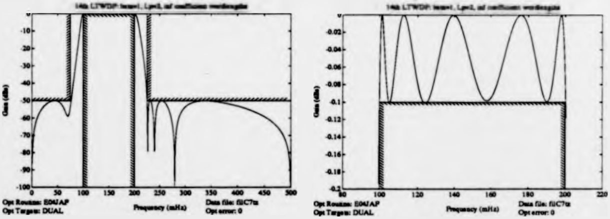

(a) (b)

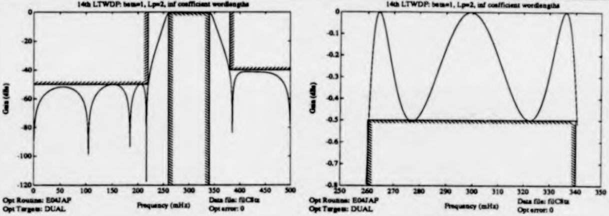

(c) (d)

Figure 5.28 Magnitude responses that satisfy the specifications of Table(5.13); example 1 (a) overall and (b) passband and example 2 (c) overall and (d) passband.

Results from these tests proved the versatility and efficiency of optimization procedures based upon the dual line template scheme and the quasi-Newton algorithms. Results also supported most of the optimization parameter rules and settings developed for lowpass designs based upon the dual line template scheme. These settings concerned the weighting values, the number and distribution of error points and the transition band descriptions.

Tests were most successful with weighting values that followed the equal deviation/equal error rule described in Chapter 3 and an error point distribution technique that group more points around the regions of greatest change. The number of error points per band used for the single and dual band responses was lower than for lowpass specifications. The number of error point represents a compromise between the time taken to calculate the error function at each iteration and the accuracy with which the actual response was measured. Because of the increased number of bands within the response and consequently the total number of error points, the number of points per band was limited to the range $10 < x < 35$.

5.5.2 Simultaneous designs

Having shown that the ideas of optimization and frequency transformations can be applied to arbitrary magnitude-only designs, the investigation was extended to incorporate simultaneous specifications The work within this area of research followed the procedures used for the magnitude-only designs of first satisfying symmetric bandpass responses that could be transformed from simultaneous lowpass solutions and then moving to specifications that cannot be produced from transformed lowpass solutions.

Using the specification of Table(5.15), the multipliers of a 13th order lowpass lattice WDF were generated through optimization and are given in Table(5.16).

Specification		passband	stopband
Gain	atten (dB)	0.1	50
	Freq (Hz)	0 → 0.1	0.15 → 0.5
Group Delay	dev (%)	5	/
	Freq (Hz)	0 → 0.1	0.15 → 0.5

Table 5.15 Simultaneous lowpass lattice WDF frequency specification.

Upper lattice arm			Lower lattice arm		
APS No.	APS type	multiplier values	APS No.	APS type	multiplier value
1	2nd	$x_1 = -0.617480$	5	2nd	$x_8 = -0.706464$
		$x_2 = 0.842052$			$x_9 = 0.718120$
2	2nd	$x_3 = -0.347365$	6	2nd	$x_{10} = -0.302902$
		$x_4 = 0.839724$			$x_{11} = 0.880970$
3	2nd	$x_5 = -0.878290$	7	2nd	$x_{12} = -0.630416$
		$x_6 = 0.711525$			$x_{13} = 0.914474$
4	1st	$x_7 = 0.758694$			

Table 5.16 Multiplier values that satisfy the specification of Table(5.15).

The equivalent symmetric bandpass response to the lowpass specification of Table(5.15) was determined and is shown in Table(5.17). The design of a filter to satisfy the specification of Table(5.17) was first approached with a 26th order bandpass structure that had equal frequency transformation values, all set to zero as the specification is symmetric. The multipliers of this structure were then optimized using the techniques discussed for the magnitude-only design and are shown in Table(5.18), with frequency responses illustrated by Fig.(5.29).

Specification		lower stopband	passband	upper stopband
Gain	atten (dB)	50	0.1	50
	Freq (Hz)	0 → 0.175	0.2 → 0.3	0.325 → 0.5
Group Delay	dev (%)	/	5	/
	Freq (Hz)	0 → 0.175	0.2 → 0.3	0.325 → 0.5

Table 5.17 Symmetric bandpass lattice WDF frequency specification.

lattice arm	APS Nos.	APS type	APS multipliers			
Upper	1	4th	$x_1 =$ -0.86796	$x_2 =$ 0.72104	$x_3 =$ 0.0	$x_4 =$ 0.0
	2	4th	$x_5 =$ -0.63142	$x_6 =$ 0.88310	$x_7 =$ 0.0	$x_8 =$ 0.0
	3	4th	$x_9 =$ -0.38430	$x_{10} =$ 0.73722	$x_{11} =$ 0.0	$x_{12} =$ 0.0
	4	2nd	$x_{13} =$ 0.82093	$x_{14} =$ 0.0		
Lower	5	4th	$x_{15} =$ -0.43064	$x_{16} =$ 0.86135	$x_{17} =$ 0.0	$x_{18} =$ 0.0
	6	4th	$x_{19} =$ -0.58006	$x_{20} =$ 0.93014	$x_{21} =$ 0.0	$x_{22} =$ 0.0
	7	4th	$x_{23} =$ -0.65916	$x_{24} =$ 0.72048	$x_{25} =$ 0.0	$x_{26} =$ 0.0

Table 5.18 Bandpass lattice WDF multiplier values that satisfy the specifications of Table(5.17).

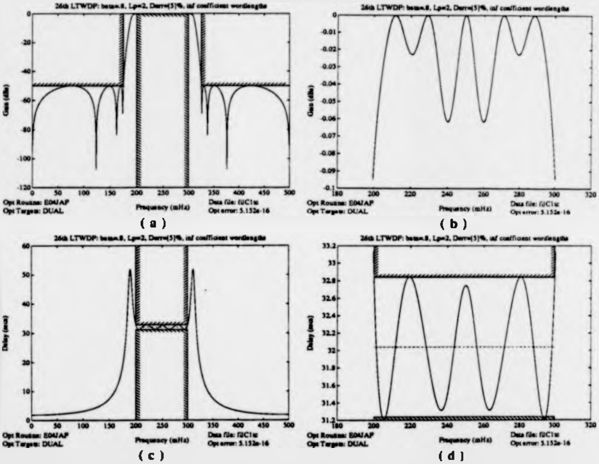

Figure 5.29 Frequency responses of symmetric bandpass filter: magnitude (a) overall and (b) passband and group delay (c) overall and (d) passband.

The specification of Table(5.17) was then approached with a 26th order bandpass structure where the frequency transformation values for each APS were optimization parameters. This was to ensure that for the symmetric specification the solutions with and without the frequency transformation values as optimization parameters were equivalent. The multipliers from this bandpass filter are shown in Table(5.19) while its frequency responses given in Fig.(3.30).

lattice arm	APS Nos.	APS type	APS multipliers			
Upper	1	4^{th}	$x_1 = -0.52561$	$x_2 = 0.84669$	$x_3 = -0.04464$	$x_4 = -0.04464$
	2	4^{th}	$x_5 = -0.53216$	$x_6 = 0.82934$	$x_7 = 0.04543$	$x_8 = 0.04543$
	3	4^{th}	$x_9 = -0.87453$	$x_{10} = 0.70422$	$x_{11} = 0.00175$	$x_{12} = 0.00175$
	4	2^{nd}	$x_{13} = 0.75564$	$x_{14} = 0.02427$		
Lower	5	4^{th}	$x_{15} = -0.49930$	$x_{16} = 0.94488$	$x_{17} = -0.13618$	$x_{18} = -0.13618$
	6	4^{th}	$x_{19} = -0.49872$	$x_{20} = 0.93975$	$x_{21} = 0.14387$	$x_{22} = 0.14387$
	7	4^{th}	$x_{23} = -0.71434$	$x_{24} = 0.69962$	$x_{25} = 0.00239$	$x_{26} = 0.00239$

Table 5.19 Multiplier values that satisfy the specifications of Table(5.17) using the frequency transformation values as optimization parameters.

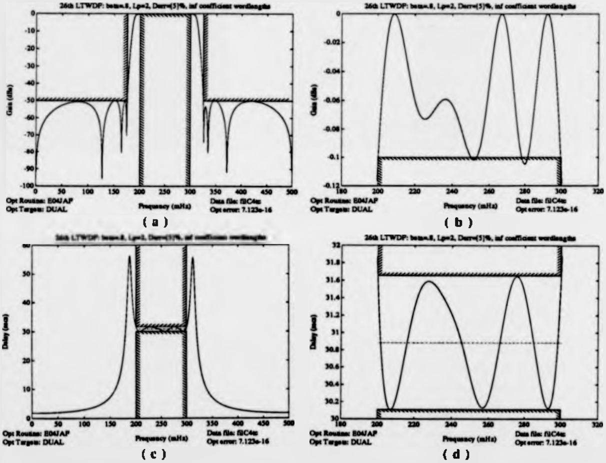

(a) (b)

(c) (d)

Figure 5.30 Frequency responses of symmetric bandpass filter: magnitude (a) overall and (b) passband and group delay (c) overall and (d) passband.

The next step in the simultaneous design investigation involved the asymmetric bandpass specifications of Table(5.6). Although the magnitude side of these specifications can be satisfied by a transformed lowpass solution, the transformation process distorts the phase linearity. As a result the simultaneous specifications can only be approached with structures that use the frequency transformation values as optimization parameters. Results confirmed the design assumptions by generating linear phase solutions to various asymmetric specifications.

The last area of concern with simultaneous specifications involved magnitude responses that could not be satisfied by transformed lowpass solutions. This entailed finding simultaneous solutions to the asymmetric bandpass specifications with equal transition band widths, such as those given in Table(5.20).

Example	Specification		lower stopband	passband	upper stopband
1	Gain	att (dB)	50	0.1	50
		freq (Hz)	0 → 0.075	0.1 → 0.2	0.225 → 0.5
	Group	dev (%)	/	10	/
	Delay	freq (Hz)	0 → 0.075	0.1 → 0.2	0.225 → 0.5
2	Gain	att (dB)	50	0.5	40
		freq (Hz)	0 → 0.22	0.26 → 0.34	0.38 → 0.5
	Group	dev (%)	/	1	/
	Delay	freq (Hz)	0 → 0.22	0.26 → 0.34	0.38 → 0.5

Table 5.20 Asymmetric bandpass lattice WDF frequency specifications.

Frequency responses for the solution to the second specification of Table(5.20) are shown in Fig.(5.31) and Fig.(5.32) respectively. The multiplier values for these structures are given in Table(5.21).

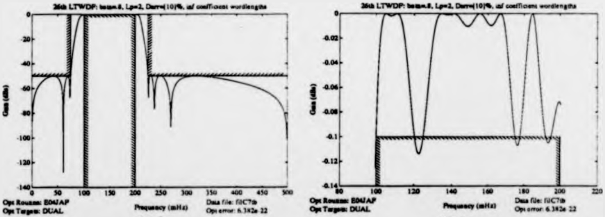

(a) (b)

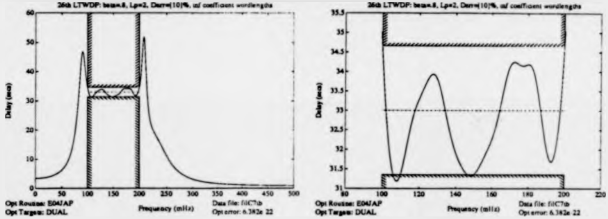

(c) (d)

Figure 5.31 Frequency responses of first asymmetric bandpass filter from Table(5.20); magnitude (a) overall and (b) passband and group delay (c) overall and (d) passband.

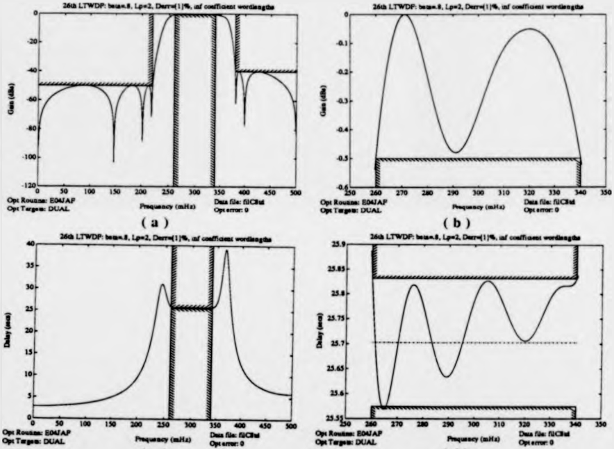

(c) (d)

Figure 5.32 Frequency responses of second asymmetric bandpass filter from Table(5.20); magnitude (a) overall and (b) passband and group delay (c) overall and (d) passband.

lattice arm	APS Nos.	APS type	APS multipliers
Solution for first asymmetric bandpass specification from Table(5.20)			
Upper	1	4th	$x_1 = -0.56014$ $x_2 = 0.64167$ $x_3 = 0.55382$ $x_4 = 0.55382$
	2	4th	$x_5 = -0.77667$ $x_6 = 0.82524$ $x_7 = 0.68055$ $x_8 = 0.68055$
	3	4th	$x_9 = -0.68855$ $x_{10} = 0.96786$ $x_{11} = 0.62429$ $x_{12} = 0.62429$
	4	2nd	$x_{13} = 0.93524$ $x_{14} = 0.25619$
Lower	5	4th	$x_{15} = -0.70454$ $x_{16} = 0.96762$ $x_{17} = 0.39553$ $x_{18} = 0.39553$
	6	4th	$x_{19} = -0.58225$ $x_{20} = 0.60327$ $x_{21} = 0.59594$ $x_{22} = 0.59594$
	7	4th	$x_{23} = -0.67877$ $x_{24} = 0.96814$ $x_{25} = 0.68790$ $x_{26} = 0.68790$
Solution for second asymmetric bandpass specification from Table(5.20)			
Upper	1	4th	$x_1 = -0.75288$ $x_2 = 0.70138$ $x_3 = -0.36515$ $x_4 = -0.36515$
	2	4th	$x_5 = -0.30943$ $x_6 = 0.88422$ $x_7 = -0.14055$ $x_8 = -0.14055$
	3	4th	$x_9 = -0.11397$ $x_{10} = 0.63292$ $x_{11} = -0.42628$ $x_{12} = -0.42628$
	4	2nd	$x_{13} = 0.70898$ $x_{14} = -0.51125$
Lower	5	4th	$x_{15} = -0.14717$ $x_{16} = 0.72472$ $x_{17} = -0.37688$ $x_{18} = -0.37688$
	6	4th	$x_{19} = -0.20425$ $x_{20} = 0.81318$ $x_{21} = -0.31070$ $x_{22} = -0.31070$
	7	4th	$x_{23} = -0.58097$ $x_{24} = 0.66856$ $x_{25} = -0.35744$ $x_{26} = -0.35744$

Table 5.21 Bandpass lattice WDF multiplier values that satisfy the specifications of Table(5.20).

5.6 Conclusions

This Chapter has discussed the ideas of frequency transformations and how they can be applied to lattice WDF structures to produce highpass, bandpass and bandstop type responses. Experiments have shown that simple frequency transformations that do not alter the width of passbands or move the centre frequency point, are linear in their effects upon gain and group delay. Frequency transformations that create asymmetric bandpass or bandstop type responses, distort the phase and the relative widths of transition bands in the process.

To counteract the non-linearities of the frequency transformations, optimization was applied to the bandpass and bandstop lattice structures directly. A further technique to compensate for the transforms' non-linearities was to consider the frequency transformation value of each APS of a structure as an optimization variable. This technique follows the ideas used in analogue filter designs where the resonant frequency of a section within the filter is tuned to a slightly different point to achieve the desired cut-off rate. Different frequency transformation values for each APS within the lattice WDF structure allows the same principle to be applied within the digital domain.

The performance of this technique and the optimization procedures was verified through a large number of design examples. These examples included symmetric specifications that required the frequency transformation value for each APS to be zero, symmetric specifications that required the frequency transformation value of each APS to be equal and asymmetric specifications that possessed equal transition band widths and unequal stopband attenuations that could only be satisfied with a different transformation value for each APS.

The procedure of applying a different frequency transformation value to each APS of a structure increases the degrees of freedom of the structure as a whole. An increase in the degrees of freedom of the lattice WDF improves the versatility and performance of the structure, allowing it to satisfy a wider range of arbitrary magnitude and phase specifications. The transformed APS's suggested in this Chapter do not exploit all the degrees of freedom available, determined by the number of independent multipliers in an APS. Therefore, although the 4th order bandpass and bandstop APS's contain four multipliers, only three are independent while the 8th order dual bandpass and bandstop APS's only possess four independent multipliers.

Maximizing the degrees of freedom available to the overall structure requires APS's that do not contain dependent multipliers, such as the 1st and 2nd order lowpass APS's or more general 4th and 8th order APS's. Designs involving lowpass APS's would entail applying single and multi-band frequency specifications directly to the lowpass lattice WDF detailed in Chapter 4. For the range of examples considered, the limited degrees of freedom of the 2nd and 4th order bandpass and bandstop APS's did not hinder the design process. However, this was not true for the 4th and 8th order dual band APS's which imposed a severe limitation upon the performance of the lattice structure.

Optimization of the highpass, bandpass and bandstop type magnitude and simultaneous specifications confirmed the effectiveness of the ideas and procedures developed for lowpass designs. These optimization techniques included the dual line templates, the weighted L_p-metric error function and the quasi-Newton algorithms. A number of the optimization settings developed for the lowpass designs held true for these arbitrary specifications.

These settings included an equal deviation/equal error weighting scheme and the clustering of error points in regions of greatest change. Error points were spaced under the ideas outlined in Chapter 4, where for gain templates they were placed around the edge(s) of a template band. Within group delay templates the error points were spaced evenly over the passband(s). The ratio, β, controls the contributions of gain and group delay errors to the overall error function. Its value was limited to the range $0.6 < \beta < 0.9$ so that for simultaneous designs more emphasis was placed upon the gain response to ensure it was established before trying to satisfy the group delay specification. This procedure follows the ideas discussed in Chapter 3. In all optimization tests the initial multiplier values were started from zero.

In most design cases the number of error points per band was reduced to $15 < x < 35$ to decrease the time taken to calculate the error at each iteration and as a result improves the speed of the design process. However, low densities of error points made bandpass specifications with very wide stopbands more susceptible to spikes. To avoid this possibility the density of error points in narrower stopbands was reduced in favour of higher densities in the wider stopbands. Repositioning the error points within the stopbands of a specification allows the total number of error points to be kept to a minimum. Use of the transition band templates within arbitrary magnitude and phase specifications confirmed the ideas developed for lowpass design in Chapter 4, where the more closely the goal response could be modelled, the more acceptable any design solutions. The shape of the transition band template, defined through an upper and lower angle, was varied to encouraging a rapid cut-off around the edge of a passband and a slower cut-off toward the edge of a stopband.

The purpose of this Chapter has been to outline the ideas and models for frequency transformations of the lattice WDF and its application to arbitrary magnitude and phase specifications. Examples provided in this Chapter show that the transformed APS's detailed are capable of satisfying a wide range of frequency specification. Although the dual band APS's can be implemented to achieve selective magnitude-only frequency specifications, their limited degrees of freedom and the introduction of linear phase prompted dual band specifications to be addressed using lattice structures with the simpler 1st and 2nd order lowpass and highpass APS's.

With descriptions and equations for all the APS's considered, the next area of research entailed producing finite wordlength designs for arbitrary magnitude and phase specifications. An outline and discussion of the techniques involved in the finite wordlength design process is provided in Chapter 6.

References

1) Ali, A. M., "Design of Low-Sensitivity Digital Filters by Linear Transformations", IEEE Trans. Circuits and Systems, Vol CAS-27, No. 6, June 198, pp435-444.

2) Constantinides, A. G., "Spectral Transformations for Digital Filters", Proc. IEE, Vol 117, No. 8, August 1970, pp1585-1590.

3) Gulluoglu, S. N., "Frequency Transformations for Wave Digital Filters", Signal Processing III: Theories and Applications, Vol C3.11, No. 11, November 1986, pp199-202.

4) Lawson, S. S., "Frequency Transformations for the simple 2-port Wave Digital Filter Adaptor Chain", Proc. IEE, Vol 132, Pt. G, No. 5, October 1985, pp237-240.

5) Mathematica, Wolfram, S., Addison-Wesley, California, 1988.

6) Orchard, H. J. and Temes, G. C., "Filter Design using Transformed Variables", IEEE Trans. Circuit Theory, Vol CT-15, No. 5, December 1968, pp385-408.

7) Swamy, M. N. S. and Thyagarajan, K. S, "Digital Bandpass and Bandstop Filters with Variable Center Frequency and Bandwidth", Proc. IEEE, Vol 123, No. 11, November 1976, pp1632-1634.

Chapter 6

Finite Wordlength Designs

The final objective of any digital filter design is a set of finite wordlength coefficients that satisfy a given specification. The main thrust of this research has been to investigate and develop techniques for the design of WDF's capable of satisfying arbitrary magnitude and phase designs. These techniques have been based upon lattice WDF's and optimization. Initial designs have provided solutions to arbitrary specifications with coefficient values that require a high degree of accuracy. The next step in the design process entails starting with these high accuracy or ideal coefficient values and producing equivalent finite wordlength solutions.

The first part of this Chapter details the effects of finite wordlength constraints upon the responses of the lattice WDF determined in both the frequency and time domains. The Chapter then outlines the options for finite wordlength designs and the optimization techniques adopted. The Chapter concludes with a number of finite wordlength designs for magnitude-only and simultaneous frequency specifications and a discussion of the effects of finite wordlength constraints upon digital filter designs.

6.1 Finite Wordlength Effects

The errors introduced by finite wordlength criterion may be grouped into two areas. The first area relates to the transfer function of the filter and with what accuracy its coefficient values are represented. The other area concerns the hardware upon which a digital filter is implemented.

The frequency response of a transfer function may be calculated analytically for an arbitrary set of filter coefficients with a large degree of accuracy. The filter coefficients may themselves be represented with a large degree of accuracy or limited to a specific wordlength. Calculating the response of the transfer function analytically with finite wordlength coefficient values provides an indication of their effects in isolation to the finite wordlength effects introduced by any hardware implementation. To consider the effects of quantizing the filter coefficient values on the lattice WDF, the responses of a filter were determined in the frequency domain with a range of finite coefficient wordlengths quantized under a range of procedures.

Finite wordlength errors due to hardware implementation relate to the accuracy with which the transfer function can be determined. This is limited by the wordlength of the hardware, in the form of multiplier, adder, input and output data wordlengths and the rounding, overflow and scaling techniques applied. Hardware limitations can only be simulated in the time domain and the filter's response must be evaluated by applying a FFT to the impulse response. Using this technique the effects of different rounding, overflow and scaling procedures can be modelled and related to a filter's frequency responses.

The only method of confirming the accuracy of these simulated results involves generating the lattice WDF upon a DSP chip and measuring the actual frequency responses with a spectrum analyser. Results from implementing lattice WDF's upon a DSP chip are detailed later on in this Chapter.

6.1.1 Frequency domain simulation

Frequency domain calculations are based upon an analytical evaluation of the transfer function of a filter. These calculations are performed to the full accuracy of a computer system and do not allow the effects of rounding and overflow to be modelled. As a consequence the only finite wordlength effect that can be modelled in the frequency domain is the distortion of the frequency response resulting from quantizing the filter coefficient values.

The low coefficient sensitivity properties of WDF structures enable them to retain a desired frequency response with low coefficient wordlengths. This can be illustrated through the 7^{th} order lattice WDF of Fig.(6.1) which satisfies the lowpass specification of Table(6.1) with the coefficient values given in Table(6.2).

Gain passband		Gain stopband		Samp.
att (dB)	edge (Hz)	att (dB)	edge (Hz)	freq (Hz)
0.1	0.1	50	0.15	1

Table 6.1 Lowpass filter specification.

For this example, the multiplier values of Table(6.2) were treated as ideal and then used to produce 16, 12, 8, 7, 6 and 5 bits quantized versions. In all the design considered the bit length specified includes a sign bit. The magnitude frequency response of this 7th order lattice WDF was then determined for each set of quantized coefficients. Distortion of the filter's frequency response due to coefficient quantization can be seen in Fig.(6.2), showing the frequency responses for each different coefficient set.

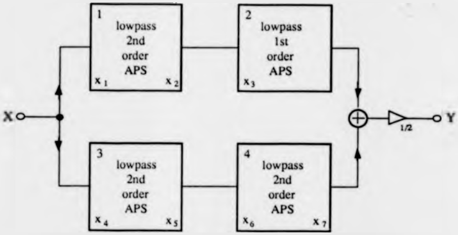

Figure 6.1 7th order lowpass lattice WDF structure.

Upper lattice arm			Lower lattice arm		
APS No.	APS type	multiplier values	APS No.	APS type	multiplier values
1	2nd	x_1 = -0.783992 x_2 = 0.840820	3	2nd	x_4 = -0.635752 x_5 = 0.916427
2	1st	x_3 = 0.751907	4	2nd	x_6 = -0.930190 x_7 = 0.796660

Table 6.2 Lowpass lattice WDF multiplier values that satisfy the lowpass specification of Table(6.1) with an elliptic function.

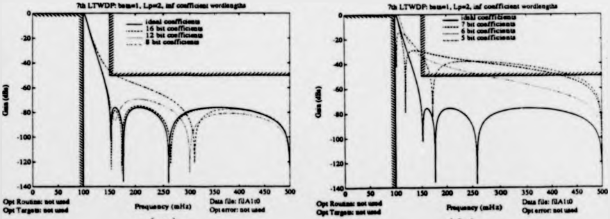

(a) (b)

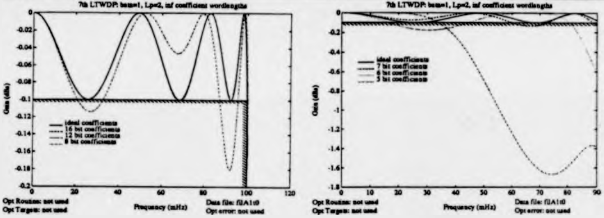

(c) (d)

Figure 6.2 (a)-(b) overall and (c)-(d) passband magnitude frequency responses using quantized versions of the multipliers of Table(6.2).

The frequency responses of Fig.(6.2) clearly show that the lattice structure is less sensitive to coefficient changes in the passband region of its response than the stopband region. This feature is a property of the lattice structure and can be further illustrated if the coefficient sensitivities for this structure are calculated. Fig.(6.3) shows the gain coefficient sensitivities for the upper and lower lattice arm multipliers.

The gain coefficient sensitivities of Fig.(6.3) show a higher sensitivity across its stopband region. This property is a feature of the lattice structure. Across the stopband region the action of the lattice is to subtract two virtually identical numbers, generating a very small number that is susceptible to noise. Despite the higher sensitivity in the stopband, the lattice structure is still able to retain an acceptable frequency response under very short coefficient wordlengths.

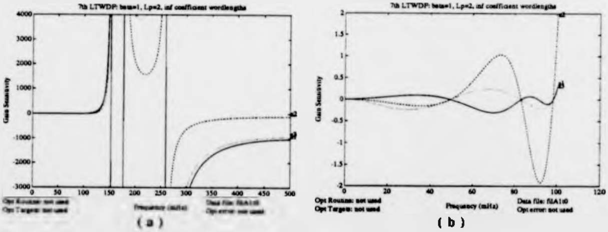

(a) (b)

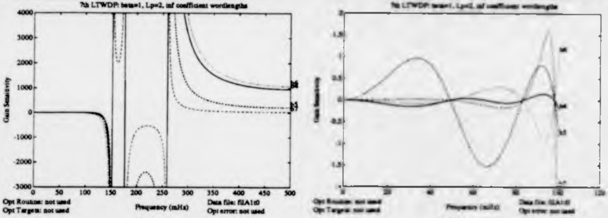

(c) (d)

Figure 6.3 Gain coefficient sensitivities for upper arm (a) overall and (c) passband and lower arm (b) overall and (d) passband responses.

Research to date has only considered the effects of finite wordlength coefficients upon the magnitude response of WDF's and the corresponding gain coefficient sensitivities. The addition of group delay constraints into a specification, dramatically alters the minimum wordlength that can be achieved before frequency responses become unacceptable. The presence of finite wordlength coefficients in simultaneous specifications can be illustrated through a number of examples introduced in Chapter 4 and Chapter 5.

First consider the 11th order lattice WDF of Fig.(6.4). Using a filter of this order the design programs and optimization techniques discussed in Chapter 4 were applied to produce a solution that satisfied the simultaneous lowpass specification of Table(6.3). The coefficient values of this solution are given in Table(6.4). These coefficient values were calculated with the full 64 bit accuracy of the computer system. The coefficients of Table(6.4) therefore represent an ideal set of values that can only be reproduced with a large wordlength system.

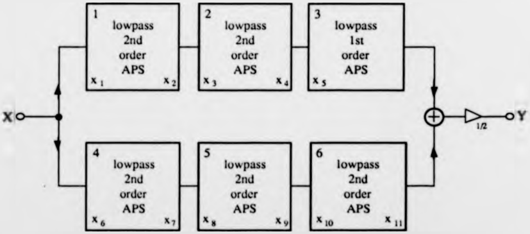

Figure 6.4 11th order lowpass lattice WDF structure.

Gain passband		Gain stopband		Delay passband		Samp.
att (dB)	edge (Hz)	att (dB)	edge (Hz)	dev (%)	edge (Hz)	freq (Hz)
0.1	0.1	50	0.15	10	0.1	1

Table 6.3 Simultaneous lowpass filter specification.

Upper lattice arm			Lower lattice arm		
APS No.	APS type	multiplier values	APS No.	APS type	multiplier values
1	2^{nd}	$x_1 =$ -0.716631 $x_2 =$ 0.938000	4	2^{nd}	$x_6 =$ -0.668982 $x_7 =$ 0.971084
2	2^{nd}	$x_3 =$ -0.753809 $x_4 =$ 0.793809	5	2^{nd}	$x_8 =$ -0.748782 $x_9 =$ 0.886975
3	1^{st}	$x_5 =$ 0.848703	6	2^{nd}	$x_{10} =$ -0.898191 $x_{11} =$ 0.748912

Table 6.4 Lowpass lattice WDF multiplier values that satisfy the simultaneous lowpass specification of Table(6.3).

Fig.(6.5) shows the magnitude response of the lattice WDF of Fig.(6.4) under different sets of coefficient values. Each coefficient set represents a quantized version of the 'ideal' multipliers of Table(6.4). The coefficient sets used for this comparison were generated by quantizing the multiplier values to 16, 12, 10, 9, 8 and 7 bits. Fig.(6.6) shows a comparison of the corresponding group delay responses using the same set of finite wordlength coefficient values.

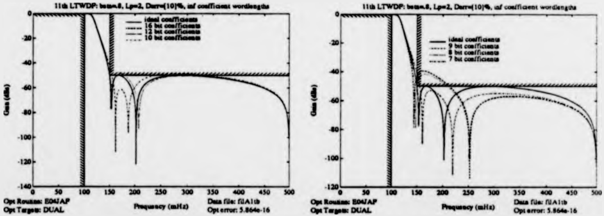

(a) (b)

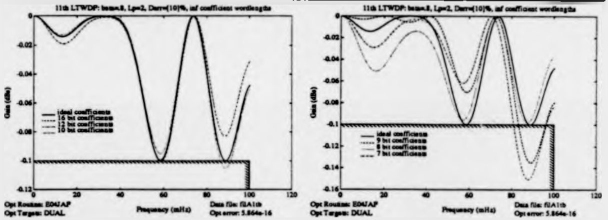

(c) (d)

Figure 6.5 Magnitude responses for different coefficients wordlengths showing (a)-(b) overall and (c)-(d) passband responses.

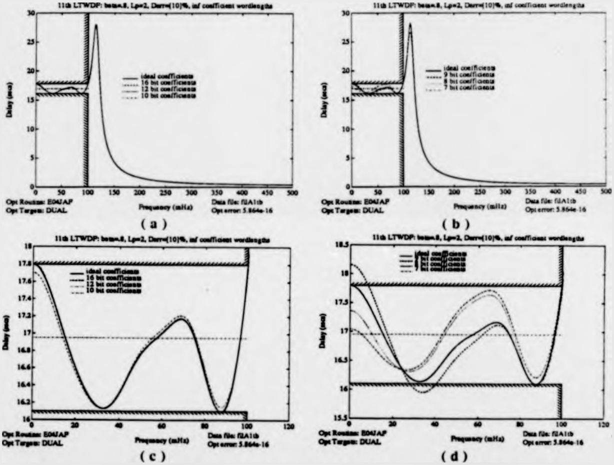

(a) (b)

(c) (d)

Figure 6.6 Group delay responses for different coefficients wordlengths showing (a)-(b) overall and (c)-(d) passband responses.

The magnitude responses of Fig.(6.5) confirm the low coefficient sensitivity properties of the lattice structure. It is the group delay responses of Fig.(6.6) that are of interest. Reducing the coefficient wordlength has a greater effect upon the group delay response. An indication of the effects of reducing the coefficient wordlength can be provided by calculating the gain and group delay coefficient sensitivities. The passband region of the gain coefficient sensitivities for the multipliers of Table(6.4) is shown in Fig.(6.7), while the corresponding group delay coefficient sensitivities are illustrated in Fig.(6.8).

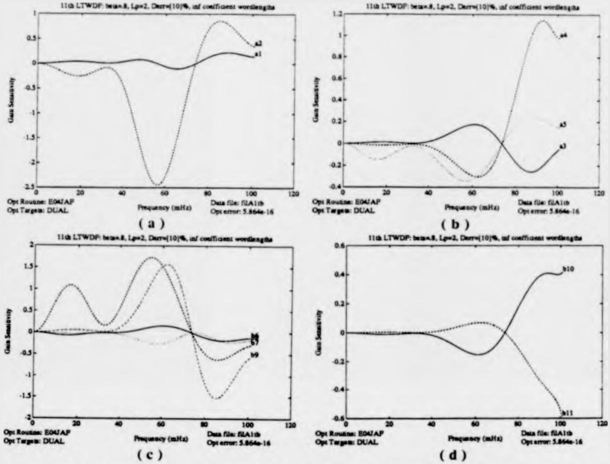

(a) (b) (c) (d)

Figure 6.7 11^{th} order lattice gain coefficient sensitivity responses across the passband with respect to (a)-(b) upper arm and (c)-(d) lower arm multipliers.

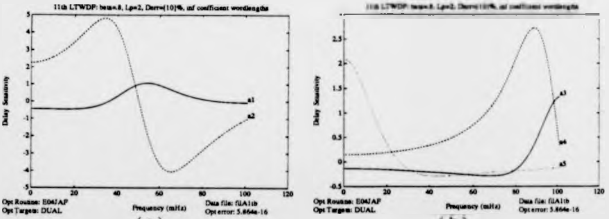

(a) (b)

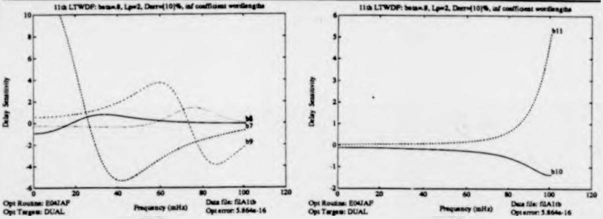

(c) (d)

Figure 6.8 11th order lattice delay coefficient sensitivity responses across the passband with respect to (a)-(b) upper arm and (c)-(d) lower arm multipliers.

The group delay coefficient sensitivity of a particular multiplier is higher than the corresponding gain sensitivity. This indicates that the group delay response of a lattice WDF is more susceptible to changes in coefficient values than the gain response. As a result simultaneous designs require a higher minimum coefficient wordlength to satisfy a finite wordlength specification than equivalent magnitude-only designs. This higher group delay coefficient sensitivity was also exhibited by highpass, bandpass and bandstop type structures. The effects of finite wordlength constraints upon a bandpass structure can be illustrated by comparing the frequency responses of a solution to a simultaneous specification under different coefficients wordlengths and then calculating its gain and group delay coefficient sensitivities.

Consider the 26th order bandpass lattice WDF of Fig.(6.9) which satisfies the simultaneous specification of Table(6.5) with the coefficient of Table(6.6).

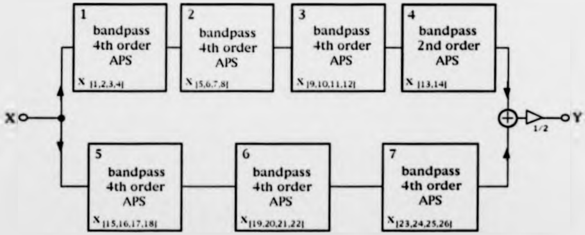

Figure 6.9 26th order bandpass lattice WDF structure.

Specification		lower stopband	passband	upper stopband
Gain	atten (dB)	50	0.5	40
	freq (Hz)	0 → 0.22	0.26 → 0.34	0.38 → 0.5
Group Delay	dev (%)	/	1	/
	freq (Hz)	0 → 0.22	0.26 → 0.34	0.38 → 0.5

Table 6.5 Simultaneous bandpass lattice WDF frequency specification.

lattice arm	APS Nos	APS type	APS multipliers			
Upper	1	4th	$x_1 =$ -0.75288	$x_2 =$ 0.70138	$x_3 =$ -0.36515	$x_4 =$ -0.36515
	2	4th	$x_5 =$ -0.30943	$x_6 =$ 0.88422	$x_7 =$ -0.14055	$x_8 =$ -0.14055
	3	4th	$x_9 =$ -0.11397	$x_{10} =$ 0.63292	$x_{11} =$ -0.42628	$x_{12} =$ -0.42628
	4	2nd	$x_{13} =$ 0.70898	$x_{14} =$ -0.51125		
Lower	5	4th	$x_{15} =$ -0.14717	$x_{16} =$ 0.72472	$x_{17} =$ -0.37688	$x_{18} =$ -0.37688
	6	4th	$x_{19} =$ -0.20425	$x_{20} =$ 0.81318	$x_{21} =$ -0.31070	$x_{22} =$ -0.31070
	7	4th	$x_{23} =$ -0.58097	$x_{24} =$ 0.66856	$x_{25} =$ -0.35744	$x_{26} =$ -0.35744

Table 6.6 Bandpass lattice WDF multiplier values that satisfy the simultaneous specification of Table(6.5).

The magnitude responses of the lattice WDF of Fig.(6.9) using 16, 12, 10, 9, 8 and 7 bit quantized versions of the multipliers of Table(6.6) are shown in Fig.(6.10). The corresponding group delay responses are detailed in Fig.(6.11). In both Fig.(6.10) and Fig.(6.11) the ideal responses were generated using the multipliers of Table(6.6) unquantized.

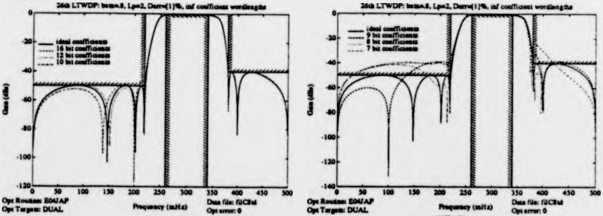

(a) (b)

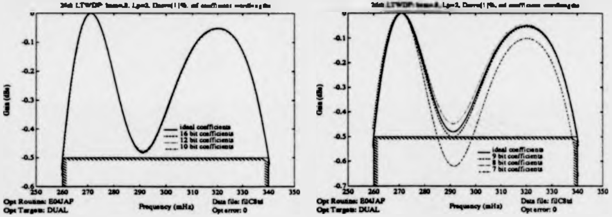

(c) (d)

Figure 6.10 Magnitude responses with different coefficients wordlengths showing (a)-(b) overall and (c)-(d) passband responses.

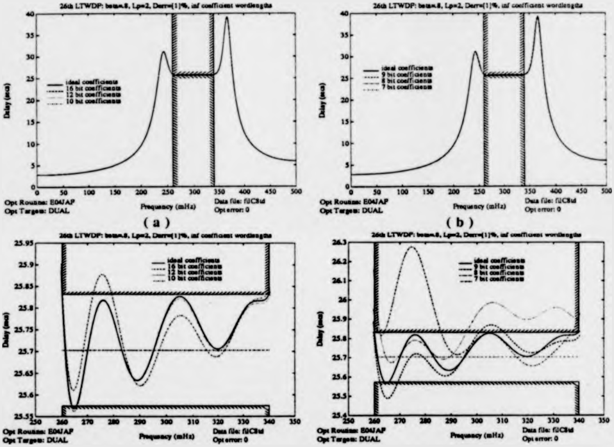

(a) (b)

(c) (d)

Figure 6.11 Group delay responses with different coefficients wordlengths showing (a)-(b) overall and (c)-(d) passband responses.

The gain and group delay coefficient sensitivities of the bandpass lattice WDF of Fig.(6.9) can be calculated for each multiplier. Gain and group delay coefficient sensitivity responses across the passband region for the multipliers in the first

4th order APS of the upper arm, the 2nd order APS and the first 4th order APS of the lower arm, are shown in Fig.(6.12), Fig.(6.13) and Fig.(6.14) respectively.

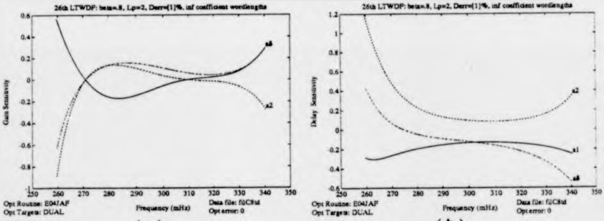

(a) (b)

Figure 6.12 Passband (a) gain and (b) group delay coefficient sensitivities of the first 4th order APS in the upper arm of Fig.(6.9).

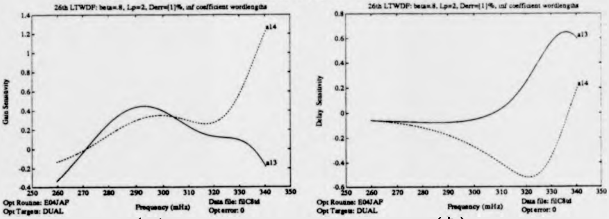

(a) (b)

Figure 6.13 Passband (a) gain and (b) group delay coefficient sensitivities of the 2nd order APS in the upper arm of Fig.(6.9).

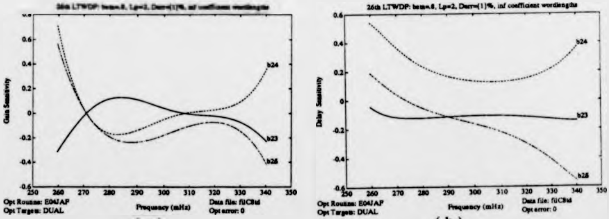

(a) (b)

Figure 6.14 Passband (a) gain and (b) group delay coefficient sensitivities of the first 4th order APS in the lower arm of Fig.(6.9).

Group delay coefficient sensitivities provide an indication of the effects on phase linearity by showing how the gradient of the phase response would alter under finite wordlength conditions. As a consequence the values for gain and group delay sensitivity cannot be compared directly. However the group delay sensitivities of a wide range of examples indicated that finite wordlength distortion of simultaneous responses was more pronounced within the phase specification. As a result, the minimum coefficient wordlength for a filter order and frequency specification would be constrained by the desired phase linearity.

The coefficient quantization applied in the examples considered so far has been rounding. This is not the only method of quantizing however and the effects of rounding, value truncation and magnitude truncation can be determined if each method is applied to the same set of coefficient values and the responses using these multipliers compared. To illustrate these effects the multiplier values of the lowpass structure of Fig.(6.4), given in Table(6.4), were quantized to 8 and 10 bits under rounding, value truncation and magnitude truncation. The resulting magnitude and group delay responses are given in Fig.(6.15).

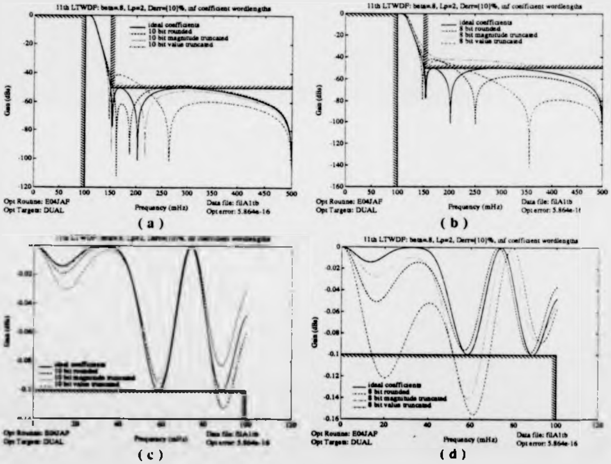

(a) (b)

(c) (d)

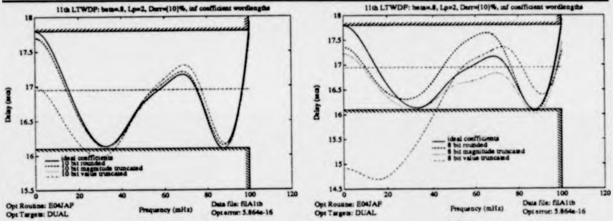

(e) (f)

Figure 6.15 Frequency responses showing passband (a) 8 and (b) 10 bit and overall (c) 8 and (d) 10 bit magnitude and passband (e) 8 and (f) 10 bit delay responses under different quantization procedures.

Comparing the various quantizing procedures for a number of different filter specifications and wordlengths showed that no one procedure was better for all occasions. Results from a range of comparisons of different quantization procedures led to the conclusion that the performance of various finite wordlength solutions could be improved if the coefficient quantization was replaced by some form of optimization that applied rounding or truncation to the coefficient values that best retained the desired frequency responses.

6.1.2 Time domain simulations

To simulate the lattice WDF in the time domain it is necessary to model the action of the lattice arms and the APS's to determine the transfer function. The first step in simulating the lattice WDF in the time domain is to generate a mathematical model for the two-port adaptor that forms the basis of all APS's. The equation for the two-port adaptor is given by Eq.(6.1) with a possible signal flow graph shown by Fig.(6.16).

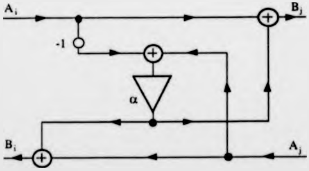

Figure 6.16 Possible signal flow graph for a two-port adaptor.

$$\begin{bmatrix} B_i \\ B_j \end{bmatrix} = \begin{bmatrix} -\alpha & 1+\alpha \\ 1-\alpha & \alpha \end{bmatrix} \cdot \begin{bmatrix} A_i \\ A_j \end{bmatrix} \qquad -1 < \alpha < 1 \qquad (6.1)$$

Any software model of the two-port adaptor would require that the calculations for B_i and B_j were carried out using values of A_i, A_j and α limited to a particular wordlength. Therefore the fixed point operations of the multiplier and adders within the two-port adaptor must be modelled. The action of a fixed point multiplier is to multiply two *b* bit numbers and then quantize the 2*b* bit result to *b* bits. As a result any signal multiplication within the modelled two-port adaptor must be associated with a quantization to reduce the accuracy of the result to the limit of the modelled hardware system. Within a digital hardware system, the number range would be limited to $-1.0 < x < 1.0 - 2^{-(b-1)}$ and b is wordlength of the system. Therefore if an adder was to sum two positive or negative numbers close to this limit, then an overflow would occur. To ensure that this operation was modelled accurately all add operation must be monitored to flag the occurrence of an overflow and the result altered according to a defined overflow strategy.

Any time domain simulation must also limit the wordlength of input and output data, the coefficients and the internal storage registers. Software modelling allows these various wordlengths to be specified individually. Quantizing procedures, such as rounding or truncation, arithmetic operations, such as 1's or 2's complement and overflow procedures, such as reset or saturation can also be included to produce a more versatile time domain simulation program.

Following the time domain requirements outlined, a mathematical model for the two-port adaptor was generated and is shown in Fig.(6.17).

```
READ "$A_i$", "$A_j$"                      (quantized to internal data wordlength)
READ "$\alpha$"                            (quantized to coefficient wordlength)

"sum inputs" = "$A_j$" - "$A_i$"
if "sum inputs" > overflow limit,          apply overflow strategy to "temp"

"sum inputs" = "sum inputs" * "$\alpha$"
Quantize "temp" to internal data wordlength

"$B_i$" = "$A_i$" + "sum inputs"
if "$B_i$" > overflow limit,               apply overflow strategy to "$B_i$"

"$B_j$" = "$A_j$" + "sum inputs"
if "$B_j$" > overflow limit,               apply overflow strategy to "$B_j$"

WRITE "$B_i$", "$B_j$"
```

Figure 6.17 Mathematical model of two-port adaptor.

Using the model for the two-port adaptor given in Fig.(6.17), it was easy to generate models for the APS's used in the lowpass, highpass and band type lattice WDF structures. Computer code written in fortran to implement the two-port adaptor and the various APS's required is detailed in Appendix D1-7. With software models of the lattice WDF structure and the various APS's it was possible to investigate the effects of different quantizing, overflow and scaling strategies on the lattice structure through time domain simulation.

Three standard time domain responses are generated by applying an impulse, step and ramp function to a system. Applying these functions to a time domain model of the lattice WDF of Fig.(6.4) with the multipliers of Table(6.4), produced an ideal set of time domain responses when all system wordlengths were modelled as 64 bits long. A more realistic set of wordlengths would be to limit the input and output data wordlength to 12 bits, restrict the internal data wordlength to 16 bits and reduce the coefficient wordlength to 8 bits. The impulse, step and ramp responses under these reduced wordlength conditions are shown in Fig.(6.18). Differences between the responses of Fig.(6.18) are solely due to the quantization of the filter coefficients.

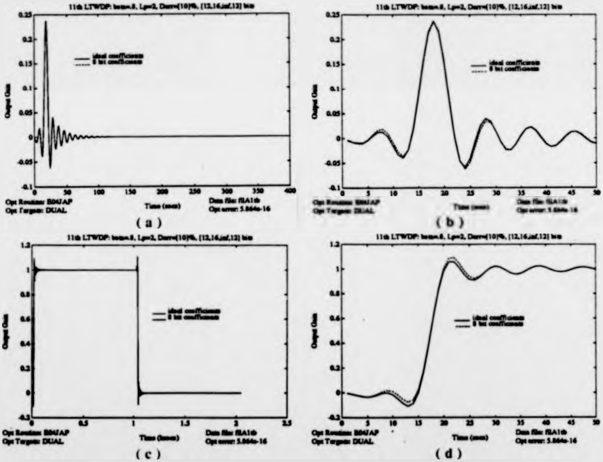

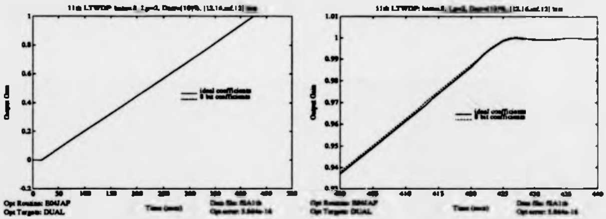

(e) (f)

Figure 6.18 Time domain simulations showing (a) overall and (b) initial impulse response, (c) overall and (d) initial step response and (e) overall and (f) initial ramp response with ideal and finite wordlength coefficients.

Through the FFT the impulse response of a lattice WDF structure can be converted into the frequency domain and displayed in terms of its gain and group delay. By altering the wordlength of the various parameters within the time domain simulation, the effects of coefficient quantization can be determined in isolation to finite wordlength hardware effects. Fig.(6.19) shows the magnitude and group delay responses generated from the impulse response of the lattice WDF of Fig.(6.4) using 64 bits for the input, output and internal signal wordlengths. Responses of Fig.(6.19) therefore illustrate the frequency response distortion due solely to coefficient quantization. These frequency responses, calculated from a time domain simulation, coincide with the finite wordlength coefficient responses determined within the frequency domain, illustrated in Fig.(6.5) and Fig.(6.6).

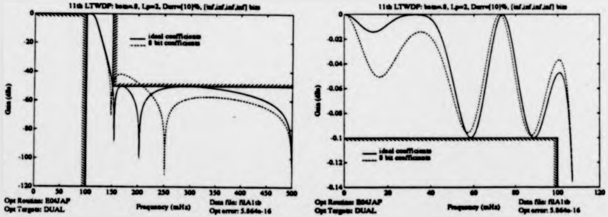

(a) (b)

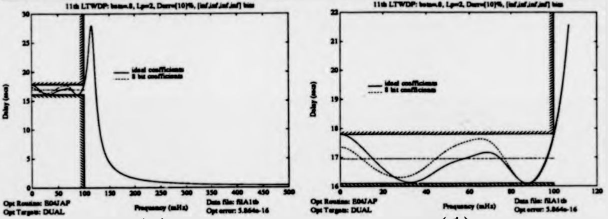

(c) (d)

Figure 6.19 Time domain calculations for magnitude (a) passband and (b) overall and delay (c) passband and (d) overall frequency responses with ideal hardware and finite wordlength coefficients.

Although the FFT allows the various finite wordlength effects to be related to frequency response distortion, it must be remembered that the FFT itself introduces noise to the frequency responses as the DFT is only an approximation to the Fourier transform. The amount of noise introduced will depend upon the frequency resolution of the FFT that is determined by the number of points used to sample the impulse response.

A more detailed investigation of the properties of the FFT is provided by Brigham[1]. All the frequency responses shown in this Chapter were generated through FFT's that used 2048 points. An explanation of the FFT and its characteristics can also be found in a number of DSP text books[7,6,8].

Introducing finite wordlengths for the input, output and internal signals but applying the filter coefficients unquantized within a time domain simulation allowed just the effects of hardware implementation to be displayed in terms of frequency response distortion. Using this technique the distortion to the frequency responses of the filter of Fig.(6.4), with the input and output wordlengths set to 12 bits and the internal signal wordlength set to 16 bits, can be determined and are shown in Fig.(6.20).

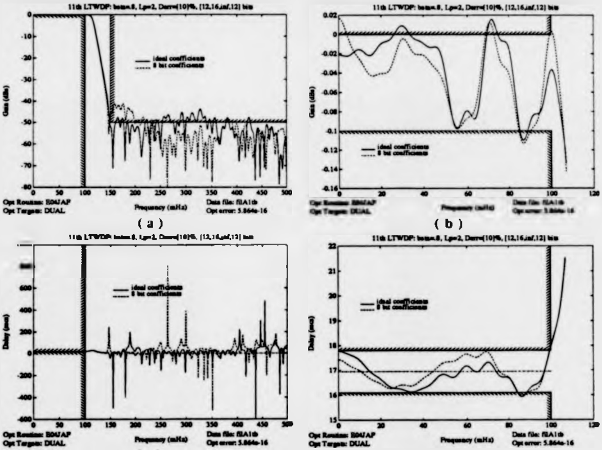

(a) (b)

(c) (d)

Figure 6.20 Time domain simulations showing magnitude (a) passband and (b) overall and delay (c) passband and (d) overall frequency responses under ideal coefficient and finite wordlength hardware conditions.

The effects of scaling on a lattice WDF are more difficult to establish. An ideal hardware implementation would require that the signal at each point within the structure is at a level that produces the best possible signal to noise ratio. This ideal signal level would vary across the structure due to the size of the coefficients. Therefore if an internal signal was multiplied by a small coefficient value then a higher overall accuracy could be achieved if the signal before that multiplier was scaled up.

This process could also be applied around large coefficient values, where to prevent overflows the signal level before an adder would be scaled down. This scaling process would not effect the overall signal level if the result of all these scaling factors was unity. To reduce the complexity introduced by these scaling techniques all scaling values should be a power of two so that the scaling action could be performed through a register shift in physical hardware.

The practical effects of scaling upon the dynamic range and performance of the lattice WDF are very difficult to simulate through software. To determine the actual impulse response of the lattice WDF under different wordlength and scaling strategies the structure was implemented upon a DSP chip.

6.1.3 Lattice WDF implementation

Implementation of a lattice WDF capable of exhibiting various lowpass, highpass and band type responses was approached upon a Loughborough board[4] using the TMS32010 DSP chip[10]. This board was plugged into an IBM compatible machine and the lattice WDF produced under the Texas Instruments development tools.

To test the performance of the lattice WDF, the coefficients of a solution to the simultaneous lowpass design example of Table(6.7) were rounded to 16 bits and are shown in Table(6.8). Using the symmetric frequency transformations discussed in Chapter 5, this simultaneous lowpass example was converted into equivalent single and dual bandpass structures with the same set of multiplier values.

Filter Type	Filter Spec		Frequency edges (Hz)	trans α/β	f_o (Hz)
lowpass	Atten	dBs	0.1 → 34	n / a	n / a
		Hz	0 → 0.08 → 0.16 → 0.5		
	Delay	%dev	0.5 → /		
		Hz	0 → 0.09 → 0.16 → 0.5		
single	Atten	dBs	34 → 0.1 → 34	$\alpha =$	$f_o =$
bandpass		Hz	0 → 0.17 → 0.21 → 0.29 → 0.33 → 0.5	0	0.25
	Delay	%dev	/ → 0.5 → /		
		Hz	0 → 0.17 → 0.21 → 0.29 → 0.33 → 0.5		
dual	Atten	dBs	34 → 0.1 → 34 → 0.1 → 34	$\alpha =$	$f_{o,1} =$
bandpass		Hz	0 → 0.085 → 0.105 → 0.145 → 0.165 → 0.335 → 0.355 → 0.395 → 0.415 → 0.5	0	0.125
	Delay	%dev	/ → 0.5 → / → 0.5 → /	$\beta =$	$f_{o,2} =$
		Hz	0 → 0.085 → 0.105 → 0.145 → 0.165 → 0.335 → 0.355 → 0.395 → 0.415 → 0.5	0	0.375

Table 6.7 Filter specifications for a lowpass filter with equivalent bandpass and dual bandpass specifications.

Upper lattice arm			Lower lattice arm		
APS No.	APS type	multiplier values	APS No.	APS type	multiplier values
1	2nd	$x_1 =$ -0.8828314045 $x_2 =$ 0.6172207384	4	2nd	$x_6 =$ -0.7152976626 $x_7 =$ 0.6370727390
2	2nd	$x_3 =$ -0.5456894656 $x_4 =$ 0.8245115507	5	2nd	$x_8 =$ -0.4759607014 $x_9 =$ 0.9079765957
3	1st	$x_5 =$ 0.6571687539			

Table 6.8 Multiplier values used for the lowpass, bandpass and dual bandpass lattice WDF specifications of Table(6.7).

The gain and group delay responses of these three examples, generated through a software simulation of their impulse responses and using the FFT, are illustrated in Fig.(6.21). In Fig.(6.21) the responses correspond to a time domain simulation with 16 bit wordlengths for coefficients and signals.

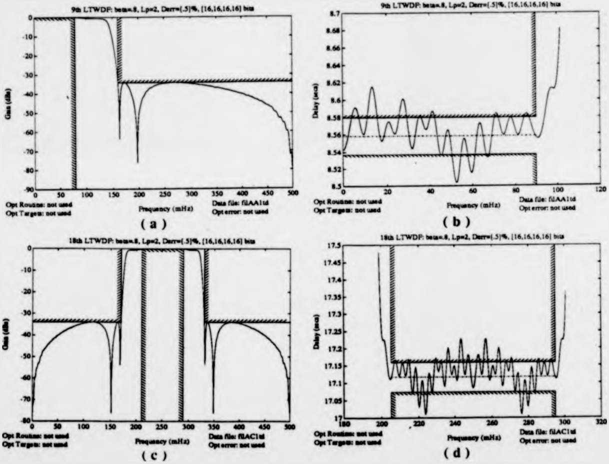

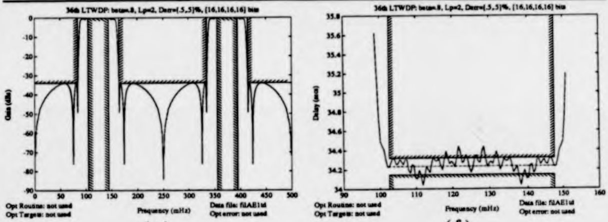

(e) (f)

Figure 6.21 Frequency responses generated through time domain simulations showing magnitude (a) lowpass, (c) bandpass and (e) dual bandpass and group delay (b) lowpass, (d) bandpass and (e) dual bandpass responses.

With the aid of a digital spectrum analyser performing a swept sine operation, the frequency response of the lattice WDF implemented on the TMS chip was measured directly for each of the design examples considered. The simultaneous specifications of Table(6.7) were based upon a sampling frequency of 1 Hz. To utilise the resolution of the digital spectrum analyser, the sampling frequency of the filters implemented upon the DSP chip was increased to 10 kHz. The frequency responses of the three lattice WDF's considered were measured through the digital spectrum analyser and the results are shown by Fig.(6.22), Fig.(6.23) and Fig.(6.24).

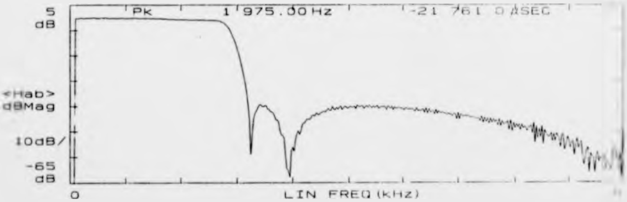

(a)

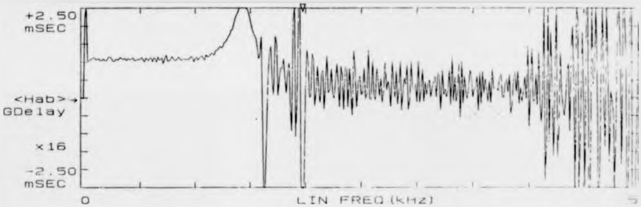

(b)

Figure 6.22 Frequency responses of lowpass lattice WDF showing (a) magnitude and (b) group delay responses.

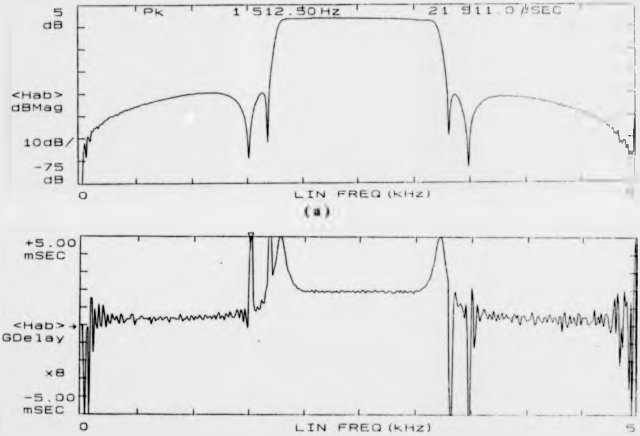

(a)

(b)

Figure 6.23 Frequency responses of single bandpass lattice WDF showing (a) magnitude and (b) group delay responses.

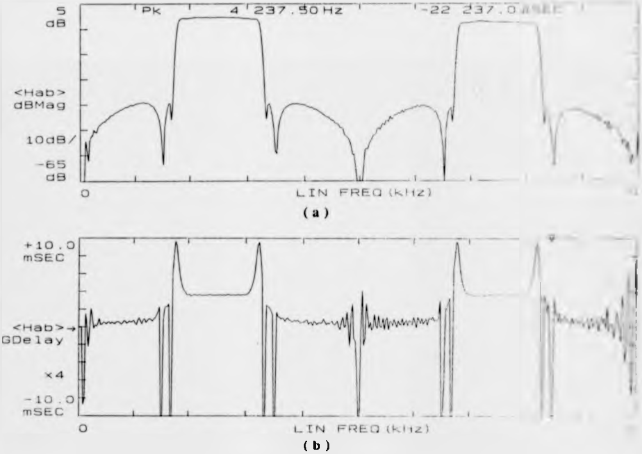

Figure 6.24 Frequency responses of dual bandpass lattice WDF showing (a) magnitude and (b) group delay responses.

The methods of scaling applied within the DSP software entailed halving the input signal and then doubling the output signal, first to the overall structure and then to each arm of the lattice. Both methods appeared to improve the performance of the system compared with the unscaled version but it was felt that further research into the aspects of scaling on the lattice structure fell outside the bounds and time scales of this current research project.

Research into the effects of finite wordlength on the lattice WDF structure has shown that its low gain coefficient sensitivity is a clear indication of its performance under finite wordlength conditions. This performance, however, only relates to the gain response and the inclusion of the group delay into a filter specification reduces the amount of information that can be obtained from the gain coefficient sensitivities. Calculation of the group delay coefficient sensitivities provides a better indication to the performance of a lattice WDF to a finite wordlength simultaneous specification. Several design examples have shown that the minimum wordlength for an acceptable simultaneous solution was higher than for the magnitude-only design. Further investigation into the effects of rounding and truncation upon group delay responses indicated that the performance could be improved if coefficients were selectively rounded or truncated. A more systematic approach to this idea entailed optimization of the finite wordlength filter coefficient values to satisfy an arbitrary magnitude and phase design.

6.2 Design for finite wordlength

6.2.1 Optimization considerations

Finite wordlength design of any digital filter structure may be approached in a number of different ways. However each method must involve some optimization as there is no other method of determining the best set of finite wordlength coefficients for a given frequency specification. The main optimization considerations for finite wordlength design parallel those discussed in Chapter 2 for general filter design. These include the domain in which the filter response is simulated, how the problem is described in terms of a function to be minimized and the optimization algorithm.

The first of these decisions concerns the domain in which the filter is simulated. Filter responses can either be generated analytically in the frequency domain with finite wordlength coefficients or in the time domain with finite wordlength criteria applied to all aspects of the response calculations. The purpose of generating the filter's frequency response is to use an error parameter based upon the sampled function concept. The principle of this idea is to determine the error between the actual and desired function at a number of sample points and then sum these errors under a weighted L_p-metric. Therefore the speed and accuracy of any optimization routine will depend on the number of sample points used and the time taken to calculate the error at each sample point.

Simulation of the filter in the frequency or time domain represents a compromise between accuracy and speed. Although frequency domain simulations are unable to model the effects of finite wordlength signals and different quantization procedures, it is able to evaluate the frequency response at a given sample point quickly and with an accuracy that is independent of the total number of sample points. Simulation of a filter's frequency response through the time domain and the FFT represents a more comprehensive method of modelling all the finite wordlength effects present in a digital structure. However, the accuracy with which the frequency response at each sample point can be generated is dependant upon the total number of points used for the FFT. Ensuring that the FFT has enough points to generate an accurate frequency response to be sampled by the error function makes the method very slow.

Comparing the speed and modelling accuracy of the frequency domain and time domain approaches prompted the selection of the frequency domain. This decision was based upon the very large time taken to generate accurate frequency responses through the FFT.

Using the frequency domain as a basis for finite wordlength coefficient designs, the next design decision concerned the optimization routine, its error function and algorithm. Success with the dual line templates and weighted L_p-metric error function used for coefficient optimization in Chapters 4 and Chapter 5 made these techniques an obvious choice for finite wordlength designs. The selection of an optimization algorithm was more difficult. Optimization of the filter coefficients with a very large accuracy for simultaneous specifications only placed simple boundary constraints upon the optimization algorithm. The addition of finite wordlength criteria upon the coefficient values increases the complexity of any constraints. Increasing the complexity of the constraints of the quasi-Newton type algorithms tends to limit their efficiency as more time is spent ensuring that the coefficients satisfy the wordlength criteria than searching the solution space. An alternative is to apply an optimization algorithm that only moves around the search space with a discrete interval that corresponds to the finite wordlength required. Under this technique the coefficients will always to limited to the desired wordlength and extra calculations to ensure that the finite wordlength constraints had not been violated would not be required.

Optimization algorithms that can be applied to this discrete search problem include the methods suggested by Fletcher & Powell[2] and Hooke & Jeeves[3]. The direct search method of Hooke and Jeeves was adopted because of its success with finite wordlength designs for cascaded second order sections investigated by Steiglitz[9] and because it could be easily modified to include boundary constraints. Boundary constraints were essential to ensure the stability and pseudopassivity of the WDF structure. Application of this optimization algorithm to magnitude-only finite wordlength designs was considered by Mirzai[5] with reference to the implementation of lattice WDF's upon systolic arrays.

6.2.2 Design techniques

Having decided to apply the Hooke-Jeeves algorithm to the finite wordlength coefficient design problem, the next step is to consider the design options available. The main design option concerns the initial coefficient values and their wordlengths. The direct search nature of the Hooke-Jeeves algorithm tends to make it very slow for large numbers of variables. Therefore to speed the convergence rate, the initial coefficient values should be finite wordlength versions of the solutions generated with the quasi-Newton techniques.

Under this technique a filter specification, simultaneous or magnitude-only, would be approached with the quasi-Newton algorithm and procedures discussed in Chapter 4. Having generated a solution for the specification, the ideal filter coefficients would be rounded or truncated to a particular wordlength and then applied to the Hooke-Jeeves based finite wordlength routine.

This design procedure suggests a further choice concerning the initial wordlength for these ideal coefficients. Three options exist :-

(i) Quantize ideal coefficients to desired wordlength and then optimize until a solution can be found within a given threshold.

(ii) Quantize the ideal coefficients to a shorter wordlength than that required and optimize. If no solution can be found below a given threshold then the wordlength would be increased by one bit and optimization reapplied. Continue until a solution can be found.

(iii) Quantize the ideal coefficients to a larger wordlength than that required and optimize. When a solution has been found below a given threshold, reduce the wordlength by one bit and reapply optimization. Continue until a solution cannot be found.

Each optimization procedure has its merits but the first method would only confirm if a given wordlength was possible, not the minimum wordlength for a given frequency specification and filter order. Therefore the other two design procedures represent a better approach for finding minimum finite wordlength solutions.

The first of these two design techniques starts with a very short wordlength and as a consequence has a search step in the optimization routine that would be quite large. This allows a large proportion of the solution space to be searched. If no solution could be found below a given threshold, the wordlength would be increased and as a result the search step would be reduced. Starting from the best solution under the previous wordlength, the optimization routine would be reapplied. If no solution could be found the wordlength would again be increased and the process continued until a solution was generated. The increase in wordlength decreases the search step of the optimization routine, which in turn limits the solution space it can cover.

The process relies upon previous iterations, generating shorter wordlengths solutions, to move closer to a global solution. For this procedure the loss of accuracy in quantizing the ideal solution coefficients to a very short wordlength is compensated by initially searching a wider region of the solution space. This approach would work better with functions that have relatively smooth surfaces, such as magnitude-only specifications.

The other design approach starts with the ideal coefficients quantized to a very large wordlength. This large wordlength would enforce a very small search step upon the Hooke-Jeeves algorithm. A small search step restricts the optimization routine to the region around the ideal solution and ensures that a solution would be found quickly. From a finite wordlength solution, the wordlength would be decreased and starting from the previous solution, the optimization routine would be reapplied. This process would be repeated until a solution could not be found under a given threshold. Reducing the wordlength at each stage would remove a number of coefficient values from the solution space and the corresponding increase in the search step would force the optimization routine to use finite wordlength coefficient values remaining.

Simultaneous specifications approached using this technique showed that the best results were achieved by starting from a very large wordlength, around 20-30 bits, so that there was little difference between the ideal and initial finite wordlength design and then reducing the wordlength by one bit at a time. With this technique, although the initial large wordlength solutions were achieved quickly, the overall design procedure can be slow.

Inserting the modified Hooke-Jeeves algorithm within design program "WDF" allowed a wide range of filter specifications to be approached. Magnitude-only or simultaneous specifications could be described and solved through the quasi-Newton techniques to produce an ideal solution. With this ideal solution the coefficients could then be applied to the Hooke-Jeeves based optimization routine and approached through either of the design procedures discussed to find the minimum wordlength for a given specification. The performance of any finite wordlength solution could then be analysed in the time or frequency domains through the lattice WDF analysis package written for MatLab and discussed in Chapter 4.

6.3 Design examples

The benefits of using the Hooke-Jeeves algorithm to find a finite wordlength solution can be illustrated through a number of design examples using magnitude-only and simultaneous specifications. These examples also show the effect of narrow group delay tolerances upon the minimum achievable coefficient wordlength.

The first example is a 5th order lowpass WDF that satisfies the specification of Table(6.9) with the multipliers of Table(6.10).

Gain passband		Gain stopband		Samp
att (dB)	edge (Hz)	att (dB)	edge (Hz)	freq (Hz)
0.1	0.08	34	0.16	1

Table 6.9 Lowpass filter specification.

Upper lattice arm			Lower lattice arm		
APS No.	APS type	multiplier values	APS No.	APS type	multiplier values
1	2nd	$x_1 =$ -0.8726701 $x_2 =$ 0.8562082	3	2nd	$x_4 =$ -0.6510824 $x_5 =$ 0.9124413
2	1st	$x_3 =$ 0.7395416			

Table 6.10 Lowpass lattice WDF multiplier values that satisfy the lowpass specification of Table(6.9) using an elliptic function.

By applying the Hooke-Jeeves based optimization routine to 4 bit quantized versions of the multipliers of Table(6.10) and increasing the bit length until a solution was found, generated the multipliers of Table(6.11). These multipliers have a wordlength of 7 bits.

Upper lattice arm			Lower lattice arm		
APS No.	APS type	multiplier values	APS No.	APS type	multiplier values
1	2nd	$x_1 =$ -0.828125 $x_2 =$ 0.843750	3	2nd	$x_4 =$ -0.593750 $x_5 =$ 0.906250
2	1st	$x_3 =$ 0.718750			

Table 6.11 Finite wordlength multiplier values that satisfy the lowpass specification of Table(6.9).

The frequency responses of the 5th order lattice structure with quantized versions of the multipliers of Table(6.10) and the optimized coefficients of Table(6.11) can be evaluated to demonstrate the improvements possible. These frequency responses can be calculated analytically in the frequency domain or through an FFT conversion of the impulse response generated in the time domain. Fig.(6.25) shows the magnitude response of the 5th order lattice with the coefficients of Table(6.10) quantized to 7 bits through rounding and truncating and with the coefficients of Table(6.11). These responses purely show the effects of finite wordlength coefficients because they are calculated in the frequency domain. Fig.(6.26) shows the corresponding magnitude responses simulated in the time domain with the input, output and internal data wordlengths set to 16 bits.

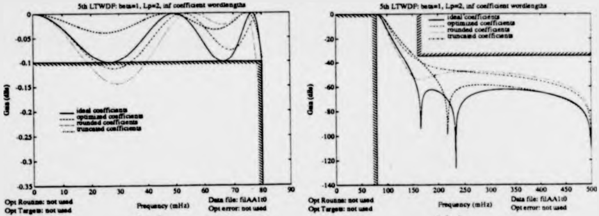

(a) (b)

Figure 6.25 Frequency responses showing magnitude (a) passband and (b) overall responses with ideal and finite wordlength coefficients.

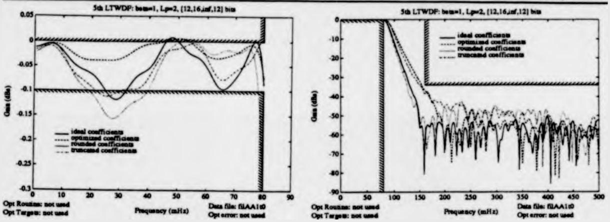

(a) (b)

Figure 6.26 Frequency responses calculated from time domain simulations showing magnitude (a) passband and (b) overall responses under ideal and finite wordlength conditions.

The second example is a simultaneous lowpass specification with a range of group delay tolerances. This specification is given in Table(6.12). Ideal solutions to this specification were produced with the quasi-Newton optimization techniques. The coefficient values of each solution were then quantized and then applied to the Hooke-Jeeves algorithm. Table(6.13) shows the minimum filters order that satisfied the specifications of Table(6.12) along with the minimum coefficient wordlengths that could be achieved with that filter order.

Gain passband		Gain stopband		Delay passband		Samp.
att (dB)	edge (Hz)	att (dB)	edge (Hz)	dev (%)	edge (Hz)	freq (Hz)
0.1	0.1	50	0.15	20 - 0.005	0.1	1

Table 6.12 Simultaneous lowpass filter specification.

	Lattice WDF										Linear
	Ellip	Group delay deviation (%)									phase
	fun	20	10	5	1	0.5	0.1	0.05	0.01	0.005	FIR
filter order	7	11	11	13	15	17	19	19	23	23	52
min. word length	10	15	12	18	18	17	15	17	17	19	/

Table 6.13 Filter orders satisfying the specification of Table(6.12).

The wordlengths of Table(6.13) do not represent the minimum wordlength that can be achieved for a particular simultaneous specification but the minimum wordlength for that specification and filter order. To reduce the wordlength required, especially for very narrow group delay tolerances, the filter order has to be increased. This entails finding a new ideal solution with the quasi-Newton routines and then reapplying this solution to the Hooke-Jeeves routine.

Frequency responses of the 10% group delay deviation example from Table(6.12) are shown by Fig.(6.27) and Fig.(6.28), while Fig.(6.29) and Fig.(6.30) show the frequency responses of the 1% deviation example. Fig.(6.27) and Fig.(6.29) illustrate the magnitude and group delay responses calculated analytically in the frequency domain and compare the responses produced when the ideal coefficients are optimized, rounded and truncated. The frequency responses shown in Fig.(6.28) and Fig.(6.30) are the result of applying a FFT to an impulse response generated in the time domain with input, output and internal data wordlengths limited to 16 bits and the coefficients optimized, rounded and truncated to the same bit length.

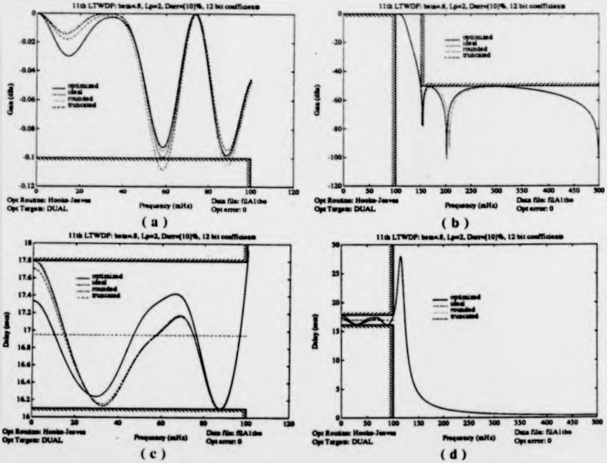

Figure 6.27 Frequency responses of 10% delay deviation showing (a) passband and (b) overall magnitude and (c) passband and (d) overall group delay responses under ideal and finite wordlength conditions.

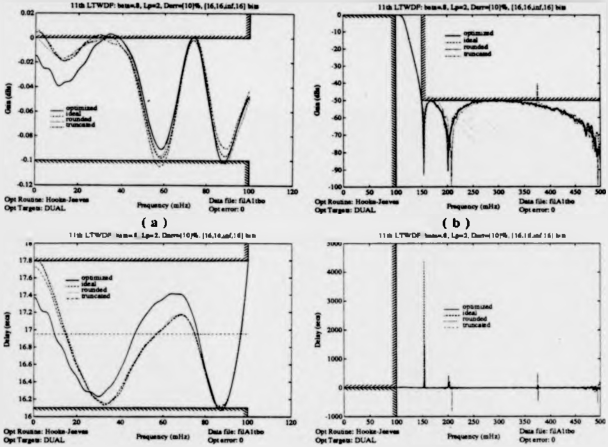

(c) (d)

Figure 6.28 Frequency responses of 10% delay deviation calculated from time domain simulation showing (a) passband and (b) overall magnitude and (c) passband and (d) overall group delay responses under ideal and finite wordlength conditions.

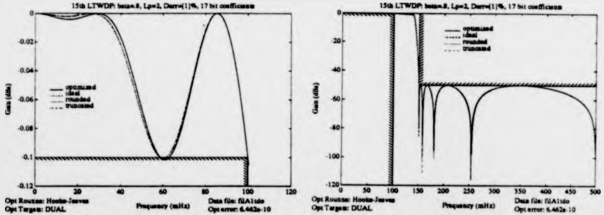

(a) (b)

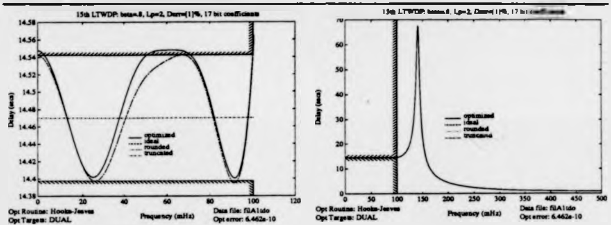

(c) (d)

Figure 6.29 Frequency responses of 1% delay deviation showing (a) passband and (b) overall magnitude and (c) passband and (d) overall group delay responses under ideal and finite wordlength conditions.

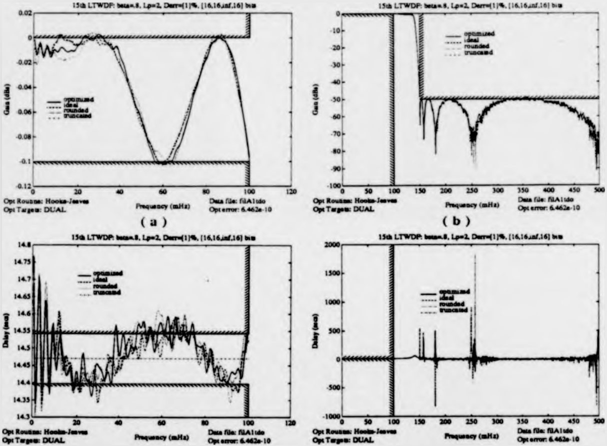

(a) (b)

(c) (d)

Figure 6.30 Frequency responses of 1% delay deviation calculated from time domain simulation showing (a) passband and (b) overall magnitude and (c) passband and (d) overall group delay responses under ideal and finite wordlength conditions.

The final example is a single bandpass simultaneous specification that is given in Table(6.14). This specification cannot be achieved by transforming a lowpass design and therefore must use a different transformation value for each APS within the structure. Using the quasi-Newton routine and the procedures outlined in Chapter 5, a set of filter orders and ideal coefficients was determined. With these coefficient values as a starting point, the Hooke-Jeeves procedures were applied to each specification to evaluate the minimum possible wordlength. The results of these calculations are shown in Table(6.15).

Specification		lower stopband	passband	upper stopband
Gain	atten (dB)	50	0.1	50
	freq (Hz)	0 → 0.075	0.1 → 0.2	0.225 → 0.5
Group Delay	dev (%)	/	20 - 0.005	/
	freq (Hz)	0 → 0.075	0.1 → 0.2	0.225 → 0.5

Table 6.14 Simultaneous single bandpass lattice WDF specifications.

	Bandpass Lattice WDF										Linear phase FIR
	Gain only	Group delay deviation (%)									
		20	10	5	1	0.5	0.1	0.05	0.01	0.005	
filter order	14	26	26	34	38	42	46	50	54	62	105
min. word length	14	13	15	16	16	15	18	19	20	19	/

Table 6.15 Filter orders satisfying the specification of Table(6.15).

Frequency responses of the 5% group delay deviation example from Table(6.15) are shown in Fig.(6.31).

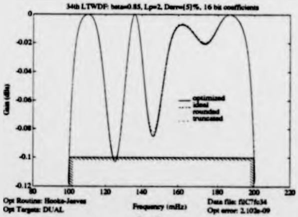

(a)

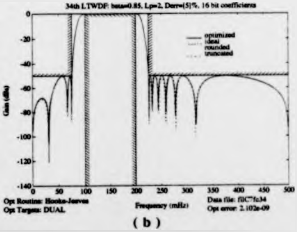

(b)

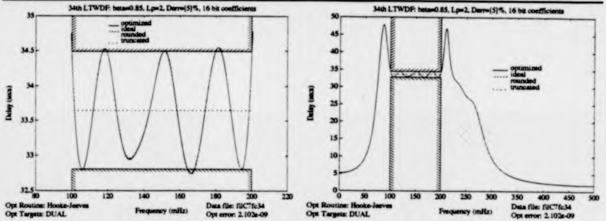

(c) (d)

Figure 6.31 Frequency responses of 5% delay deviation showing (a) passband and (b) overall magnitude and (c) passband and (d) overall group delay responses under ideal and finite wordlength conditions.

6.4 Conclusions

The objective of this Chapter has been to illustrate the performance of the lattice WDF under various finite wordlength conditions and then to outline a number of techniques to counteract these effects.

Errors due to finite wordlength effects within a digital filter may be attributed to distortion of the frequency response by finite wordlength coefficients or the introduction of noise by digital hardware. An indication of the frequency response distortion can be obtained by calculating the frequency response of a filter analytically with finite wordlength coefficient values. The effect of digital hardware on the performance of a digital filter can only be modelled through a time domain simulation.

This Chapter has illustrated a number of different finite wordlength effects in terms of coefficient quantization and confirmed the validity of these results through simulation in the frequency and time domains and actual implementation upon a DSP chip. The main techniques that can be used to improve the performance of a digital filter involve an appropriate selection of finite wordlength filter coefficient values that best retain the desired frequency response(s) and a set of scaling factors that result in the greatest signal to noise ratio for a given hardware implementation. Research of this project has concentrated upon the finite wordlength coefficient aspect of the problem although future work may be expanded to include the scaling and other hardware implementation considerations.

Optimization is based upon the minimization of an error function, which for filter design is a sum of errors generated by sampling the frequency response(s) at a number of points. The frequency response(s) can be generated analytically in the frequency domain or produced through a FFT of an impulse response simulated in the time domain. Time domain simulations provide an ability to model a wide range of finite wordlength effects such as quantization, overflow and scaling that are not possible in the frequency domain. However the time required to generate an accurate frequency response(s) from an impulse response through the FFT makes the techniques impractical for use within an optimization routine. Therefore the finite wordlength optimization routine(s) were concerned only with minimizing the frequency response distortion due to finite wordlength coefficient values based in the frequency domain.

Design of finite wordlength solutions to arbitrary frequency specifications was approached through the optimization techniques developed for the large precision solutions discussed in Chapter 4 and Chapter 5. Although the design templates and error functions from these techniques could be applied directly, the nature of the finite wordlength constraints prompted the selection of a non-quasi-Newton algorithm. The optimization routine adopted was based upon a direct search technique, developed by Hooke-Jeeves, where the search step was determined by the required coefficient bit length.

The nature of the direct search optimization algorithm made it very slow, so the procedure developed for finite wordlength designs involved first producing a solution to the frequency specification with large precision or ideal coefficient values and then using a quantized version of these coefficient values as a starting point for the finite wordlength optimization routine. This process suggested a number of options concerning the bit length of these initial coefficient values. Three methods exist, quantize the coefficients to the desired bit length, quantize coefficients to a bit length shorter than required and then increase until a solution is found, or quantize to a bit length larger than required and reduce until a solution cannot be found. The first method only determines if a solution exists for that bit length while the other two methods produce the minimum bit length for a given specification.

Experiments have shown that the method of quantizing the ideal coefficient values to a very low bit length and then increasing it until a solution is found worked best on magnitude-only frequency specifications with an initial bit length of 4-6 bits. The method of quantizing the ideal coefficient values to a large bit length and then decreasing the bit length was more efficient with simultaneous designs and very large initial bit lengths, around 24-30 bits. Both methods performed better when the bit length was incremented or decremented by one bit at each iteration.

Results from this Chapter have shown that the direct search based optimization routines provide a viable approach to finite wordlength digital filter designs. The techniques suggested also determined the minimum coefficient wordlength that can be achieved for a given frequency specification, filter order and error tolerance. Experiments have confirmed the low bit lengths achievable with the lattice WDF for magnitude-only designs. However, work on simultaneous designs has shown that the inclusion of a group delay specification greatly increases the minimum wordlength possible, sometimes around 12-18 bits. This property may counter the advantages, such as lower filter order, gained against alternative filter designs, namely the exactly linear phase FIR filter.

Using the techniques developed and outlined in this Chapter for finite wordlength designs, the final stage of this research project concerned the design and simulation of a simultaneous dual bandpass frequency specification. The design procedures for this process are detailed in Chapter 7.

References

1) Brigham, E. O., *The Fast Fourier Transform*, Prentice-Hall, New Jersey, 1972.

2) Fletcher, R. and Powell, M. J. D., "A Rapid Convergent Descent Method for Minimization", Computer Journal, Vol 6, No. 2, July 1963, pp163-168.

3) Hooke, R. and Jeeves, T. A., "'Direct Search' Solution of Numerical and Statistical Problems", Jour. Assoc. Comput. Mach., Vol 8, No. 2, April 1961, pp212-229.

4) Loughborough Sound Images Ltd., "TMS 320C10 System Board", The Technology Centre, Epinal Way, Loughborough.

5) Mirzai, A. R., "Finite Wordlength Design and VLSI Implementation of Wave Digital Filters", Ph. D. Thesis, The City University, London, 1986.

6) Oppenheim, A. V. and Schafer, R. W., *Digital Signal Processing*, Prentice-Hall International, London, 1975.

7) Rabiner, L. R. and Gold, B., *Theory and Application of Digital Signal Processing*, Prentice-Hall, New Jersey, 1975.

8) Roberts, R. A. and Mullis, C. T., *Digital Signal Processing*, Addison-Wesley, Massachusetts, 1987.

9) Steiglitz, K., "Designing Short-Word Recursive Digital Filters", Proc. 9th Annual Allerton Conf. Cir. and System Theory, October 1971, pp778-788.

10) Texas Instruments Ltd., "DSP C compiler development Suite", Beffordis House, Prebend Street, Bedford.

Chapter 7

Lattice WDF Design Example

7.1 Introduction

The overall objective of this research project entailed the design of WDF's capable of satisfying a finite wordlength linear phase dual bandpass frequency specification. The previous Chapters have outlined the various WDF's structures considered and the design techniques investigated. Results of this research prompted the selection of the lattice WDF structure. Design techniques were based upon optimization using quasi-Newton algorithms to determine large precision solutions and a modified Hooke-Jeeves routine for finite wordlength solutions. The purpose of this Chapter is to detail the stages of the design process proposed through a dual bandpass example.

The first step concerns the filter specification, detailing the cut-off frequencies, attenuation levels, group delay linearity and final coefficient wordlengths. From the specification, the order of filter required to satisfy the magnitude-only part of the specification would be estimated. Starting with a lattice WDF of that order, the quasi-Newton based optimization routines, detailed in Chapter 4, would be applied in an attempt to generate a solution to the magnitude-only part of the specification.

With optimization parameter values determined for the magnitude-only design, the group delay element of the specification would be introduced. The order of the filter would be retained and the group delay tolerance increased until a simultaneous solution could be produced. Using the optimization settings developed to produce this simultaneous solution, the group delay tolerance would be reduced, nominally by a factor of two, and the filter order increased until a new simultaneous solution could be generated. This process would continue until the desired group delay deviation was achieved.

Simultaneous solutions obtained with the quasi-Newton algorithms would be based upon coefficients specified to a large degree of accuracy. As a consequence the frequency response will distort when the coefficients are quantized. To offset the finite wordlength effects, the coefficients' values would then be applied to the

Hooke-Jeeves routine detailed in Chapter 6. Using this algorithm and the 'ideal' coefficient values generated by the quazi-Newton routine as initial values, the best set of finite wordlength coefficients for a particular bit length or function error would be determined. For simultaneous specifications this finite wordlength design process would begin with the ideal coefficient values quantized to a very large bit length, nominally around 32 bits and applied to the Hooke-Jeeves routine. When a solution was found the bit length would be reduced and the resulting coefficient values reapplied to the optimization routine. The bit length would be reduced in this manner until the desired finite wordlength was achieved or the frequency response distortion becomes unacceptable. If the desired wordlength could not be achieved, a simultaneous solution to a higher order filter would be generated and the finite wordlength optimization process repeated until the desired wordlength attained.

The steps involved in this design procedure can be better illustrated through a design example. The example chosen represents a design that cannot be achieved other than through optimization and details the stages in the design process.

7.2 Filter Specification

The frequency specification of the dual bandpass filter example considered is detailed by Table(7.1), while the templates for the response are shown in Fig.(7.1).

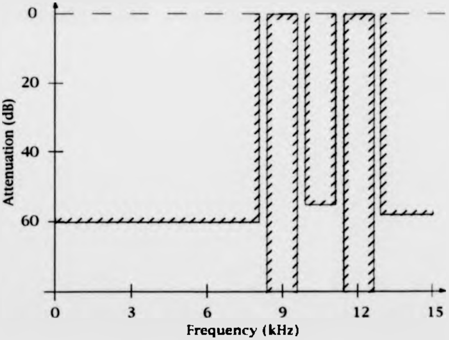

(a)

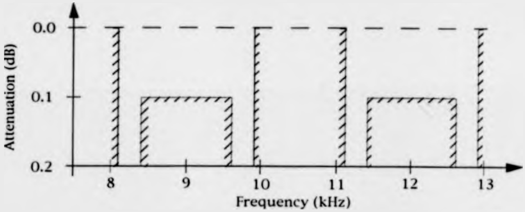

(b)

Figure 7.1 Graphical representation showing the attenuation (a) overall and (b) across the passband, for the frequency specification of Table(7.1).

Specifications		1st stop	1st pass	2nd stop	2nd pass	3rd stop
Atten	dB	600	01	550	01	580
	kHz	0 ⇔ 8.1	8.4 ⇔ 9.6	9.9 ⇔ 11.1	11.4 ⇔ 12.6	12.9 ⇔ 15
Delay	dev(%)	/	1	/	1	/
	kHz	0 ⇔ 8.1	8.4 ⇔ 9.6	9.9 ⇔ 11.1	11.4 ⇔ 12.6	12.9 ⇔ 15
F_s = 30 kHz		maximum coefficient bit length = 16				

Table 7.1 Simultaneous filter specification.

The first step in the design process is to establish limits for the filter order with this frequency specification. The lower value of the limit is set by the minimum filter order that satisfies the magnitude-only side of the specification. An upper limit is imposed to ensure the filter order for an approximately phase design using the lattice WDF does not exceed that of an equivalent FIR filter which possesses exactly linear phase.

A number of different software packages can be used to determine the filter order of an exactly linear phase FIR filter equivalent to the specification of Table(7.1). Using software written within MatLab especially for this purpose, the equivalent FIR filter order for this design was determined as 286. The symmetric nature of an exactly linear phase FIR filter imposes a need for only (N+1)/2 independent multipliers, or for this design example 143 multipliers.

The operational speed of a digital filter is limited by the amount of computation required within each sample period. By far the slowest component within any digital filter's operation is multiplication and as a result a more realistic comparison between a lattice WDF and an exactly linear phase FIR filter would involve the number of multiplications per sample. Under this principle, the upper limit on the lattice filter order would be set to half the order of the equivalent exactly linear phase FIR filter.

The lower filter order limit is set by the minimum order that will satisfy the magnitude-only part of a specification. For lowpass specifications the minimum filter order can be calculated from standard polynomial equations widely used in filter designs. The most efficient polynomial for magnitude-only filter designs is the elliptic polynomial. Standard polynomials can only be applied directly to lowpass specifications. To determine the filer order of highpass, bandpass or dual bandpass specifications requires an equivalent lowpass specification. The filter order of an equivalent lowpass specification may not be very accurate, but provide a good initial guess. With complex specifications, such as the dual bandpass example of Table(7.1), the only method of determining the minimum filter order is through optimization. Calculation of the minimum lattice WDF order that satisfied the magnitude-only part of the specification of Table(7.1) should therefore be approached through the quasi-Newton and dual line template ideas discussed in previous Chapters.

The final area of the specification is the filter structure. Ladder WDF structures have proved unsuitable for simultaneous frequency specifications because of their minimum-phase characteristics. Dual band designs upon the lattice WDF structure using the transformed APS's detailed in Chapter 5, have also met with little success. For this reason dual bandpass and bandstop specification, such as Table(7.1), should be approached with the standard 1st and 2nd order APS's described in Chapter 4.

The lattice WDF, Fig.(7.2), can be simplified if the second input, A2, is set to zero. The resulting basic one-port structures are shown by Fig.(7.3). These simplified lattice WDF's are polyphase structures whose transfer functions are the sum or difference of the transfer functions of two branches. The structure of Fig.(7.3)(a) has the transfer function given by Eq.(7.1), while the structure of Fig.(7.3)(b) corresponds to Eq.(7.2).

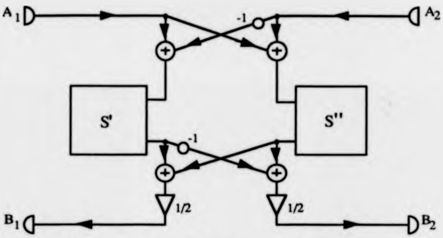

Figure 7.2 Complete Lattice WDF Structure.

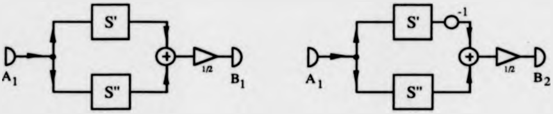

(a) (b)

Figure 7.3 Simplified lattice WDF's structures using (a) output port B_1 and (b) output port B_2.

$$G(z) = \frac{B_1}{A_1} = \frac{S'' + S'}{2} \qquad (7.1)$$

$$G(z) = \frac{B_2}{A_1} = \frac{S'' - S'}{2} \qquad (7.2)$$

Due to the nature of the lattice structure the transfer functions Eq.(7.1) and Eq.(7.2) are complementary, such that if the structure of Fig.(7.2)(a) has a lowpass frequency response, then with the same coefficients, the structure of Fig.(7.3)(b) will exhibit a highpass response.

Designs using the transformed APS's described in Chapter 5 have been based upon the lattice structure of Fig.(7.3)(a), however, to satisfy single and dual bandpass specifications using the standard 1st and 2nd order APS's, requires the lattice structure of Fig.(7.3)(b).

7.3 Magnitude-Only Design (Ideal)

The main purpose of this design stage is to determine the minimum filter order and optimization settings for a simultaneous design. The magnitude-only solution to a given filter specification provides a basis for the simultaneous case and initial coefficient values for finite wordlength magnitude-only designs. The software tools developed within in this research project allow for both magnitude-only and simultaneous finite wordlength designs. Both procedures are outlined in this Chapter.

In order to apply optimization to the magnitude-only part of the specification of Table(7.1), a number of parameters need to be evaluated or estimated. The main parameter is the initial filter order. This can be estimated by calculating the order of a polynomial that can satisfy an equivalent lowpass specification. An approximate method of converting a general specification into a lowpass specification is to sum the widths of the various passbands and stopbands to generate the edge frequencies and the most severe attenuation levels. The final step involves normalising the frequency edge values to coincide with a sampling frequency of 1 Hz. Applying this method to the magnitude-only part of the specification of Table(7.1), shown in Table(7.2), produces the lowpass specification of Table(7.3).

Specification		1st stop	1st pass	2nd stop	2nd pass	3rd stop
Atten	dB	60	0.1	55	0.1	58
	kHz	0 ⇔ 8.1	8.4 ⇔ 9.6	9.9 ⇔ 11.1	11.4 ⇔ 12.6	12.9 ⇔ 15
F_s = 30 kHz		maximum coefficient bit length = 16				

Table 7.2 Magnitude-only part of the filter specification of Table(7.1).

Specification		Passband	Stopband
Atten	dB	0.1	60
	Hz	0 ⇔ 0.08	0.12 ⇔ 0.5
F_s = 1 Hz		max. coefficient bit length = 16	

Table 7.3 Estimated lowpass equivalent of the specification of Table(7.2).

The minimum elliptic polynomial that can satisfy the specification of Table(7.3) is 7th order. Applying the optimization techniques to this lowpass specification allows a range of weights, error point and transition and template angle to be investigated. Optimization parameters were varied until the optimization routine generated a response that fitted within the design templates. Coefficient values from this solution were then applied to the finite wordlength design procedures to determine the minimum coefficient wordlength for this specification. Responses from the large and finite wordlength solution are shown in Fig.(7.4).

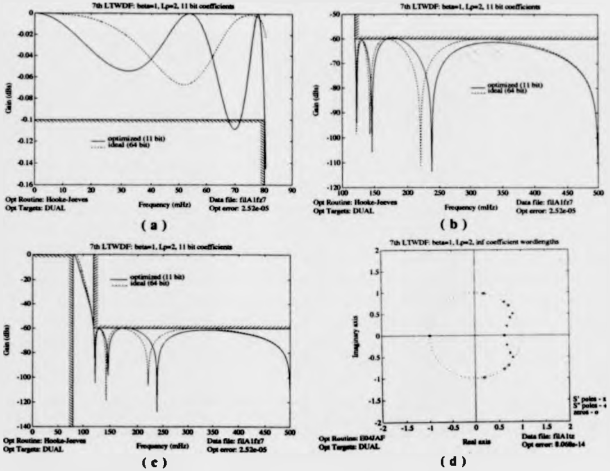

(a) (b) (c) (d)

Figure 7.4 Magnitude (a) passband, (b) stopband and (c) overall frequency responses and (d) pole/zero plot of a solution to the specification of Table(7.3).

Transformation of a lowpass filter structure into a dual bandpass form, detailed in Chapter 5, requires the filter order to be doubled to produce a bandpass structure and then doubled again to generate a dual bandpass response. A 28th order lattice WDF of this type and the coefficient values from the lowpass solution can then be used to create an equivalent dual bandpass response. If the frequency transformation values for each APS were set to 0.86 and -0.65 then the transformed response closely matched the magnitude-only specification of Table(7.2). The frequency responses of a dual bandpass lattice structure under these conditions are illustrated by Fig.(7.5).

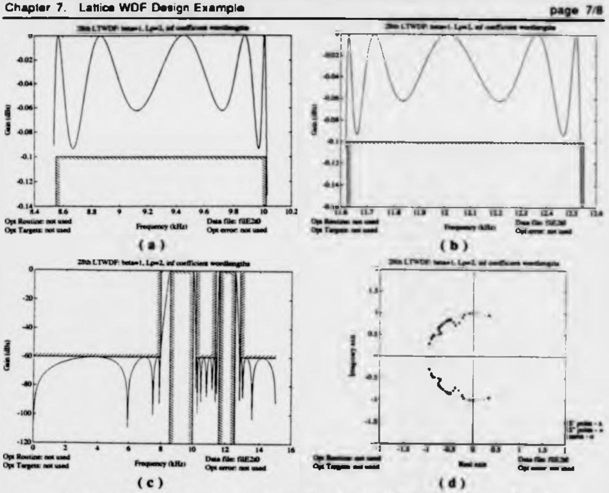

(a) (b) (c) (d)

Figure 7.5 Magnitude (a) lower passband, (b) upper passband and (c) overall frequency responses and (d) pole/zero plot of a transformed solution from the lowpass specification to Table(7.3).

Due to the limited performance of the transformed APS's for dual bandpass designs, an exact solution to the specification of Table(7.2) could not be generated even using the frequency transformation values for each APS as an optimization parameter. Further designs were switched to the standard 1st and 2nd order APS's upon the lattice WDF structure shown by Fig.(7.3)(b). The filter order of the transformed APS design was used as an initial guess for this design method.

Optimization parameters that produced the equivalent lowpass solution were modified to incorporate changes in transition band width and attenuation levels. Experience gained through a number of filter designs has shown that the most effective optimization solutions were generated with an error function based upon an L_2-metric and error points that were clustered around the regions of greatest change, weights that produced an equal deviation/equal error effect and all the initial multiplier values set to zero. Parameter values selected for the design of a dual bandpass filter to satisfy the specification of Table(7.2) are detailed in Table(7.4).

Filter order	28
Initial multiplier values	all zero
Lp-metric value	2
Beta ratio (i.e. magnitude-only design)	1

Parameters per band	1st stop	1st tran	1st pass	2nd tran	2nd stop	3rd tran	2nd pass	4th tran	3rd stop
Error points	37	11	21	11	21	11	21	11	15
Error point spacing	sine	linear	dual cos	linear	dual cos	linear	dual cos	linear	cos
weights	5000	200	50	200	5000	200	50	200	5000

Table 7.4(a) Initial optimization parameter values.

Transition bands		1st	2nd	3rd	4th
template angles (degs)	upper	35	35	35	35
	lower	30	30	30	30

Table 7.4(b) Initial optimization parameter values.

Using the initial parameter settings of Table(7.4), dual line template and quasi-Newton based optimization was applied to the design specification. Results from the design process very closely approached the desired solution, but tended to spike at the edges of stopband. Spikes are most prominent when the filter order is too large for a specification. Other signs that the filter order was too high could be seen in the frequency response of the solution, Fig.(7.6), where the middle stopband attenuation was lower than necessary.

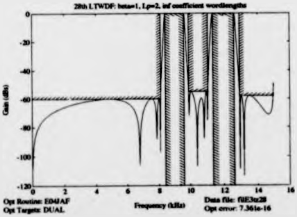

Figure 7.6 Overall magnitude responses of a 28th order solution to the specification of Table(7.2).

Following the results of the 28th order design solution, the filter order was reduced to 26 and the optimization process re-applied with the same initial optimization parameter values. Solutions from this design process were more successful. The frequency responses of the solution are shown in Fig.(7.7).

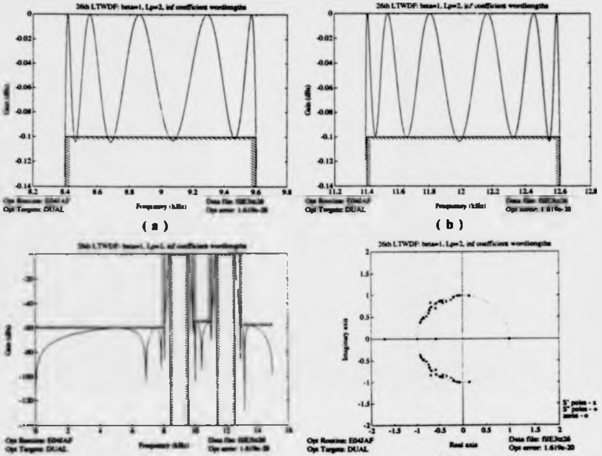

(a) (b) (c) (d)

Figure 7.7 Magnitude (a) lower passband, (b) upper passband and (c) overall frequency responses and (d) pole/zero plot of a 26th order solution to the specification to Table(7.2).

7.4 Magnitude-Only Design (Finite)

Starting with the coefficient values generated in the previous section and the optimization parameter values of Table(7.4), the design example was applied to the finite wordlength routine. This process would determine the minimum coefficient wordlength for this filter order and specification. The finite wordlength coefficient values produced through the optimization process were 16 bits in length and are given in Table(7.5).

Upper lattice arm			Lower lattice arm		
APS No.	APS type	multiplier values	APS No.	APS type	multiplier values
1	2nd	x_1 = -0.93023681640625 x_2 = -0.20568847656250	7	2nd	x_{13} = -0.86846923828125 x_{14} = -0.26959228515625
2	2nd	x_3 = -0.88696289062500 x_4 = -0.45800781250000	8	2nd	x_{15} = -0.98004150390625 x_{16} = -0.18164062500000
3	2nd	x_5 = -0.85473632812500 x_6 = -0.37414550781250	9	2nd	x_{17} = -0.96643066406250 x_{18} = -0.43701171875000
4	2nd	x_7 = -0.88385009765625 x_8 = -0.77886962890625	10	2nd	x_{19} = -0.86120605468750 x_{20} = -0.45568847656250
5	2nd	x_9 = -0.98028564453125 x_{10} = -0.72448730468750	11	2nd	x_{21} = -0.93420410156250 x_{22} = -0.74029541015625
6	2nd	x_{11} = -0.93237304587500 x_{12} = -0.86633300781250	12	2nd	x_{23} = -0.88232421875000 x_{24} = -0.83197021484375
			13	2nd	x_{25} = -0.98010253906250 x_{26} = -0.87896728515625

Table 7.5 16 bit coefficient values that satisfy the dual bandpass specification of Table(7.2).

Impulse responses of the 26^{th} order lattice WDF's with the ideal and finite wordlength coefficients are illustrated in Fig.(7.8), while the frequency responses are shown in Fig.(7.9).

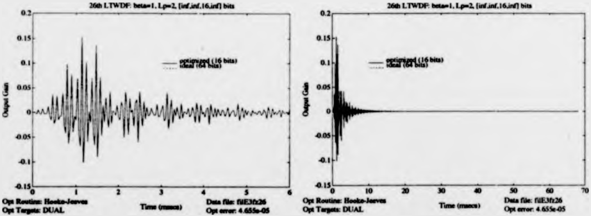

(a) (b)

Figure 7.8 (a) Initial and (b) overall impulse responses of a 26th order solution to the specification to Table(7.2) under ideal and finite wordlength conditions.

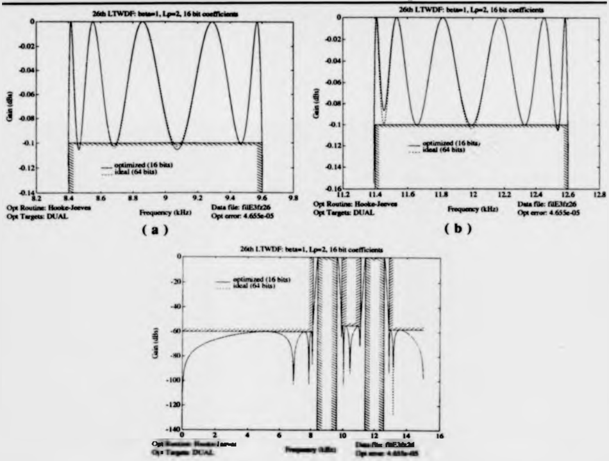

(a) (b)

(c)

Figure 7.9 Magnitude (a) lower passband, (b) upper passband and (c) overall frequency responses of a 26th order solution to the specification to Table(7.2) under ideal and finite wordlength conditions.

7.5 Simultaneous Design (Ideal)

The filter order for the magnitude-only part of the specification of Table(7.1) was determined to be 26. Using a 26th order solution as a starting point, the group delay part of the specification was introduced. With the optimization parameter values of Table(7.6), the group delay tolerance was started at 200%.

Filter order	26
Initial multiplier values	Ideal
Lp-metric value	2
Beta ratio (i.e. magnitude-only design)	0.8
Group Delay tolerance	200%
Initial mean passband group delay value	0.0025 sec

Parameters per band	1st stop	1st tran	1st pass	2nd tran	2nd stop	3rd tran	2nd pass	4th tran	3rd stop
Gain template values									
Error points	37	11	21	11	21	11	21	11	15
Pt spacing	sine	linear	dual cos	linear	dual cos	linear	dual cos	linear	cos
Weights	5000	200	50	200	5000	200	50	200	5000
Group Delay template values									
Error points	/	/	19	/	/	/	19	/	/
Pt spacing	/	/	linear	/	/	/	linear	/	/
Weights	/	/	60000	/	/	/	60000	/	/

Table 7.6(a) Initial optimization parameter values.

Transition bands		1st	2nd	3rd	4th
template angles (degs)	upper	35	35	35	35
	lower	30	30	30	30

Table 7.6(b) Initial optimization parameter values.

When a solution was generated for this specification, the group delay tolerance was reduced until a 26th order simultaneous solution could not be created. For the specification of Table(7.1), the minimum group delay deviation for a 26th order lattice WDF was 90%.

Having determined a set of optimization parameters from the initial simultaneous designs, the filter order was increased and the group delay tolerance again lowered until a solution could not be generated. The filter order was increased so that there was always a larger number of poles in the upper, S", branch of the lattice structure. Following this rule the next filter order considered was 30. Optimization determined that the minimum group delay deviation for the 30th order lattice WDF example was 70%. Repeating this design process for a 34th order example produced a minimum deviation of 50%. Using the reduction in group delay per filter order, as a rule of thumb, a 20% deviation example was considered upon a 42nd order lattice WDF. The actual solution was achieved upon a 46th order lattice structure.

The specification of Table(7.1) requires a group delay deviation of 1%. Applying the rule of thumb concerning filter order, the 1% tolerance example was first considered upon a 54th order lattice structure. Fig.(7.10) shows the responses of the 54th order solution generated through the quazi-Newton, dual line templates and optimization parameter settings of Table(7.6).

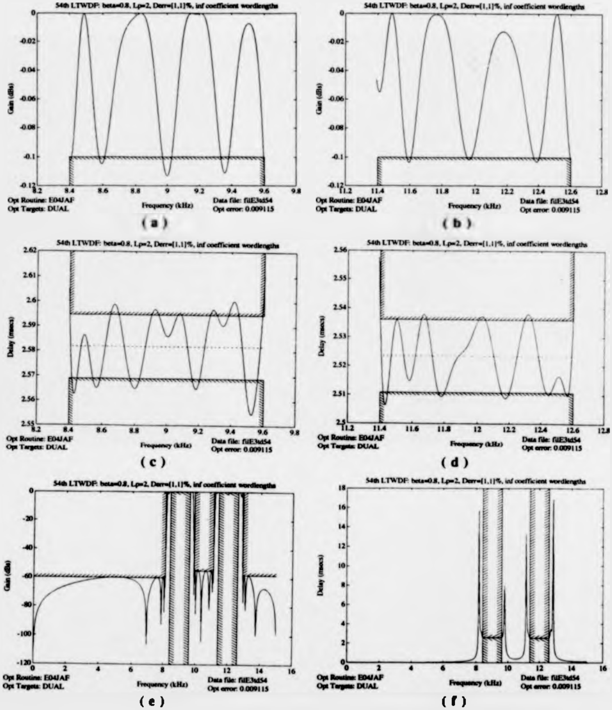

(a) (b) (c) (d) (e) (f)

Figure 7.10 Passband (a) lower and (b) upper magnitude, passband (c) lower and (d) upper group delay and overall (e) magnitude and (f) group delay frequency responses of a 54th order lattice WDF.

The responses of Fig.(7.10) fail to satisfy the specification of Table(7.1), although only just for the upper passband responses. Failure to satisfy any region of the specification suggests the filter order was too low. Retaining the optimization parameter values from this solution, the filter order was increased until an acceptable solution was achieved.

A final solution was produced upon a 66th order lattice structure. The frequency responses of this solution are illustrated in Fig.(7.11).

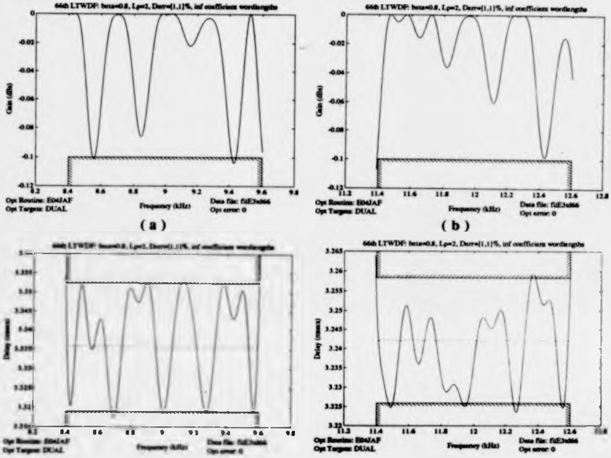

(a) (b)

(c) (d)

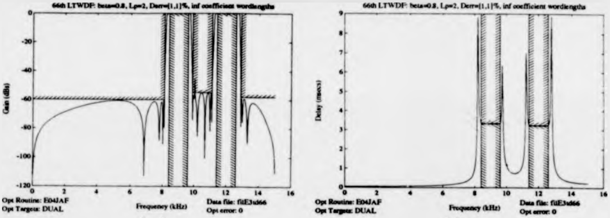

(e) (f)

Figure 7.11 Passband (a) lower and (b) upper magnitude, passband (c) lower and (d) upper group delay and overall (e) magnitude and (f) group delay frequency responses of a 66th order lattice WDF.

7.6 Simultaneous Design (Finite)

The final step in the design process involved generating a finite wordlength solution to the specification. Using the ideal coefficients determined in the previous section as a starting point, the modified Hooke-Jeeves optimization routine was applied to the problem. With the same optimization parameters used for the ideal coefficient solution and an initial wordlength of 32 bits, the optimization routine produced a solution with a minimum wordlength of 26 bits. This therefore represented the minimum coefficient wordlength for the specification of Table(7.1) and a 66th order lattice WDF.

Satisfying the 16 bit requirement of Table(7.1) involved increasing the filter order, finding an ideal coefficient simultaneous solution and reapplying the finite wordlength optimization routine. Each iteration of this process determined the minimum coefficient wordlength for that order of filter. A solution was finally achieved with a 74th order lattice WDF. Frequency responses of this solution using ideal and finite wordlength coefficient values are illustrated in Fig.(7.12). As a comparison the frequency responses of the equivalent exactly linear phase FIR filter are shown by Fig.(7.13). The finite coefficient values are detailed in Table(7.7).

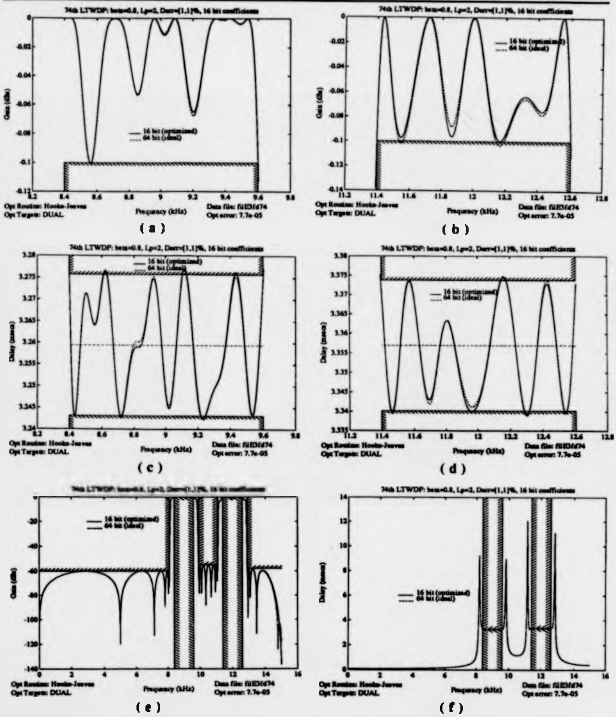

(a) (b)

(c) (d)

(e) (f)

Figure 7.12 Passband (a) lower and (b) upper magnitude, passband (c) lower and (d) upper group delay and overall (e) magnitude and (f) group delay frequency responses of a 74th order lattice WDF with ideal and 16 bit coefficients.

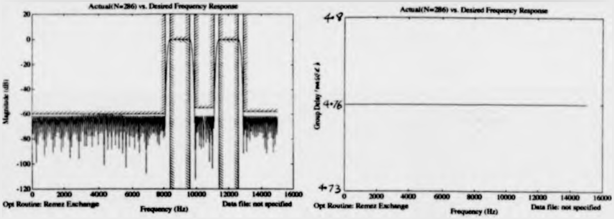

(a) (b)

Figure 7.13 Overall (a) magnitude and (b) group delay frequency responses of a 286th order exactly linear phase FIR filter.

Upper lattice arm					
APS No.	APS type	multiplier values	APS No.	APS type	multiplier values
1	2nd	x_1 = -0.973602294921875 x_2 = -0.146820068359375	10	2nd	x_{19} = -0.896209716796875 x_{20} = -0.804107666015625
2	2nd	x_3 = -0.929443359375000 x_4 = -0.331054687500000	11	2nd	x_{21} = -0.290618896484375 x_{22} = -0.664215087890625
3	2nd	x_5 = -0.940582275390625 x_6 = -0.203704833984375	12	2nd	x_{23} = -0.892364501953125 x_{24} = -0.750670386718750
4	2nd	x_7 = -0.930328369140625 x_8 = -0.264984130859375	13	2nd	x_{25} = -0.990173339843750 x_{26} = -0.692535400390625
5	2nd	x_9 = -0.927276611328125 x_{10} = -0.396972656250000	14	2nd	x_{27} = -0.940399169921875 x_{28} = -0.721130371093750
6	2nd	x_{11} = -0.633209228515625 x_{12} = -0.502838134765625	15	2nd	x_{29} = -0.859039306640625 x_{30} = -0.816162109375000
7	2nd	x_{13} = -0.682342529296875 x_{14} = -0.395141601562500	16	2nd	x_{31} = -0.908416748046875 x_{32} = -0.858947753906250
8	2nd	x_{15} = -0.971496582031250 x_{16} = -0.465240478515625	17	2nd	x_{33} = -0.794433593750000 x_{34} = -0.855102539062500
9	2nd	x_{17} = -0.402252197265625 x_{18} = -0.600219726562500	18	2nd	x_{35} = -0.979400634765625 x_{36} = -0.897888183593750

Table 7.7(a) Upper lattice arm coefficient values of the 74th order filter that satisfies the dual bandpass specification of Table(7.1).

Lower lattice arm					
APS No.	APS type	multiplier values	APS No.	APS type	multiplier values
19	2nd	x_{37} = -0.987823486328125 x_{38} = -0.143890380859375	29	2nd	x_{57} = -0.476043701171875 x_{58} = -0.692962646484375
20	2nd	x_{39} = -0.935546875000000 x_{40} = -0.233306884765625	30	2nd	x_{59} = -0.583312988281250 x_{60} = -0.747924804687500
21	2nd	x_{41} = -0.934753417968750 x_{42} = -0.431701660156250	31	2nd	x_{61} = -0.890014648437500 x_{62} = -0.860351562500000
22	2nd	x_{43} = -0.951782226562500 x_{44} = -0.171783447265625	32	2nd	x_{63} = -0.911865234375000 x_{64} = -0.781402587890625
23	2nd	x_{45} = -0.930389404296875 x_{46} = -0.295989990234375	33	2nd	x_{65} = -0.907165527343750 x_{66} = -0.830352783203125
24	2nd	x_{47} = -0.986450195312500 x_{48} = -0.467132568359375	34	2nd	x_{67} = -0.982116699218750 x_{68} = -0.693756103515625
25	2nd	x_{49} = -0.922424316406250 x_{50} = -0.364593505859375	35	2nd	x_{69} = -0.938568115234375 x_{70} = -0.881622314453125
26	2nd	x_{51} = -0.779571533203125 x_{52} = -0.414459228515625	36	2nd	x_{71} = -0.912658691406250 x_{72} = -0.749114990234375
27	2nd	x_{53} = -0.439819335937500 x_{54} = -0.535522460937500	37	2nd	x_{73} = -0.989349365234375 x_{74} = -0.898895263671875
28	2nd	x_{55} = -0.423156738281250 x_{56} = -0.606597900390625			

Table 7.7(b) Lower lattice arm coefficient values of the 74th order filter that satisfies the dual bandpass specification of Table(7.1).

7.7 Design Summary

The purpose of this Chapter was to demonstrate the design of a linear phase dual bandpass filter with finite wordlength coefficients and discuss of number of properties of the proposed design techniques that have emerged though the wide range of designs considered during the period of this research project.

Principle among the reasons for exchanging the exact phase linearity of FIR filters to the approximately linear phase lattice WDF's was a possible reduction in filter order and increased operational performance. The compromise between filter order and phase linearity is heavily dependant upon the frequency specification of a filter design. Phase linearity is only required across the passbands of a response and is sensitive to rapid changes in gain. FIR filters, due to their non-recursive nature, have poor frequency selectivity and exactly linear phase designs possess phase linearity across the whole frequency band. Therefore the combination of phase linearity, narrow passbands and sharp cut-off rates in a design specification, such as the dual bandpass considered in this Chapter, results in a very large FIR filter order.

The superior frequency selectivity of recursive filter structures and the linear phase techniques discussed in this thesis, allow solutions to be generated with considerably lower filter orders. However this improvement is dependent upon the phase linearity required and frequency specification of the example. Overall, the performance of a linear phase lattice WDF over an exactly linear phase FIR filter will depend upon the nature of the frequency specification.

Experience of the dual-line template based optimization techniques proposed has highlighted a number of parameters that need to be considered to improve design process. Principle among these parameters is the transition band templates. For magnitude-only designs the transition band templates should force a rapid cut-off rate from the edge of the passband. However for simultaneous designs, because rapid changes in gain distort the phase response, a sharp cut-off rate from the edge of the passband increases the constraints upon the group delay side of the problem. Therefore with simultaneous designs a more appropriate transition band template scheme involves a slow cut-off from the edge of the passband and then a rapid cut-off toward the edge of the stopband. This feature is especially true for very narrow transition bands.

Another property of the optimization techniques is due to the nature of the error function. Since the error is generated at a finite number of points, it is possible that the peak error of a particular region may fall between two error points and not register. To ensure this characteristic is reduced, a design solution should be re-run with a different arrangement of error points, usually achieved by increasing the points by 10 % across the passbands and stopbands.

Chapter 8

Discussion and Conclusions

8.1 Project Outline

The main objective of this research project entailed the design of linear phase multi-band digital filters that could operate at high sampling rates while maintaining the desired response under finite wordlength conditions. Sampling rates and the finite wordlength performance of a digital filter are related and dependant upon hardware implementation. The maximum sampling rate of a digital filter is limited by a system's ability to perform basic operations, such as multiplication and addition and the maximum number of these operations a particular digital filter is required to perform in one sample period. For the basic FIR filter structure, a sample period entails the multiplication and accumulation of N samples, where N is the order, while for the lattice WDF structure, a sample period involves one multiplication and three additions for each two-port adaptor. The sampling rate limit is therefore constrained by the structure of the filter and the speed of multiplication and addition operations. Of the hardware operations, the most computationally expensive is multiplication.

A technique for improving the performance of hardware multipliers involves reducing the number of operations required to generate the product by shortening the wordlength of one of the multiplicands. In this way, a X by X bit multiplier producing a 2X bit result, would be replaced by a X by Y bit multiplier generating a (X + Y) bit answer. The increase in speed of operation of the modified multiplier is approximately X/Y. Maintaining system accuracy with this modified multiplier technique requires that the signal wordlength be kept as long as possible. Central to most DSP applications is the Multiply and Accumulate (MAC) function, where the input signal is multiplied by a coefficient value and the result added to the contents of a register. Therefore the only filter wordlength that could be modified to incorporate the modified multiplier technique are those of the coefficient values.

Adopting this multiplier technique to improve the sampling rate performance of a system requires filter structures that can satisfy the desired frequency response with short coefficient wordlengths. These limitations prompted research to consider the WDF and its properties.

Since the development of WDF's by Fettweis in 1972, very little research had been published regarding the design of linear phase WDF's. To this end, the research project was concerned with investigating the properties of ladder and lattice WDF's in relation to linear phase and possible design techniques. The final goal of the project was to develop tools to design and analyse WDF's that satisfied dual bandpass magnitude specifications with an approximately linear phase response across the passbands and finite wordlength coefficients.

8.2 Summary of WDF structures and properties.

The WDF was designed to possess low coefficient sensitivity by mimicing the properties of analogue DTL networks, such as LC ladder circuits. Under the techniques proposed by Fettweis, digital equivalents of analogue elements were modelled through wave parameters and a digital filter constructed using these components. The modelled digital components can be considered as one-port elements interconnected by special adaptors or as two-port elements cascaded together. Using digital models for a range of analogue components, the analogue lossless ladder and lattice DTL networks can be constructed in the digital domain as ladder and lattice WDF's respectively.

8.2.1 WDF structures

Although both ladder and lattice WDF structures can satisfy arbitrary magnitude-only specifications, it is the property of minimum- or nonminimum-phase that dictates their performance with respect to linear phase. A linear phase response is dependent upon the position of its poles and zeros. Stability requires that the poles of a system remain within the unit circle while the pole/zero plot of exactly linear phase FIR filters clearly shows that the zeros have to exist in complex conjugate pairs. Structures that exhibit minimum-phase do so by forcing all zeros to remain on or within the unit circle. This is to ensure that a stable and causal inverse of the system exists. Of the two main WDF structures, the ladder WDF can only satisfy the minimum-phase criteria while the lattice WDF may be configured to possess minimum- or nonminimum-phase characteristics.

The property of minimum-phase suggests that the ladder WDF is unsuitable for linear or arbitrary phase specifications, while the lattice WDF provides a basis for both simultaneous and magnitude-only designs. The lattice WDF structure can be specified in a form that corresponds to a polyphase network, in which each branch is an allpass function. For the lattice WDF, these branches are a cascade of APS's, where the nature of the APS's will determine the overall frequency response of the filter.

8.2.2 Frequency Transforms

Lattice WDF's can be designed to satisfy lowpass, highpass and bandpass type responses using the standard 1st and 2nd order APS's detailed in Chapter 4 or the transformed APS's described in Chapter 5. The alternative APS's were designed by describing frequency transformation equations in terms of WDF building blocks and then applying them to the standard 1st and 2nd order APS's. This design method created 1st and 2nd order APS's for highpass designs, 2nd and 4th order APS's for bandpass designs, and 4th and 8th order APS's for dual band designs that could be used as direct replacements for APS's in the lowpass lattice structure. Their construction allowed the coefficient values from lowpass designs to be applied directly to the alternative APS's to create equivalent transformed solutions. However, this construction method imposed a restriction upon the 4th and 8th order APS's by making a number of the multipliers within the APS dependent and reducing their degrees of freedom. This dependence limits the performance of the APS's and therefore the overall response of a lattice structure using them.

A reduction in performance using the transformed APS's did not present a problem for the range of single bandpass and bandstop magnitude-only and simultaneous specifications considered. Dual band designs, however, were severely limited by the performance of the transformed 4th and 8th order APS's. To avoid these limitations dual band frequency designs were considered upon a lattice structure using the standard 1st and 2nd order APS's. For these designs, the overall equations for the lattice structure had to be modified to implement the difference of the two lattice branch responses for single and dual bandpass specifications rather than their sum which had been used for the transformed APS's.

8.2.3 Finite Wordlength Effects

Effects of finite wordlength upon ladder and lattice WDF structures can be observed by calculating their coefficient sensitivity responses and by comparing the frequency responses determined with ideal and reduced accuracy coefficient values. Coefficient sensitivities illustrate the amount by which a filter's gain, phase and group delay responses will vary as coefficient values are altered. For DTL structures, this sensitivity can approach zero at its MAP points within the passband. Finite wordlength characteristics illustrated in Chapter 6, demonstrate the high tolerance of the lattice WDF's magnitude response to changes in the coefficient wordlengths. This was also confirmed by the structure's low magnitude coefficient sensitivities across its passband, again reaching zero at MAP points within the passband(s) of lowpass, highpass and bandpass specifications. Extending the ideas of sensitivity to group delay allowed the variation of the group delay response to be determined with respect to coefficient changes. The coefficient sensitivities provide an indication of the distortion introduced into the frequency response as the coefficient wordlengths are reduced.

8.3 Summary of Design Options

With the ladder and lattice WDF structures as a basis for this research project, the main design decision concerned the method of generating the filter coefficients. Ultimately, these filter coefficients would satisfy simultaneous magnitude and phase specifications with finite wordlengths. A number of design options are available but the three main methods consist of using analytical equations, optimization or a combination of both techniques. Magnitude-only designs can be solved by minimum-phase polynomials, such as the elliptic or Butterworth functions and be implemented directly upon lattice or ladder WDF's. Calculating these polynomials for magnitude-only frequency specifications results in a set of large wordlength coefficients. However, the frequency responses of ladder and lattice WDF's with these coefficients may become unacceptably distorted if the coefficient wordlengths were reduced too far.

To offset this effect some type of finite wordlength optimization should be applied to achieve the desired frequency response with short wordlength coefficients. This mixed approach to magnitude-only frequency specifications cannot be applied to simultaneous designs as nonminimum-phase polynomials do not exist which can satisfy arbitrary magnitude and phase specifications. For these design cases, optimization must be applied from the start. Under these conditions, optimization techniques would be directed at generating a set of large wordlength, or ideal filter coefficients, that satisfy the simultaneous frequency specification. These ideal simultaneous solutions, along with large coefficient solutions from magnitude-only designs, would then be applied to optimization techniques suited to finding finite wordlength solutions.

8.3.1 Optimization Techniques

The three main steps in applying optimization to a problem concern: describing the problem in a form that has a goal, a process for measuring the difference between the current state and the goal, and a method of moving from the current state to the goal. For filter design, the goal is a set of coefficients that generate the desired frequency responses. The error to be minimized is the difference between the frequency response with the current set of coefficients and the goal frequency response. The optimization algorithm is therefore responsible for altering the values of the filter coefficients to achieve the desired frequency response.

To determine an error function to minimise, the response of the system must be gauged against an ideal response. However, for a wide range of design cases, the ideal response will not be specified as a continuous function, but as a piece-wise linear approximation or template. This is usually defined as a maximum attenuation across the passband(s) and minimum attenuation across the stopband(s). Therefore, to determine an error function, the actual response must be compared with a template function created from the frequency specification. Of the template functions considered in Chapter 2, and applied in both Chapters 3 and 4, the most effective template scheme used the frequency response specification to determine an upper and lower limit line for each band of the response. Under these dual line template targets, the optimization routine would only be concerned with minimizing excursions of the frequency response outside the template limits. This also allowed the error function to reach zero if the frequency response fell within the template targets.

The format of the error function applied within the optimization process was to sum the differences between the template targets and the actual frequency response at various points over the frequency spectrum. The overall difference was generated using a weighted L_p-metric function. The dependent relationship between magnitude and group delay responses meant that both responses had to be considered simultaneously within the optimization problem. To cater for this, a weighted L_p-metric error was generated for each frequency response template and a ratio of the two errors summed together. Introducing a ratio of the two functions allowed overall control of the contributions of the two errors into the magnitude-only designs, would then be applied to optimization techniques suited to finding finite wordlength solutions.

8.3.1 Optimization Techniques

The three main steps in applying optimization to a problem concern: describing the problem in a form that has a goal, a process for measuring the difference between the current state and the goal, and a method of moving from the current state to the goal. For filter design, the goal is a set of coefficients that generate the desired frequency responses. The error to be minimized is the difference between the frequency response with the current set of coefficients and the goal frequency response. The optimization algorithm is therefore responsible for altering the values of the filter coefficients to achieve the desired frequency response.

To determine an error function to minimise, the response of the system must be gauged against an ideal response. However, for a wide range of design cases, the ideal response will not be specified as a continuous function, but as a piece-wise linear approximation or template. This is usually defined as a maximum attenuation across the passband(s) and minimum attenuation across the stopband(s). Therefore, to determine an error function, the actual response must be compared with a template function created from the frequency specification. Of the template functions considered in Chapter 2, and applied in both Chapters 3 and 4, the most effective template scheme used the frequency response specification to determine an upper and lower limit line for each band of the response. Under these dual line template targets, the optimization routine would only be concerned with minimizing excursions of the frequency response outside the template limits. This also allowed the error function to reach zero if the frequency response fell within the template targets.

The format of the error function applied within the optimization process was to sum the differences between the template targets and the actual frequency response at various points over the frequency spectrum. The overall difference was generated using a weighted L_p-metric function. The dependent relationship between magnitude and group delay responses meant that both responses had to be considered simultaneously within the optimization problem. To cater for this, a weighted L_p-metric error was generated for each frequency response template and a ratio of the two errors summed together. Introducing a ratio of the two functions allowed overall control of the contributions of the two errors into the optimization routine. Altering this factor also allowed magnitude and group delay only problems to be addressed with the same error function and optimization routine.

The weighted L_p-metric error function forces the optimization routine to emphasize parts of the frequency response by increasing the weights on points within a specific region. However, the effects of the number and position of the points at which the L_p-metric function was determined are more difficult to quantify. Calculating the L_p-metric function for a frequency response represents an approximation of the error between the actual response and the ideal or target response. Increasing the number of frequency points with which the L_p-metric error was determined improves the accuracy of the error function, but also increased the time taken to generate the overall error for each iteration of the optimization routine. A method of reducing the number of error points, without unduly effecting the accuracy of the overall error function, was to place the error points around the regions of greatest activity within the frequency response. For filter designs, this was at the edge of the transition bands. Details of the selections of weights, error points and the L_p-metric error function adopted for these filter designs were detailed in Chapters 2, 3 and 4.

Central to applying optimization to a problem is the algorithm. The performance of any optimization algorithm will depend upon the nature of the problem to which it is applied and the information it requires to calculate its search directions. Of the types of algorithm considered, quasi-Newton techniques were best suited to an error function calculated against the dual line templates used in the simultaneous filter designs. The availability of a wide range of optimization routines, through the NAG libraries, allowed the performance of a number of optimization algorithms to be compared for magnitude-only and simultaneous design examples. Of the algorithms considered, the simple quasi-Newton function, E04JAF, proved to be the most effective for large wordlength coefficient simultaneous frequency specifications using the dual line template scheme.

Introducing finite wordlength conditions into an optimization problem imposes a set of non-linear constraints upon the algorithm and a solution search space. Optimization algorithms can deal with these constraints in a number of ways. One method is to determine the next 'best' solution with ideal coefficients in the search space and then select a set of coefficients that satisfy the finite wordlength constraints while remaining closest to this 'best' solution. Another method is to only select finite wordlength coefficients and then search the solution space for the 'best' solution with those coefficients.

Although the first method is an extension of the techniques used for large wordlength coefficient solutions, it suffers a time penalty as the algorithm is not finding the 'best' solution with a given finite wordlength but a finite wordlength approximation to a large wordlength solution. As a result, for short wordlengths, the 'best' finite wordlength solution may only bear a small correlation to the best large wordlength solution. To improve the optimization process for finite wordlength designs, a direct search algorithm was adopted. This modified Hooke-Jeeves method only increases or decreases the coefficient values corresponding to the finite wordlength required. In this way, the algorithm always moved between the 'best' finite wordlength solutions within its search space until it found a global or local minimum.

8.3.2 WDF Design Methodologies

With the WDF structure as the basis for research into simultaneous filter designs, the two main design decisions concerned how best to describe and analyse the various WDF structures and how to achieve the final goal of finite wordlength solutions to dual bandpass frequency specifications.

The design elements to construct WDF's may be considered as one-port or two-port components. The one-port approach represents the general case design technique, as any number of one-port elements may be interconnected through N-port serial or parallel adaptors that can, in turn, be connected to other adaptors. However, the overall format of a WDF structure is a two-port device and it is more appropriate to consider it as a cascade of two-port elements. Therefore, for the ladder WDF, the design process should consider cascading two-port building blocks, such as the parallel capacitor and series inductor described in Chapter 3. The lattice WDF, however, is more generally considered in its simplified one-port format. In this form, the lattice WDF is best described in terms of cascaded one-port APS's, described in Chapter 4.

The second design decision entailed developing techniques to move from the large wordlength coefficient solutions of magnitude-only specifications using minimum-phase polynomial based formulae, to finite wordlength solutions for simultaneous multi-band frequency specifications.

Initially research concentrated upon investigating optimization techniques and algorithms that could generate solutions to known large wordlength lowpass magnitude-only examples. Techniques were adapted and modified until magnitude-only solutions could be generated quickly and accurately. The most effective of these optimization techniques were then expanded to include a linear phase requirement. A wide range of simultaneous lowpass design examples were investigated using these techniques upon ladder and lattice WDF's.

Although the minimum-phase properties of the ladder WDF prevented it from completely satisfying simultaneous specifications, partial solutions highlighted a number of problems that could be addressed through better template definitions and error point distributions. Among these problems was a tendency of the optimized frequency response to spike within the transition band and at the edge of stop bands. These effects were counteracted by defining transition band templates that more closely mimicked the shape of the desired response and by placing more error points around the regions of the response susceptible to spiking.

Other properties of the simultaneous design techniques concerned the weights and relative contributions of the gain and group delay errors. Due to the nature of the target templates, each region of a template may possess a different width. This is especially true for the gain template. If a specification has a passband attenuation of 0.1 dB and a stopband attenuation of 40 dB, then the gain template widths differ by approximately 230:1 passband to stopband. To counter this effect, weights were set so that an equal deviation relative to the width of a template region, would generate an equal absolute error. Weights following this procedure were also applied to the group delay templates.

Using a weighting scheme that placed equal importance upon each error point within the gain and group delay templates, simultaneous design examples upon the lattice WDF were considered. These provided an insight into successful initial settings for the coefficient values and the relative contributions of the gain and group delay errors. Large changes in gain are contrary to the requirements for linear phase design and it is difficult to achieve linear phase around the transition bands of the response. Therefore combining equal contributions of the gain and group delay errors to the overall error function tends to prohibit the optimization routine from establishing the desired shape of the gain response. This is mainly due the to group delay errors overriding the effects to attain the stopband gain templates by limiting the cut-off rate in the transition band. To offset this effect the relative contributions of the gain and group delay errors were set so that the shape of the gain response was established before the group delay error was considered. Experiments placed the ratio of the two error functions in the region of 1.8 to 5.6, or in terms of the β factor of the L_p-metric function discussed, a ratio 0.65 to 0.85.

Having successfully applied optimization techniques to generate simultaneous lowpass solutions upon the lattice WDF, the next step involved creating lattice WDF structures capable of satisfying bandpass specifications. Using these structures, the optimization techniques were again adapted until arbitrary magnitude-only and simultaneous frequency specifications could be satisfied.

Lattice WDF structures considered for these designs consisted of the transformed 2nd and 4th order APS's described in Chapter 5. With these transformed APS's the optimization techniques were modified to include the frequency transformation value for all or each APS, as an optimization parameter. Using this technique mimics the design procedure of adjusting the resonant frequencies of second order sections in analogue filters to achieve the desired cut-off rates

With experience gained from single band frequency designs, solutions to dual band specifications were considered. Initial work concentrated upon the transformed 4th and 8th order APS's detailed in Chapter 5 and using the frequency transformation values as optimization parameters. However the constrained characteristics of these 4th and 8th order APS's due to their dependent multipliers proved to be a severe limitation on the performance of the lattice structure.

To avoid this limitation dual band frequency designs were considered upon an alternative lattice structure using the standard 1st and 2nd order APS's. Using this structure a range of dual band magnitude-only and simultaneous frequency specifications were considered and the performance of the optimization techniques investigated. For this design process the frequency transformation values were no longer required and the optimization techniques reverted to those used for lowpass designs. In addition a mean group delay value optimization parameter was considered for each passband. Details of the overall design process were provided through a design example in Chapter 7.

The final step in the overall design process concerned developing techniques to determine acceptable finite wordlength lowpass, single band and dual band frequency responses from large wordlengths coefficient solutions. The nature of the Hooke-Jeeves direct search algorithm made it very inefficient for locating the general area of a the global solution to a problem. Therefore, the first step of the finite wordlength design process was to start close to the region of the large wordlength coefficient solution. With the large wordlength coefficients as a starting point, the wordlength of the coefficients was reduced to the desired length. This process could be approached by reducing the coefficient wordlength to the final desired wordlength and then looking for a solution or by moving the wordlength up and down by one bit until the desired wordlength or the 'best' finite wordlength solution was achieved. Some coefficient wordlengths are too short for a given frequency specification and filter order, and therefore the second approach of increasing or decreasing the coefficient wordlength was more versatile.

8.4 Conclusions

The work carried out within this research project, and therefore its conclusions, relate directly to the investigation of WDF structures and their properties, or the design techniques and tools proposed to generate finite wordlength coefficient solutions to arbitrary magnitude and phase frequency specifications.

8.4.1 WDF's for Linear Phase Design

Recursive filter structures, such as the ladder and lattice WDF, cannot possess exactly linear phase. This property therefore precludes their use in applications that require this level of linearity and force the selection of a non-recursive filter structure. However, for a wide range of design specifications, a small amount of non-linearity in the phase response is acceptable. Allowing this non-linearity opens the door to recursive structures for linear phase design.

All digital systems suffer from finite wordlength effects. When selecting recursive structures for finite coefficient designs it is important to compare their dynamic range and finite wordlength properties. Discussion detailed in Chapters 1 and 2 prompted the selection of the WDF structures because of their low coefficient sensitivities and the canonic nature of the lattice WDF.

Investigations into the properties and requirements for linear phase design highlighted the need for nonminimum-phase structures so that the zeros of the transfer function could be arrange into complex conjugate pairs. Ladder WDF's, with their purely minimum-phase structures, were therefore unable to satisfy a linear phase requirement. This property was confirmed through examples, detailed in Chapter 3, under a wide range of optimization techniques and frequency specifications.

Lattice WDF structures, however, can be designed to possess transfer functions that exhibit a minimum- or nonminimum-phase type response, prompting their selection for simultaneous frequency response designs. The ability of the lattice WDF structure to satisfy simultaneous frequency specification was illustrated in Chapter 4 through a wide range of lowpass design examples. Solutions from Chapter 4 allowed the actual pole and zero positions of lattice WDF to be calculated. In these pole/zero plots, the poles lay upon an arc within the unit circle that was symmetrical about the real axis, while the zeros occupied the predicted complex conjugate pairings. Within the z-domain an APS possesses poles and zeros that exist in reciprocal pairs, forcing the gain of the APS to be unity. Pole/zero plots of the roots of the transfer function of the lattice WDF revealed that the poles and zeros no longer conformed to this relationship. This was due to the structure of the lattice WDF, where although the poles of the lattice were the poles of the individual APS's, the zeros do not relate to the APS's directly, allowing the structure to exhibit a non allpass magnitude response.

Adapting the 1st and 2nd order APS's of the lowpass lattice WDF structure enabled highpass, single and dual band-type filter responses to be considered. Construction of the APS's through the application of frequency transformation techniques caused some of the multipliers within an APS to become dependent upon each other, reducing a section's degrees of freedom. The transformed APS's considered represent a set of special case APS's that can be applied as direct replacements for the standard 1st and 2nd order APS's and using the coefficient values from lowpass solutions, create equivalent highpass, single and dual band type responses.

Although lattice WDF structures using these transformed APS's experienced a limitation in their possible performance, this did not prove a restriction for the bandpass and bandstop frequency specifications considered. However the transformed APS's for dual band specifications severely limited the overall performance of lattice structure and forced future designs to be addressed with a modified lattice structure and the standard 1st and 2nd order APS's.

Selection of the format of the lattice WDF structure and its' APS's is determined by their performance and flexibility. Under these conditions lattice WDF's using the transformed APS's cannot compete with structures based upon the standard 1st and 2nd order APS's. This is because the transformed APS's have lower degrees of freedom that their order due to dependent multipliers. Lattice filter orders are limited by the smallest APS that can be added. For dual band designs using the transformed APS's this is the 4th order APS, further limiting the flexibility of the structure. Selection of the standard 1st and 2nd order APS's over the transformed APS's becomes more certain when additions properties are considered, such as the ability of the standard 1st and 2nd order APS's to be configured to satisfy highpass, single bandpass and bandstop designs along with any multi-band specifications.

The main purpose behind the transformed APS's was to combine existing frequency transformation techniques and WDF elements to produce a lattice structure that could exhibit a wide range of frequency responses. Overall, future arbitrary magnitude-only and simultaneous would be considered with the standard 1st and 2nd order APS's upon a lattice structure an appropriate selection of the sum or difference of the lattice arm responses rather than the transformed APS's considered in this thesis.

Examples of solutions to simultaneous bandpass frequency specifications are illustrated in Chapter 5 and Chapter 7. Pole/zero plots from these solutions can be compared to simultaneous lowpass solutions. As expected the zeros exist in complex conjugate sets, but the poles and zeros now lie in a symmetrical format about the centre of the passband, which for lowpass designs was the real axis.

Investigating the properties of the lattice WDF structure with relation to finite wordlength designs highlighted a number of features concerning its phase response. Principle among these properties was illustrated by the group delay coefficient sensitivities. The magnitude and group delay coefficient sensitivities for a number of design examples were provided in Chapters 4 and 5. Magnitude coefficient sensitivities calculated for these examples confirm the low coefficient properties of the WDF structure. However, the group delay sensitivities for a particular coefficient tend to be higher, on average, than its magnitude sensitivity and for some coefficients, usually the end of a lattice branch, the group delay sensitivity can be relatively large at the beginning or end of the passband. This property suggested that the group delay response of a lattice WDF structure would be more prone to distortion than the magnitude response, as the coefficient values were changed.

The outcome of these coefficient sensitivity calculations was to suggest that the limit on the minimum achievable coefficient wordlength was imposed by the amount of group delay distortion that was acceptable. However, for both magnitude-only and simultaneous designs, the actual minimum achievable wordlength is constrained by the frequency specification and filter order. Finite wordlength coefficients distort the frequency response relative to its large wordlength solution and therefore if the large wordlength solution only just satisfied a frequency specification, this may leave little scope for coefficient wordlength reduction before the response became unacceptably distorted. The minimum acceptable coefficient wordlength is therefore a minimum for a given frequency specification and filter order and the minimum wordlength could be improved if the filter order was increased. Higher sensitivity of the group delay response to coefficient changes also means that to achieve a given simultaneous finite wordlength solution, the increase in filter order from the large coefficient solution would be larger than that for the magnitude-only design, especially for very narrow group delay tolerances.

Overall the lattice WDF has proved to be a versatile and appropriate structure for the design of magnitude-only and simultaneous design specifications. A limitation on its use, as with all recursive structures capable of satisfying a simultaneous specification, is that as the group delay tolerance is narrowed, the filter order required to satisfy the specification rises above that of an exactly linear phase FIR filter. With this limitation in mind, the lattice WDF has been successfully applied to the design of arbitrary magnitude-only and linear phase frequency specifications, including the linear phase dual bandpass designs that formed one of the objectives of this research project.

8.4.2 Design Technique Performance

The purpose of the second area of the research project was to develop techniques for the design of digital filters to satisfy simultaneous specifications. An optimization approach was adopted to speed the design process since it was not known if solutions existed for some of the filter structures and specifications.

A wide selection of optimization algorithms and error functions were considered for magnitude-only and simultaneous frequency specifications. The most successful optimization technique for general filter specifications was based upon a weighted L_2-metric error function using a dual line template scheme to define upper and lower limits for the desired response. The L_2-metric error function was incorporated into an optimization routine allowing a direct comparison of optimization alogrithms for this problem. For large wordlength coefficient solutions a simple quasi-Newton algorithm was best suited to the dual line template scheme. Finite wordlength solutions were better addressed with a bounded Hooke-Jeeves direct search algorithm.

Optimization techniques that have proved successful for simultaneous designs include the introduction of the mean passband group delay value as an optimization parameter, better defined transition band targets and error point positioning and spacing. All these modifications have been directed toward creating target templates that closer reflect the desired frequency response.

Other successful techniques included an equal deviation/equal error weighting scheme and the selection of the ratio of gain to group delay errors that forced the optimization routine to establish the shape of the gain response before introducing the group delay specification.

Overall the error functions and optimization techniques have proved successful in creating finite wordlength solutions to simultaneous frequency specification for a particular lattice WDF order. However, general finite wordlength filter designs are specified as a frequency response and desired wordlength, leaving the filter order as a parameter to be determined. This reveals a limitation of the optimization techniques discussed since they determine the minimum coefficient wordlength for a frequency response and filter order, not the filter order for a coefficient wordlength and frequency response.

Another limitation of these optimization techniques is the need for two separate optimization algorithms, one to find the large wordlength solution and the other to find the finite wordlength solution using the large wordlength solution as a starting point.

8.5 Future Work

Future work into the area of linear phase lattice WDF's, in line with the conclusions, may be divided into the areas concerning the elements of lattice WDF structure or alterations to the design/optimization techniques.

A lattice WDF structure is a basic polyphase structure containing a cascade of APS's. Future work on this structure may therefore entail a wider comparison of

APS's to include general and bi-reciprocal 4th and 8th order sections or extending the design and linear phase optimization techniques to N-branch polyphase structures used in decimating and interpolation filters.

Design techniques provide a wide scope for investigation, particularly with respect to optimization algorithms to determine finite wordlength solutions. Work has already been directed into using simulated annealing to generate finite wordlength solutions directly without the need for large wordlength solutions as a starting point. Such techniques would determine the minimum filter order for a given frequency specification and coefficient wordlength. Another interesting design avenue would be to use the knowledge gained about pole/zero positions from existing simultaneous frequency solutions to create better initial guesses to speed up the optimization process.

A final area of work could involve extending the recently published techniques for the design of linear phase microwave filters into the digital domain on Unit Element WDF's.

Appendix A

Two-port Building Blocks

This Appendix contains the design equations for seven building blocks for WDF's based upon two-port elements. Each set of equations can be used in the calculation of the gain, phase and group delay frequency responses of the overall structure. Equations for the calculation of the gain, phase and group delay coefficient sensitivities are also detailed. All the building blocks are considered under each of the three design approaches outlined in Chapter 3. Each building block contains the three variations of the general equation for each design option. The final part of this Appendix details a number of examples using the three possible design approaches for ladder WDF designs. The contents of this appendix are :-

A 1 Series Inductor

This two-port element can be considered as :

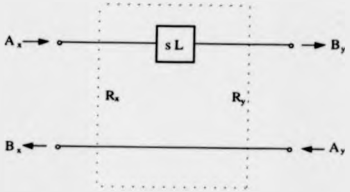

The chain matrix, $X_s(L)$, of a series inductor element, in terms of voltage and current, is given by Eq.(A1.1). The equivalent voltage wave chain matrix description, calculated from the voltage wave transforms of Eq.(A1.2) and using the bilinear transform, is shown by Eq.(A1.3).

$$\begin{bmatrix} V_x \\ I_x \end{bmatrix} = \left[X_s(L)\right] \cdot \begin{bmatrix} V_y \\ I_y \end{bmatrix} \quad \text{where} \quad X_s(L) = \begin{bmatrix} 1 & -sL \\ 0 & -1 \end{bmatrix} \qquad \text{(A1.1)}$$

$$P = \begin{bmatrix} 1 & R_x \\ 1 & -R_x \end{bmatrix} \qquad Q = \begin{bmatrix} 1 & R_y \\ 1 & -R_y \end{bmatrix} \qquad \text{(A1.2)}$$

$$\begin{bmatrix} A_x \\ B_x \end{bmatrix} = \left[P\right] \cdot \left[X_s(L)\right] \cdot \left[Q\right]^{-1} \begin{bmatrix} A_y \\ B_y \end{bmatrix} \qquad \text{(A1.3a)}$$

or

$$\begin{bmatrix} A_x \\ B_x \end{bmatrix} = \left[C_{ms}(L)\right] \cdot \begin{bmatrix} A_y \\ B_y \end{bmatrix} \qquad \text{(A1.3b)}$$

where

$$C_{ms}(L) = \begin{bmatrix} \dfrac{\beta_2 + (1 - \beta_1 + \beta_2)z^{-1}}{(1 + \beta_2)(1 + z^{-1})} & \dfrac{1 + \beta_1 z^{-1}}{(1 + \beta_2)(1 + z^{-1})} \\ \dfrac{\beta_1 + z^{-1}}{(1 + \beta_2)(1 + z^{-1})} & \dfrac{(1 - \beta_1 + \beta_2) + \beta_2 z^{-1}}{(1 + \beta_2)(1 + z^{-1})} \end{bmatrix}$$

and

$$\beta_1 = \frac{R_y + R_x - L'}{R_y + R_x + L'} \quad \text{and} \quad \beta_2 = \frac{R_y - R_x - L'}{R_y + R_x + L'} \quad \text{and} \quad L' = \frac{2L}{T}$$

Following the design procedures outlined in Chapter 3, delay free loops can be eliminated if the constant terms in the $S_{ms}(L)_{11}$ element or $S_{ms}(L)_{22}$ element of the scattering matrices are removed. The scattering matrix for this element is given by Eq.(A1.4).

$$\begin{bmatrix} B_x \\ B_y \end{bmatrix} = \left[S_{ms}(L) \right] \cdot \begin{bmatrix} A_x \\ A_y \end{bmatrix} \qquad \text{(A1.4)}$$

where

$$S_{ms}(L) = \begin{bmatrix} \dfrac{(1 - \beta_1 + \beta_2) + \beta_2 z^{-1}}{(1 + \beta_1 z^{-1})} & \dfrac{(\beta_1 - \beta_2)(1 + z^{-1})}{(1 + \beta_1 z^{-1})} \\[2ex] \dfrac{(1 + \beta_2)(1 + z^{-1})}{(1 + \beta_1 z^{-1})} & -\left(\dfrac{\beta_2 + (1 - \beta_1 + \beta_2) z^{-1}}{(1 + \beta_1 z^{-1})} \right) \end{bmatrix}$$

Source Design

To remove the constant term from the $S_{ms}(L)_{22}$ element, then $\beta_2 \Rightarrow 0$ and the resulting source design chain matrix may be defined as :

$$\begin{bmatrix} A_x \\ B_x \end{bmatrix} = \left[C_{ss}(L) \right] \cdot \begin{bmatrix} A_y \\ B_y \end{bmatrix} \qquad \text{(A1.5)}$$

where

$$C_{ss}(L) = \begin{bmatrix} \dfrac{(1 - \beta_3)\, z^{-1}}{1 + z^{-1}} & \dfrac{1 + \beta_3 z^{-1}}{1 + z^{-1}} \\[2ex] \dfrac{\beta_3 + z^{-1}}{1 + z^{-1}} & \dfrac{1 - \beta_3}{1 + z^{-1}} \end{bmatrix}, \quad \beta_3 = \frac{R_x}{L' + R_x} \quad \text{and} \quad R_y = R_x + L'$$

Load Design

To remove the constant term from the $S_{ms}(L)_{11}$ element, then $1 - \beta_1 + \beta_2 \Rightarrow 0$ and the resulting load design chain matrix may be defined as :

$$\begin{bmatrix} A_x \\ B_x \end{bmatrix} = \left[C_{ls}(L) \right] \cdot \begin{bmatrix} A_y \\ B_y \end{bmatrix} \qquad \text{(A1.6)}$$

where

$$C_{ls}(L) = \begin{bmatrix} -\left(\dfrac{1 - \beta_4}{\beta_4 (1 + z^{-1})} \right) & \dfrac{1 + \beta_4 z^{-1}}{\beta_4 (1 + z^{-1})} \\[2ex] \dfrac{\beta_4 + z^{-1}}{\beta_4 (1 + z^{-1})} & -\left(\dfrac{(1 - \beta_4)\, z^{-1}}{\beta_4 (1 + z^{-1})} \right) \end{bmatrix}, \quad \beta_4 = \frac{R_y}{L' + R_y} \quad \text{and} \quad R_x = R_y + L'$$

Appendix A

Two-port Building Blocks

This Appendix contains the design equations for seven building blocks for WDF's based upon two-port elements. Each set of equations can be used in the calculation of the gain, phase and group delay frequency responses of the overall structure. Equations for the calculation of the gain, phase and group delay coefficient sensitivities are also detailed. All the building blocks are considered under each of the three design approaches outlined in Chapter 3. Each building block contains the three variations of the general equation for each design option. The final part of this Appendix details a number of examples using the three possible design approaches for ladder WDF designs. The contents of this appendix are :-

(A1).............Series Inductor
(A2).............Series Capacitor
(A3).............Series Tuned LC circuit
(A4).............Parallel Inductor
(A5).............Parallel Capacitor
(A6).............Parallel Tuned LC circuit
(A7).............Unit Element
(A8).............Design Examples - ladder WDF designs

A 1 Series Inductor

This two-port element can be considered as ;

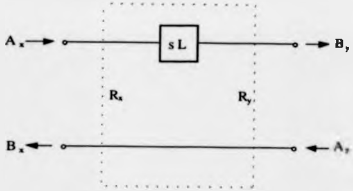

The chain matrix, $\mathbf{X}_s(L)$, of a series inductor element, in terms of voltage and current, is given by Eq.(A1.1). The equivalent voltage wave chain matrix description, calculated from the voltage wave transforms of Eq.(A1.2) and using the bilinear transform, is shown by Eq.(A1.3).

$$\begin{bmatrix} V_x \\ I_x \end{bmatrix} = \left[\mathbf{X}_{s(L)}\right] \cdot \begin{bmatrix} V_y \\ I_y \end{bmatrix} \quad \text{where} \quad \mathbf{X}_{s(L)} = \begin{bmatrix} 1 & -s\,L \\ 0 & -1 \end{bmatrix} \tag{A1.1}$$

$$\mathbf{P} = \begin{bmatrix} 1 & R_x \\ 1 & -R_x \end{bmatrix} \qquad \mathbf{Q} = \begin{bmatrix} 1 & R_y \\ 1 & -R_y \end{bmatrix} \tag{A1.2}$$

$$\begin{bmatrix} A_x \\ B_x \end{bmatrix} = [\mathbf{P}] \cdot \left[\mathbf{X}_{s(L)}\right] \cdot [\mathbf{Q}]^{-1} \begin{bmatrix} A_y \\ B_y \end{bmatrix} \tag{A1.3a}$$

or

$$\begin{bmatrix} A_x \\ B_x \end{bmatrix} = \left[\mathbf{C}_{ms(L)}\right] \cdot \begin{bmatrix} A_y \\ B_y \end{bmatrix} \tag{A1.3b}$$

where

$$\mathbf{C}_{ms(L)} = \begin{bmatrix} \dfrac{\beta_2 + (1 - \beta_1 + \beta_2)z^{-1}}{(1 + \beta_2)(1 + z^{-1})} & \dfrac{1 + \beta_1\, z^{-1}}{(1 + \beta_2)(1 + z^{-1})} \\ \dfrac{\beta_1 + z^{-1}}{(1 + \beta_2)(1 + z^{-1})} & \dfrac{(1 - \beta_1 + \beta_2) + \beta_2\, z^{-1}}{(1 + \beta_2)(1 + z^{-1})} \end{bmatrix}$$

and

$$\beta_1 = \frac{R_y + R_x - L'}{R_y + R_x + L'} \quad \text{and} \quad \beta_2 = \frac{R_y - R_x - L'}{R_y + R_x + L'} \quad \text{and} \quad L' = \frac{2\,L}{T}$$

PAGINATION ERROR

A|2

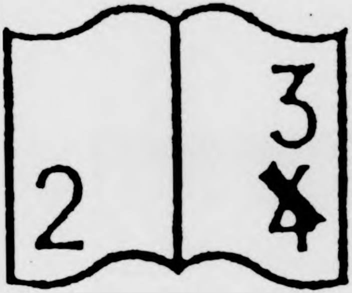

Following the design procedures outlined in Chapter 3, delay free loops can be eliminated if the constant terms in the $S_{ms}(L)_{11}$ element or $S_{ms}(L)_{22}$ element of the scattering matrices are removed. The scattering matrix for this element is given by Eq.(A1.4).

$$\begin{bmatrix} B_x \\ B_y \end{bmatrix} = \begin{bmatrix} S_{ms}(L) \end{bmatrix} \cdot \begin{bmatrix} A_x \\ A_y \end{bmatrix} \tag{A1.4}$$

where

$$S_{ms}(L) = \begin{bmatrix} \dfrac{(1 - \beta_1 + \beta_2) + \beta_2\, z^{-1}}{(1 + \beta_1\, z^{-1})} & \dfrac{(\beta_1 - \beta_2)(1 + z^{-1})}{(1 + \beta_1\, z^{-1})} \\[2ex] \dfrac{(1 + \beta_2)(1 + z^{-1})}{(1 + \beta_1\, z^{-1})} & -\left(\dfrac{\beta_2 + (1 - \beta_1 + \beta_2)z^{-1}}{(1 + \beta_1\, z^{-1})}\right) \end{bmatrix}$$

Source Design

To remove the constant term from the $S_{ms}(L)_{22}$ element, then $\beta_2 \Rightarrow 0$ and the resulting source design chain matrix may be defined as :

$$\begin{bmatrix} A_x \\ B_x \end{bmatrix} = \begin{bmatrix} C_{ss}(L) \end{bmatrix} \cdot \begin{bmatrix} A_y \\ B_y \end{bmatrix} \tag{A1.5}$$

where

$$C_{ss}(L) = \begin{bmatrix} \dfrac{(1 - \beta_3)\, z^{-1}}{1 + z^{-1}} & \dfrac{1 + \beta_3\, z^{-1}}{1 + z^{-1}} \\[2ex] \dfrac{\beta_3 + z^{-1}}{1 + z^{-1}} & \dfrac{1 - \beta_3}{1 + z^{-1}} \end{bmatrix}, \quad \beta_3 = \frac{R_x}{L' + R_x} \quad \text{and} \quad R_y = R_x + L'$$

Load Design

To remove the constant term from the $S_{ms}(L)_{11}$ element, then $1 - \beta_1 + \beta_2 \Rightarrow 0$ and the resulting load design chain matrix may be defined as :

$$\begin{bmatrix} A_x \\ B_x \end{bmatrix} = \begin{bmatrix} C_{ls}(L) \end{bmatrix} \cdot \begin{bmatrix} A_y \\ B_y \end{bmatrix} \tag{A1.6}$$

where

$$C_{ls}(L) = \begin{bmatrix} -\left(\dfrac{1 - \beta_4}{\beta_4\,(1 + z^{-1})}\right) & \dfrac{1 + \beta_4\, z^{-1}}{\beta_4\,(1 + z^{-1})} \\[2ex] \dfrac{\beta_4 + z^{-1}}{\beta_4\,(1 + z^{-1})} & -\left(\dfrac{(1 - \beta_4)\, z^{-1}}{\beta_4\,(1 + z^{-1})}\right) \end{bmatrix}, \quad \beta_4 = \frac{R_y}{L' + R_y} \quad \text{and} \quad R_x = R_y + L'$$

The group delay calculations require the derivatives of the chain matrices, $C_{ss}(L)$ for the source design, $C_{ms}(L)$ for the middle design and $C_{ls}(L)$ for the load design, with respect to the frequency, ω. Therefore, for the three design procedures the appropriate equations are :-

Middle Design

$$\frac{dC_{ms}(L)}{d\omega} = j\,\frac{z^{-1}(1-\beta_1)}{(1+\beta_2)(1+z^{-1})^2} \cdot \begin{bmatrix} -1 & 1 \\ -1 & 1 \end{bmatrix} \qquad (A1.7)$$

where

$$\beta_1 = \frac{R_y + R_x - L'}{R_y + R_x + L'} \quad \text{and} \quad \beta_2 = \frac{R_y - R_x - L'}{R_y + R_x + L'}$$

Source Design

$$\frac{dC_{ss}(L)}{d\omega} = j\,\frac{z^{-1}(1-\beta_3)}{(1+z^{-1})^2} \cdot \begin{bmatrix} -1 & 1 \\ -1 & 1 \end{bmatrix} \qquad (A1.8)$$

where

$$\beta_3 = \frac{R_x}{L' + R_x} \quad \text{and} \quad R_y = R_x + L'$$

Load Design

$$\frac{dC_{ls}(L)}{d\omega} = j\,\frac{z^{-1}(1-\beta_4)}{\beta_4(1+z^{-1})^2} \cdot \begin{bmatrix} -1 & 1 \\ -1 & 1 \end{bmatrix} \qquad (A1.9)$$

where

$$\beta_4 = \frac{R_y}{L' + R_y} \quad \text{and} \quad R_x = R_y + L'$$

In the above equations, $j = \sqrt{-1}$

The coefficient sensitivities for the magnitude and phase response calculations, require the derivatives of the chain matrices, $\mathbf{C}_{ss}(L)$, $\mathbf{C}_{ms}(L)$ and $\mathbf{C}_{ls}(L)$, with respect to each of the multipliers within that section. For the three design procedures these equations are :-

Middle Design

$$\frac{d\mathbf{C}_{ms}(L)}{d\beta_1} = \frac{1}{(1+\beta_2)(1+z^{-1})} \cdot \begin{bmatrix} -z^{-1} & z^{-1} \\ 1 & -1 \end{bmatrix} \tag{A1.10}$$

and

$$\frac{d\mathbf{C}_{ms}(L)}{d\beta_2} = \frac{1}{(1+\beta_2)^2(1+z^{-1})} \cdot \begin{bmatrix} 1+\beta_1 z^{-1} & -(1+\beta_1 z^{-1}) \\ -(\beta_1+z^{-1}) & \beta_1+z^{-1} \end{bmatrix} \tag{A1.11}$$

where

$$\beta_1 = \frac{R_y + R_x - L'}{R_y + R_x + L'} \quad \text{and} \quad \beta_2 = \frac{R_y - R_x - L'}{R_y + R_x + L'}$$

Source Design

$$\frac{d\mathbf{C}_{ss}(L)}{d\beta_3} = \frac{1}{(1+z^{-1})} \cdot \begin{bmatrix} -z^{-1} & z^{-1} \\ 1 & -1 \end{bmatrix} \tag{A1.12}$$

where

$$\beta_3 = \frac{R_x}{L' + R_x} \quad \text{and} \quad R_y = R_x + L'$$

Load Design

$$\frac{d\mathbf{C}_{ls}(L)}{d\beta_4} = \frac{1}{\beta_4^2\,(1+z^{-1})} \cdot \begin{bmatrix} 1 & -1 \\ -z^{-1} & z^{-1} \end{bmatrix} \tag{A1.13}$$

where

$$\beta_4 = \frac{R_y}{L' + R_y} \quad \text{and} \quad R_x = R_y + L'$$

The group delay coefficient sensitivities require the derivatives of the chain matrices, $C_{ss}(L)$, $C_{ms}(L)$ and $C_{ls}(L)$, with respect to the frequency, ω and then each of the multipliers within that section. The three design procedures generate the following matrices :-

Middle Design

$$\frac{d\left(\frac{dC_{ms}(L)}{d\omega}\right)}{d\beta_1} = j\,\frac{z^{-1}}{(1+\beta_2)(1+z^{-1})^2}\cdot\begin{bmatrix}1 & -1\\ 1 & -1\end{bmatrix} \qquad (A1.14)$$

and

$$\frac{d\left(\frac{dC_{ms}(L)}{d\omega}\right)}{d\beta_2} = j\,\frac{z^{-1}(1-\beta_1)}{(1+\beta_2)^2(1+z^{-1})^2}\cdot\begin{bmatrix}1 & -1\\ 1 & -1\end{bmatrix} \qquad (A1.15)$$

where

$$\beta_1 = \frac{R_y + R_x - L'}{R_y + R_x + L'} \quad \text{and} \quad \beta_2 = \frac{R_y - R_x - L'}{R_y + R_x + L'}$$

Source Design

$$\frac{d\left(\frac{dC_{ss}(L)}{d\omega}\right)}{d\beta_3} = j\,\frac{z^{-1}}{(1+z^{-1})^2}\cdot\begin{bmatrix}1 & -1\\ 1 & -1\end{bmatrix} \qquad (A1.16)$$

where

$$\beta_3 = \frac{R_x}{L' + R_x} \quad \text{and} \quad R_y = R_x + L'$$

Load Design

$$\frac{d\left(\frac{dC_{ls}(L)}{d\omega}\right)}{d\beta_4} = j\,\frac{z^{-1}}{\beta_4^2\,(1+z^{-1})^2}\cdot\begin{bmatrix}1 & -1\\ 1 & -1\end{bmatrix} \qquad (A1.17)$$

where

$$\beta_4 = \frac{R_y}{L' + R_y} \quad \text{and} \quad R_l = R_y + L'$$

A 2 Series Capacitor

This two-port element can be considered as ;

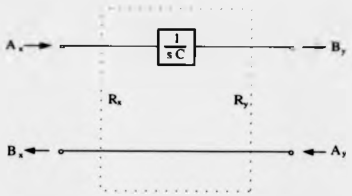

The chain matrix, $\mathbf{X}_s(C)$, of a series capacitor element, in terms of voltage and current, is given by Eq.(A2.1). The equivalent voltage wave chain matrix description, calculated from the voltage wave transforms of Eq.(A2.2) and using the bilinear transform, is shown by Eq.(A2.3).

$$\begin{bmatrix} V_x \\ I_x \end{bmatrix} = \left[\mathbf{X}_s(C)\right] \cdot \begin{bmatrix} V_y \\ I_y \end{bmatrix} \quad \text{where} \quad \mathbf{X}_s(C) = \begin{bmatrix} 1 & -\frac{1}{s\ C} \\ 0 & -1 \end{bmatrix} \qquad \text{(A2.1)}$$

$$\mathbf{P} = \begin{bmatrix} 1 & R_x \\ 1 & -R_x \end{bmatrix} \qquad \mathbf{Q} = \begin{bmatrix} 1 & R_y \\ 1 & -R_y \end{bmatrix} \qquad \text{(A2.2)}$$

$$\begin{bmatrix} A_x \\ B_x \end{bmatrix} = \left[\mathbf{P}\right] \cdot \left[\mathbf{X}_s(C)\right] \cdot \left[\mathbf{Q}\right]^{-1} \begin{bmatrix} A_y \\ B_y \end{bmatrix} \qquad \text{(A2.3a)}$$

or

$$\begin{bmatrix} A_x \\ B_x \end{bmatrix} = \left[\mathbf{C}_{ms}(C)\right] \cdot \begin{bmatrix} A_y \\ B_y \end{bmatrix} \qquad \text{(A2.3b)}$$

where

$$\mathbf{C}_{ms}(C) = \begin{bmatrix} \frac{\beta_2 - (1 - \beta_1 + \beta_2)z^{-1}}{(1 + \beta_2)(1 - z^{-1})} & \frac{1 - \beta_1\ z^{-1}}{(1 + \beta_2)(1 - z^{-1})} \\ \frac{\beta_1 - z^{-1}}{(1 + \beta_2)(1 - z^{-1})} & \frac{(1 - \beta_1 + \beta_2) - \beta_2\ z^{-1}}{(1 + \beta_2)(1 - z^{-1})} \end{bmatrix}$$

and

$$\beta_1 = \frac{R_y + R_x - 1/C'}{R_y + R_x + 1/C'} \quad \text{and} \quad \beta_2 = \frac{R_y - R_x - 1/C'}{R_y + R_x + 1/C'} \quad \text{and} \quad C' = \frac{2\ C}{T}$$

A 2 Series Capacitor

This two-port element can be considered as :

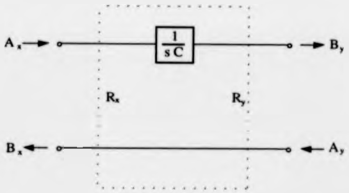

The chain matrix, $X_s(C)$, of a series capacitor element, in terms of voltage and current, is given by Eq.(A2.1). The equivalent voltage wave chain matrix description, calculated from the voltage wave transforms of Eq.(A2.2) and using the bilinear transform, is shown by Eq.(A2.3).

$$\begin{bmatrix} V_x \\ I_x \end{bmatrix} = \left[\mathbf{X}_s(C) \right] \cdot \begin{bmatrix} V_y \\ I_y \end{bmatrix} \quad \text{where} \quad \mathbf{X}_s(C) = \begin{bmatrix} 1 & -\frac{1}{s\,C} \\ 0 & -1 \end{bmatrix} \tag{A2.1}$$

$$\mathbf{P} = \begin{bmatrix} 1 & R_x \\ 1 & -R_x \end{bmatrix} \qquad \mathbf{Q} = \begin{bmatrix} 1 & R_y \\ 1 & -R_y \end{bmatrix} \tag{A2.2}$$

$$\begin{bmatrix} A_x \\ B_x \end{bmatrix} = [\mathbf{P}] \cdot [\mathbf{X}_s(C)] \cdot [\mathbf{Q}]^{-1} \begin{bmatrix} A_y \\ B_y \end{bmatrix} \tag{A2.3a}$$

or

$$\begin{bmatrix} A_x \\ B_x \end{bmatrix} = [C_{ms}(C)] \cdot \begin{bmatrix} A_y \\ B_y \end{bmatrix} \tag{A2.3b}$$

where

$$C_{ms}(C) = \begin{bmatrix} \dfrac{\beta_2 - (1 - \beta_1 + \beta_2)z^{-1}}{(1 + \beta_2)(1 - z^{-1})} & \dfrac{1 - \beta_1 z^{-1}}{(1 + \beta_2)(1 - z^{-1})} \\ \dfrac{\beta_1 - z^{-1}}{(1 + \beta_2)(1 - z^{-1})} & \dfrac{(1 - \beta_1 + \beta_2) - \beta_2 z^{-1}}{(1 + \beta_2)(1 - z^{-1})} \end{bmatrix}$$

and

$$\beta_1 = \frac{R_y + R_x - 1/C'}{R_y + R_x + 1/C'} \quad \text{and} \quad \beta_2 = \frac{R_y - R_x - 1/C'}{R_y + R_x + 1/C'} \quad \text{and} \quad C' = \frac{2\,C}{T}$$

Following the design procedures outlined in Chapter 3, delay free loops can be eliminated if the constant terms in the $S_{ms}(C)_{11}$ element or $S_{ms}(C)_{22}$ element of the scattering matrices are removed. The scattering matrix for this element is given by Eq.(A2.4).

$$\begin{bmatrix} B_x \\ B_y \end{bmatrix} = \left[S_{ms}(C)\right] \cdot \begin{bmatrix} A_x \\ A_y \end{bmatrix} \tag{A2.4}$$

where

$$S_{ms}(C) = \begin{bmatrix} \dfrac{(1 - \beta_1 + \beta_2) - \beta_2\, z^{-1}}{(1 - \beta_1\, z^{-1})} & \dfrac{(\beta_1 - \beta_2)(1 - z^{-1})}{(1 - \beta_1\, z^{-1})} \\[2ex] \dfrac{(1 + \beta_2)(1 - z^{-1})}{(1 - \beta_1\, z^{-1})} & -\left(\dfrac{\beta_2 - (1 - \beta_1 + \beta_2) z^{-1}}{(1 - \beta_1\, z^{-1})}\right) \end{bmatrix}$$

Source Design

To remove the constant term from the $S_{ms}(C)_{22}$ element, then $\beta_2 \Rightarrow 0$ and the resulting source design chain matrix may be defined as :

$$\begin{bmatrix} A_x \\ B_x \end{bmatrix} = \left[C_{ss}(C)\right] \cdot \begin{bmatrix} A_y \\ B_y \end{bmatrix} \tag{A2.5}$$

where

$$C_{ss}(C) = \begin{bmatrix} -\left(\dfrac{(1 - \beta_3) z^{-1}}{1 - z^{-1}}\right) & \dfrac{1 - \beta_3\, z^{-1}}{1 - z^{-1}} \\[2ex] \dfrac{\beta_3 - z^{-1}}{1 - z^{-1}} & \dfrac{1 - \beta_3}{1 - z^{-1}} \end{bmatrix}, \quad \beta_3 = \frac{C'\, R_y}{1 + C'\, R_x} \quad \text{and} \quad R_y = R_x + \frac{1}{C}$$

Load Design

To remove the constant term from the $S_{ms}(C)_{11}$ element, then $1 - \beta_1 + \beta_2 \Rightarrow 0$ and the resulting load design chain matrix may be defined as :

$$\begin{bmatrix} A_x \\ B_x \end{bmatrix} = \left[C_{ls}(C)\right] \cdot \begin{bmatrix} A_y \\ B_y \end{bmatrix} \tag{A2.6}$$

where

$$C_{ls}(C) = \begin{bmatrix} -\left(\dfrac{1 - \beta_4}{\beta_4\, (1 - z^{-1})}\right) & \dfrac{1 - \beta_4\, z^{-1}}{\beta_4\, (1 - z^{-1})} \\[2ex] \dfrac{\beta_4 - z^{-1}}{\beta_4\, (1 - z^{-1})} & \dfrac{(1 - \beta_4) z^{-1}}{\beta_4\, (1 - z^{-1})} \end{bmatrix}, \quad \beta_4 = \frac{C'\, R_x}{1 + C'\, R_y} \quad \text{and} \quad R_x = R_y + \frac{1}{C}$$

The group delay calculations require the derivatives of the chain matrices, $C_{ss}(C)$ for the source design, $C_{ms}(C)$ for the middle design and $C_{ls}(C)$ for the load design, with respect to the frequency, ω. Therefore, for the three design procedures the appropriate equations are :-

Middle Design

$$\frac{dC_{ms}(C)}{d\omega} = j\,\frac{z^{-1}(1-\beta_1)}{(1+\beta_2)(1-z^{-1})^2}\cdot\begin{bmatrix}1 & -1\\ 1 & -1\end{bmatrix} \qquad \text{(A2.7)}$$

where

$$\beta_1 = \frac{R_y + R_x - 1/C'}{R_y + R_x + 1/C'} \quad \text{and} \quad \beta_2 = \frac{R_y - R_x - 1/C'}{R_y + R_x + 1/C'}$$

Source Design

$$\frac{dC_{ss}(C)}{d\omega} = j\,\frac{z^{-1}(1-\beta_3)}{(1-z^{-1})^2}\cdot\begin{bmatrix}1 & -1\\ 1 & -1\end{bmatrix} \qquad \text{(A2.8)}$$

where

$$\beta_3 = \frac{C'\,R_x}{1 + C'\,R_x} \quad \text{and} \quad R_y = R_x + \frac{1}{C'}$$

Load Design

$$\frac{dC_{ls}(C)}{d\omega} = j\,\frac{z^{-1}(1-\beta_4)}{\beta_4(1-z^{-1})^2}\cdot\begin{bmatrix}1 & -1\\ 1 & -1\end{bmatrix} \qquad \text{(A2.9)}$$

where

$$\beta_4 = \frac{C'\,R_y}{1 + C'\,R_y} \quad \text{and} \quad R_x = R_y + \frac{1}{C'}$$

In the above equations, $j = \sqrt{-1}$

The coefficient sensitivities for the magnitude and phase response calculations, require the derivatives of the chain matrices, $\mathbf{C}_{ss}(C)$, $\mathbf{C}_{ms}(C)$ and $\mathbf{C}_{ls}(C)$, with respect to each of the multipliers within that section. For the three design procedures these equations are :-

Middle Design

$$\frac{d\mathbf{C}_{ms}(C)}{d\beta_1} = \frac{1}{(1+\beta_2)(1-z^{-1})} \cdot \begin{bmatrix} z^{-1} & -z^{-1} \\ 1 & -1 \end{bmatrix} \tag{A2.10}$$

and

$$\frac{d\mathbf{C}_{ms}(C)}{d\beta_2} = \frac{1}{(1+\beta_2)^2(1-z^{-1})} \cdot \begin{bmatrix} 1-\beta_1 z^{-1} & -(1-\beta_1 z^{-1}) \\ -(\beta_1 - z^{-1}) & \beta_1 - z^{-1} \end{bmatrix} \tag{A2.11}$$

where

$$\beta_1 = \frac{R_y + R_x - 1/C'}{R_y + R_x + 1/C'} \quad \text{and} \quad \beta_2 = \frac{R_y - R_x - 1/C'}{R_y + R_x + 1/C'}$$

Source Design

$$\frac{d\mathbf{C}_{ss}(C)}{d\beta_3} = \frac{1}{(1-z^{-1})} \cdot \begin{bmatrix} z^{-1} & -z^{-1} \\ 1 & -1 \end{bmatrix} \tag{A2.12}$$

where

$$\beta_3 = \frac{C'\,R_x}{1 + C'\,R_x} \quad \text{and} \quad R_y = R_x + \frac{1}{C'}$$

Load Design

$$\frac{d\mathbf{C}_{ls}(C)}{d\beta_4} = \frac{1}{\beta_4^2\,(1-z^{-1})} \cdot \begin{bmatrix} 1 & -1 \\ z^{-1} & -z^{-1} \end{bmatrix} \tag{A2.13}$$

where

$$\beta_4 = \frac{C'\,R_y}{1 + C'\,R_y} \quad \text{and} \quad R_x = R_y + \frac{1}{C'}$$

The group delay coefficient sensitivities require the derivatives of the chain matrices, $\mathbf{C}_{ss}(C)$, $\mathbf{C}_{ms}(C)$ and $\mathbf{C}_{ls}(C)$, with respect to the frequency, ω and then each of the multipliers within that section. The three design procedures generate the following matrices :-

Middle Design

$$\frac{d\left(\dfrac{d\mathbf{C}_{ms}(C)}{d\omega}\right)}{d\beta_1} = j\,\frac{z^{-1}}{(1+\beta_2)(1-z^{-1})^2}\cdot\begin{bmatrix}-1 & 1\\ -1 & 1\end{bmatrix} \qquad \text{(A2.14)}$$

and

$$\frac{d\left(\dfrac{d\mathbf{C}_{ms}(C)}{d\omega}\right)}{d\beta_2} = j\,\frac{z^{-1}(1-\beta_1)}{(1+\beta_2)^2(1-z^{-1})^2}\cdot\begin{bmatrix}-1 & 1\\ -1 & 1\end{bmatrix} \qquad \text{(A2.15)}$$

where

$$\beta_1 = \frac{R_y + R_x - 1/C'}{R_y + R_x + 1/C'} \quad \text{and} \quad \beta_2 = \frac{R_y - R_x - 1/C'}{R_y + R_x + 1/C'}$$

Source Design

$$\frac{d\left(\dfrac{d\mathbf{C}_{ss}(C)}{d\omega}\right)}{d\beta_3} = j\,\frac{z^{-1}}{(1-z^{-1})^2}\cdot\begin{bmatrix}-1 & 1\\ -1 & 1\end{bmatrix} \qquad \text{(A2.16)}$$

where

$$\beta_3 = \frac{C'\,R_x}{1 + C'\,R_x} \quad \text{and} \quad R_y = R_x + \frac{1}{C}$$

Load Design

$$\frac{d\left(\dfrac{d\mathbf{C}_{ls}(C)}{d\omega}\right)}{d\beta_4} = j\,\frac{z^{-1}}{\beta_4^2\,(1-z^{-1})^2}\cdot\begin{bmatrix}-1 & 1\\ -1 & 1\end{bmatrix} \qquad \text{(A2.17)}$$

where

$$\beta_4 = \frac{C'\,R_y}{1 + C'\,R_y} \quad \text{and} \quad R_x = R_y + \frac{1}{C}$$

A 3 Series Tuned Inductor/Capacitor

This two-port element can be considered as ;

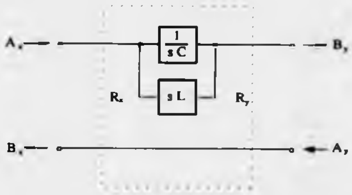

The chain matrix, $X_s(LC)$, of a series tuned inductor/capacitor element, in terms of voltage and current, is given by Eq.(A3.1). The equivalent voltage wave chain matrix description, calculated from the voltage wave transforms of Eq.(A3.2) and using the bilinear transform, is shown by Eq.(A3.3).

$$\begin{bmatrix} V_x \\ I_x \end{bmatrix} = \left[X_s(LC)\right] \cdot \begin{bmatrix} V_y \\ I_y \end{bmatrix} \quad \text{where} \quad X_s(LC) = \begin{bmatrix} 1 & \dfrac{-s\,L}{1 + L\,C\,s^2} \\ 0 & -1 \end{bmatrix} \tag{A3.1}$$

$$P = \begin{bmatrix} 1 & R_x \\ 1 & -R_x \end{bmatrix} \qquad Q = \begin{bmatrix} 1 & R_y \\ 1 & -R_y \end{bmatrix} \tag{A3.2}$$

$$\begin{bmatrix} A_x \\ B_x \end{bmatrix} = [P] \cdot \left[X_s(LC)\right] \cdot [Q]^{-1} \begin{bmatrix} A_y \\ B_y \end{bmatrix} \tag{A3.3a}$$

or

$$\begin{bmatrix} A_x \\ B_x \end{bmatrix} = \left[C_{ms}(LC)\right] \cdot \begin{bmatrix} A_y \\ B_y \end{bmatrix} \tag{A3.3b}$$

where

$$C_{ms}(LC) = \begin{bmatrix} \dfrac{\beta_2 + \alpha(1-\beta_1+2\beta_2)z^{-1} + (1-\beta_1+\beta_2)z^{-2}}{(1+\beta_2)(1+2\alpha z^{-1} + z^{-2})} & \dfrac{1 + \alpha(1+\beta_1)z^{-1} + \beta_1\, z^{-2}}{(1+\beta_2)(1+2\alpha z^{-1} + z^{-2})} \\ \dfrac{\beta_1 + \alpha(1+\beta_1)z^{-1} + z^{-2}}{(1+\beta_2)(1+2\alpha z^{-1} + z^{-2})} & \dfrac{(1-\beta_1+\beta_2) + \alpha(1-\beta_1+2\beta_2)z^{-1} + \beta_2\, z^{-2}}{(1+\beta_2)(1+2\alpha z^{-1} + z^{-2})} \end{bmatrix}$$

$$\beta_1 = \frac{(R_y + R_x)(1 + L'C') - L'}{(R_y + R_x)(1 + L'C') + L'}\ , \quad \beta_2 = \frac{(R_y - R_x)(1 + L'C') - L'}{(R_y + R_x)(1 + L'C') + L'}\ , \quad \alpha = \frac{1 - L'C'}{1 + L'C'}$$

$$L' = \frac{2\,L}{T} \quad \text{and} \quad C' = \frac{2\,C}{T}$$

Following the design procedures outlined in Chapter 3, delay free loops can be eliminated if the constant terms in the $S_{ms}(LC)_{11}$ element or $S_{ms}(LC)_{22}$ element of the scattering matrices are removed. The scattering matrix for this element is given by Eq.(A3.4).

$$\begin{bmatrix} B_x \\ B_y \end{bmatrix} = \begin{bmatrix} S_{ms}(LC) \end{bmatrix} \cdot \begin{bmatrix} A_x \\ A_y \end{bmatrix} \tag{A3.4}$$

where

$$S_{ms}(LC) = \begin{bmatrix} \dfrac{(1-\beta_1+\beta_2)+\alpha(1-\beta_1+2\beta_2)z^{-1}+\beta_2 z^{-2}}{1+\alpha(1+\beta_1)z^{-1}+\beta_1 z^{-2}} & \dfrac{(\beta_1-\beta_2)(1+2\alpha z^{-1}+z^{-2})}{1+\alpha(1+\beta_1)z^{-1}+\beta_1 z^{-2}} \\ \dfrac{(1+\beta_2)(1+2\alpha z^{-1}+z^{-2})}{1+\alpha(1+\beta_1)z^{-1}+\beta_1 z^{-2}} & -\left(\dfrac{\beta_2+\alpha(1-\beta_1+2\beta_2)z^{-1}+(1-\beta_1+\beta_2)z^{-2}}{1+\alpha(1+\beta_1)z^{-1}+\beta_1 z^{-2}}\right) \end{bmatrix}$$

Source Design :- To remove the constant term from the $S_{ms}(LC)_{22}$ element, then $\beta_2 \Rightarrow 0$ and the resulting source design chain matrix may be defined as:

$$\begin{bmatrix} A_x \\ B_x \end{bmatrix} = \begin{bmatrix} C_{ss}(LC) \end{bmatrix} \cdot \begin{bmatrix} A_y \\ B_y \end{bmatrix} \tag{A3.5}$$

where

$$C_{ss}(LC) = \begin{bmatrix} \dfrac{(1-\beta_3)z^{-1}(\alpha+z^{-1})}{1+2\alpha z^{-1}+z^{-2}} & \dfrac{1+\alpha(1+\beta_3)z^{-1}+\beta_3 z^{-2}}{1+2\alpha z^{-1}+z^{-2}} \\ \dfrac{\beta_3+\alpha(1+\beta_3)z^{-1}+z^{-2}}{1+2\alpha z^{-1}+z^{-2}} & \dfrac{(1-\beta_3)(1+\alpha z^{-1})}{1+2\alpha z^{-1}+z^{-2}} \end{bmatrix}$$

and

$$\alpha = \frac{1-L'C'}{1+L'C'} , \quad \beta_3 = \frac{R_x(1+L'C')}{L'+R_x(1+L'C')} \quad \text{and} \quad R_y = R_x + \frac{L'}{1+L'C'}$$

Load Design :- To remove the constant term from the $S_{ms}(LC)_{11}$ element, then $1 - \beta_1 + \beta_2 \Rightarrow 0$ and the resulting load design chain matrix may be defined as :

$$\begin{bmatrix} A_x \\ B_x \end{bmatrix} = \begin{bmatrix} C_{ls}(LC) \end{bmatrix} \cdot \begin{bmatrix} A_y \\ B_y \end{bmatrix} \tag{A3.6}$$

where

$$C_{ls}(LC) = \begin{bmatrix} -\left(\dfrac{(1-\beta_4)(1+\alpha z^{-1})}{\beta_4(1+2\alpha z^{-1}+z^{-2})}\right) & \dfrac{1+\alpha(1+\beta_4)z^{-1}+\beta_4 z^{-2}}{\beta_4(1+2\alpha z^{-1}+z^{-2})} \\ \dfrac{\beta_4+\alpha(1+\beta_4)z^{-1}+z^{-2}}{\beta_4(1+2\alpha z^{-1}+z^{-2})} & -\left(\dfrac{(1-\beta_4)z^{-1}(\alpha+z^{-1})}{\beta_4(1+2\alpha z^{-1}+z^{-2})}\right) \end{bmatrix}$$

and

$$\alpha = \frac{1-L'C'}{1+L'C'} , \quad \beta_4 = \frac{R_y(1+L'C')}{L'+R_y(1+L'C')} \quad \text{and} \quad R_x = R_y + \frac{L'}{1+L'C'}$$

The group delay calculations require the derivatives of the chain matrices, $C_{ss}(LC)$ for the source design, $C_{ms}(LC)$ for the middle design and $C_{ls}(LC)$ for the load design, with respect to the frequency, ω. Therefore, for the three design procedures the appropriate equations are :-

Middle Design

$$\frac{dC_{ms}(LC)}{d\omega} = j\,\frac{z^{-1}\,(1-\beta_1)(\alpha + 2z^{-1} + \alpha z^{-2})}{(1+\beta_2)(1 + 2\alpha z^{-1} + z^{-2})^2} \cdot \begin{bmatrix} -1 & 1 \\ -1 & 1 \end{bmatrix} \qquad \text{(A3.7)}$$

where

$$\beta_1 = \frac{(R_y + R_x)(1 + L'C') - L'}{(R_y + R_x)(1 + L'C') + L'}, \quad \beta_2 = \frac{(R_y - R_x)(1 + L'C') - L'}{(R_y + R_x)(1 + L'C') + L'}, \quad \alpha = \frac{1 - L'C'}{1 + L'C'}$$

Source Design

$$\frac{dC_{ss}(LC)}{d\omega} = j\,\frac{z^{-1}\,(1-\beta_3)(\alpha + 2z^{-1} + \alpha z^{-2})}{(1 + 2\alpha z^{-1} + z^{-2})^2} \cdot \begin{bmatrix} -1 & 1 \\ -1 & 1 \end{bmatrix} \qquad \text{(A3.8)}$$

where

$$\alpha = \frac{1 - L'C'}{1 + L'C'}, \quad \beta_3 = \frac{R_x(1 + L'C')}{L' + R_x(1 + L'C')} \quad \text{and} \quad R_y = R_x + \frac{L'}{1 + L'C'}$$

Load Design

$$\frac{dC_{ls}(LC)}{d\omega} = j\,\frac{z^{-1}\,(1-\beta_4)(\alpha + 2z^{-1} + \alpha z^{-2})}{\beta_4\,(1 + 2\alpha z^{-1} + z^{-2})^2} \cdot \begin{bmatrix} -1 & 1 \\ -1 & 1 \end{bmatrix} \qquad \text{(A3.9)}$$

where

$$\alpha = \frac{1 - L'C'}{1 + L'C'}, \quad \beta_4 = \frac{R_y(1 + L'C')}{L' + R_y(1 + L'C')} \quad \text{and} \quad R_x = R_y + \frac{L'}{1 + L'C'}$$

In the above equations, $j = \sqrt{-1}$

The coefficient sensitivities for the magnitude and phase response calculations require the derivatives of the chain matrices, $C_{ss}(LC)$, $C_{ms}(LC)$ and $C_{ls}(LC)$, with respect to each of the multipliers within that section. For the three design procedures these equations are :-

Middle Design

$$\frac{dC_{ms}(LC)}{d\beta_1} = \frac{1}{(1+\beta_2)(1+2\alpha z^{-1}+z^{-2})} \cdot \begin{bmatrix} -z^{-1}(\alpha+z^{-1}) & z^{-1}(\alpha+z^{-1}) \\ 1+\alpha z^{-1} & -(1+\alpha z^{-1}) \end{bmatrix} \qquad (A3.10)$$

and

$$\frac{dC_{ms}(LC)}{d\beta_2} = \begin{bmatrix} \dfrac{1+\alpha(1+\beta_1)z^{-1}+\beta_1 z^{-2}}{(1+\beta_2)^2(1+2\alpha z^{-1}+z^{-2})} & -\left(\dfrac{1+\alpha(1+\beta_1)z^{-1}+\beta_1 z^{-2}}{(1+\beta_2)^2(1+2\alpha z^{-1}+z^{-2})}\right) \\ -\left(\dfrac{\beta_1+\alpha(1+\beta_1)z^{-1}+z^{-2}}{(1+\beta_2)^2(1+2\alpha z^{-1}+z^{-2})}\right) & \dfrac{\beta_1+\alpha(1+\beta_1)z^{-1}+z^{-2}}{(1+\beta_2)^2(1+2\alpha z^{-1}+z^{-2})} \end{bmatrix} \qquad (A3.11)$$

and

$$\frac{dC_{ms}(LC)}{d\alpha} = \frac{z^{-1}(1-z^{-2})(1-\beta_1)}{(1+\beta_2)(1+2\alpha z^{-1}+z^{-2})^2} \cdot \begin{bmatrix} 1 & -1 \\ 1 & -1 \end{bmatrix} \qquad (A3.12)$$

where

$$\beta_1 = \frac{(R_y+R_x)(1+L'C')-L'}{(R_y+R_x)(1+L'C')+L'}, \quad \beta_2 = \frac{(R_y-R_x)(1+L'C')-L'}{(R_y+R_x)(1+L'C')+L'}, \quad \alpha = \frac{1-L'C'}{1+L'C'}$$

Source Design

$$\frac{dC_{ss}(LC)}{d\beta_3} = \frac{1}{(1+2\alpha z^{-1}+z^{-2})} \cdot \begin{bmatrix} -z^{-1}(\alpha+z^{-1}) & z^{-1}(\alpha+z^{-1}) \\ 1+\alpha z^{-1} & -(1+\alpha z^{-1}) \end{bmatrix} \qquad (A3.13)$$

$$\frac{dC_{ss}(LC)}{d\alpha} = \frac{z^{-1}(1-z^{-2})(1-\beta_3)}{(1+2\alpha z^{-1}+z^{-2})^2} \cdot \begin{bmatrix} 1 & -1 \\ 1 & -1 \end{bmatrix} \qquad (A3.14)$$

where

$$\alpha = \frac{1-L'C'}{1+L'C'}, \quad \beta_3 = \frac{R_x(1+L'C')}{L'+R_x(1+L'C')} \quad \text{and} \quad R_y = R_x + \frac{L'}{1+L'C'}$$

Load Design

$$\frac{dC_{ls}(LC)}{d\beta_4} = \frac{1}{\beta_4^2(1+2\alpha z^{-1}+z^{-2})} \cdot \begin{bmatrix} 1+\alpha z^{-1} & -(1+\alpha z^{-1}) \\ -z^{-1}(\alpha+z^{-1}) & z^{-1}(\alpha+z^{-1}) \end{bmatrix} \qquad (A3.15)$$

$$\frac{dC_{ls}(LC)}{d\alpha} = \frac{z^{-1}(1-z^{-2})(1-\beta_4)}{\beta_4(1+2\alpha z^{-1}+z^{-2})^2} \cdot \begin{bmatrix} 1 & -1 \\ 1 & -1 \end{bmatrix} \qquad (A3.16)$$

where

$$\alpha = \frac{1-L'C'}{1+L'C'}, \quad \beta_4 = \frac{R_y(1+L'C')}{L'+R_y(1+L'C')} \quad \text{and} \quad R_x = R_y + \frac{L'}{1+L'C'}$$

The group delay coefficient sensitivities require the derivatives of the chain matrices, $\mathbf{C}_{ss}(LC)$, $\mathbf{C}_{ms}(LC)$ and $\mathbf{C}_{ls}(LC)$, with respect to the frequency, ω and then each of the multipliers within that section. The three design procedures generate the following matrices :-

Middle Design

$$\frac{d\left(\frac{dC_{ms}(LC)}{d\omega}\right)}{d\beta_1} = j\,\frac{z^{-1}(\alpha + 2z^{-1} + \alpha z^{-2})}{(1 + \beta_2)(1 + 2\alpha z^{-1} + z^{-2})^2} \cdot \begin{bmatrix} 1 & -1 \\ 1 & -1 \end{bmatrix} \tag{A3.17}$$

and

$$\frac{d\left(\frac{dC_{ms}(LC)}{d\omega}\right)}{d\beta_2} = j\,\frac{z^{-1}(1 - \beta_1)(\alpha + 2z^{-1} + \alpha z^{-2})}{(1 + \beta_2)^2(1 + 2\alpha z^{-1} + z^{-2})^2} \cdot \begin{bmatrix} 1 & -1 \\ 1 & -1 \end{bmatrix} \tag{A3.18}$$

and

$$\frac{d\left(\frac{dC_{ms}(LC)}{d\omega}\right)}{d\alpha} = j\,\frac{z^{-1}(1-\beta_1)(1-2\alpha z^{-1}-6z^{-2}-2\alpha z^{-3}+z^{-4})}{(1 + \beta_2)(1 + 2\alpha z^{-1} + z^{-2})^3} \cdot \begin{bmatrix} -1 & 1 \\ -1 & 1 \end{bmatrix} \tag{A3.19}$$

where

$$\beta_1 = \frac{(R_y + R_x)(1 + L'C') - L'}{(R_y + R_x)(1 + L'C') + L'},\quad \beta_2 = \frac{(R_y - R_x)(1 + L'C') - L'}{(R_y + R_x)(1 + L'C') + L'},\quad \alpha = \frac{1 - L'C'}{1 + L'C'}$$

Source Design

$$\frac{d\left(\frac{dC_{ss}(LC)}{d\omega}\right)}{d\beta_3} = j\,\frac{z^{-1}(\alpha + 2z^{-1} + \alpha z^{-2})}{(1 + 2\alpha z^{-1} + z^{-2})^2} \cdot \begin{bmatrix} 1 & -1 \\ 1 & -1 \end{bmatrix} \tag{A3.20}$$

and

$$\frac{d\left(\frac{dC_{ss}(LC)}{d\omega}\right)}{d\alpha} = j\,\frac{z^{-1}(1-\beta_3)(1-2\alpha z^{-1}-6z^{-2}-2\alpha z^{-3}+z^{-4})}{(1 + 2\alpha z^{-1} + z^{-2})^3} \cdot \begin{bmatrix} -1 & 1 \\ -1 & 1 \end{bmatrix} \tag{A3.21}$$

where

$$\alpha = \frac{1 - L'C'}{1 + L'C'},\quad \beta_3 = \frac{R_x(1 + L'C')}{L' + R_x(1 + L'C')}\quad \text{and}\quad R_y = R_x + \frac{L'}{1 + L'C'}$$

Load Design

$$\frac{d\left(\frac{dC_{ls}(LC)}{d\omega}\right)}{d\beta_4} = j\,\frac{z^{-1}(\alpha + 2z^{-1} + \alpha z^{-2})}{\beta_4^2\,(1 + 2\alpha z^{-1} + z^{-2})^2} \cdot \begin{bmatrix} 1 & -1 \\ 1 & -1 \end{bmatrix} \tag{A3.22}$$

and

$$\frac{d\left(\frac{dC_{ls}(LC)}{d\omega}\right)}{d\alpha} = j\,\frac{z^{-1}(1-\beta_4)(1-2\alpha z^{-1}-6z^{-2}-2\alpha z^{-3}+z^{-4})}{\beta_4\,(1 + 2\alpha z^{-1} + z^{-2})^3} \cdot \begin{bmatrix} -1 & 1 \\ -1 & 1 \end{bmatrix} \tag{A3.23}$$

where

$$\alpha = \frac{1 - L'C'}{1 + L'C'},\quad \beta_4 = \frac{R_y(1 + L'C')}{L' + R_y(1 + L'C')}\quad \text{and}\quad R_x = R_y + \frac{L'}{1 + L'C'}$$

A 4 Parallel Inductor

This two-port element can be considered as :

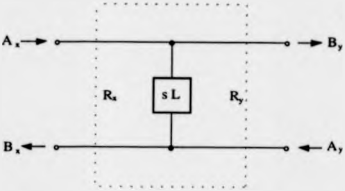

The chain matrix, $X_{p(L)}$, of a parallel inductor element, in terms of voltage and current, is given by Eq.(A4.1). The equivalent voltage wave chain matrix description, calculated from the voltage wave transforms of Eq.(A4.2) and using the bilinear transform, is shown by Eq.(A4.3).

$$\begin{bmatrix} V_x \\ I_x \end{bmatrix} = \left[X_{p(L)}\right] \cdot \begin{bmatrix} V_y \\ I_y \end{bmatrix} \quad \text{where} \quad X_{p(L)} = \begin{bmatrix} 1 & 0 \\ \frac{1}{s\,L} & -1 \end{bmatrix} \tag{A4.1}$$

$$P = \begin{bmatrix} 1 & R_x \\ 1 & -R_x \end{bmatrix} \qquad Q = \begin{bmatrix} 1 & R_y \\ 1 & -R_y \end{bmatrix} \tag{A4.2}$$

$$\begin{bmatrix} A_x \\ B_x \end{bmatrix} = [P] \cdot \left[X_{p(L)}\right] \cdot [Q]^{-1} \begin{bmatrix} A_y \\ B_y \end{bmatrix} \tag{A4.3a}$$

or

$$\begin{bmatrix} A_x \\ B_x \end{bmatrix} = \left[C_{mp(L)}\right] \cdot \begin{bmatrix} A_y \\ B_y \end{bmatrix} \tag{A4.3b}$$

where

$$C_{mp(L)} = \begin{bmatrix} \dfrac{(1 - \beta_1 + \beta_2) - \beta_2\, z^{-1}}{(1 + \beta_2)(1 - z^{-1})} & \dfrac{1 - \beta_1\, z^{-1}}{(1 + \beta_2)(1 - z^{-1})} \\ \dfrac{\beta_1 - z^{-1}}{(1 + \beta_2)(1 - z^{-1})} & \dfrac{\beta_2 - (1 - \beta_1 + \beta_2)z^{-1}}{(1 + \beta_2)(1 - z^{-1})} \end{bmatrix}$$

and

$$\beta_1 = \frac{R_y + R_x - R_y R_x / L'}{R_y + R_x + R_y R_x / L'} \quad \text{and} \quad \beta_2 = \frac{R_y - R_x - R_y R_x / L'}{R_y + R_x + R_y R_x / L'} \quad \text{and} \quad L' = \frac{2\,L}{T}$$

Following the design procedures outlined in Chapter 3, delay free loops can be eliminated if the constant terms in the $S_{mp}(L)_{11}$ element or $S_{mp}(L)_{22}$ element of the scattering matrices are removed. The scattering matrix for this element is given by Eq.(A4.4).

$$\begin{bmatrix} B_x \\ B_y \end{bmatrix} = \left[S_{mp}(L)\right] \cdot \begin{bmatrix} A_x \\ A_y \end{bmatrix} \tag{A4.4}$$

where

$$S_{mp}(L) = \begin{bmatrix} \dfrac{\beta_2 - (1 - \beta_1 + \beta_2)z^{-1}}{(1 - \beta_1 z^{-1})} & \dfrac{(\beta_1 - \beta_2)(1 - z^{-1})}{(1 - \beta_1 z^{-1})} \\ \dfrac{(1 + \beta_2)(1 - z^{-1})}{(1 - \beta_1 z^{-1})} & -\left(\dfrac{(1 - \beta_1 + \beta_2) - \beta_2 z^{-1}}{(1 - \beta_1 z^{-1})}\right) \end{bmatrix}$$

Source Design

To remove the constant term from the $S_{mp}(L)_{22}$ element, then $1 - \beta_1 + \beta_2 \Rightarrow 0$ and the resulting source design chain matrix may be defined as :

$$\begin{bmatrix} A_x \\ B_x \end{bmatrix} = \left[C_{sp}(L)\right] \cdot \begin{bmatrix} A_y \\ B_y \end{bmatrix} \tag{A4.5}$$

where

$$C_{sp}(L) = \begin{bmatrix} \dfrac{(1 - \beta_3)\ z^{-1}}{\beta_3\,(1 - z^{-1})} & \dfrac{1 - \beta_3\ z^{-1}}{\beta_3\,(1 - z^{-1})} \\ \dfrac{\beta_3 - z^{-1}}{\beta_3\,(1 - z^{-1})} & -\left(\dfrac{1 - \beta_3}{\beta_3\,(1 - z^{-1})}\right) \end{bmatrix},\ \beta_3 = \frac{L'}{L' + R_x} \quad \text{and} \quad R_y = \frac{L'\,R_x}{L' + R_x}$$

Load Design

To remove the constant term from the $S_{mp}(L)_{11}$ element, then $\beta_2 \Rightarrow 0$ and the resulting load design chain matrix may be defined as :

$$\begin{bmatrix} A_x \\ B_x \end{bmatrix} = \left[C_{lp}(L)\right] \cdot \begin{bmatrix} A_y \\ B_y \end{bmatrix} \tag{A4.6}$$

where

$$C_{lp}(L) = \begin{bmatrix} \dfrac{1 - \beta_4}{1 - z^{-1}} & \dfrac{1 - \beta_4\ z^{-1}}{1 - z^{-1}} \\ \dfrac{\beta_4 - z^{-1}}{1 - z^{-1}} & -\left(\dfrac{(1 - \beta_4)\ z^{-1}}{1 - z^{-1}}\right) \end{bmatrix},\ \beta_4 = \frac{L'}{L' + R_y} \quad \text{and} \quad R_x = \frac{L'\,R_y}{L' + R_y}$$

The group delay calculations require the derivatives of the chain matrices, $C_{sp}(L)$ for the source design, $C_{mp}(L)$ for the middle design and $C_{lp}(L)$ for the load design, with respect to the frequency, ω. Therefore, for the three design procedures the appropriate equations are :-

Middle Design

$$\frac{dC_{mp}(L)}{d\omega} = j\,\frac{z^{-1}(1-\beta_1)}{(1+\beta_2)(1-z^{-1})^2} \cdot \begin{bmatrix} -1 & -1 \\ 1 & 1 \end{bmatrix} \tag{A4.7}$$

where

$$\beta_1 = \frac{R_y + R_x - R_yR_x/L'}{R_y + R_x + R_yR_x/L'} \quad \text{and} \quad \beta_2 = \frac{R_y - R_x - R_yR_x/L'}{R_y + R_x + R_yR_x/L'}$$

Source Design

$$\frac{dC_{sp}(L)}{d\omega} = j\,\frac{z^{-1}(1-\beta_3)}{\beta_3(1-z^{-1})^2} \cdot \begin{bmatrix} -1 & -1 \\ 1 & 1 \end{bmatrix} \tag{A4.8}$$

where

$$\beta_3 = \frac{L'}{L' + R_x} \quad \text{and} \quad R_y = \frac{L'R_x}{L' + R_x}$$

Load Design

$$\frac{dC_{lp}(L)}{d\omega} = j\,\frac{z^{-1}(1-\beta_4)}{(1-z^{-1})^2} \cdot \begin{bmatrix} -1 & -1 \\ 1 & 1 \end{bmatrix} \tag{A4.9}$$

where

$$\beta_4 = \frac{L'}{L' + R_y} \quad \text{and} \quad R_x = \frac{L'R_y}{L' + R_y}$$

In the above equations, $j = \sqrt{-1}$

The coefficient sensitivities for the magnitude and phase response calculations require the derivatives of the chain matrices, $C_{sp}(L)$, $C_{mp}(L)$ and $C_{lp}(L)$, with respect to each of the multipliers within that section. For the three design procedures these equations are :-

Middle Design

$$\frac{dC_{mp}(L)}{d\beta_1} = \frac{1}{(1 + \beta_2)(1 - z^{-1})} \cdot \begin{bmatrix} -1 & -z^{-1} \\ 1 & z^{-1} \end{bmatrix} \qquad (A4.10)$$

and

$$\frac{dC_{mp}(L)}{d\beta_2} = \frac{1}{(1 + \beta_2)^2(1 - z^{-1})} \cdot \begin{bmatrix} \beta_1 - z^{-1} & -(1 - \beta_1 z^{-1}) \\ -(\beta_1 - z^{-1}) & 1 - \beta_1 z^{-1} \end{bmatrix} \qquad (A4.11)$$

where

$$\beta_1 = \frac{R_y + R_x - R_y R_x / L'}{R_y + R_x + R_y R_x / L'} \quad \text{and} \quad \beta_2 = \frac{R_y - R_x - R_y R_x / L'}{R_y + R_x + R_y R_x / L'}$$

Source Design

$$\frac{dC_{sp}(L)}{d\beta_3} = \frac{1}{\beta_3^2 (1 - z^{-1})} \cdot \begin{bmatrix} -z^{-1} & -1 \\ z^{-1} & 1 \end{bmatrix} \qquad (A4.12)$$

where

$$\beta_3 = \frac{L'}{L' + R_x} \quad \text{and} \quad R_y = \frac{L' R_x}{L' + R_x}$$

Load Design

$$\frac{dC_{lp}(L)}{d\beta_4} = \frac{1}{(1 - z^{-1})} \cdot \begin{bmatrix} -1 & -z^{-1} \\ 1 & z^{-1} \end{bmatrix} \qquad (A4.13)$$

where

$$\beta_4 = \frac{L'}{L' + R_y} \quad \text{and} \quad R_x = \frac{L' R_y}{L' + R_y}$$

The group delay coefficient sensitivities require the derivatives of the chain matrices, $C_{sp}(L)$, $C_{mp}(L)$ and $C_{lp}(L)$, with respect to the frequency, ω and then each of the multipliers within that section. The three design procedures generate the following matrices :-

Middle Design

$$\frac{d\left(\frac{dC_{mp}(L)}{d\omega}\right)}{d\beta_1} = j\,\frac{z^{-1}}{(1+\beta_2)(1-z^{-1})^2}\cdot\begin{bmatrix} 1 & 1 \\ -1 & -1 \end{bmatrix} \qquad \text{(A4.14)}$$

and

$$\frac{d\left(\frac{dC_{mp}(L)}{d\omega}\right)}{d\beta_2} = j\,\frac{z^{-1}(1-\beta_1)}{(1+\beta_2)^2(1-z^{-1})^2}\cdot\begin{bmatrix} 1 & 1 \\ -1 & -1 \end{bmatrix} \qquad \text{(A4.15)}$$

where

$$\beta_1 = \frac{R_y + R_x - R_yR_x/L'}{R_y + R_x + R_yR_x/L'} \quad \text{and} \quad \beta_2 = \frac{R_y - R_x - R_yR_x/L'}{R_y + R_x + R_yR_x/L'}$$

Source Design

$$\frac{d\left(\frac{dC_{sp}(L)}{d\omega}\right)}{d\beta_3} = j\,\frac{z^{-1}}{\beta_3^2\,(1-z^{-1})^2}\cdot\begin{bmatrix} 1 & 1 \\ -1 & -1 \end{bmatrix} \qquad \text{(A4.16)}$$

where

$$\beta_3 = \frac{L'}{L' + R_x} \quad \text{and} \quad R_y = \frac{L'\,R_x}{L' + R_x}$$

Load Design

$$\frac{d\left(\frac{dC_{lp}(L)}{d\omega}\right)}{d\beta_4} = j\,\frac{z^{-1}}{(1-z^{-1})^2}\cdot\begin{bmatrix} 1 & 1 \\ -1 & -1 \end{bmatrix} \qquad \text{(A4.17)}$$

where

$$\beta_4 = \frac{L'}{L' + R_y} \quad \text{and} \quad R_x = \frac{L'\,R_y}{L' + R_y}$$

A 5 Parallel Capacitor

This two-port element can be considered as ;

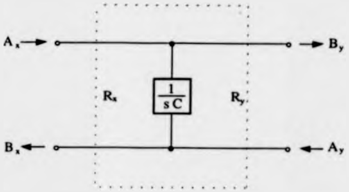

The chain matrix, $X_p(C)$, of a parallel capacitor element, in terms of voltage and current, is given by Eq.(A5.1). The equivalent voltage wave chain matrix description, calculated from the voltage wave transforms of Eq.(A5.2) and using the bilinear transform, is shown by Eq.(A5.3).

$$\begin{bmatrix} V_x \\ I_x \end{bmatrix} = \left[X_{p(C)} \right] \cdot \begin{bmatrix} V_y \\ I_y \end{bmatrix} \quad \text{where} \quad X_{p(C)} = \begin{bmatrix} 1 & 0 \\ s\,C & -1 \end{bmatrix} \tag{A5.1}$$

$$P = \begin{bmatrix} 1 & R_x \\ 1 & -R_x \end{bmatrix} \qquad Q = \begin{bmatrix} 1 & R_y \\ 1 & -R_y \end{bmatrix} \tag{A5.2}$$

$$\begin{bmatrix} A_x \\ B_x \end{bmatrix} = [P] \cdot \left[X_{p(C)} \right] \cdot [Q]^{-1} \begin{bmatrix} A_y \\ B_y \end{bmatrix} \tag{A5.3a}$$

or

$$\begin{bmatrix} A_x \\ B_x \end{bmatrix} = \left[C_{mp(C)} \right] \cdot \begin{bmatrix} A_y \\ B_y \end{bmatrix} \tag{A5.3b}$$

where

$$C_{mp(C)} = \begin{bmatrix} \dfrac{(1 - \beta_1 + \beta_2) + \beta_2 \, z^{-1}}{(1 + \beta_2)(1 + z^{-1})} & \dfrac{1 + \beta_1 \, z^{-1}}{(1 + \beta_2)(1 + z^{-1})} \\[2ex] \dfrac{\beta_1 + z^{-1}}{(1 + \beta_2)(1 + z^{-1})} & \dfrac{\beta_2 + (1 - \beta_1 + \beta_2) z^{-1}}{(1 + \beta_2)(1 + z^{-1})} \end{bmatrix}$$

and

$$\beta_1 = \frac{R_y + R_x - R_y \, R_x \, C'}{R_y + R_x + R_y \, R_x \, C'} \quad \text{and} \quad \beta_2 = \frac{R_y - R_x - R_y \, R_x \, C'}{R_y + R_x + R_y \, R_x \, C'} \quad \text{and} \quad C' = \frac{2\,C}{T}$$

Following the design procedures outlined in Chapter 3, delay free loops can be eliminated if the constant terms in the $S_{mp}(C)_{11}$ element or $S_{mp}(C)_{22}$ element of the scattering matrices are removed. The scattering matrix for this element is given by Eq.(A5.4).

$$\begin{bmatrix} B_x \\ B_y \end{bmatrix} = \left[S_{mp}(C)\right] \cdot \begin{bmatrix} A_x \\ A_y \end{bmatrix} \tag{A5.4}$$

where

$$S_{mp}(C) = \begin{bmatrix} \dfrac{\beta_2 + (1 - \beta_1 + \beta_2)\, z^{-1}}{(1 + \beta_1\, z^{-1})} & \dfrac{(\beta_1 - \beta_2)(1 + z^{-1})}{(1 + \beta_1\, z^{-1})} \\[2ex] \dfrac{(1 + \beta_2)(1 + z^{-1})}{(1 + \beta_1\, z^{-1})} & -\left(\dfrac{(1 - \beta_1 + \beta_2) + \beta_2\, z^{-1}}{(1 + \beta_1\, z^{-1})}\right) \end{bmatrix}$$

<u>Source Design</u>

To remove the constant term from the $S_{mp}(C)_{22}$ element, then $1 - \beta_1 + \beta_2 \Rightarrow 0$ and the resulting source design chain matrix may be defined as :

$$\begin{bmatrix} A_x \\ B_x \end{bmatrix} = \left[C_{sp}(C)\right] \cdot \begin{bmatrix} A_y \\ B_y \end{bmatrix} \tag{A5.5}$$

where

$$C_{sp}(C) = \begin{bmatrix} -\left(\dfrac{(1 - \beta_3)z^{-1}}{\beta_3\,(1 + z^{-1})}\right) & \dfrac{1 + \beta_3\, z^{-1}}{\beta_3\,(1 + z^{-1})} \\[2ex] \dfrac{\beta_3 + z^{-1}}{\beta_3\,(1 + z^{-1})} & -\left(\dfrac{1 - \beta_3}{\beta_3\,(1 + z^{-1})}\right) \end{bmatrix}, \quad \beta_3 = \frac{1}{1 + C'R_x} \quad \text{and} \quad R_y = \frac{R_x}{1 + C'R_x}$$

<u>Load Design</u>

To remove the constant term from the $S_{mp}(C)_{11}$ element, then $\beta_2 \Rightarrow 0$ and the resulting load design chain matrix may be defined as :

$$\begin{bmatrix} A_x \\ B_x \end{bmatrix} = \left[C_{lp}(C)\right] \cdot \begin{bmatrix} A_y \\ B_y \end{bmatrix} \tag{A5.6}$$

where

$$C_{lp}(C) = \begin{bmatrix} \dfrac{1 - \beta_4}{1 + z^{-1}} & \dfrac{1 + \beta_4\, z^{-1}}{1 + z^{-1}} \\[2ex] \dfrac{\beta_4 + z^{-1}}{1 + z^{-1}} & \dfrac{(1 - \beta_4)\, z^{-1}}{1 + z^{-1}} \end{bmatrix}, \quad \beta_4 = \frac{1}{1 + C'\,R_y} \quad \text{and} \quad R_x = \frac{R_y}{1 + C'\,R_y}$$

The group delay calculations require the derivatives of the chain matrices, $C_{sp}(C)$ for the source design, $C_{mp}(C)$ for the middle design and $C_{lp}(C)$ for the load design, with respect to the frequency, ω. Therefore, for the three design procedures the appropriate equations are :-

Middle Design

$$\frac{dC_{mp}(C)}{d\omega} = j\,\frac{z^{-1}(1-\beta_1)}{(1+\beta_2)(1+z^{-1})^2}\cdot\begin{bmatrix}1 & 1\\ -1 & -1\end{bmatrix} \qquad (A5.7)$$

where

$$\beta_1 = \frac{R_y + R_x - R_y R_x C'}{R_y + R_x + R_y R_x C'} \quad \text{and} \quad \beta_2 = \frac{R_y - R_x - R_y R_x C'}{R_y + R_x + R_y R_x C'}$$

Source Design

$$\frac{dC_{sp}(C)}{d\omega} = j\,\frac{z^{-1}(1-\beta_3)}{\beta_3(1+z^{-1})^2}\cdot\begin{bmatrix}1 & 1\\ -1 & -1\end{bmatrix} \qquad (A5.8)$$

where

$$\beta_3 = \frac{1}{1 + C' R_x} \quad \text{and} \quad R_y = \frac{R_x}{1 + C' R_x}$$

Load Design

$$\frac{dC_{lp}(C)}{d\omega} = j\,\frac{z^{-1}(1-\beta_4)}{(1+z^{-1})^2}\cdot\begin{bmatrix}1 & 1\\ -1 & -1\end{bmatrix} \qquad (A5.9)$$

where

$$\beta_4 = \frac{1}{1 + C' R_y} \quad \text{and} \quad R_x = \frac{R_y}{1 + C' R_y}$$

In the above equations, $j = \sqrt{-1}$

The coefficient sensitivities for the magnitude and phase response calculations require the derivatives of the chain matrices, $C_{sp}(C)$, $C_{mp}(C)$ and $C_{lp}(C)$, with respect to each of the multipliers within that section. For the three design procedures these equations are :-

Middle Design

$$\frac{dC_{mp}(C)}{d\beta_1} = \frac{1}{(1+\beta_2)(1+z^{-1})} \cdot \begin{bmatrix} -1 & z^{-1} \\ 1 & -z^{-1} \end{bmatrix} \tag{A5.10}$$

and

$$\frac{dC_{mp}(C)}{d\beta_2} = \frac{1}{(1+\beta_2)^2(1+z^{-1})} \cdot \begin{bmatrix} \beta_1 + z^{-1} & -(1+\beta_1 z^{-1}) \\ -(\beta_1 + z^{-1}) & 1+\beta_1 z^{-1} \end{bmatrix} \tag{A5.11}$$

where

$$\beta_1 = \frac{R_y + R_x - R_y R_x C'}{R_y + R_x + R_y R_x C'} \quad \text{and} \quad \beta_2 = \frac{R_y - R_x - R_y R_x C'}{R_y + R_x + R_y R_x C'}$$

Source Design

$$\frac{dC_{sp}(C)}{d\beta_3} = \frac{1}{\beta_3^2\,(1+z^{-1})} \cdot \begin{bmatrix} z^{-1} & -1 \\ -z^{-1} & 1 \end{bmatrix} \tag{A5.12}$$

where

$$\beta_3 = \frac{1}{1 + C' R_x} \quad \text{and} \quad R_y = \frac{R_x}{1 + C' R_x}$$

Load Design

$$\frac{dC_{lp}(C)}{d\beta_4} = \frac{1}{(1+z^{-1})} \cdot \begin{bmatrix} -1 & z^{-1} \\ 1 & -z^{-1} \end{bmatrix} \tag{A5.13}$$

where

$$\beta_4 = \frac{1}{1 + C' R_y} \quad \text{and} \quad R_x = \frac{R_y}{1 + C' R_y}$$

The group delay coefficient sensitivities response require the derivatives of the chain matrices, $\mathbf{C}_{sp}(C)$, $\mathbf{C}_{mp}(C)$ and $\mathbf{C}_{lp}(C)$, with respect to the frequency, ω and then each of the multipliers within that section. The three design procedures generate the following matrices :-

Middle Design

$$\frac{d\left(\frac{d\mathbf{C}_{mp}(C)}{d\omega}\right)}{d\beta_1} = j\,\frac{z^{-1}}{(1+\beta_2)(1+z^{-1})^2}\cdot\begin{bmatrix}-1 & -1\\ 1 & 1\end{bmatrix} \qquad \textbf{(A5.14)}$$

and

$$\frac{d\left(\frac{d\mathbf{C}_{mp}(C)}{d\omega}\right)}{d\beta_2} = j\,\frac{z^{-1}(1-\beta_1)}{(1+\beta_2)^2(1+z^{-1})^2}\cdot\begin{bmatrix}-1 & -1\\ 1 & 1\end{bmatrix} \qquad \textbf{(A5.15)}$$

where

$$\beta_1 = \frac{R_y + R_x - R_y R_x C'}{R_y + R_x + R_y R_x C'} \quad \text{and} \quad \beta_2 = \frac{R_y - R_x - R_y R_x C'}{R_y + R_x + R_y R_x C'}$$

Source Design

$$\frac{d\left(\frac{d\mathbf{C}_{sp}(C)}{d\omega}\right)}{d\beta_3} = j\,\frac{z^{-1}}{\beta_3^2\,(1+z^{-1})^2}\cdot\begin{bmatrix}-1 & -1\\ 1 & 1\end{bmatrix} \qquad \textbf{(A5.16)}$$

where

$$\beta_3 = \frac{1}{1 + C' R_x} \quad \text{and} \quad R_y = \frac{R_x}{1 + C' R_x}$$

Load Design

$$\frac{d\left(\frac{d\mathbf{C}_{lp}(C)}{d\omega}\right)}{d\beta_4} = j\,\frac{z^{-1}}{(1+z^{-1})^2}\cdot\begin{bmatrix}-1 & -1\\ 1 & 1\end{bmatrix} \qquad \textbf{(A5.17)}$$

where

$$\beta_4 = \frac{1}{1 + C' R_y} \quad \text{and} \quad R_x = \frac{R_y}{1 + C' R_y}$$

A 6 Parallel Tuned Inductor/Capacitor

This two-port element can be considered as ;

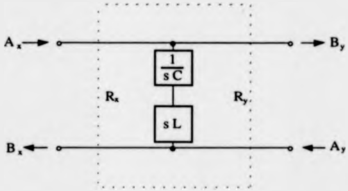

The chain matrix, $X_p(LC)$, of a parallel tuned inductor/capacitor element, in terms of voltage and current, is given by Eq.(A6.1). The equivalent voltage wave chain matrix description, calculated from the voltage wave transforms of Eq.(A6.2) and using the bilinear transform is shown by Eq.(A6.3).

$$\begin{bmatrix} V_x \\ I_x \end{bmatrix} = \left[X_{p(LC)}\right] \cdot \begin{bmatrix} V_y \\ I_y \end{bmatrix} \quad \text{where} \quad X_{p(LC)} = \begin{bmatrix} 1 & 0 \\ \dfrac{s\,C}{1 + L\,C\,s^2} & -1 \end{bmatrix} \qquad \text{(A6.1)}$$

$$P = \begin{bmatrix} 1 & R_x \\ 1 & -R_x \end{bmatrix} \qquad Q = \begin{bmatrix} 1 & R_y \\ 1 & -R_y \end{bmatrix} \qquad \text{(A6.2)}$$

$$\begin{bmatrix} A_x \\ B_x \end{bmatrix} = [P] \cdot \left[X_{p(LC)}\right] \cdot [Q]^{-1} \begin{bmatrix} A_y \\ B_y \end{bmatrix} \qquad \text{(A6.3a)}$$

or

$$\begin{bmatrix} A_x \\ B_x \end{bmatrix} = \left[C_{mp(LC)}\right] \cdot \begin{bmatrix} A_y \\ B_y \end{bmatrix} \qquad \text{(A6.3b)}$$

where

$$C_{mp(LC)} = \begin{bmatrix} \dfrac{(1-\beta_1+\beta_2)+\alpha(1-\beta_1+2\beta_2)z^{-1}+\beta_2\,z^{-2}}{(1+\beta_2)(1+2\alpha z^{-1}+z^{-2})} & \dfrac{1+\alpha(1+\beta_1)z^{-1}+\beta_1\,z^{-2}}{(1+\beta_2)(1+2\alpha z^{-1}+z^{-2})} \\ \dfrac{\beta_1+\alpha(1+\beta_1)z^{-1}+z^{-2}}{(1+\beta_2)(1+2\alpha z^{-1}+z^{-2})} & \dfrac{\beta_2+\alpha(1-\beta_1+2\beta_2)z^{-1}+(1-\beta_1+\beta_2)z^{-2}}{(1+\beta_2)(1+2\alpha z^{-1}+z^{-2})} \end{bmatrix}$$

$$\beta_1 = \frac{(R_y + R_x)(1+L'C') - C'R_yR_x}{(R_y + R_x)(1+L'C') + C'R_yR_x}, \quad \beta_2 = \frac{(R_y - R_x)(1+L'C') - C'R_yR_x}{(R_y + R_x)(1+L'C') + C'R_yR_x}, \quad \alpha = \frac{1 - L'C'}{1 + L'C'}$$

$$L' = \frac{2\,L}{T} \quad \text{and} \quad C' = \frac{2\,C}{T}$$

Following the design procedures outlined in Chapter 3, delay free loops can be eliminated if the constant terms in the $S_{mp}(LC)_{11}$ element or $S_{mp}(LC)_{22}$ element of the scattering matrices are removed. The scattering matrix for this element is given by Eq.(A6.4).

$$\begin{bmatrix} B_x \\ B_y \end{bmatrix} = \left[S_{mp}(LC)\right] \cdot \begin{bmatrix} A_x \\ A_y \end{bmatrix} \qquad \text{(A6.4)}$$

where

$$S_{mp}(LC) = \begin{bmatrix} \dfrac{\beta_2+\alpha(1-\beta_1+2\beta_2)z^{-1}+(1-\beta_1+\beta_2)z^{-2}}{1+\alpha(1+\beta_1)z^{-1}+\beta_1\ z^{-2}} & \dfrac{(\beta_1-\beta_2)(1+2\alpha z^{-1}+z^{-2})}{1+\alpha(1+\beta_1)z^{-1}+\beta_1\ z^{-2}} \\ \dfrac{(1+\beta_2)(1+2\alpha z^{-1}+z^{-2})}{1+\alpha(1+\beta_1)z^{-1}+\beta_1\ z^{-2}} & -\left(\dfrac{(1-\beta_1+\beta_2)+\alpha(1-\beta_1+2\beta_2)z^{-1}+\beta_2\ z^{-2}}{1+\alpha(1+\beta_1)z^{-1}+\beta_1\ z^{-2}}\right) \end{bmatrix}$$

<u>Source Design</u> :- To remove the constant term from the $S_{mp}(LC)_{22}$ element, then $1 - \beta_1 + \beta_2 \Rightarrow 0$ and the resulting source design chain matrix may be defined as :

$$\begin{bmatrix} A_x \\ B_x \end{bmatrix} = \left[C_{sp}(LC)\right] \cdot \begin{bmatrix} A_y \\ B_y \end{bmatrix} \qquad \text{(A6.5)}$$

where

$$C_{sp}(LC) = \begin{bmatrix} -\left(\dfrac{(1-\beta_3)\ z^{-1}\ (\alpha+z^{-1})}{\beta_3\,(1+2\alpha z^{-1}+z^{-2})}\right) & \dfrac{1+\alpha(1+\beta_3)z^{-1}+\beta_3\ z^{-2}}{\beta_3\,(1+2\alpha z^{-1}+z^{-2})} \\ \dfrac{\beta_3+\alpha(1+\beta_4)z^{-1}+z^{-2}}{\beta_3\,(1+2\alpha z^{-1}+z^{-2})} & -\left(\dfrac{(1-\beta_3)(1+\alpha\ z^{-1})}{\beta_4\,(1+2\alpha z^{-1}+z^{-2})}\right) \end{bmatrix}$$

and

$$\alpha = \frac{1-L'\,C'}{1+L'\,C'}\ ,\ \beta_3 = \frac{(1+L'\,C')}{1+L'\,C'+C'\,R_x} \quad \text{and} \quad R_y = \frac{R_x\,(1+L'\,C')}{1+L'\,C'+C'\,R_x}$$

<u>Load Design</u> :- To remove the constant term from the $S_{mp}(LC)_{11}$ element, then $\beta_2 \Rightarrow 0$ and the resulting load design chain matrix may be defined as :

$$\begin{bmatrix} A_x \\ B_x \end{bmatrix} = \left[C_{lp}(LC)\right] \cdot \begin{bmatrix} A_y \\ B_y \end{bmatrix} \qquad \text{(A6.6)}$$

where

$$C_{lp}(LC) = \begin{bmatrix} \dfrac{(1-\beta_3)(1+\alpha\ z^{-1})}{(1+2\alpha z^{-1}+z^{-2})} & \dfrac{1+\alpha(1+\beta_3)z^{-1}+\beta_3\ z^{-2}}{(1+2\alpha z^{-1}+z^{-2})} \\ \dfrac{\beta_3+\alpha(1+\beta_3)z^{-1}+z^{-2}}{(1+2\alpha z^{-1}+z^{-2})} & \dfrac{(1-\beta_3)\ z^{-1}\,(\alpha+z^{-1})}{(1+2\alpha z^{-1}+z^{-2})} \end{bmatrix}$$

and

$$\alpha = \frac{1-L'\,C'}{1+L'\,C'}\ ,\ \beta_4 = \frac{(1+L'\,C')}{1+L'\,C'+C'\,R_y} \quad \text{and} \quad R_x = \frac{R_y\,(1+L'\,C')}{1+L'\,C'+C'\,R_y}$$

The group delay calculations require the derivatives of the chain matrices, $C_{sp}(LC)$ for the source design, $C_{mp}(LC)$ for the middle design and $C_{lp}(LC)$ for the load design, with respect to the frequency, ω. Therefore, for the three design procedures the appropriate equations are :-

Middle Design

$$\frac{dC_{mp}(LC)}{d\omega} = j\,\frac{z^{-1}\,(1-\beta_1)(\alpha+2z^{-1}+\alpha z^{-2})}{(1+\beta_2)(1+2\alpha z^{-1}+z^{-2})^2}\cdot\begin{bmatrix}1 & 1\\ -1 & -1\end{bmatrix} \qquad (A6.7)$$

where

$$\beta_1=\frac{(R_y+R_x)(1+L'C')-C'R_yR_x}{(R_y+R_x)(1+L'C')+C'R_yR_x},\ \beta_2=\frac{(R_y-R_x)(1+L'C')-C'R_yR_x}{(R_y+R_x)(1+L'C')+C'R_yR_x},\ \alpha=\frac{1-L'C'}{1+L'C'}$$

Source Design

$$\frac{dC_{sp}(LC)}{d\omega} = j\,\frac{z^{-1}\,(1-\beta_3)(\alpha+2z^{-1}+\alpha z^{-2})}{\beta_3\,(1+2\alpha z^{-1}+z^{-2})^2}\cdot\begin{bmatrix}1 & 1\\ -1 & -1\end{bmatrix} \qquad (A6.8)$$

where

$$\alpha=\frac{1-L'C'}{1+L'C'},\ \beta_3=\frac{(1+L'C')}{1+L'C'+C'R_x}\ \text{ and }\ R_y=\frac{R_x\,(1+L'C')}{1+L'C'+C'R_x}$$

Load Design

$$\frac{dC_{lp}(LC)}{d\omega} = j\,\frac{z^{-1}\,(1-\beta_4)(\alpha+2z^{-1}+\alpha z^{-2})}{(1+2\alpha z^{-1}+z^{-2})^2}\cdot\begin{bmatrix}1 & 1\\ -1 & -1\end{bmatrix} \qquad (A6.9)$$

where

$$\alpha=\frac{1-L'C'}{1+L'C'},\ \beta_4=\frac{(1+L'C')}{1+L'C'+C'R_y}\ \text{ and }\ R_x=\frac{R_y\,(1+L'C')}{1+L'C'+C'R_y}$$

In the above equations, $j=\sqrt{-1}$

The coefficient sensitivities for the magnitude and phase response calculations require the derivatives of the chain matrices, $C_{sp}(LC)$, $C_{mp}(LC)$ and $C_{lp}(LC)$, with respect to each of the multipliers within that section. For the three design procedures these equations are :-

Middle Design

$$\frac{dC_{mp}(LC)}{d\beta_1} = \frac{1}{(1+\beta_2)(1+2\alpha z^{-1}+z^{-2})} \cdot \begin{bmatrix} -(1+\alpha z^{-1}) & z^{-1}(\alpha+z^{-1}) \\ 1+\alpha z^{-1} & -z^{-1}(\alpha+z^{-1}) \end{bmatrix} \qquad \text{(A6.10)}$$

and

$$\frac{dC_{mp}(LC)}{d\beta_2} = \begin{bmatrix} \dfrac{\beta_1+\alpha(1+\beta_1)z^{-1}+z^{-2}}{(1+\beta_2)^2(1+2\alpha z^{-1}+z^{-2})} & -\left(\dfrac{1+\alpha(1+\beta_1)z^{-1}+\beta_1 z^{-2}}{(1+\beta_2)^2(1+2\alpha z^{-1}+z^{-2})}\right) \\ -\left(\dfrac{\beta_1+\alpha(1+\beta_1)z^{-1}+z^{-2}}{(1+\beta_2)^2(1+2\alpha z^{-1}+z^{-2})}\right) & \dfrac{1+\alpha(1+\beta_1)z^{-1}+\beta_1 z^{-2}}{(1+\beta_2)^2(1+2\alpha z^{-1}+z^{-2})} \end{bmatrix} \qquad \text{(A6.11)}$$

and

$$\frac{dC_{mp}(LC)}{d\alpha} = \frac{z^{-1}(1-z^{-2})(1-\beta_1)}{(1+\beta_2)(1+2\alpha z^{-1}+z^{-2})^2} \cdot \begin{bmatrix} -1 & -1 \\ 1 & 1 \end{bmatrix} \qquad \text{(A6.12)}$$

where

$$\beta_1 = \frac{(R_y+R_x)(1+L'C') - C'R_yR_x}{(R_y+R_x)(1+L'C') + C'R_yR_x}, \quad \beta_2 = \frac{(R_y-R_x)(1+L'C') - C'R_yR_x}{(R_y+R_x)(1+L'C') + C'R_yR_x}, \quad \alpha = \frac{1-L'C'}{1+L'C'}$$

Source Design

$$\frac{dC_{sp}(LC)}{d\beta_3} = \frac{1}{\beta_3^2(1+2\alpha z^{-1}+z^{-2})} \cdot \begin{bmatrix} z^{-1}(\alpha+z^{-1}) & -(1+\alpha z^{-1}) \\ -z^{-1}(\alpha+z^{-1}) & 1+\alpha z^{-1} \end{bmatrix} \qquad \text{(A6.13)}$$

$$\frac{dC_{sp}(LC)}{d\alpha} = \frac{z^{-1}(1-z^{-2})(1-\beta_3)}{\beta_3(1+2\alpha z^{-1}+z^{-2})^2} \cdot \begin{bmatrix} -1 & -1 \\ 1 & 1 \end{bmatrix} \qquad \text{(A6.14)}$$

where

$$\alpha = \frac{1-L'C'}{1+L'C'}, \quad \beta_3 = \frac{(1+L'C')}{1+L'C'+C'R_x} \quad \text{and} \quad R_y = \frac{R_x(1+L'C')}{1+L'C'+C'R_x}$$

Load Design

$$\frac{dC_{lp}(LC)}{d\beta_4} = \frac{1}{1+2\alpha z^{-1}+z^{-2}} \cdot \begin{bmatrix} -(1+\alpha z^{-1}) & z^{-1}(\alpha+z^{-1}) \\ 1+\alpha z^{-1} & -z^{-1}(\alpha+z^{-1}) \end{bmatrix} \qquad \text{(A6.15)}$$

$$\frac{dC_{lp}(LC)}{d\alpha} = \frac{z^{-1}(1-z^{-2})(1-\beta_4)}{(1+2\alpha z^{-1}+z^{-2})^2} \cdot \begin{bmatrix} -1 & -1 \\ 1 & 1 \end{bmatrix} \qquad \text{(A6.16)}$$

where

$$\alpha = \frac{1-L'C'}{1+L'C'}, \quad \beta_4 = \frac{(1+L'C')}{1+L'C'+C'R_y} \quad \text{and} \quad R_x = \frac{R_y(1+L'C')}{1+L'C'+C'R_y}$$

The group delay coefficient sensitivities require the derivatives of the chain matrices, $\mathbf{C}_{sp}(LC)$, $\mathbf{C}_{mp}(LC)$ and $\mathbf{C}_{lp}(LC)$, with respect to the frequency, ω and then each of the multipliers within that section. The three design procedures generate the following matrices :-

Middle Design

$$\frac{d\left(\dfrac{d\mathbf{C}_{mp}(LC)}{d\omega}\right)}{d\beta_1} = j\,\frac{z^{-1}(\alpha + 2z^{-1} + \alpha z^{-2})}{(1+\beta_2)(1+2\alpha z^{-1}+z^{-2})^2}\cdot\begin{bmatrix} -1 & -1 \\ 1 & 1 \end{bmatrix} \qquad \text{(A6.17)}$$

and

$$\frac{d\left(\dfrac{d\mathbf{C}_{mp}(LC)}{d\omega}\right)}{d\beta_2} = j\,\frac{z^{-1}(1-\beta_1)(\alpha + 2z^{-1} + \alpha z^{-2})}{(1+\beta_2)^2(1+2\alpha z^{-1}+z^{-2})^2}\cdot\begin{bmatrix} -1 & -1 \\ 1 & 1 \end{bmatrix} \qquad \text{(A6.18)}$$

and

$$\frac{d\left(\dfrac{d\mathbf{C}_{mp}(LC)}{d\omega}\right)}{d\alpha} = j\,\frac{z^{-1}(1-\beta_1)(1-2\alpha z^{-1}-6z^{-2}-2\alpha z^{-3}+z^{-4})}{(1+\beta_2)(1+2\alpha z^{-1}+z^{-2})^3}\cdot\begin{bmatrix} 1 & 1 \\ -1 & -1 \end{bmatrix} \qquad \text{(A6.19)}$$

where

$$\beta_1 = \frac{(R_y + R_x)(1+L'C') - C'R_yR_x}{(R_y + R_x)(1+L'C') + C'R_yR_x}\,,\quad \beta_2 = \frac{(R_y - R_x)(1+L'C') - C'R_yR_x}{(R_y + R_x)(1+L'C') + C'R_yR_x}\,,\quad \alpha = \frac{1 - L'C'}{1 + L'C'}$$

Source Design

$$\frac{d\left(\dfrac{d\mathbf{C}_{sp}(LC)}{d\omega}\right)}{d\beta_3} = j\,\frac{z^{-1}(\alpha + 2z^{-1} + \alpha z^{-2})}{\beta_3^2\,(1+2\alpha z^{-1}+z^{-2})^2}\cdot\begin{bmatrix} -1 & -1 \\ 1 & 1 \end{bmatrix} \qquad \text{(A6.20)}$$

and

$$\frac{d\left(\dfrac{d\mathbf{C}_{sp}(LC)}{d\omega}\right)}{d\alpha} = j\,\frac{z^{-1}(1-\beta_3)(1-2\alpha z^{-1}-6z^{-2}-2\alpha z^{-3}+z^{-4})}{\beta_3\,(1+2\alpha z^{-1}+z^{-2})^3}\cdot\begin{bmatrix} 1 & 1 \\ -1 & -1 \end{bmatrix} \qquad \text{(A6.21)}$$

where

$$\alpha = \frac{1 - L'C'}{1 + L'C'}\,,\quad \beta_3 = \frac{(1 + L'C')}{1 + L'C' + C'R_x} \quad \text{and} \quad R_y = \frac{R_x\,(1 + L'C')}{1 + L'C' + C'R_x}$$

Load Design

$$\frac{d\left(\dfrac{d\mathbf{C}_{lp}(LC)}{d\omega}\right)}{d\beta_4} = j\,\frac{z^{-1}(\alpha + 2z^{-1} + \alpha z^{-2})}{(1+2\alpha z^{-1}+z^{-2})^2}\cdot\begin{bmatrix} -1 & -1 \\ 1 & 1 \end{bmatrix} \qquad \text{(A6.22)}$$

and

$$\frac{d\left(\dfrac{d\mathbf{C}_{lp}(LC)}{d\omega}\right)}{d\alpha} = j\,\frac{z^{-1}(1-\beta_4)(1-2\alpha z^{-1}-6z^{-2}-2\alpha z^{-3}+z^{-4})}{(1+2\alpha z^{-1}+z^{-2})^3}\cdot\begin{bmatrix} 1 & 1 \\ -1 & -1 \end{bmatrix} \qquad \text{(A6.23)}$$

where

$$\alpha = \frac{1 - L'C'}{1 + L'C'}\,,\quad \beta_4 = \frac{(1 + L'C')}{1 + L'C' + C'R_y} \quad \text{and} \quad R_x = \frac{R_y\,(1 + L'C')}{1 + L'C' + C'R_y}$$

A 7 Unit Element

This two-port element can be considered as ;

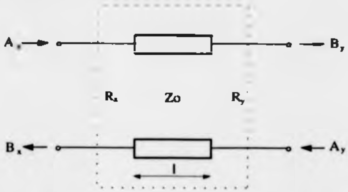

The chain matrix, X(UE), of a lossless transmission line or unit element of characteristic impedance, Z_o, is given by Eq.(A7.1) in terms of voltage and current. The equivalent incident and reflected voltage wave chain matrix description, calculated from the voltage wave transforms of Eq.(A7.2) is shown by Eq.(A7.3).

$$\begin{bmatrix} V_x \\ I_x \end{bmatrix} = \left[X(UE) \right] \cdot \begin{bmatrix} V_y \\ I_y \end{bmatrix} \quad \text{where} \quad X(UE) = \begin{bmatrix} \cos\theta & -j\,Z_o \sin\theta \\ j\,Y_o \sin\theta & -\cos\theta \end{bmatrix} \tag{A7.1}$$

where

$Y_o = 1/Z_o$, $\theta = k\,\Omega$, k is the line constant and Ω is the angular frequency.

$$P = \begin{bmatrix} 1 & R_x \\ 1 & -R_x \end{bmatrix} \qquad Q = \begin{bmatrix} 1 & R_y \\ 1 & -R_y \end{bmatrix} \tag{A7.2}$$

$$\begin{bmatrix} A_x \\ B_x \end{bmatrix} = [P] \cdot [X(UE)] \cdot [Q]^{-1} \begin{bmatrix} A_y \\ B_y \end{bmatrix} \tag{A7.3a}$$

or

$$\begin{bmatrix} A_x \\ B_x \end{bmatrix} = [C_m(UE)] \cdot \begin{bmatrix} A_y \\ B_y \end{bmatrix} \tag{A7.3b}$$

where

$$C_m(UE) = \frac{1}{2} \begin{bmatrix} \alpha \cos\theta + j\,\delta \sin\theta & \beta \cos\theta + j\,\gamma \sin\theta \\ \beta \cos\theta - j\,\gamma \sin\theta & \alpha \cos\theta - j\,\delta \sin\theta \end{bmatrix}$$

and

$$\alpha = \frac{R_2 - R_1}{R_2}, \ \beta = \frac{R_2 + R_1}{R_2}, \ \delta = \frac{R_1 R_2 - Z_o^2}{Z_o R_2} \ \text{and} \ \gamma = \frac{R_1 R_2 + Z_o^2}{Z_o R_2}$$

Following the design procedures outlined in Chapter 3, delay free loops can be eliminated if the constant terms in the $S_m(UE)_{11}$ element or $S_m(UE)_{22}$ element of the scattering matrices are removed. The scattering matrix for this element, generated through the transform $\theta = \omega T/2$, is given by Eq.(A7.4).

$$\begin{bmatrix} B_x \\ B_y \end{bmatrix} = \begin{bmatrix} S_m(UE) \end{bmatrix} \cdot \begin{bmatrix} A_x \\ A_y \end{bmatrix} \qquad \text{(A7.4)}$$

where

$$S_m(UE) = \begin{bmatrix} \dfrac{\beta_4 + \beta_3 z^{-1}}{\beta_1 + \beta_2 z^{-1}} & \dfrac{4 R_1 G_2 z^{-1/2}}{\beta_1 + \beta_2 z^{-1}} \\ \dfrac{4 z^{-1/2}}{(1 + \beta_1 z^{-1})} & \dfrac{-\beta_3 + \beta_4 z^{-1}}{\beta_1 + \beta_2 z^{-1}} \end{bmatrix}$$

and

$$\beta_1 = 1 + R_1G_2 + R_1Y_o + G_2Z_o \ , \quad \beta_2 = 1 + R_1G_2 - R_1Y_o - G_2Z_o$$

$$\beta_3 = 1 - R_1G_2 + R_1Y_o - G_2Z_o \ , \quad \beta_4 = 1 - R_1G_2 - R_1Y_o - G_2Z_o$$

Source Design

To remove the constant term from the $S_m(UE)_{22}$ element, then $\beta_3 \Rightarrow 0$ and the resulting source design chain matrix may be defined as :

$$\begin{bmatrix} A_x \\ B_x \end{bmatrix} = \begin{bmatrix} C_s(UE) \end{bmatrix} \cdot \begin{bmatrix} A_y \\ B_y \end{bmatrix} \qquad \text{(A1.5)}$$

where

$$C_s(UE) = \begin{bmatrix} \dfrac{(1 - \beta_3)\ z^{-1}}{1 + z^{-1}} & \dfrac{1 + \beta_3 z^{-1}}{1 + z^{-1}} \\ \dfrac{\beta_3 + z^{-1}}{1 + z^{-1}} & \dfrac{1 - \beta_3}{1 + z^{-1}} \end{bmatrix} , \ \beta = \frac{R_x - Z_o}{R_x + Z_o} \quad \text{and} \quad R_y = Z_o$$

Load Design

To remove the constant term from the $S_m(UE)_{11}$ element, then $\beta_4 \Rightarrow 0$ and the resulting load design chain matrix may be defined as :

$$\begin{bmatrix} A_x \\ B_x \end{bmatrix} = \begin{bmatrix} C_l(UE) \end{bmatrix} \cdot \begin{bmatrix} A_y \\ B_y \end{bmatrix} \qquad \text{(A1.6)}$$

where

$$C_l(UE) = \begin{bmatrix} -\left(\dfrac{1 - \beta_4}{\beta_4\ (1 + z^{-1})}\right) & \dfrac{1 + \beta_4 z^{-1}}{\beta_4\ (1 + z^{-1})} \\ \dfrac{\beta_4 + z^{-1}}{\beta_4\ (1 + z^{-1})} & -\left(\dfrac{(1 - \beta_4)\ z^{-1}}{\beta_4\ (1 + z^{-1})}\right) \end{bmatrix} , \ \beta = \frac{R_y - Z_o}{R_y + Z_o} \quad \text{and} \quad R_x = Z_o$$

A 8 Design Examples

To illustrate the three design procedures outlined in the Chapter 3, consider the 7th order ladder DTL circuit shown by Fig.(A8.1).

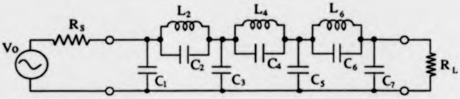

Figure A8.1 A 7th order DTL filter

Using the two-port design approach, suggested by Lawson, a general ladder WDF equivalent of this circuit can be constructed and is shown by Fig.(A8.2).

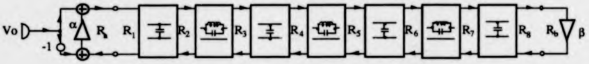

Figure A8.2 General two-port ladder WDF equivalent of the circuit of Fig.(A8.1).

with

$$\alpha = \frac{R_s - R_a}{R_s + R_a} \quad \text{and} \quad \beta = \frac{R_L - R_b}{R_L + R_b}$$

where R_a is the port resistance of the digital equivalent of a resistive voltage source, V_0, with resistance R_s. The port resistance R_b and external multiplier, β, correspond to a digital equivalent of the load resistor, R_L, of Fig.(A8.1).

A8.1 Source Design

Applying the source design procedure to the general ladder WDF circuit of Fig.(A8.2), the first step is to remove the delay free path provided by the external multiplier, α. This can be achieved by setting $\alpha = 0$ or $R_a = R_s$, and therefore $R_1 = R_s$. The first element of the circuit of Fig.(A8.2) is a parallel capacitor. This section has a source design chain matrix given by Eq.(A8.1).

$$\begin{bmatrix} A_1 \\ \\ B_1 \end{bmatrix} = \begin{bmatrix} -\left(\frac{(1-\delta_3)\,z^{-1}}{\delta_1\,(1+z^{-1})}\right) & \frac{1+\delta_1\,z^{-1}}{\delta_1\,(1+z^{-1})} \\ \frac{\delta_1+z^{-1}}{\delta_1\,(1+z^{-1})} & -\left(\frac{1-\delta_1}{\delta_1\,(1+z^{-1})}\right) \end{bmatrix} \cdot \begin{bmatrix} A_2 \\ \\ B_2 \end{bmatrix} \qquad (A8.1)$$

where

$$\delta_1 = \frac{1}{1 + C_1' R_1}, \quad R_2 = \frac{R_1}{1 + C_1' R_1} \quad \text{and} \quad C_1' = \frac{2\,C_1}{T}$$

or

$$\delta_1 = \frac{1}{1 + C_1' R_s} \quad \text{and} \quad R_2 = \frac{R_s}{1 + C_1' R_s}$$

The next section is a series tuned inductor/capacitor element. The source design chain matrix of this element is given by Eq.(A8.2).

$$\begin{bmatrix} A_3 \\ \\ B_3 \end{bmatrix} = \begin{bmatrix} \dfrac{(1 - \delta_3)\, z^{-1} (\delta_2 + z^{-1})}{1 + 2\delta_2 z^{-1} + z^{-2}} & \dfrac{1 + \delta_2(1 + \delta_3) z^{-1} + \delta_3 z^{-2}}{1 + 2\delta_2 z^{-1} + z^{-2}} \\ \dfrac{\delta_3 + \delta_2(1 + \delta_3) z^{-1} + z^{-2}}{1 + 2\delta_2 z^{-1} + z^{-2}} & \dfrac{(1 - \delta_3)(1 + \delta_2 z^{-1})}{1 + 2\delta_2 z^{-1} + z^{-2}} \end{bmatrix} \cdot \begin{bmatrix} A_4 \\ \\ B_4 \end{bmatrix} \qquad (A8.2)$$

where

$$\delta_2 = \frac{1 - L_2' C_2'}{1 + L_2' C_2'}, \quad \delta_3 = \frac{R_2(1 + L_2' C_2')}{L_2' + R_2(1 + L_2' C_2')} \quad \text{and} \quad R_3 = R_2 + \frac{L_2'}{1 + L_2' C_2'}$$

with

$$C_2' = \frac{2\,C_2}{T} \quad \text{and} \quad L_2' = \frac{2\,L_2}{T}$$

Since the value of R_2 has been expressed in terms of R_s, then it can be substituted to express δ_3 and R_3 as,

$$\delta_3 = \frac{R_s(1 + L_2' C_2')}{L_2'(1 + C_1' R_s) + R_s(1 + L_2' C_2')} \quad \text{and} \quad R_3 = \frac{R_s}{1 + C_1' R_s} + \frac{L_2'}{1 + L_2' C_2'}$$

Continuing the design process using the chain matrices of the form of Eq.(A8.1) and (A8.2), the multiplier values for the overall circuit can be determined and applied to the resulting structure of Fig.(A8.3).

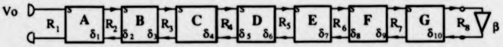

Figure A8.3 Ladder WDF circuit using source design procedure.

In the circuit of Fig.(A8.3) the parallel capacitor of the first section has the chain matrix, **A**, given by Eq.(A8.1), while the series tuned inductor/capacitor in the second section has a chain matrix, **B**, of Eq.(A8.2). The chain matrix **C**, **E** and **G** have the same form as Eq.(A8.1) but in terms of δ_4, δ_7 and δ_{10} respectively. Similarly, the matrices **D** and **F** have the form of Eq.(A8.2), but with multipliers δ_5/δ_6 and δ_8/δ_9 respectively. The multiplier equations for the source design ladder WDF circuit of Fig.(A8.3) are given in Table(A8.1).

$\delta_1 = \dfrac{1}{1 + C_1' R_1}$	$R_2 = \dfrac{R_1}{1 + C_1' R_1}$	
$\delta_2 = \dfrac{1 - L_2' C_2'}{1 + L_2' C_2'}$	$\delta_3 = \dfrac{R_2(1 + L_2' C_2')}{L_2' + R_2(1 + L_2' C_2')}$	$R_3 = R_2 + \dfrac{L_2'}{1 + L_2' C_2'}$
$\delta_4 = \dfrac{1}{1 + C_3' R_3}$	$R_4 = \dfrac{R_3}{1 + C_3' R_1}$	
$\delta_5 = \dfrac{1 - L_4' C_4'}{1 + L_4' C_4'}$	$\delta_6 = \dfrac{R_4(1 + L_4' C_4')}{L_4' + R_4(1 + L_4' C_4')}$	$R_5 = R_4 + \dfrac{L_4'}{1 + L_4' C_4'}$
$\delta_7 = \dfrac{1}{1 + C_5' R_5}$	$R_6 = \dfrac{R_5}{1 + C_5' R_5}$	
$\delta_8 = \dfrac{1 - L_6' C_6'}{1 + L_6' C_6'}$	$\delta_9 = \dfrac{R_6(1 + L_6' C_6')}{L_6' + R_6(1 + L_6' C_6')}$	$R_7 = R_6 + \dfrac{L'_6'}{1 + L'_6' C'_6'}$
$\delta_{10} = \dfrac{1}{1 + C_7' R_7}$	$R_8 = \dfrac{R_7}{1 + C_7' R_7}$	
$\beta = \dfrac{R_L - R_8}{R_L + R_8}$		

Table A8.1 Multiplier equations for source design ladder WDF of Fig.(A8.3).

The transfer function for the circuit is given by Eq.(A8.3) where **X** represents a cascade of the chain matrices **A** to **G**, or a multiplication of the modified chain matrices **A'** to **G'**.

$$H(z) = \frac{1}{x_{11} + \beta\, x_{12}} \tag{A8.3}$$

and

$$X' = A' B' C' D' E' F' G' \quad \text{when} \quad X' = \begin{bmatrix} x_{12} & x_{11} \\ x_{22} & x_{21} \end{bmatrix}$$

To simulate a given magnitude specification using a ladder WDF circuit then existing analogue design tables can be used. From tables a set of analogue DTL filter components can be found and used to determine the multiplier coefficients for ladder WDF. This type of analogue design table is given in terms of lowpass filter responses, such as elliptic, Butterworth and Chebyshev, with various pass and stopband tolerances.

A digital lowpass filter is to be designed from tables with an elliptic shape and the specification

$$|G| \le 0.1\ \text{dB} \qquad 0 \le f_{dp} \le 0.1$$
$$|G| \ge 50\ \text{dB} \qquad 0.12 \le f_{ds} \le F_s/2$$

with a sampling frequency, $F_s = 1$ Hz. The first step is to convert the discrete frequencies into equivalent analogue values. Under the bilinear transform the frequencies are subject to a non-linear mapping, characterised by Eq.(A8.4).

$$\omega_d = \frac{2}{T}\tan^{-1}\left(\frac{\omega_a T}{2}\right) \qquad \omega_a = \frac{2}{T}\tan\left(\frac{\omega_d T}{2}\right) \tag{A8.4}$$

where ω_d discrete frequency in rad/s

ω_a analogue frequency in rad/s

To compensate for this effect, the frequency values are pre-warped. Using Eq.(A8.4) the specification, given in terms of a discrete frequency in Hz, can be converted to a continuous frequency in rad/s. The modified specification becomes

$$|G| \le 0.1 \text{ dB} \qquad 0 \le \omega_{ap} \le 0.64984$$
$$|G| \ge 50 \text{ dB} \qquad 0.79186 \le \omega_{as} \le \infty$$

The Zverev tables are given in terms of a set of normalized magnitude responses which have a passband edge at 1 rad/s. To use the values in the table, the specification needs to be divided by the required passband edge. The resulting specification would then be

$$|G| \le 0.1 \text{ dB} \qquad 0 \le \omega'_{ap} \le 1$$
$$|G| \ge 50 \text{ dB} \qquad 1.2185 \le \omega'_{as} \le \infty$$

An entry in the Zverev tables which most closely matches this specification is CC_07_15_56, where CC denotes an elliptic shape and 07 is the order of the filter. The number 15 represents a reflection coefficient. The term indicates the passband attenuation, given as a reflection coefficient, ρ, which can be calculated from an attenuation in dBs through Eq.(A8.5).

$$\rho = \sqrt{1 - 10^{-\left(\frac{A_{dB}}{10}\right)}} \tag{A8.5}$$

The final term in the catalogue reference is 56, which is an angle indicating the sharpness of magnitude cut-off. This table entry corresponds to the specification

$$|G| \le 0.098 \text{ dB} \qquad 0 \le \omega'_{ap} \le 1$$
$$|G| \ge 56.5 \text{ dB} \qquad 1.2062 \le \omega'_{as} \le \infty$$

To achieve the desired filter specification, the component values from this table entry need to be divided by the required passband frequency, in this case, the value is 0.64984.

The resulting component elements are :-

R_s = 1.0	
C_1 = 1.61592	
C_2 = 0.24303	L_2 = 1.92723
C_3 = 2.29469	
C_4 = 1.22503	L_4 = 1.29234
C_5 = 1.99623	
C_6 = 0.88576	L_6 = 1.35875
C_7 = 1.16738	
R_L = 1.0	

Table A8.2 Component values for a 7th order DTL filter.

Because the filter order of this specification is 7, then the design can be implemented through the ladder WDF of Fig.(A8.3). The multipliers for this ladder WDF circuit, derived from the component values of Table(A8.2) and the equations of Table(A8.1), are illustrated in Table(A8.3).

R_1 = 1.0	δ_1 = 0.236304	
R_2 = 0.236304	δ_2 = -0.303984	δ_3 = 0.149779
R_3 = 1.577686	δ_4 = 0.121350	
R_4 = 0.191453	δ_5 = -0.727246	δ_6 = 0.351972
R_5 = 0.543943	δ_7 = 0.315291	
R_6 = 0.171501	δ_8 = -0.656009	δ_9 = 0.268432
R_7 = 0.638898	δ_{10} = 0.401337	
R_8 = 0.256413	β = 0.591833	

Table A8.3 Multiplier values for the ladder WDF using the source design procedure.

A8.2 Load Design

The first step of a load design procedure using the general ladder WDF circuit of Fig.(A8.2), is to remove the delay free path provided through the load external multiplier, β. This can be achieved by setting $\beta = 0$ or $R_b = R_L$, and therefore $R_8 = R_L$. The last element of the circuit of Fig.(A8.2) is a parallel capacitor. This section has a load design chain matrix given by Eq.(A8.6).

$$\begin{bmatrix} A_{13} \\ \\ B_{13} \end{bmatrix} = \begin{bmatrix} \dfrac{1-\delta_1}{1+z^{-1}} & \dfrac{1+\delta_1 z^{-1}}{1+z^{-1}} \\ \\ \dfrac{\delta_1+z^{-1}}{1+z^{-1}} & \dfrac{(1-\delta_1)\,z^{-1}}{1+z^{-1}} \end{bmatrix} \cdot \begin{bmatrix} A_{14} \\ \\ B_{14} \end{bmatrix} \qquad (A8.6)$$

where

$$\delta_1 = \frac{1}{1+C_7'\,R_8}\ ,\ R_7 = \frac{R_8}{1+C_7'\,R_8} \quad \text{and} \quad C_7' = \frac{2\,C_7}{T}$$

or

$$\delta_1 = \frac{1}{1+C_7'\,R_L} \quad \text{and} \quad R_7 = \frac{R_L}{1+C_7'\,R_L}$$

The next section is a series tuned inductor/capacitor element. The load design chain matrix of this element is given by Eq.(A8.7).

$$\begin{bmatrix} A_{11} \\ \\ B_{11} \end{bmatrix} = \begin{bmatrix} -\left(\dfrac{(1-\delta_3)(1+\delta_2 z^{-1})}{\delta_3\,(1+2\delta_2 z^{-1}+z^{-2})}\right) & \dfrac{1+\delta_2(1+\delta_3)z^{-1}+\delta_3 z^{-2}}{\delta_3\,(1+2\delta_2 z^{-1}+z^{-2})} \\ \\ \dfrac{\delta_3+\delta_2(1+\delta_3)z^{-1}+z^{-2}}{\delta_3\,(1+2\delta_2 z^{-1}+z^{-2})} & -\left(\dfrac{(1-\delta_3)z^{-1}(\delta_2+z^{-1})}{\delta_3\,(1+2\delta_2 z^{-1}+z^{-2})}\right) \end{bmatrix} \cdot \begin{bmatrix} A_{12} \\ \\ B_{12} \end{bmatrix} \qquad (A8.7)$$

with

$$\delta_2 = \frac{1-L_6'\,C_6'}{1+L_6'\,C_6'}\ ,\ \delta_3 = \frac{R_7(1+L_6'\,C_6')}{L_6'+R_7(1+L_6'\,C_6')} \quad \text{and} \quad R_6 = R_7 + \frac{L_6'}{1+L_6'\,C_6'}$$

and

$$C_6' = \frac{2\,C_6}{T} \quad \text{and} \quad L_6' = \frac{2\,L_6}{T}$$

Since the value of R_7 has been expressed in terms of R_L, then it can be substituted to express δ_3 and R_6 as,

$$\delta_3 = \frac{R_L(1+L_6'\,C_6')}{L_6'(1+C_7'\,R_L)+R_L(1+L_6'\,C_6')} \quad \text{and} \quad R_6 = \frac{R_L}{1+C_7'\,R_L} + \frac{L_6'}{1+L_6'\,C_6'}$$

Continuing the design process using chain matrices of the form of Eq.(A8.6) and (A8.7), the multiplier values for the overall circuit can be determined and applied to the load design structure of Fig.(A8.4).

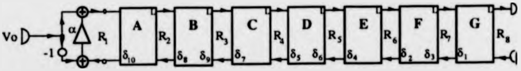

Figure A8.4 Ladder WDF circuit using load design procedure.

In the circuit of Fig.(A8.4), the parallel capacitor of the last section has the chain matrix, G, given by Eq.(A8.6), while the series tuned inductor/capacitor in the second to last section has the chain matrix, F, of Eq.(A8.7). The chain matrix A, C and E have the same form as Eq.(A8.6) but in terms of δ_{10}, δ_7 and δ_4 respectively.

Similarly, the matrices **B** and **D** have the form of Eq.(A8.7) with multipliers δ_8/δ_9 and δ_2/δ_3 respectively. The multiplier equations for the load design ladder WDF circuit of Fig.(A8.4) are given in Table(A8.4).

$\delta_1 = \dfrac{1}{1 + C_7' R_8}$	$R_7 = \dfrac{R_8}{1 + C_7' R_8}$	
$\delta_2 = \dfrac{1 - L_6' C_6'}{1 + L_6' C_6'}$	$\delta_3 = \dfrac{R_7(1 + L_6' C_6')}{L_6' + R_7(1 + L_6' C_6')}$	$R_6 = R_7 + \dfrac{L_6'}{1 + L_6' C_6'}$
$\delta_4 = \dfrac{1}{1 + C_5' R_6}$	$R_5 = \dfrac{R_6}{1 + C_5' R_6}$	
$\delta_5 = \dfrac{1 - L_4' C_4'}{1 + L_4' C_4'}$	$\delta_6 = \dfrac{R_5(1 + L_4' C_4')}{L_4' + R_5(1 + L_4' C_4')}$	$R_4 = R_5 + \dfrac{L_4'}{1 + L_4' C_4'}$
$\delta_7 = \dfrac{1}{1 + C_3' R_4}$	$R_3 = f(R_4, 1 + C_3' R_4)$	
$\delta_8 = \dfrac{1 - L_2' C_2'}{1 + L_2' C_2'}$	$\delta_9 = \dfrac{R_3(1 + L_2' C_2')}{L_2' + R_3(1 + L_2' C_2')}$	$R_2 = R_3 + \dfrac{L_2'}{1 + L_2' C_2'}$
$\delta_{10} = \dfrac{1}{1 + C_1' R_2}$	$R_1 = \dfrac{R_2}{1 + C_1' R_2}$	
$\alpha = \dfrac{R_s - R_1}{R_s + R_1}$		

Table A8.4 Multiplier equations for load design ladder WDF of Fig.(A8.4).

The transfer function for the circuit is given by Eq.(A8.8) where **X** represents a cascade of the chain matrices **A** to **G**.

$$H(z) = \frac{1 - \alpha}{x_{11} - \alpha\, x_{22}} \qquad \text{(A8.8)}$$

and

$$\mathbf{X}' = \mathbf{A}'\mathbf{B}'\mathbf{C}'\mathbf{D}'\mathbf{E}'\mathbf{F}'\mathbf{G}' \quad \text{when} \quad \mathbf{X}' = \begin{bmatrix} x_{12} & x_{11} \\ x_{22} & x_{21} \end{bmatrix}$$

If the load design procedure is applied to the same filter specification as that used for the source design example, then the lumped component value will be the same, shown in Table(A8.2). The resulting load design multipliers are given in Table(A8.5).

$R_8 = 1.0$	$\delta_1 = 0.299872$	
$R_7 = 0.299872$	$\delta_2 = -0.656009$	$\delta_3 = 0.390830$
$R_6 = 0.767269$	$\delta_4 = 0.246106$	
$R_5 = 0.188829$	$\delta_5 = -0.727246$	$\delta_6 = 0.348831$
$R_4 = 0.541320$	$\delta_7 = 0.287000$	
$R_3 = 0.155359$	$\delta_8 = -0.303984$	$\delta_9 = 0.103798$
$R_2 = 1.496741$	$\delta_{10} = 0.171314$	
$R_1 = 0.256413$	$\alpha = 0.591833$	

Table A8.5 Multiplier values for the ladder WDF using the load design procedure

A8.3 Middle Design

The objective of the middle design procedure is to use the ideas from the source and load design techniques simultaneously to meet at some port near the middle of the circuit. If the middle design approach is applied to the general ladder WDF circuit of Fig.(A8.2), then the middle of the circuit would be the second series tuned element. The first step of this design procedure would be to follow the source design approach, eliminating the constant terms from the circuit connected to the input port of each element, until the port resistance R_4 has been determined. The next stage is to follow the load design procedure until the value of R_5 has been calculated. The resulting middle design ladder WDF circuit is shown by Fig.(A8.5).

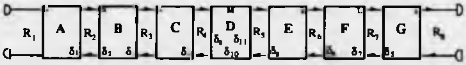

Figure A8.5 Ladder WDF circuit using middle design procedure.

Using the middle design procedure, sections **A** and **C** have chain matrices of the form of Eq.(A8.1), but in terms of δ_1 and δ_4 respectively, while the sections **G** and **E** have the form of Eq.(A8.6) in terms of δ_5 and δ_8 respectively.

Section **B** has the source design chain matrix of Eq.(A8.2), while section **F** has the load chain matrix of Eq.(A8.7) in terms of δ_6 and δ_7. The final section, **D**, has both its input and output port resistances determined by sections **C** and **E**, which ensure the removal of delay free loops. The chain matrix for the series tuned circuit, under the middle design procedure, is given by Eq.(A8.9).

$$\begin{bmatrix} A_7 \\ B_7 \end{bmatrix} = \left[C_{ms}(LC)\right] \cdot \begin{bmatrix} A_8 \\ B_8 \end{bmatrix} \tag{A8.9}$$

where

$$C_{ms}(LC) = \begin{bmatrix} \dfrac{\delta_{11}+\delta_9(1-\delta_{10}+2\delta_{11})z^{-1}+(1-\delta_{10}+\delta_{11})z^{-2}}{(1+\delta_{11})(1+2\delta_9 z^{-1}+z^{-2})} & \dfrac{1+\delta_9(1+\delta_{10})z^{-1}+\delta_{10}\ z^{-2}}{(1+\delta_{11})(1+2\delta_9 z^{-1}+z^{-2})} \\ \dfrac{\delta_{10}+\delta_9(1+\delta_{10})z^{-1}+z^{-2}}{(1+\delta_{11})(1+2\delta_9 z^{-1}+z^{-2})} & \dfrac{(1-\delta_{10}+\delta_{11})+\delta_9(1-\delta_{10}+2\delta_{11})z^{-1}+\delta_{11}z^{-2}}{(1+\delta_{11})(1+2\delta_9 z^{-1}+z^{-2})} \end{bmatrix}$$

$$\delta_9 = \frac{1 - L_4'C_4'}{1 + L_4'C_4'} \ , \ \delta_{10} = \frac{(R_5 + R_4)(1 + L_4'C_4') - L_4'}{(R_5 + R_4)(1 + L_4'C_4') + L_4'}$$

$$\delta_{11} = \frac{(R_5 - R_4)(1 + L_4'C_4') - L_4'}{(R_5 + R_4)(1 + L_4'C_4') + L_4'} \ , \ L_4' = \frac{2\,L_4}{T} \quad \text{and} \quad C_4' = \frac{2\,C_4}{T}$$

The transfer function for this circuit is given by Eq.(A8.10), where **X** represents a cascade of the chain matrices **A** to **G**.

$$H(z) = \frac{1}{x_{11}} \tag{A8.10}$$

The multiplier equations for the ladder WDF, shown by Fig.(A8.5), under the middle design procedure, are shown by Table(A8.6).

$\delta_1 = \dfrac{1}{1 + C_1'\,R_1}$	$R_2 = \dfrac{R_1}{1 + C_1'\,R_1}$	
$\delta_2 = \dfrac{1 - L_2'\,C_2'}{1 + L_2'\,C_2'}$	$\delta_3 = \dfrac{R_2(1 + L_2'\,C_2')}{L_2' + R_2(1 + L_2'\,C_2')}$	$R_3 = R_2 + \dfrac{L_2'}{1 + L_2'\,C_2'}$
$\delta_4 = \dfrac{1}{1 + C_3'\,R_3}$	$R_4 = \dfrac{R_3}{1 + C_3'\,R_1}$	
$\delta_5 = \dfrac{1}{1 + C_7'\,R_8}$	$R_7 = \dfrac{R_8}{1 + C_7'\,R_8}$	
$\delta_6 = \dfrac{1 - L_6'\,C_6'}{1 + L_6'\,C_6'}$	$\delta_7 = \dfrac{R_7(1 + L_6'\,C_6')}{L_6' + R_7(1 + L_6'\,C_6')}$	$R_6 = R_7 + \dfrac{L_6'}{1 + L_6'\,C_6'}$
$\delta_8 = \dfrac{1}{1 + C_5'\,R_6}$	$R_5 = \dfrac{R_6}{1 + C_5'\,R_6}$	
$\delta_9 = \dfrac{1 - L_4'\,C_4'}{1 + L_4'\,C_4'}$	$\delta_{10} = \dfrac{(R_5+R_4)(1+L_4'C_4') - L_4'}{(R_5+R_4)(1+L_4'C_4') + L_4'}$	$\delta_{11} = \dfrac{(R_5-R_4)(1+L_4'C_4') - L_4'}{(R_5+R_4)(1+L_4'C_4') + L_4'}$

Table A8.6 Multiplier equations for middle design ladder WDF of Fig.(A8.5).

If the component value, given in Table(A8.2), used in the previous examples are applied to the ladder WDF of Fig.(A8.5), then the resulting multiplier values can be determined are illustrated in Table(A8.7).

R_1 = 1.0	δ_1 = 0.236304	
R_2 = 0.236304	δ_2 = -0.303984	δ_3 = 0.149779
R_3 = 1.577686	δ_4 = 0.121350	
R_4 = 0.191453		
R_8 = 1.0	δ_5 = 0.299872	
R_7 = 0.299872	δ_6 = -0.656009	δ_7 = 0.390830
R_6 = 0.767269	δ_8 = 0.246106	
R_5 = 0.188829		
δ_9 = -0.727246	δ_{10} = 0.037926	δ_{11} = -0.484618

Table A8.7 Multiplier values for the ladder WDF using the middle design procedure.

This whole design process can be performed through the computer program WAVE. This program also applies the optimization techniques discussed in Chapters 2 and 3 to the design of arbitrary simultaneous magnitude and phase specifications.

Appendix B

Design Program Descriptions

This Appendix provides a menu walk through of the software tools developed within this research project for the design and analysis of lattice WDF's. The design and analysis functions are split into two separate programs. The design program is called `'wdf'` and was written in Fortran. Lattice WDF analysis was provided through a program called `'mltwdf'` which was written for a package called MatLab. The final program, `'ellip'`, is an implementation of the design equations developed by Gazsi to calculate the order and multipliers values of lattice WDF's that can satisfy lowpass magnitude only specifications using Elliptical, Butterworth and Chebyshev polynomials.

The options and operation of each program is illustrated through a menu walk through and a number of design examples. This contents of this Appendix is :-

B1 Design Program '`ellip`'

To illustrate the operation of the design program, '`ellip`', consider the specification shown in Table(B1.1).

Gain passband		Gain stopband		Samp freq (Hz)
att (dB)	edge (Hz)	att (dB)	edge (Hz)	
0.1	0.1	50	0.15	1

Table B1.1 Lowpass filter specification.

The program, '`ellip`', can be used to determine the order of Elliptic, Butterworth and Chebyshev polynomial required to satisfy the specification of Table(B1.1). The program can then calculate the multiplier values for a lattice WDF to exhibit the desired polynomial response.

On entry, the program, '`ellip`', will display the menu structure shown by Fig.(B1.1).

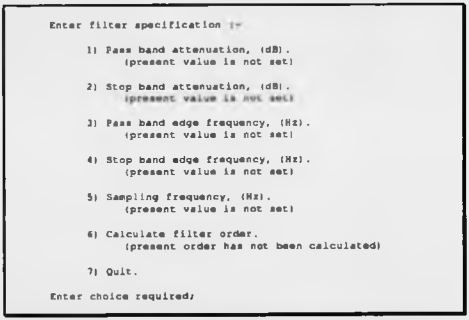

```
Enter filter specification :-

      1) Pass band attenuation, (dB).
            (present value is not set)

      2) Stop band attenuation, (dB).
            (present value is not set)

      3) Pass band edge frequency, (Hz).
            (present value is not set)

      4) Stop band edge frequency, (Hz).
            (present value is not set)

      5) Sampling frequency, (Hz).
            (present value is not set)

      6) Calculate filter order.
            (present order has not been calculated)

      7) Quit.

Enter choice required;
```

Figure B1.1 Filter specification menu of '`ellip`'.

By selecting the options 1 though 5 from the menu shown by Fig.(B1.1), the lowpass specification of Table(B1.1) can be entered into the program. While the specification is entered, the menu structure of Fig.(B1.1) will alter to display the current values. The program menu with the specification of Table(B1.1) entered, is shown by Fig.(B1.2).

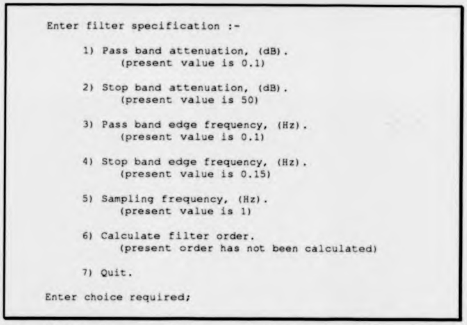

```
Enter filter specification :-

      1) Pass band attenuation, (dB).
          (present value is 0.1)

      2) Stop band attenuation, (dB).
          (present value is 50)

      3) Pass band edge frequency, (Hz).
          (present value is 0.1)

      4) Stop band edge frequency, (Hz).
          (present value is 0.15)

      5) Sampling frequency, (Hz).
          (present value is 1)

      6) Calculate filter order.
          (present order has not been calculated)

      7) Quit.

Enter choice required;
```

Figure B1.2 Filter specification menu of `'ellip'` with specification.

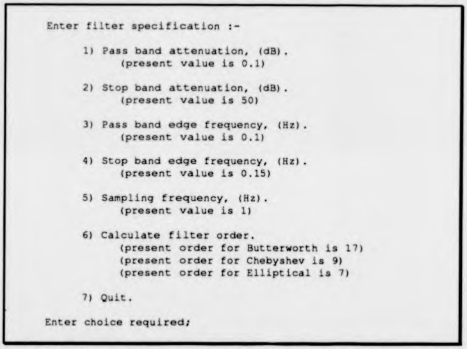

```
Enter filter specification :-

      1) Pass band attenuation, (dB).
          (present value is 0.1)

      2) Stop band attenuation, (dB).
          (present value is 50)

      3) Pass band edge frequency, (Hz).
          (present value is 0.1)

      4) Stop band edge frequency, (Hz).
          (present value is 0.15)

      5) Sampling frequency, (Hz).
          (present value is 1)

      6) Calculate filter order.
          (present order for Butterworth is 17)
          (present order for Chebyshev is 9)
          (present order for Elliptical is 7)

      7) Quit.

Enter choice required;
```

Figure B1.3 Menu with specification and minimum polynomial orders.

Option '6' of the main menu will calculate the order of the Elliptic, Butterworth and Chebyshev polynomials for the current filter specification. This features allows the orders of a number of different specification to be found quickly. Selecting option '6' was for the specification of Table(B1.1) results in the Butterworth, Chebyshev and Elliptic polynomial orders being added to the program menu, illustrated by Fig.(B1.3).

Having completed the entry of the filter specification, the next step is the calculation of the multipliers for a lattice WDF. Selection of option '7' from the menu of Fig.(B1.3) moves the program onto the next menu. This menu structure allows the required filter order to be selected, shown in Fig.(B1.4).

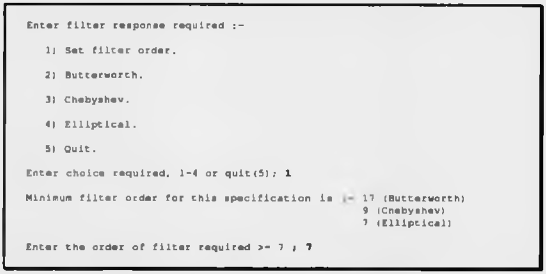

```
Enter filter response required :-

    1) Set filter order.

    2) Butterworth.

    3) Chebyshev.

    4) Elliptical.

    5) Quit.

Enter choice required, 1-4 or quit(5); 1

Minimum filter order for this specification is :- 17 (Butterworth)
                                                    9 (Chebyshev)
                                                    7 (Elliptical)

Enter the order of filter required >= 7 ; 7
```

Figure B1.4 Selection of lattice WDF orders.

With the filter order selected, the next step is to select the polynomial type required. A particular filter order for a polynomial allows a small amount of freedom upon the frequency specification. This is expressed as a range of possible stopband edge frequencies and passband attenuations. If the elliptical polynomial is required and option '4' selected from the menu of Fig.(B1.4), then the program will provide the limits for the stopband edge frequencies and passband attenuations allowed for that particular filter order, passband edge frequency and stopband attenuation. This information will be presented in the format shown by Fig.(B1.5).

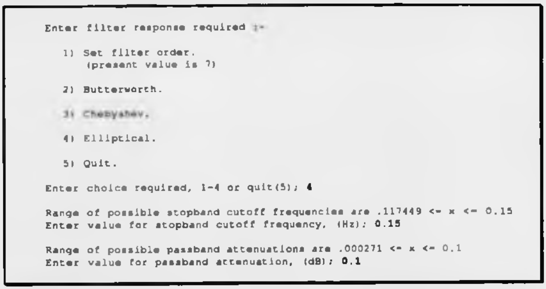

```
Enter filter response required :-

   1) Set filter order.
      (present value is 7)

   2) Butterworth.

   3) Chebyshev.

   4) Elliptical.

   5) Quit.

Enter choice required, 1-4 or quit(5); 4

Range of possible stopband cutoff frequencies are .117449 <= x <= 0.15
Enter value for stopband cutoff frequency, (Hz): 0.15

Range of possible passband attenuations are .000271 <= x <= 0.1
Enter value for passband attenuation, (dB); 0.1
```

Figure B1.5 Final selection of specification values for an elliptic polynomial response.

With a final frequency specification, the program will calculate the lattice WDF multiplier values for a particular polynomial type and display them in the form illustrated by Fig.(B1.6).

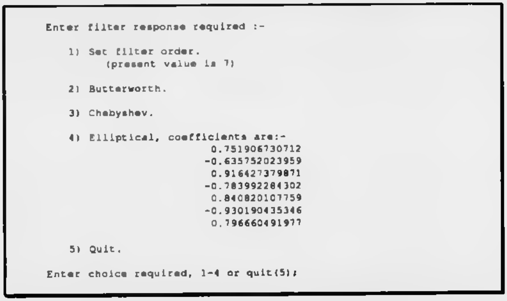

```
Enter filter response required :-

   1) Set filter order.
      (present value is 7)

   2) Butterworth.

   3) Chebyshev.

   4) Elliptical, coefficients are:-
                           0.751906730712
                          -0.635752023959
                           0.916427379871
                          -0.783992284302
                           0.840820107759
                          -0.930190435346
                           0.796660491977

   5) Quit.

Enter choice required, 1-4 or quit(5);
```

Figure B1.6 Display of filter coefficients for the desired elliptic polynomial response.

The multiplier values from the program, '`ellip`', are given in the format specified by Gazsi, so that the first multiplier value is that of the only 1st order APS, the next two multipliers belong to the first 2nd order APS of the lower arm and the next two for the first 2nd order APS of the upper arm. Pairs of multipliers then alternate between upper and lower arm 2nd order APS's. On exit the program will convert the current set of multiplier values into the format used within the `'wdf'` and `'mltwdf'` programs. Within this format first half of the multipliers belong to the upper arm and the other half for the lower arm. Where appropriate, the last multiplier for the upper lattice arm set will belong to the single 1st order APS.

B 2 Design Program `wdf`

The `wdf` program has three main functions :-

(i) Entry and alteration of general filter specification.
(ii) Design through the application of optimization routines.
(iii) Retrieval and storage of filter/optimization parameters.

The operation and structure of this program can be illustrated through the filter specifications of Table(B1.1) and Table(B2.1).

Gain passband		Gain stopband		Delay passband		Samp.
att (dB)	edge (Hz)	att (dB)	edge (Hz)	dev (%)	edge (Hz)	freq (Hz)
0.1	0.1	50	0.15	1	0.1	1

Table B2.1 Simultaneous lowpass filter specification.

The main menu of the `wdf` program is shown by Fig.(B2.1).

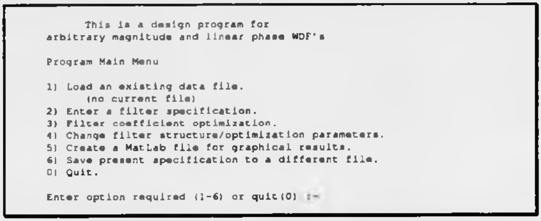

```
      This is a design program for
arbitrary magnitude and linear phase WDF's

Program Main Menu

1) Load an existing data file.
     (no current file)
2) Enter a filter specification.
3) Filter coefficient optimization.
4) Change filter structure/optimization parameters.
5) Create a MatLab file for graphical results.
6) Save present specification to a different file.
0) Quit.

Enter option required (1-6) or quit(0) :-
```

Figure B2.1 Main menu structure of the `wdf` program.

The operation of the `wdf` program is controlled through the main menu structure of Fig.(B2.1). Frequency specifications can be entered into the program through option '2'. With an initial frequency specification, option '4' can be used to amend the specification and optimization parameter values. These specification and optimization settings can then be saved to a plain ASCII data file though option '6'. Alternatively an existing data file can be loaded into the program using option '1' and the appropriate parameter values changed to satisfy a new specification.

Analysis of the time and frequency domain responses of the various lattice WDF designs is carried out within the program `mltwdf`. This program was written to operate within MatLab which possess its own data file format. To utilise the efficiency of the MatLab file format the plain data files of the `wdf` program can be converted into an equivalent MatLab format file through option '5' of the main menu of Fig.(B2.1).

The procedures under options '3' and '4' constitute the main features of the `wdf` program. The menu structure and operation of each option will be considered in turn. Option '4' of the main menu, shown by Fig.(B2.1) provides the operator with the ability to change all the parameters directly related to the design and optimization of a lattice WDF. Selection of option '4' will invoke the alteration menu illustrated by Fig.(B2.2).

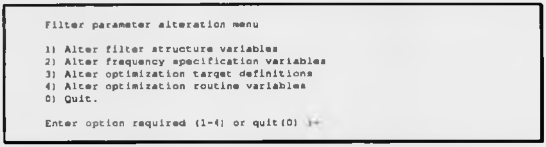

```
Filter parameter alteration menu

1) Alter filter structure variables
2) Alter frequency specification variables
3) Alter optimization target definitions
4) Alter optimization routine variables
0) Quit.

Enter option required (1-4) or quit(0) :-
```

Figure B2.2 Filter parameter alteration menu structure.

The first two options of the menu of Fig.(B2.2) relate directly to the filter structure and specification parameters. These elements include filter order, frequency specification and desired finite wordlength. If the magnitude-only filter specification of Table(B1.1) had been entered into the program, then selecting option '1' from the menu of Fig.(B2.2) would show the '`Filter structure menu`', illustrated by Fig.(B2.3).

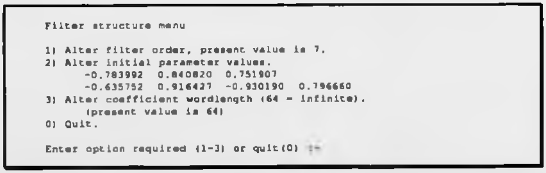

```
Filter structure menu

1) Alter filter order, present value is 7.
2) Alter initial parameter values.
     -0.783992  0.840820  0.751907
     -0.635752  0.916427  -0.930190  0.796660
3) Alter coefficient wordlength (64 = infinite).
     (present value is 64)
0) Quit.

Enter option required (1-3) or quit(0) :-
```

Figure B2.3 Filter structure menu options showing value from Table(B1.1).

The three options shown in Fig.(B2.3) allow the user to change the filter order, initial coefficient values or desired filter coefficient wordlength. If the filter order is changed, using option '1', then all coefficient values will be set to zero.

The menu structure invoked by selecting option '2' from the '`Filter parameter alteration menu`', Fig.(B2.2), is illustrated by Fig.(B2.4) containing the lowpass specification values from Table(B2.1).

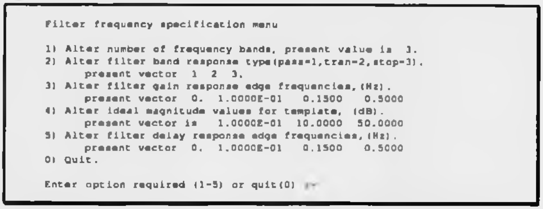

```
Filter frequency specification menu

1) Alter number of frequency bands, present value is  3.
2) Alter filter band response type(pass=1,tran=2,stop=3).
     present vector  1  2  3.
3) Alter filter gain response edge frequencies,(Hz).
     present vector  0.  1.0000E-01   0.1500   0.5000
4) Alter ideal magnitude values for template, (dB).
     present vector is   1.0000E-01  10.0000  50.0000
5) Alter filter delay response edge frequencies,(Hz).
     present vector  0.  1.0000E-01   0.1500   0.5000
0) Quit.

Enter option required (1-5) or quit(0) ?
```

Figure B2.4 Filter frequency specification menu shown for the specification of Table(B2.1).

Option '3' of the '`Filter parameter alteration menu`', Fig.(B2.2), allows the definition for the optimization targets to be altered between the single and dual line schemes described in Chapter 2. Finally option '4' from Fig.(B2.2) allows the operator control over all the optimization parameters relevant to the quasi-Newton and modified Hooke-Jeeves routines. Fig.(B2.5) shows a typical set of parameter values for a simultaneous lowpass specification.

The options within the menu structure of Fig.(B2.5) directly control the optimization algorithm, templates and error function parameters. Selection of particular values for these various parameters requires a small amount of experimentation for a particular specification. A parameter which may not be obvious is the frequency transformation procedure, option '15'. In the design of single and dual bandpass and bandstop lattice WDF's, the APS's contain either one or two parameters which determine the movement of the frequency band(s). The value of these parameters may be common within all APS's of a filter or used as an optimization variable to increase the flexibility of bandpass and bandstop type designs.

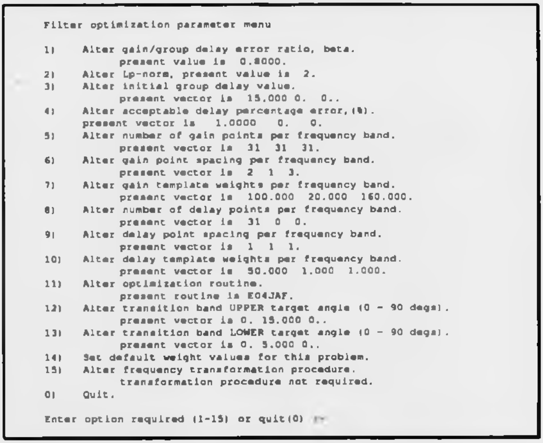

```
Filter optimization parameter menu

1)    Alter gain/group delay error ratio, beta.
             present value is  0.8000.
2)    Alter Lp-norm, present value is  2.
3)    Alter initial group delay value.
             present vector is  15.000 0.  0..
4)    Alter acceptable delay percentage error,(%).
      present vector is   1.0000   0.   0.
5)    Alter number of gain points per frequency band.
             present vector is  31  31  31.
6)    Alter gain point spacing per frequency band.
             present vector is  2  1  3.
7)    Alter gain template weights per frequency band.
             present vector is  100.000  20.000  160.000.
8)    Alter number of delay points per frequency band.
             present vector is  31  0  0.
9)    Alter delay point spacing per frequency band.
             present vector is  1  1  1.
10)   Alter delay template weights per frequency band.
             present vector is  50.000  1.000  1.000.
11)   Alter optimization routine.
             present routine is E04JAF.
12)   Alter transition band UPPER target angle (0 - 90 degs).
             present vector is 0. 15.000 0..
13)   Alter transition band LOWER target angle (0 - 90 degs).
             present vector is 0. 5.000 0..
14)   Set default weight values for this problem.
15)   Alter frequency transformation procedure.
             transformation procedure not required.
0)    Quit.

Enter option required (1-15) or quit(0)
```

Figure B2.5 Filter optimization parameter menu showing a typical set of parameter values for a lowpass specification.

With the desired design specification entered into the program the next step is to return the '`Program Main Menu`', Fig.(B2.1), and either save these parameters to a data file under option '6' or begin optimization through option '3'. The various quasi-Newton optimization algorithms are implemented to produce filter coefficients values to the full accuracy of the computer system. These algorithms can therefore only be implemented when the desired wordlength, set in the '`Filter structure menu`' of Fig.(B2.4), is equal to the upper limit, i.e. 64 bits. If the wordlength is shorter than this value, then the program will automatically invoke the Hooke-Jeeves algorithm. Upon starting any optimization, the user will be asked for a filename into which the design parameters will be stored. These results consist of a '.dat' file which contains the filter structure information which can be loaded back into the '`wdf`' program, a '.res' file which holds a list of all the initial optimization settings, multipliers values and a history of error function values and a '.mat' file created in the MatLab format. The '.mat' file contains virtually the same information as the .'dat' file expect that it is compressed and stored in a binary form that cannot be edited. This format allows a rapid loading into the '`mltwdf`' program and ensures that parameters within a solution data file cannot be accidentally altered.

The design process using a quasi-Newton algorithm is illustrated in Fig.(B2.6)(a-c) for the simultaneous specification of Table(B2.1). Having prompted the operator for a filename, the program will display the initial parameters values.

```
Enter name for optimization data files
      (creating ".res", ".mat" and ".dat" files)
fil_test

Filter coefficient wordlength is 'ideal' = (64 bits)

Initial optimization vector values are :-
      parameter[  1] =   0.00000000000000000000
      parameter[  2] =   0.00000000000000000000
      parameter[  3] =   0.00000000000000000000
      parameter[  4] =   0.00000000000000000000
      parameter[  5] =   0.00000000000000000000
      parameter[  6] =   0.00000000000000000000
      parameter[  7] =   0.00000000000000000000
      parameter[  8] =   0.00000000000000000000
      parameter[  9] =   0.00000000000000000000
      parameter[ 10] =   0.00000000000000000000
      parameter[ 11] =   0.00000000000000000000
      parameter[ 12] =   0.00000000000000000000
      parameter[ 13] =   0.00000000000000000000
      parameter[ 14] =   0.00000000000000000000
      parameter[ 15] =   0.00000000000000000000
      parameter[ 16] =  15.00000000000000000000

Initial mean group delay value for passband [1] is 15.0000

Group delay error tolerance for passband [1] is 1.00000%

Initial error value is  0.12644725E+05

Optimizing coefficients ...

      Function               Function                 Function
       number                 error                improvement(%)
        100               0.48844741E+03              96.137145
        200               0.22899577E+03              53.117621
        300               0.21514542E+03               6.048297
        400               0.19540717E+03               9.174379
        500               0.99811552E+02              48.921243
        600               0.37994933E+02              61.933331
        700               0.32677623E+02              13.994787
        800               0.26852514E+02              17.825986
        900               0.23721900E+02              11.658552
       1000               0.16446858E+02              30.668040
         .                    .                         .
         .                    .                         .
       6200               0.82923786E-03               0.000002
       6300               0.82923859E-03              -0.036266
       6400               0.82923861E-03               0.036163
```

Figure B2.6(a) Display of initial optimization parameter values.

If the routine exceeds 400 times the number of optimization variables then the program will exist, display the results and restart the process using the values of the parameters on exit as the initial starting values. This process in shown in Fig.(B2.6)(b).

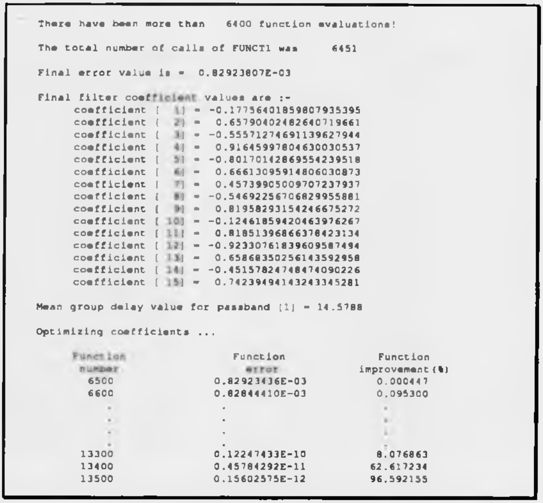

```
There have been more than   6400 function evaluations!

The total number of calls of FUNCT1 was     6451

Final error value is =  0.82923807E-03

Final filter coefficient values are :-
     coefficient [  1] = -0.17756401859807935395
     coefficient [  2] =  0.65790402482640719661
     coefficient [  3] = -0.55571274691139627944
     coefficient [  4] =  0.91645997804630030537
     coefficient [  5] = -0.80170142869554239518
     coefficient [  6] =  0.66613095914806030873
     coefficient [  7] =  0.45739905009707237937
     coefficient [  8] = -0.54692256706829955881
     coefficient [  9] =  0.81958293154246675272
     coefficient [ 10] = -0.12461859420463976267
     coefficient [ 11] =  0.81851396866378423134
     coefficient [ 12] = -0.92330761839609587494
     coefficient [ 13] =  0.65868350256143592958
     coefficient [ 14] = -0.45157824748474090226
     coefficient [ 15] =  0.74239494143243345281

Mean group delay value for passband [1] = 14.5788

Optimizing coefficients ...

     Function              Function             Function
      number                error            improvement(%)
       6500             0.82923436E-03          0.000447
       6600             0.82844410E-03          0.095300
         .                    .                    .
         .                    .                    .
         .                    .                    .
         .                    .                    .
      13300             0.12247433E-10          8.076863
      13400             0.45784292E-11         62.617234
      13500             0.15602575E-12         96.592155
```

Figure B2.6(b) Typical optimization process.

Optimization, using the NAG routines, will continue until the solution can no longer be improved or the number of iteration exceeds 400 times the number of optimization variables. If the iteration limit is reached, the program will display the number of actual function evaluation, the final error and coefficient values. The program will then re-invoke the routine with the final coefficient values as initial settings. This process will allows occur if the iteration limit is reached. On exit a NAG routine will return an error flag to indicate its reason for terminating. The program interprets this error flag for each NAG routine and uses it to re-invoke the routine if the iteration limit has been reached or exit the optimization procedure if a solution has been found. Return error flags will also indicate if a solution could not be found or if there was some doubt about the solution produced.

The final steps of the design process for the example considered are shown in Fig.(B2.6)(c).

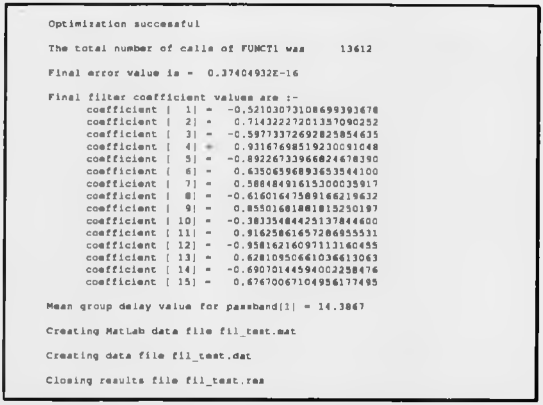

```
Optimization successful

The total number of calls of FUNCT1 was      13612

Final error value is =  0.37404932E-16

Final filter coefficient values are :-
      coefficient [  1] =  -0.52103073108699393678
      coefficient [  2] =   0.71432227201357090252
      coefficient [  3] =  -0.59773372692825854635
      coefficient [  4] =   0.93167698519230091048
      coefficient [  5] =  -0.89226733966824678390
      coefficient [  6] =   0.63506596893653544100
      coefficient [  7] =   0.58848491615300035917
      coefficient [  8] =  -0.61601647589166219632
      coefficient [  9] =   0.85501681881815250197
      coefficient [ 10] =  -0.38335484425137844600
      coefficient [ 11] =   0.91625861657286955531
      coefficient [ 12] =  -0.95816216097113160455
      coefficient [ 13] =   0.62810950661036613063
      coefficient [ 14] =  -0.69070144594002258476
      coefficient [ 15] =   0.67670067104956177495

Mean group delay value for passband[1] = 14.3867

Creating MatLab data file fil_test.mat

Creating data file fil_test.dat

Closing results file fil_test.res
```

Figure B2.6(c) Final steps in optimization design process.

Finite wordlength optimization designs expect to be started with an 'ideal' solution as its initial multiplier values. Before the optimization is started the user is asked for an initial wordlength to which the initial coefficient multipliers will be quantized. The program will then apply the Hooke-Jeeves optimization routine to the specification. If a solution can be found the current wordlength is compared to the desired wordlength defined within the specification. If it is larger, the current wordlength is reduced by one bit and the process repeated. If a solution cannot be found the wordlength is increased by one bit and reapplied. If the routine reaches a minimum limit three times without being able to achieve the desired wordlength, the process is terminated. The optimization procedure will therefore exit with a set of finite wordlength coefficients that satisfy the desired or shortest possible wordlength conditions. A typical example of a finite wordlength design using the simultaneous specification of Table(B2.1) is illustrated by Fig.(B2.7).

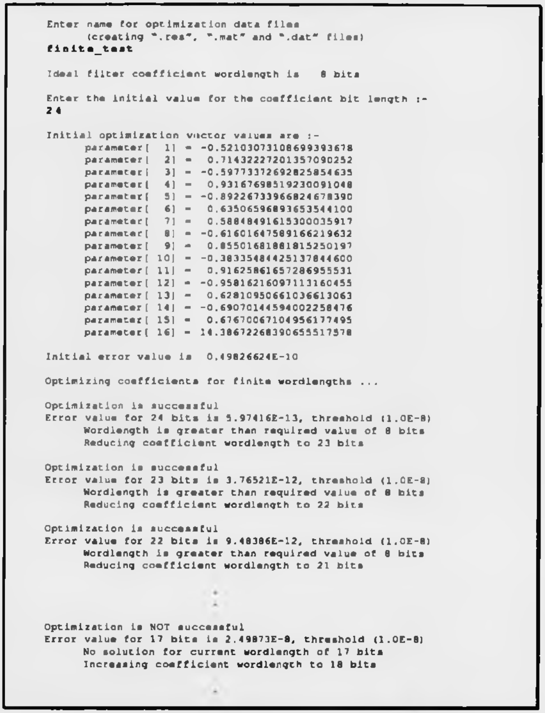

```
Enter name for optimization data files
      (creating ".res", ".mat" and ".dat" files)
finite_test

Ideal filter coefficient wordlength is   8 bits

Enter the initial value for the coefficient bit length :-
24

Initial optimization vector values are :-
      parameter[  1] = -0.52103073108699393678
      parameter[  2] =  0.71432227201357090252
      parameter[  3] = -0.59773372692825854635
      parameter[  4] =  0.93167698519230091048
      parameter[  5] = -0.89226733966824678390
      parameter[  6] =  0.63506596893653544100
      parameter[  7] =  0.58848491615300035917
      parameter[  8] = -0.61601647589166219632
      parameter[  9] =  0.85501681881815250197
      parameter[ 10] = -0.38335484425137844600
      parameter[ 11] =  0.91625861657286955531
      parameter[ 12] = -0.95816216097113160455
      parameter[ 13] =  0.62810950661036613063
      parameter[ 14] = -0.69070144594002258476
      parameter[ 15] =  0.67670067104956177495
      parameter[ 16] = 14.38672268390655517578

Initial error value is  0.49826624E-10

Optimizing coefficients for finite wordlengths ...

Optimization is successful
Error value for 24 bits is 5.97416E-13, threshold (1.0E-8)
      Wordlength is greater than required value of 8 bits
      Reducing coefficient wordlength to 23 bits

Optimization is successful
Error value for 23 bits is 3.76521E-12, threshold (1.0E-8)
      Wordlength is greater than required value of 8 bits
      Reducing coefficient wordlength to 22 bits

Optimization is successful
Error value for 22 bits is 9.48386E-12, threshold (1.0E-8)
      Wordlength is greater than required value of 8 bits
      Reducing coefficient wordlength to 21 bits

                          .
                          .


Optimization is NOT successful
Error value for 17 bits is 2.49873E-8, threshold (1.0E-8)
      No solution for current wordlength of 17 bits
      Increasing coefficient wordlength to 18 bits

                          .
```

Figure B2.7 Display of finite wordlength optimization.

B 3 Analysis Program '`mltwdf`'

This program utilise the features and graphical procedures of MatLab to generate and display the results of a number of responses of the lattice WDF. These responses can be calculated within the frequency domain through a set of analytical equations which describe the lattice WDF's or determined within the time domain by modelling the physical element of the two-port adaptor and lattice WDF APS's.

Frequency domain characteristics calculated by the '`mltwdf`' program are :-

- (i) Frequency response ;
  - (a) Gain vs. Frequency
  - (b) Magnitude vs. Frequency
  - (c) Phase vs. Frequency
  - (d) Group Delay vs. Frequency
- (ii) Coefficient Sensitivity ;
  - (a) Gain vs. Frequency
  - (b) Phase vs. Frequency
  - (c) Group Delay vs. Frequency
- (iii) Pole/Zero Plots

Time domain characteristics calculated by the '`mltwdf`' program are :-

- (i) Time response ;
  - (a) Impulse vs. Time
  - (b) Ramp vs. Time
  - (c) Step vs. Time
  - (d) Triangular vs. Time
  - (e) Pulse vs. Time
  - (f) Sine vs. Time
  - (g) Cosine vs. Time
- (ii) Frequency response ;
  - (a) Gain vs. Frequency
  - (b) Magnitude vs. Frequency
  - (c) Phase vs. Frequency
  - (d) Group Delay vs. Frequency

The main menu of the 'mltwdf' MatLab program is illustrated by Fig.(B3.1).

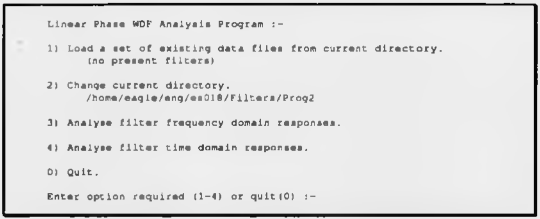

```
Linear Phase WDF Analysis Program :-

1) Load a set of existing data files from current directory.
     (no present filters)

2) Change current directory.
     /home/eagle/eng/es018/Filters/Prog2

3) Analyse filter frequency domain responses.

4) Analyse filter time domain responses.

0) Quit.

Enter option required (1-4) or quit(0) :-
```

Figure B3.1 Main menu structure of the 'mltwdf' program.

This software package does not generate any lattice WDF designs so all solutions must be load into the program from data files created by the 'wdf' program. The first two items of the main menu of Fig.(B3.1) are only concerned with loading data file(s) and moving around the system directories. Fig.(B3.2) shows the menu structure for changing directories, available through option '2' of the 'Linear Phase WDF Analysis Program' menu.

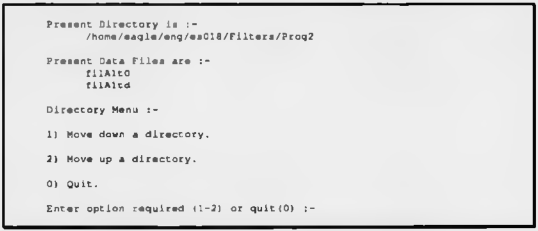

```
Present Directory is :-
     /home/eagle/eng/es018/Filters/Prog2

Present Data Files are :-
     filAlt0
     filAltd

Directory Menu :-

1) Move down a directory.

2) Move up a directory.

0) Quit.

Enter option required (1-2) or quit(0) :-
```

Figure B3.2 Change directory menu structure.

Changing directory until the file or files of interest are located, the next step is to load them into the program. Data files can either be loaded individually or a family of solutions that have the same filter order and frequency response. This last feature allows a direct comparison of large and finite wordlength coefficient solutions to the same problem.

Selecting option '1' from the 'Linear Phase WDF Analysis Program' displays the menu shown by Fig.(B3.3). This menu will list the data files available in that directory and prompt for the number of data files to be load into the program. Fig.(B3.3) illustrates the sequence for loading one data file. If more than one data file is loaded, the user is given the option of adding a label to each response that will be displayed in all frequency response plots.

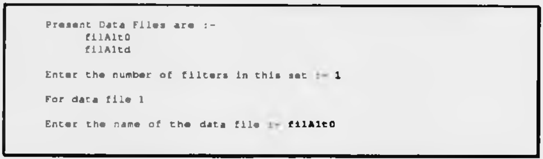

```
Present Data Files are :-
      filAlt0
      filAltd

Enter the number of filters in this set :- 1

For data file 1

Enter the name of the data file :- filAlt0
```

Figure B3.3 Menu for loading data file.

Having loaded a data file into the program the remaining two options of the main menu will become active, allowing the time or frequency responses of that particular lattice WDF to be determined. Frequency domain responses can be calculated through option '3' from the main program menu, Fig.(B3.4), while the time domain responses are available through option '4'.

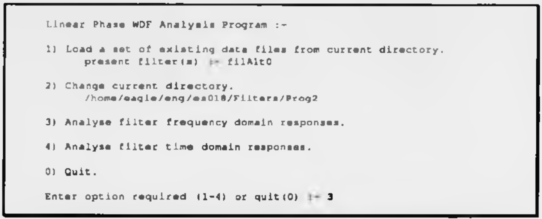

```
Linear Phase WDF Analysis Program :-

1) Load a set of existing data files from current directory.
     present filter(s) :- filAlt0

2) Change current directory.
     /home/eagle/eng/es018/Filters/Prog2

3) Analyse filter frequency domain responses.

4) Analyse filter time domain responses.

0) Quit.

Enter option required (1-4) or quit(0) :- 3
```

Figure B3.4 Main menu structure with loaded data file.

Selecting option '3' from the main program menu will move the user to the menu structure shown by Fig.(B3.5). The lattice responses available through this menu include the magnitude, gain, phase and group delay frequency responses, option '1', the gain, phase and group delay sensitivity responses, option '2' and the pole/zero positions, option '4'. The frequency and sensitivity responses can be calculated over an arbitrary frequency range set by option '7' and for an arbitrary number point specified with option '8'.

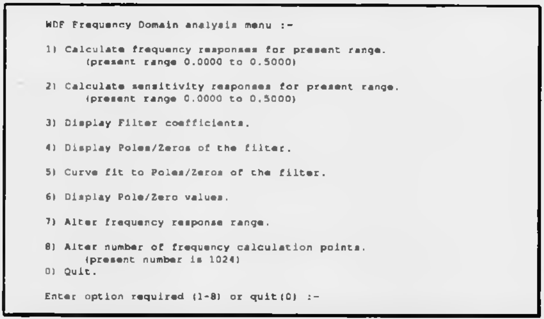

```
WDF Frequency Domain analysis menu :-

1) Calculate frequency responses for present range.
     (present range 0.0000 to 0.5000)

2) Calculate sensitivity responses for present range.
     (present range 0.0000 to 0.5000)

3) Display Filter coefficients.

4) Display Poles/Zeros of the filter.

5) Curve fit to Poles/Zeros of the filter.

6) Display Pole/Zero values.

7) Alter frequency response range.

8) Alter number of frequency calculation points.
     (present number is 1024)
0) Quit.

Enter option required (1-8) or quit(0) :-
```

Figure B3.5 Main frequency domain menu structure.

Selecting option '3' from the menu show by Fig.(B3.5) will display the filter coefficients of the data file or data files loaded. Filter coefficients for the design example considered in Appendix B1 are displayed in Fig.(B3.6). The final stage of this option is to provide the user with the option to generate a hard copy of these filter coefficients which can be to a file or a direct print.

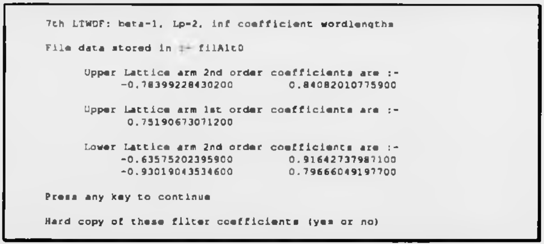

```
7th LTWDF: beta-1, Lp=2, inf coefficient wordlengths

File data stored in :- filAlt0

      Upper Lattice arm 2nd order coefficients are :-
           -0.78399228430200         0.84082010775900

      Upper Lattice arm 1st order coefficients are :-
            0.75190673071200

      Lower Lattice arm 2nd order coefficients are :-
           -0.63575202395900         0.91642737987100
           -0.93019043534600         0.79666049197700

Press any key to continue

Hard copy of these filter coefficients (yes or no)
```

Figure B3.6 Example of a filter coefficient display.

Selecting option '4' from the '`WDF Frequency Domain analysis menu`', Fig.(B3.5), will prompt the program to calculate and display the roots of the transfer function of the lattice WDF on a pole/zero plot. The program displays the roots of the transfer function in set, first the upper lattice branch poles, then the lower lattice branch poles and finally the zeros of the overall transfer function. Option '5' of the same menu, 'Curve fit to Poles/Zeros of the filter' displays the same information but allow the user to select roots from the pole/zero plots to apply to a curve fitting function. A pole/zero plot of the elliptic design example considered is shown in Fig.(B3.7)(a), while a plot/zero plot with a curve fitted to the upper and lower branch poles is shown in Fig.(B3.7)(b).

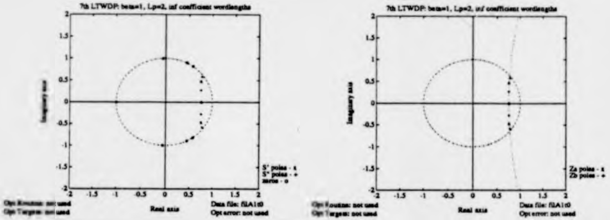

(a) (b)

Figure B3.7 Pole/zero plots showing (a) all poles and zeros of a lattice WDF structure and (b) a curve fitted to the poles of the structure.

The numerical values of the pole and zero locations can be displayed and printed though option '6' of the '`WDF Frequency Domain analysis menu`'. The values of the roots for the example considered are shown in Fig.(B3.8).

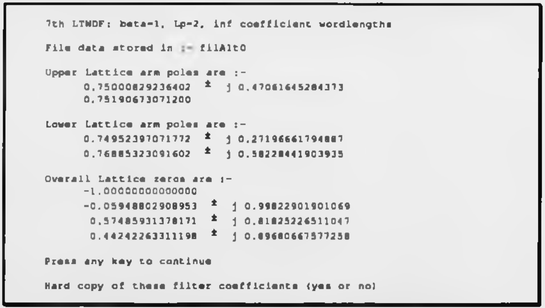

```
7th LTWDF: beta=1, Lp=2, inf coefficient wordlengths

File data stored in := filA1t0

Upper Lattice arm poles are :-
      0.75000829236402  ±  j 0.47061645284373
      0.75190673071200

Lower Lattice arm poles are :-
      0.74952397071772  ±  j 0.27196661794887
      0.76885323091602  ±  j 0.58228441903935

Overall Lattice zeros are :-
      -1.00000000000000
      -0.05948802908953  ±  j 0.99822901901069
       0.57485931378171  ±  j 0.81825226511047
       0.44242263311198  ±  j 0.89680667577258

Press any key to continue

Hard copy of these filter coefficients (yes or no)
```

Figure B3.8 Pole/zero values for design example.

Selecting option '1' from the '`WDF Frequency Domain analysis menu`' will cause the program to calculate the magnitude, gain, phase and group delay frequency responses at the number of points and over the frequency region specified. Having determined the responses, the program will display the menu of Fig.(B3.9).

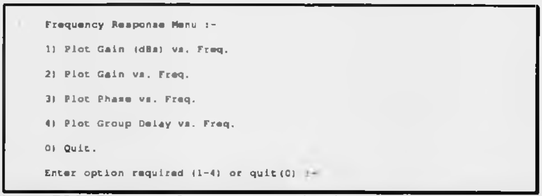

```
Frequency Response Menu :-

1) Plot Gain (dBs) vs. Freq.

2) Plot Gain vs. Freq.

3) Plot Phase vs. Freq.

4) Plot Group Delay vs. Freq.

0) Quit.

Enter option required (1-4) or quit(0) :-
```

Figure B3.9 Frequency Response Menu for frequency domain calculations.

Through options '1' - '4' the user can display the corresponding frequency responses to the screen. Again the option to generate a hard copy of the plot is offered to the user. Typical frequency response plots for the example loaded are shown in Fig.(B3.10).

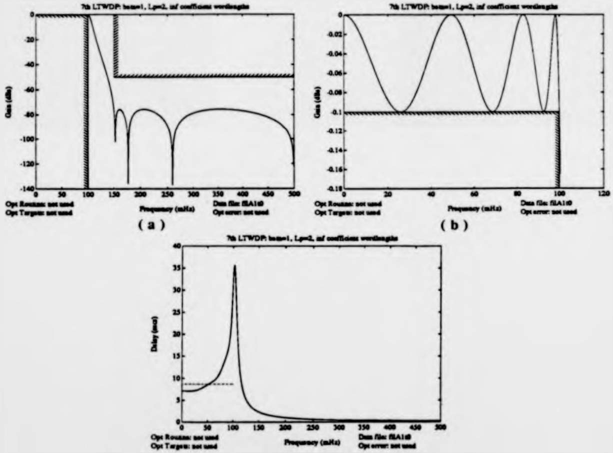

(a) (b)

(c)

Figure B3.10 Frequency responses showing (a) overall and (b) passband magnitude and (c) overall group delay responses for the example considered.

Selecting option '2' from the `WDF Frequency Domain analysis menu'` will cause the program to calculate the gain, phase and group delay coefficient sensitivity responses at the number of points and over the frequency region specified. When the sensitivity responses have been determined for each multiplier, the program will show the menu illustrated by Fig.(B3.11).

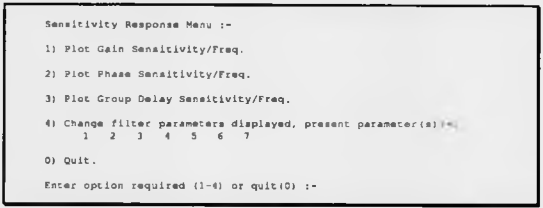

```
Sensitivity Response Menu :-

1) Plot Gain Sensitivity/Freq.

2) Plot Phase Sensitivity/Freq.

3) Plot Group Delay Sensitivity/Freq.

4) Change filter parameters displayed, present parameter(s) :-
      1    2    3    4    5    6    7

0) Quit.

Enter option required (1-4) or quit(0) :-
```

Figure B3.11 Coefficient Sensitivity Response Menu

Option '4' of the `'Sensitivity Response Menu'` allows the user to selectively display single or sets of coefficient sensitivity responses. In this way the responses for the coefficients of the upper or lower arm of the lattice WDF could be displayed together. This is illustrated in Fig.(B3.12), which shows the gain and group delay sensitivities for the upper lattice arm coefficient, Fig.(B3.12)(a-b), while those of the lower arm coefficients are shown by Fig.(B3.12)(c-d).

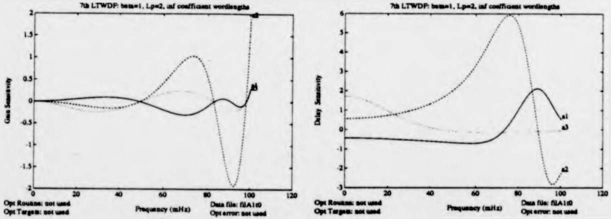

(a) (b)

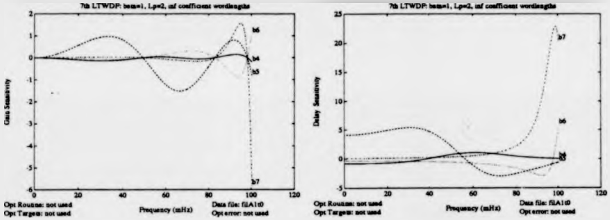

(c) (d)

Figure B3.12 Upper arm multiplier (a) gain and (b).group delay sensitivities and lower arm multiplier (c) gain and (d) group delay sensitivities

Returning to the main program menu, Fig.(B3.1), the user can determine the finite wordlength responses of the lattice WDF through the time domain menu. Selecting option '4' moves the user to the finite wordlength menu, illustrated by Fig.(B3.13).

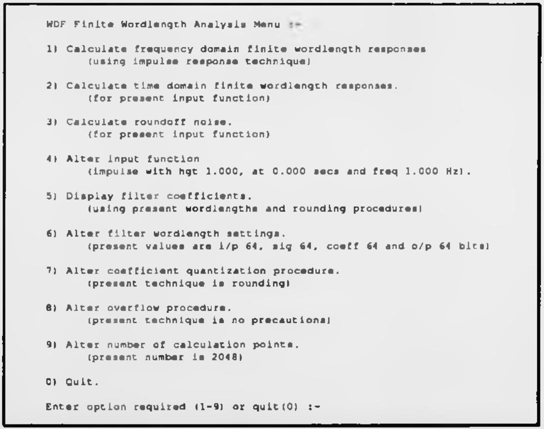

```
WDF Finite Wordlength Analysis Menu :-

1) Calculate frequency domain finite wordlength responses
     (using impulse response technique)

2) Calculate time domain finite wordlength responses.
     (for present input function)

3) Calculate roundoff noise.
     (for present input function)

4) Alter input function
     (impulse with hgt 1.000, at 0.000 secs and freq 1.000 Hz).

5) Display filter coefficients.
     (using present wordlengths and rounding procedures)

6) Alter filter wordlength settings.
     (present values are i/p 64, sig 64, coeff 64 and o/p 64 bits)

7) Alter coefficient quantization procedure.
     (present technique is rounding)

8) Alter overflow procedure.
     (present technique is no precautions)

9) Alter number of calculation points.
     (present number is 2048)

0) Quit.

Enter option required (1-9) or quit(0) :-
```

Figure B3.13 Menu structure for time domain analysis.

In line with the frequency domain analysis menu, Fig.(B3.4), this menu offers the user control over the settings under which the responses of the lattice is calculated. Each parameter is accessed through a menu detailing the options available. Option '4' of the menu shown by Fig.(B3.13) defines the input time function to be applied to the lattice WDF if the time domain responses was calculated. The menu structure of the available input functions is illustrated in Fig.(B3.14)

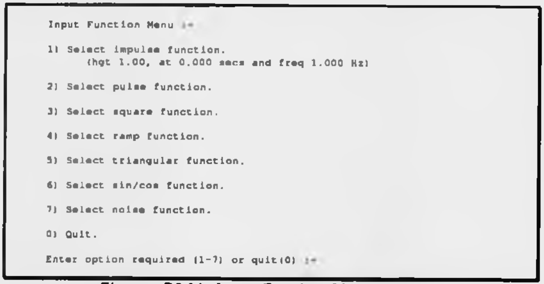

```
Input Function Menu :-

1) Select impulse function.
     (hgt 1.00, at 0.000 secs and freq 1.000 Hz)

2) Select pulse function.

3) Select square function.

4) Select ramp function.

5) Select triangular function.

6) Select sin/cos function.

7) Select noise function.

0) Quit.

Enter option required (1-7) or quit(0) :-
```

Figure B3.14 Input Function Menu structure.

For waveforms available through the '`Input function Menu`', the user is prompted for the peak amplitude, the time at which the peak amplitude is to occur and the number of the waveforms required for the input function.

The time domain calculations are performed using simulated finite wordlength effects. This means that the finite wordlength effects on particular elements of the lattice WDF can be considered in isolation to the rest of system. Control over the wordlengths of the various elements of the system is provided by the '`Filter Wordlength Menu`', available through option '6' from the main finite wordlength menu of Fig.(B3.13). The '`Filter Wordlength Menu`' structure is shown by Fig.(B3.15).

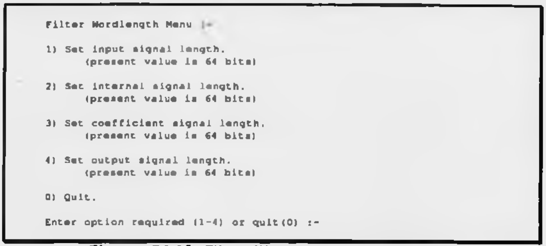

```
Filter Wordlength Menu :-

1) Set input signal length.
     (present value is 64 bits)

2) Set internal signal length.
     (present value is 64 bits)

3) Set coefficient signal length.
     (present value is 64 bits)

4) Set output signal length.
     (present value is 64 bits)

0) Quit.

Enter option required (1-4) or quit(0) :-
```

Figure B3.15 Filter Wordlength Menu structure.

Control over the type of quantization applied within the time domain calculations is provided through the menu illustrated by Fig.(B3.16), available with option '7' from the main finite wordlength menu.

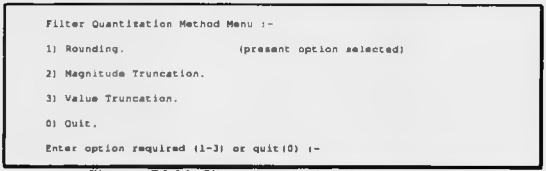

```
Filter Quantization Method Menu :-

1) Rounding.                (present option selected)

2) Magnitude Truncation.

3) Value Truncation.

0) Quit.

Enter option required (1-3) or quit(0) :-
```

Figure B3.16 Filter Quantization Menu structure.

Finally the types of overflow procedures available to the time domain calculations is determined by the '`Filter Overflow Procedure Menu`', Fig.(B3.17). This is option '8' within the main finite wordlength menu structure.

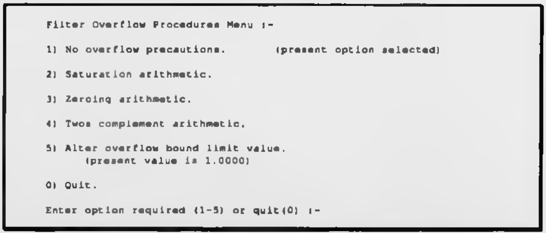

```
Filter Overflow Procedures Menu :-

1) No overflow precautions.       (present option selected)

2) Saturation arithmetic.

3) Zeroing arithmetic.

4) Twos complement arithmetic.

5) Alter overflow bound limit value.
     (present value is 1.0000)

0) Quit.

Enter option required (1-5) or quit(0) :-
```

Figure B3.17 Filter Overflow Procedure Menu structure.

With the various parameters defined, the time domain response can be calculated. These responses involved the time response for a given input function and the frequency responses determined through a FFT on the impulse response. If the frequency response option is selected then the program will calculate the values and display the menu shown by Fig.(B3.18).

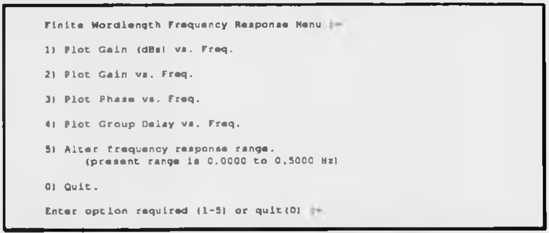

```
Finite Wordlength Frequency Response Menu :-

1) Plot Gain (dBs) vs. Freq.

2) Plot Gain vs. Freq.

3) Plot Phase vs. Freq.

4) Plot Group Delay vs. Freq.

5) Alter frequency response range.
      (present range is 0.0000 to 0.5000 Hz)

0) Quit.

Enter option required (1-5) or quit(0) :-
```

Figure B3.18 Finite Wordlength Frequency Response Menu.

Using this option the frequency responses calculated from analytical equation in the frequency domain can be directly compared to those from the time model of the lattice WDF, if the filter wordlengths are all set to 'infinite' precision. Frequency responses determined through the time domain and a FFT for the design example considered are shown in Fig.(B3.19). These responses show a high correlation to those generated in the frequency domain and shown by Fig.(B3.10).

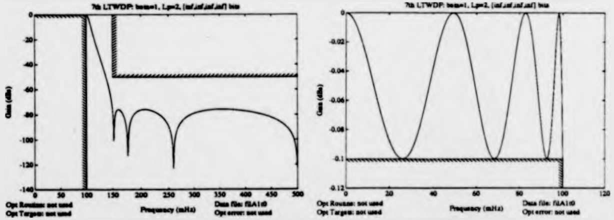

(a) (b)

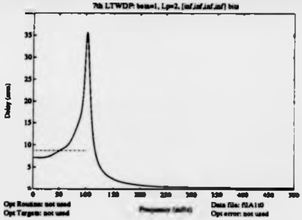

(c)

Figure B3.19 Frequency responses calculated through the time domain showing (a) overall and (b) passband magnitude and (c) overall group delay responses for the example considered.

Finally option '2' of the '`WDF Finite Wordlength Analysis Menu`' calculates the time domain response for an arbitrary input signal. The input signal, selected through the menu shown by Fig.(B3.14), is applied to the model of the lattice using the current quantization, overflow and filter wordlength. When the calculations are complete the program enters the menu shown by Fig.(B3.20)

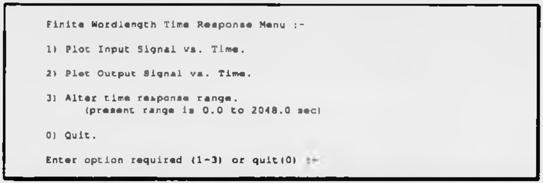

```
Finite Wordlength Time Response Menu :-

1) Plot Input Signal vs. Time.

2) Plot Output Signal vs. Time.

3) Alter time response range.
     (present range is 0.0 to 2048.0 sec)

0) Quit.

Enter option required (1-3) or quit(0) :-
```

Figure B3.20 Time Response Menu structure.

Selecting options '2' and '3', the output waveform can be displayed over any period. The output of the lattice WDF using the coefficients from the design example considered to the unit impulse, are shown in Fig.(B3.21).

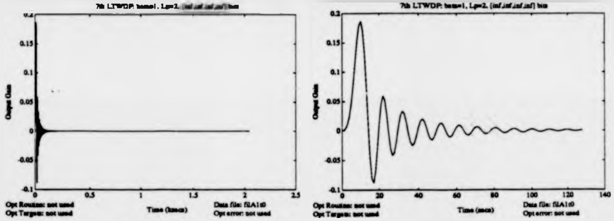

(a) (b)

Figure B3.21 Unit impulse response of lattice WDF example showing (a) overall waveform and (b) initial part of response.

Appendix C

Lattice WDF APS Models

(Frequency Domain)

This Appendix details the design equations for the various APS's required in the construction and analysis of the highpass and single and dual bandpass and bandstop lattice WDF's. The design equations are given in terms of the parameters required by the overall lattice WDF equations outlined in Chapter 4. The APS's considered are :-

(C1)..............1st and 2nd order highpass APS equations.
(C2)..............2nd and 4th order single bandpass APS equations.
(C3)..............2nd and 4th order single bandstop APS equations.
(C4)..............4th and 8th order dual bandpass APS equations.
(C5)..............4th and 8th order dual bandstop APS equations.

C1 Highpass APS Models

C1.1 1^{st} order Highpass APS

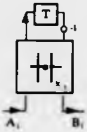

Limits :-

$-1 < x_1 < 1$

$zt_1 = -x_1 - z^{-1}$

$zt_2 = 1 + x_1 z^{-1}$

Overall transfer function :-

$$H(z) = \frac{B_i}{A_i} = \frac{zt_1}{zt_2}$$

Group delay parameter :-

$$\frac{1}{H(z)} \cdot \frac{dH(z)}{d\omega} = j z^{-1} \frac{\left(1 - x_1^{2}\right)}{zt_1\ zt_2}$$

Gain/Phase coefficient sensitivity parameters :-

$$\frac{1}{H(z)} \cdot \frac{dH(z)}{dx_1} = \frac{\left(z^{-2} - 1\right)}{zt_1\ zt_2}$$

Group delay coefficient sensitivity parameters :-

$$\frac{d\left(\frac{1}{H(z)} \cdot \frac{dH(z)}{d\omega}\right)}{dx_1} = -j z^{-1} \frac{(1 + z^{-2})(1 + x_1^{2})}{\left(zt_1\ zt_2\right)^{2}}$$

C1.2 2nd order Highpass APS

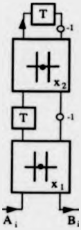

Limits :-

$-1 < x_1 < 1$

$-1 < x_2 < 0$

$$zt_1 = -x_1 + (1 - x_1)\, x_2\, z^{-1} + z^{-2}$$

$$zt_2 = 1 + (1 - x_1)\, x_2\, z^{-1} - x_1\, z^{-2}$$

Overall transfer function :-

$$H(z) = \frac{B_i}{A_i} = \frac{zt_1}{zt_2}$$

Group delay parameter :-

$$\frac{1}{H(z)} \cdot \frac{dH(z)}{d\omega} = j\, z^{-1} \frac{\left(x_1^2 - 1\right)\left(x_2 + 2z^{-1} + x_2 z^{-2}\right)}{zt_1\ zt_2}$$

Gain/Phase coefficient sensitivity parameters :-

$$\frac{1}{H(z)} \cdot \frac{dH(z)}{dx_1} = \frac{\left(z^{-2} - 1\right)\left(1 + 2x_2 z^{-1} + z^{-2}\right)}{zt_1\ zt_2}$$

$$\frac{1}{H(z)} \cdot \frac{dH(z)}{dx_2} = z^{-1} \frac{\left(z^{-2} - 1\right)\left(x_1^2 - 1\right)}{zt_1\ zt_2}$$

Group delay coefficient sensitivity parameters :-

$$\frac{d\left(\frac{1}{H(z)} \cdot \frac{dH(z)}{d\omega}\right)}{dx_1} = -j\, z^{-1} \left(x_2 + 2z^{-1} + x_2 z^{-2}\right)\left(zt_1\ zt_2\right)^{-2}$$

$$\left(2z^{-2}(x_2^2(1-x_1)^2 - 2x_1) + 2x_2 z^{-1}(1+z^{-2})(1-x_1)^2 + (1+x_1^2)(1+z^{-4})\right)$$

$$\frac{d\left(\frac{1}{H(z)} \cdot \frac{dH(z)}{d\omega}\right)}{dx_2} = -j\, z^{-1} \left(x_2^2 - 1\right)\left(zt_1\ zt_2\right)^{-2}$$

$$\left(z^{-2}(1+z^{-2})(x_3^2(1-x_2)^2 + x_2(x_2-3) + 1) + x_2(1+z^{-6})\right)$$

C 2 Single Bandpass APS Models

C2.1 2nd order Single Bandpass APS

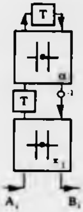

Limits :-

$-1 < x_1 < 1$

$-1 < \alpha < 1$

$$zt_1 = -(x_1 - \alpha (1 + x_1) z^{-1} + z^{-2})$$

$$zt_2 = 1 - \alpha (1 + x_1) z^{-1} + x_1 z^{-2}$$

Overall transfer function :-

$$H(z) = \frac{B_i}{A_i} = \frac{zt_1}{zt_2}$$

Group delay parameter :-

$$\frac{1}{H(z)} \cdot \frac{dH(z)}{d\omega} = j z^{-1} \frac{\left(x_1^2 - 1\right)\left(\alpha - 2 z^{-1} + \alpha z^{-2}\right)}{zt_1 \; zt_2}$$

Gain/Phase coefficient sensitivity parameters :-

$$\frac{1}{H(z)} \cdot \frac{dH(z)}{dx_1} = \frac{\left(z^{-2} - 1\right)\left(1 - 2 \alpha z^{-1} + z^{-2}\right)}{zt_1 \; zt_2}$$

$$\frac{1}{H(z)} \cdot \frac{dH(z)}{d\alpha} = z^{-1} \frac{\left(z^{-2} - 1\right)\left(x_1^2 - 1\right)}{zt_1 \; zt_2}$$

Group delay coefficient sensitivity parameters :-

$$\frac{d\left(\frac{1}{H(z)} \cdot \frac{dH(z)}{d\omega}\right)}{dx_1} = -j z^{-1} \Big((1 + z^{-4})(1 + x_1^2) - 2 \alpha z^{-1} (1 + z^{-2})(1 + x_1)^2 + 2 z^{-2} \big(2 x_1(1 + \alpha^2) + \alpha^2(1 + x_1^2)\big)\Big) \left(\alpha - 2 z^{-1} + \alpha z^{-2}\right)\left(zt_1 \; zt_2\right)^{-2}$$

$$\frac{d\left(\frac{1}{H(z)} \cdot \frac{dH(z)}{d\omega}\right)}{d\alpha} = -j z^{-1}\left(x_1^2 - 1\right)\left(zt_1 \; zt_2\right)^{-2}\Big(x_1(1 + z^{-6}) + 4 \alpha z^{-3}(1 + x_1)^2 - z^{-2}(1 + z^{-2})\big((1 + x_1)(1 + \alpha^2) + x_1(3 + 2\alpha^2)\big)\Big)$$

C2.2 4th order Single Bandpass APS

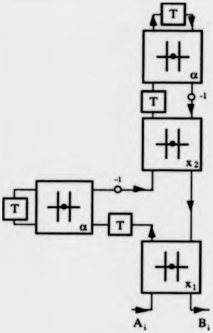

Limits :-

$-1 < x_1 < 0$

$-1 < x_2 < 1$

$-1 < \alpha < 1$

$n_1 = -\alpha\ (2x_1 + x_2(x_1 - 1))\ ,\ n_2 = (x_1 - 1)(x_2 + \alpha^2(1 + x_2))\ ,\ n_3 = \alpha\ (2 - x_2(x_1 - 1))$

$zt_1 = x_1 + n_1 z^{-1} + n_2 z^{-2} + n_3 z^{-3} - z^{-4}\ ,\ zt_2 = -1 + n_3 z^{-1} + n_2 z^{-2} + n_1 z^{-3} + x_1 z^{-4}$

Overall transfer function :-

$$H(z) = \frac{B_i}{A_i} = \frac{zt_1}{zt_2}$$

Group delay parameter :-

$$\frac{1}{H(z)} \cdot \frac{dH(z)}{d\omega} = -j z^{-1}\left(x_1^2 - 1\right)\left(\alpha - 2z^{-1} + \alpha z^{-2}\right) \\ \left((1 + z^{-4})x_2 - 2\alpha z^{-1}(1 + z^{-2})(1 + x_2) \\ + 2z^{-2}(1 + \alpha^2(1 + x_2))\right)\left(zt_1\ zt_2\right)^{-1}$$

Gain/Phase coefficient sensitivity parameters :-

$$\frac{1}{H(z)} \cdot \frac{dH(z)}{dx_1} = \left(z^{-2} - 1\right)\left(1 - 2\alpha z^{-1} + z^{-2}\right) \\ \left((1 + z^{-4}) - 2\alpha z^{-1}(1 + z^{-2})(1 + x_2) \\ + 2z^{-2}(x_2 + \alpha^2(1 + x_2))\right)\left(zt_1\ zt_2\right)^{-1}$$

$$\frac{1}{H(z)} \cdot \frac{dH(z)}{dx_2} = z^{-1}\left(z^{-2} - 1\right)\left(1 - 2\alpha z^{-1} + z^{-2}\right) \\ \left(z^{-1} - \alpha\right)\left(1 - \alpha z^{-1}\right)\left(x_1^2 - 1\right)\left(zt_1\ zt_2\right)^{-1}$$

$$\begin{aligned}\frac{1}{H(z)}\cdot\frac{dH(z)}{d\alpha} = \; & -z^{-1}\left(z^{-2}-1\right)\left(x_1{}^2-1\right)\\ & \Big((1+z^{-4})x_2 - 2\alpha z^{-1}(1+z^{-2})(1+x_2)\\ & \quad + 2z^{-2}(1+\alpha^2(1+x_2))\Big)\left(zt_1\; zt_2\right)^{-1}\end{aligned}$$

Group delay coefficient sensitivity parameters :-

$$\frac{d\left(\frac{1}{H(z)}\cdot\frac{dH(z)}{d\omega}\right)}{dx_1} = \; j\,z^{-1}\left(\alpha - 2z^{-1} + \alpha z^{-2}\right)\left(zt_1\; zt_2\right)^{-2}$$

$$\begin{aligned}&\Big((1+z^{-4})x_2 - 2\alpha z^{-1}(1+z^{-2})(1+x_2) + 2z^{-2}(1+\alpha^2(1+x_2))\Big)\\ &\Big((1+z^{-8})\left(1+x_1{}^2\right) - 2\alpha z^{-1}(1+z^{-6})\left(2(1+x_1{}^2) + x_2(x_1-1)^2\right)\\ &\quad + 2z^{-2}(1+z^{-4})\Big(x_2(x_1-1)^2 + \alpha^2\left(3(1+x_1{}^2) - 2x_1 + x_2(3+x_2)(x_1-1)^2\right)\Big)\\ &\quad - 2\alpha z^{-3}(1+z^{-2})\left(x_2(3+2x_2)(x_1-1)^2 - 4x_1 + 2\alpha^2(x_1-1)^2(x_2+1)^2\right)\\ &\quad + 2z^{-4}\Big(x_2{}^2(x_1-1)^2 - 2x_1 + 2\alpha^2\left(x_2(3+2x_2)(x_1-1)^2 - 4x_1\right)\\ &\qquad\qquad + \alpha^4(x_1-1)^2(x_2+1)^2\Big)\quad\Big)\end{aligned}$$

$$\frac{d\left(\frac{1}{H(z)}\cdot\frac{dH(z)}{d\omega}\right)}{dx_2} = j\,z^{-1}\left(x_1{}^2-1\right)\left(\alpha - 2z^{-1} + \alpha z^{-2}\right)\left(zt_1\; zt_2\right)^{-2}$$

$$\begin{aligned}&\Big((1+z^{-12})x_1 - 6\alpha z^{-1}(1+z^{-10})x_1\\ &\quad + \alpha^2 z^{-2}(1+z^{-8})\left(1 + x_1(12+x_1) + x_2{}^2(x_1-1)^2\right)\\ &\quad - 2\alpha z^{-3}(1+z^{-6})\Big(1 - x_1(3-x_1) + x_2{}^2(x_1-1)^2\\ &\qquad + 2\alpha^2\left((1+x_1)^2 + x_2(x_2+1)(x_1-1)^2\right)\Big)\\ &\quad + z^{-4}(1+z^{-4})\Big(1 - x_1(3-x_1) + x_2{}^2(x_1-1)^2\\ &\qquad + 4\alpha^2\left(2(1-x_1(3-x_1)) + x_2(3+2x_2)(x_1-1)^2\right)\\ &\qquad + \alpha^4\left(7 - x_1(6-7x_1) + x_2(12+7x_2)(x_1-1)^2\right)\Big)\\ &\quad - 2\alpha z^{-5}(1+z^{-2})\Big(2(1-x_1(3-x_1)) + x_2(3+2x_2)(x_1-1)^2\\ &\qquad + 2\alpha^2\left(4(1-x_1(3-x_1)) + x_2(9+4x_2)(x_1-1)^2\right)\\ &\qquad + 3\alpha^4(x_1-1)^2(x_2+1)^2\Big)\\ &\quad + 2z^{-6}\Big(2x_2(x_1-1)^2\\ &\qquad + 6\alpha^2\left(1 - x_1(3-x_1) + x_2(3+x_2)(x_1-1)^2\right)\\ &\qquad + 2\alpha^4\left(4(1-x_1(3-x_1)) + x_2(9+4x_2)(x_1-1)^2\right)\\ &\qquad + \alpha^6(x_1-1)^2(x_2+1)^2\Big)\Big)\end{aligned}$$

$$
\frac{d\left(\frac{1}{H(z)}\cdot\frac{dH(z)}{d\omega}\right)}{d\alpha} = j\,z^{-1}\Big(x_1^2 - 1\Big)\Big(zt_1\; zt_2\Big)^{-2}
$$

$$
\begin{aligned}
&\Big((1 + z^{-14})x_1x_2 - 4\alpha z^{-1}(1 + z^{-12})x_1(1 + x_2)\\
&\quad + z^{-2}(1 + z^{-10})\Big(3x_1(2 - x_2) + x_2^2(x_1 - 1)^2\\
&\qquad + \alpha^2\Big(14x_1 - x_2(1 - x_1(12 - x_1)) + x_2^2(1 + x_2)(x_1 - 1)^2\Big)\Big)\\
&\quad - 4\alpha z^{-3}(1 + z^{-8})\Big(4x_1 + x_2^2(2 + x_2)(x_1 - 1)^2\\
&\qquad + \alpha^2(1 + x_2)\Big(4x_1 + x_2^2(x_1 - 1)^2\Big)\Big)\\
&\quad + z^{-4}(1 + z^{-6})\Big(-10x_1 + x_2(1 + x_1(9 + x_1)) + x_2^2(1 + 3x_2)(x_1 - 1)^2\\
&\qquad + \alpha^2\Big(2(1+x_1(1+x_1)) + 3x_2(5-x_1(4-5x_1)) + x_2^2(27+17x_2)(x_1-1)^2\Big)\\
&\qquad + \alpha^4\Big(2(1+x_1)^2 + x_2(7 - x_1(6-7x_1)) + 5x_2^2(2+x_2)(x_1-1)^2\Big)\Big)\\
&\quad - 4\alpha z^{-5}(1 + z^{-4})\Big(1-x_1(11-x_1) + x_2(5-x_1(3-5x_1)) + 3x_2^2(1+x_2)(x_1-1)^2\\
&\qquad + 2\alpha^2\Big(2(x_1 - 1)^2 + 7x_2(x_1 - 1)^2 + x_2^2(8 + 3x_2)(x_1-1)^2\Big)\\
&\qquad + \alpha^4(x_1 - 1)^2(x_2 + 1)^3\Big)\\
&\quad + 2\alpha z^{-6}(1 + z^{-2})\Big(2(1+x_1^2) + x_2(5-x_1(19-5x_1)) + x_2^2(4-x_2)(x_1-1)^2\\
&\qquad + 2\alpha^2\Big(2(7-x_1(19-7x_1)) + 2x_2(19-x_1(45-19x_1)) + x_2^2(31+6x_2)(x_1-1)^2\Big)\\
&\qquad + \alpha^4\Big(4(7-x_1(16-7x_1)) + x_2(83-x_1(174-83x_1)) + 5x_2^2(16+5x_2)(x_1-1)^2\Big)\\
&\qquad + 2\alpha^6(x_1 - 1)^2(x_2 + 1)^3\Big)\\
&\quad - 8\alpha z^{-7}\Big(2(1 + x_1^2) + 4x_2(1 - x_1(4 - x_1)) + x_2^2(4-x_2)(x_1-1)^2\\
&\qquad + \alpha^2\Big(2(3 - x_1(8-3x_1)) + 4x_2(4 - x_1(9-4x_1)) + x_2^2(13+3x_2)(x_1-1)^2\Big)\\
&\qquad + 2\alpha^4(x_1-1)^2(x_2+1)^3\Big)\qquad\Big)
\end{aligned}
$$

C 3 Single Bandstop APS Models

C3.1 2^{nd} order Single Bandstop APS

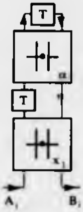

Limits :-

$-1 < x_1 < 1$

$-1 < \alpha < 1$

$$zt_1 = x_1 + \alpha\,(1 - x_1)\,z^{-1} - z^{-2}\ ,\ \ zt_2 = -1 + \alpha\,(1 - x_1)\,z^{-1} + x_1\,z^{-2}$$

Overall transfer function :-

$$H(z) = \frac{B_i}{A_i} = \frac{zt_1}{zt_2}$$

Group delay parameter :-

$$\frac{1}{H(z)} \cdot \frac{dH(z)}{d\omega} = -j\,z^{-1}\,\frac{\left(x_1^{\,2} - 1\right)\left(\alpha - 2\,z^{-1} + \alpha\,z^{-2}\right)}{zt_1\;zt_2}$$

Gain/Phase coefficient sensitivity parameters :-

$$\frac{1}{H(z)} \cdot \frac{dH(z)}{dx_1} = \frac{\left(z^{-2} - 1\right)\left(1 - 2\,\alpha\,z^{-1} + z^{-2}\right)}{zt_1\;zt_2}$$

$$\frac{1}{H(z)} \cdot \frac{dH(z)}{d\alpha} = -z^{-1}\,\frac{\left(z^{-2} - 1\right)\left(x_1^{\,2} - 1\right)}{zt_1\;zt_2}$$

Group delay coefficient sensitivity parameters :-

$$\begin{aligned}\frac{d\left(\frac{1}{H(z)} \cdot \frac{dH(z)}{d\omega}\right)}{dx_1} = j\,z^{-1}\,\Big(&(1 + z^{-4})(1 + x_1^{\,2}) - 2\,\alpha\,z^{-1}\,(1 + z^{-2})(1 - x_1)^2 \\ &+ 2\,z^{-2}\left(\alpha^2(1 - x_1)^2 - 2\,x_1\right)\Big) \\ &\left(\alpha - 2\,z^{-1} + \alpha\,z^{-2}\right)\left(zt_1\;zt_2\right)^{-2}\end{aligned}$$

$$\begin{aligned}\frac{d\left(\frac{1}{H(z)} \cdot \frac{dH(z)}{d\omega}\right)}{d\alpha} = j\,z^{-1}\left(x_1^{\,2} - 1\right)\left(zt_1\;zt_2\right)^{-2}\Big(&x_1(1 + z^{-6}) - 4\,\alpha\,z^{-3}(1 - x_1)^2 \\ &+ z^{-2}(1 + z^{-2})\left(1 + x_1(x_1 - 3) + \alpha^2(1 - x_1)^2\right)\Big)\end{aligned}$$

C3.2 4th order Single Bandstop APS

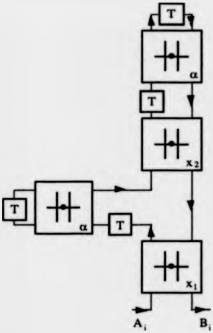

Limits :-

$-1 < x_1 < 0$

$-1 < x_2 < 1$

$-1 < \alpha < 1$

$$n_1 = \alpha\,(x_2(x_1 - 1) - 2x_1)\ ,\ n_2 = -(x_1 - 1)(x_2 + \alpha^2(x_2 - 1))\ ,\ n_3 = \alpha\,(2 + x_2(x_1 - 1))$$

$$zt_1 = x_1 + n_1 z^{-1} + n_2 z^{-2} + n_3 z^{-3} - z^{-4}\ ,\ zt_2 = -1 + n_3 z^{-1} + n_2 z^{-2} + n_1 z^{-3} + x_1 z^{-4}$$

Overall transfer function :-

$$H(z) = \frac{B_1}{A_i} = \frac{zt_1}{zt_2}$$

Group delay parameter :-

$$\frac{1}{H(z)} \cdot \frac{dH(z)}{d\omega} = j z^{-1} \left(x_1^2 - 1\right)\left(\alpha - 2z^{-1} + \alpha z^{-2}\right) \left(\left(1 + z^{-4}\right)x_2 + 2\alpha z^{-1}\left(1 + z^{-2}\right)\left(1 - x_2\right) - 2z^{-2}\left(1 - \alpha^2(x_2 - 1)\right)\right)\left(zt_1\, zt_2\right)^{-1}$$

Gain/Phase coefficient sensitivity parameters :-

$$\frac{1}{H(z)} \cdot \frac{dH(z)}{dx_1} = \left(z^{-2} - 1\right)\left(1 - 2\alpha z^{-1} + z^{-2}\right) \left(\left(1 + z^{-4}\right) + 2\alpha z^{-1}\left(1 + z^{-2}\right) - 2z^{-2}\left(x_2 + \alpha^2(x_2 - 1)\right)\right)\left(zt_1\, zt_2\right)^{-1}$$

$$\frac{1}{H(z)} \cdot \frac{dH(z)}{dx_2} = z^{-1}\left(z^{-2} - 1\right)\left(1 - 2\alpha z^{-1} + z^{-2}\right) \left(z^{-1} - \alpha\right)\left(\alpha z^{-1} - 1\right)\left(x_1^2 - 1\right)\left(zt_1\, zt_2\right)^{-1}$$

$$\begin{aligned}\frac{1}{H(z)} \cdot \frac{dH(z)}{d\alpha} = \; & z^{-1}\left(z^{-2} - 1\right)\left(x_1{}^2 - 1\right) \\ & \Big((1 + z^{-4})x_2 - 2\alpha z^{-1}(1 + z^{-2})(x_2 - 1) \\ & - 2z^{-2}(1 - \alpha^2(x_2 - 1))\Big)\left(zt_1\, zt_2\right)^{-1}\end{aligned}$$

Group delay coefficient sensitivity parameters :-

$$\frac{d\left(\frac{1}{H(z)} \cdot \frac{dH(z)}{d\omega}\right)}{dx_1} = -j\, z^{-1}\left(\alpha - 2z^{-1} + \alpha z^{-2}\right)\left(zt_1\, zt_2\right)^{-2}$$

$$\begin{aligned}& \Big((1 + z^{-4})x_2 - 2\alpha z^{-1}(1 + z^{-2})(x_2 - 1) - 2z^{-2}(1 - \alpha^2(x_2 - 1))\Big) \\ & \Big((1 + z^{-8})\left(1 + x_1{}^2\right) \\ & \quad - 2\alpha z^{-1}(1 + z^{-6})\left(2(1 + x_1{}^2) - x_2(x_1 - 1)^2\right) \\ & \quad - 2z^{-2}(1 + z^{-4})\Big(x_2(x_1 - 1)^2 - \alpha^2\left(3 - x_1(2 - 3x_1) - x_2(3 - x_2)(x_1 - 1)^2\right)\Big) \\ & \quad + 2\alpha z^{-3}(1 + z^{-2})\left(4x_1 + x_2(3 - 2x_2)(x_1 - 1)^2 - 2\alpha^2(x_1 - 1)^2(x_2 - 1)^2\right) \\ & \quad + 2z^{-4}\Big(x_2{}^2(x_1 - 1)^2 - 2x_1 - 2\alpha^2\left(x_2(3 - 2x_2)(x_1 - 1)^2 + 4x_1\right) \\ & \qquad + \alpha^4(x_1 - 1)^2(x_2 - 1)^2\Big) \quad \Big)\end{aligned}$$

$$\frac{d\left(\frac{1}{H(z)} \cdot \frac{dH(z)}{d\omega}\right)}{dx_2} = j\, z^{-1}\left(x_1{}^2 - 1\right)\left(\alpha - 2z^{-1} + \alpha z^{-2}\right)\left(zt_1\, zt_2\right)^{-2}$$

$$\begin{aligned}& \Big((1 + z^{-12})x_1 - 6\alpha z^{-1}(1 + z^{-10})x_1 \\ & \quad + \alpha^2 z^{-2}(1 + z^{-8})\left(1 + x_1(12 + x_1) + x_2{}^2(x_1 - 1)^2\right) \\ & \quad - 2\alpha z^{-3}(1 + z^{-6})\Big(1 - x_1(3 - x_1) + x_2{}^2(x_1 - 1)^2 \\ & \qquad + 2\alpha^2\left((1 + x_1)^2 + x_2(x_2 - 1)(x_1 - 1)^2\right)\Big) \\ & \quad + z^{-4}(1 + z^{-4})\Big(1 - x_1(3 - x_1) + x_2{}^2(x_1 - 1)^2 \\ & \qquad + 4\alpha^2\left(2(1 - x_1(3 - x_1)) - x_2(3 - 2x_2)(x_1 - 1)^2\right) \\ & \qquad + \alpha^4\left(7 - x_1(6 - 7x_1) - x_2(12 - 7x_2)(x_1 - 1)^2\right)\Big) \\ & \quad - 2\alpha z^{-5}(1 + z^{-2})\Big(2(1 - x_1(3 - x_1)) - x_2(3 - 2x_2)(x_1 - 1)^2 \\ & \qquad + 2\alpha^2\left(4(1 - x_1(3 - x_1)) - x_2(9 - 4x_2)(x_1 - 1)^2\right) \\ & \qquad + 3\alpha^4(x_1 - 1)^2(x_2 - 1)^2\Big) \\ & \quad + 2z^{-6}\Big(-2x_2(x_1 - 1)^2 \\ & \qquad + 6\alpha^2\left(1 - x_1(3 - x_1) - x_2(3 - x_2)(x_1 - 1)^2\right) \\ & \qquad + 2\alpha^4\left(4(1 - x_1(3 - x_1)) - x_2(9 - 4x_2)(x_1 - 1)^2\right) \\ & \qquad + \alpha^6(x_1 - 1)^2(x_2 - 1)^2\Big) \quad \Big)\end{aligned}$$

$$\frac{d\left(\frac{1}{H(z)}\cdot\frac{dH(z)}{d\omega}\right)}{d\alpha} = j\,z^{-1}\Big(x_1{}^2 - 1\Big)\Big(zt_1\ zt_2\Big)^{-2}$$

$$\begin{aligned}
&\Big((1 + z^{-14})x_1x_2 - 4\alpha z^{-1}(1 + z^{-12})x_1(x_2 - 1) \\
&\quad - z^{-2}(1 + z^{-10})\Big(3x_1(2 + x_2) + x_2{}^2(x_1 - 1)^2 \\
&\qquad + \alpha^2\Big(14x_1 + x_2(1 - x_1(12 - x_1)) - x_2{}^2(x_2 - 1)(x_1 - 1)^2\Big)\ \Big) \\
&\quad + 4\alpha z^{-3}(1 + z^{-8})\Big(4x_1 + x_2{}^2(2 - x_2)(x_1 - 1)^2 \\
&\qquad - \alpha^2(x_2 - 1)\Big(4x_1 + x_2{}^2(x_1 - 1)^2\Big)\ \Big) \\
&\quad + z^{-4}(1 + z^{-6})\Big(10x_1 + x_2(1 + x_1(9 + x_1)) - x_2{}^2(1 - 3x_2)(x_1 - 1)^2 \\
&\qquad - \alpha^2\Big(2(1+x_1(1+x_1)) - 3x_2(5-x_1(4-5x_1)) + x_2{}^2(27-17x_2)(x_1-1)^2\Big) \\
&\qquad + \alpha^4(x_2 - 1)\Big(2(1+x_1)^2 + 5x_2(x_2 - 1)(x_1-1)^2\Big)\ \Big) \\
&\quad - 4\alpha z^{-5}(1 + z^{-4})\Big(1-x_1(11-x_1) - x_2(5-x_1(3-5x_1)) - 3x_2{}^2(x_2 - 1)(x_1-1)^2 \\
&\qquad + 2\alpha^2(x_2 - 1)^2(2 - 3x_2)(x_1 - 1)^2) \\
&\qquad - \alpha^4(x_1 - 1)^2(x_2 - 1)^3\ \Big) \\
&\quad + z^{-6}(1 + z^{-2})\Big(-2(1+x_1{}^2) + x_2(5-x_1(19-5x_1)) - x_2{}^2(4+x_2)(x_1-1)^2 \\
&\qquad + 2\alpha^2\Big(-2(7-x_1(19-7x_1)) + 2x_2(19-x_1(45-19x_1)) - x_2{}^2(31-6x_2)(x_1-1)^2\Big) \\
&\qquad + \alpha^4(x_2 - 1)\Big(4(7 - x_1(16 - 7x_1)) - 5x_2(11 - 5x_2)(x_1 - 1)^2\Big) \\
&\qquad + 2\alpha^6(x_1 - 1)^2(x_2 - 1)^3\ \Big) \\
&\quad + 8\alpha z^{-7}\Big(2(1 + x_1{}^2) - 4x_2(1 - x_1(4 - x_1)) + x_2{}^2(4 - x_2)(x_1 - 1)^2 \\
&\qquad - \alpha^2(x_2 - 1)\Big(2(3 - x_1(8 - 3x_1)) - x_2(10 - 3x_2)(x_1 - 1)^2\Big) \\
&\qquad - 2\alpha^4(x_1 - 1)^2(x_2 - 1)^2\Big)\quad \Big)
\end{aligned}$$

C4 Dual Bandpass APS Models

C4.1 4th order Dual Bandpass APS

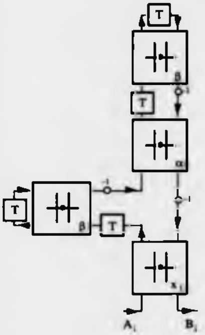

Limits :-

$-1 < x_1 < 1$

$-1 < \alpha < 1$

$-1 < \beta < 1$

$n_1 = -\beta\,(\alpha + x_1(2 + \alpha))$, $n_2 = -(1 + x_1)(\alpha + \beta^2(1 + \alpha))$, $n_3 = \beta\,(2 + \alpha(1 + x_1))$

$zt_1 = -x_1 + n_1 z^{-1} + n_2 z^{-2} + n_3 z^{-3} - z^{-4}$, $zt_2 = 1 - n_3 z^{-1} - n_2 z^{-2} - n_1 z^{-3} + x_1 z^{-4}$

Overall transfer function :-

$$H(z) = \frac{B_i}{A_i} = \frac{zt_1}{zt_2}$$

Group delay parameter :-

$$\frac{1}{H(z)} \cdot \frac{dH(z)}{d\omega} = j\,z^{-1}\left(x_1^2 - 1\right)\left(\beta - 2z^{-1} + \beta z^{-2}\right) \left(((1 + z^{-4})\alpha - 2\beta z^{-1}(1 + z^{-2})(1 + \alpha) + 2z^{-2}(1 + \beta^2(1 + \alpha))\right)\left(zt_1\, zt_2\right)^{-1}$$

Gain/Phase coefficient sensitivity parameters :-

$$\frac{1}{H(z)} \cdot \frac{dH(z)}{dx_1} = \left(z^{-2} - 1\right)\left(1 - 2\beta z^{-1} + z^{-2}\right) \left(((1 + z^{-4}) - 2\beta z^{-1}(1 + z^{-2})(1 + \alpha) + 2z^{-2}(\alpha + \beta^2(1 + \alpha))\right)\left(zt_1\, zt_2\right)^{-1}$$

$$\frac{1}{H(z)} \cdot \frac{dH(z)}{d\alpha} = z^{-1}\left(z^{-2} - 1\right)\left(1 - 2\beta z^{-1} + z^{-2}\right) \left(z^{-1} - \beta\right)\left(\beta z^{-1} - 1\right)\left(x_1^2 - 1\right)\left(zt_1\, zt_2\right)^{-1}$$

$$\begin{aligned}\frac{1}{H(z)}\cdot\frac{dH(z)}{d\beta} = {} & -z^{-1}\left(z^{-2}-1\right)\left(x_1^2-1\right)\\ & \Big((1+z^{-4})\alpha - 2\beta z^{-1}(1+z^{-2})(1+\alpha)\\ & \quad + 2z^{-2}(1+\beta^2(1+\alpha))\Big)\left(zt_1\, zt_2\right)^{-1}\end{aligned}$$

Group delay coefficient sensitivity parameters :-

$$\begin{aligned}\frac{d\left(\frac{1}{H(z)}\cdot\frac{dH(z)}{d\omega}\right)}{dx_1} = {} & -j\,z^{-1}\left(\beta - 2z^{-1} + \beta z^{-2}\right)\left(zt_1\, zt_2\right)^{-2}\\ & \Big((1+z^{-4})\alpha - 2\beta z^{-1}(1+z^{-2})(1+\alpha) + 2z^{-2}(1+\beta^2(1+\alpha))\Big)\\ & \Big((1+z^{-8})\big(1+x_1^2\big) - 2\beta z^{-1}(1+z^{-6})\big(2(1+x_1^2)+\alpha(x_1-1)^2\big)\\ & \quad + 2z^{-2}(1+z^{-4})\Big(\alpha(x_1-1)^2+\beta^2\big(3(1+x_1^2)+2x_1+\alpha(3+\alpha)(1+x_1)^2\big)\Big)\\ & \quad - 2\beta z^{-3}(1+z^{-2})\big(\alpha(3+2\alpha)(1+x_1)^2+4x_1+2\beta^2(1+x_1)^2(1+\alpha)^2\big)\\ & \quad + 2z^{-4}\Big(\alpha^2(1+x_1)^2+2x_1+2\beta^2\big(\alpha(3+2\alpha)(1+x_1)^2+4x_1\big)\\ & \qquad + \beta^4(1+x_1)^2(1+\alpha)^2\Big)\quad\Big)\end{aligned}$$

$$\begin{aligned}\frac{d\left(\frac{1}{H(z)}\cdot\frac{dH(z)}{d\omega}\right)}{d\alpha} = {} & -j\,z^{-1}\left(x_1^2-1\right)\left(\beta - 2z^{-1} + \beta z^{-2}\right)\left(zt_1\, zt_2\right)^{-2}\\ & \Big((1+z^{-12})x_1 - 6\beta z^{-1}(1+z^{-10})x_1\\ & \quad - \beta^2 z^{-2}(1+z^{-8})\big(1 - x_1(12-x_1)+\alpha^2(1+x_1)^2\big)\\ & \quad + 2\beta z^{-3}(1+z^{-6})\Big(1+x_1(3+x_1)+\alpha^2(1+x_1)^2\\ & \qquad + 2\beta^2\big((x_1-1)^2+\alpha(\alpha+1)(1+x_1)^2\big)\Big)\\ & \quad - z^{-4}(1+z^{-4})\Big(1+x_1(3+x_1)+\alpha^2(1+x_1)^2\\ & \qquad + 4\beta^2\big(2(1+x_1(3+x_1))+\alpha(3+2\alpha)(1+x_1)^2\big)\\ & \qquad + \beta^4\big(7+x_1(6+7x_1)+\alpha(12+7\alpha)(1+x_1)^2\big)\Big)\\ & \quad + 2\beta z^{-5}(1+z^{-2})\Big(2(1+x_1(3+x_1))+\alpha(3+2\alpha)(1+x_1)^2\\ & \qquad + 2\beta^2\big(4(1+x_1(3+x_1))+\alpha(9+4\alpha)(1+x_1)^2\big)\\ & \qquad + 3\beta^4(\alpha+1)^2(1+x_1)^2\Big)\\ & \quad - 2z^{-6}\Big(2\alpha(1+x_1)^2\\ & \qquad + 6\beta^2\big(1+x_1(3+x_1)+\alpha(3+\alpha)(1+x_1)^2\big)\\ & \qquad + 2\beta^4\big(4(1+x_1(3+x_1))+\alpha(9+4\alpha)(1+x_1)^2\big)\\ & \qquad + \beta^6(1+\alpha)^2(1+x_1)^2\Big)\Big)\end{aligned}$$

$$\frac{d\left(\frac{1}{H(z)}\cdot\frac{dH(z)}{d\omega}\right)}{d\beta} = j\,z^{-1}\left(x_1{}^2 - 1\right)\left(zt_1\ zt_2\right)^{-2}$$

$$\begin{aligned}
&\Big((1 + z^{-14})x_1\alpha - 4\beta z^{-1}(1 + z^{-12})x_1(1 + \alpha) \\
&\quad - z^{-2}(1 + z^{-10})\Big(3x_1(\alpha - 2) + \alpha^2(1 + x_1)^2 \\
&\qquad - \beta^2\Big(14x_1 + \alpha(1 + x_1(12 + x_1)) - \alpha^2(1 + \alpha)(1 + x_1)^2\Big)\Big) \\
&\quad + 4\beta z^{-3}(1 + z^{-8})\Big(-4x_1 + \alpha^2(2 + \alpha)(1 + x_1)^2 \\
&\qquad + \beta^2(1 + \alpha)\Big(-4x_1 + \alpha^2(1 + x_1)^2\Big)\Big) \\
&\quad - z^{-4}(1 + z^{-6})\Big(10x_1 + \alpha(1 - x_1(9 - x_1)) + \alpha^2(1 + 3\alpha)(1 + x_1)^2 \\
&\qquad + \beta^2\Big(2(1 - x_1(1-x_1)) + 3\alpha(5+x_1(4+5x_1)) + \alpha^2(27+17\alpha)(1+x_1)^2\Big) \\
&\qquad + \beta^4(1 + \alpha)\Big(2(x_1 - 1)^2 + 5\alpha(1 + \alpha)(1 + x_1)^2\Big)\Big) \\
&\quad + 4\beta z^{-5}(1 + z^{-4})\Big(1+x_1(11+x_1) + \alpha(5+x_1(3+5x_1)) + 3\alpha^2(1+\alpha)(1+x_1)^2 \\
&\qquad + 2\beta^2(1 + \alpha)^2(2 + 3\alpha)(1 + x_1)^2 \\
&\qquad + \beta^4(1 + \alpha)^3(1 + x_1)^2\Big) \\
&\quad - \beta z^{-6}(1 + z^{-2})\Big(2(1+x_1{}^2) + \alpha(5+x_1(19+5x_1)) + \alpha^2(4-\alpha)(1+x_1)^2 \\
&\qquad + 2\beta^2\Big(2(7+x_1(19+7x_1)) + 2\alpha(19+x_1(45+19x_1)) + \alpha^2(31+6\alpha)(1+x_1)^2\Big) \\
&\qquad + \beta^4(1 + \alpha)\Big(4(7 + x_1(16 + 7x_1)) + 5\alpha(11 + 5\alpha)(+ x_1)^2\Big) \\
&\qquad + 2\beta^6(1 + \alpha)^3(1 + x_1)^2\Big) \\
&\quad + 8\beta z^{-7}\Big(2(1 + x_1{}^2) + 4\alpha(1 + x_1(4 + x_1)) + \alpha^2(4 - \alpha)(1 + x_1)^2 \\
&\qquad + \beta^2(1 + \alpha)\Big(2(3 + x_1(8 + 3x_1)) + \alpha(10 + 3\alpha)(1 + x_1)^2\Big) \\
&\qquad + 2\beta^4(1 + \alpha)^3(1 + x_1)^2\Big) \qquad \Big)
\end{aligned}$$

C4.2 8th order Dual Bandpass APS

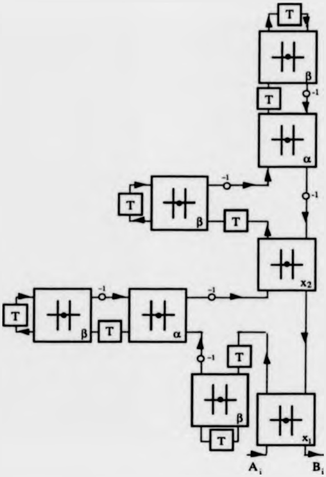

Limits :-

$-1 < x_1 < 0$

$-1 < x_2 < 1$

$-1 < \alpha < 1$

$-1 < \beta < 1$

$$zt_1 = x_1 + n_1 z^{-1} + n_2 z^{-2} + n_3 z^{-3} + n_4 z^{-4} + n_5 z^{-5} + n_6 z^{-6} + n_7 z^{-7} - z^{-8}$$

$$zt_2 = -1 + n_7 z^{-1} + n_6 z^{-2} + n_5 z^{-3} + n_4 z^{-4} + n_3 z^{-5} + n_2 z^{-6} + n_1 z^{-7} + x_1 z^{-8}$$

$$n_1 = -\beta\Big(4x_1 + \alpha(x_1(2 + x_2) - x_2)\Big)$$

$$\begin{aligned} n_2 = \alpha\Big(x_1(2 + x_2) - x_2\Big) + \beta^2\Big(&x_1(6 + x_2) - x_2 \\ &+ 3\alpha\Big(x_1(2 + x_2) - x_2\Big) + \alpha^2(x_1 - 1)(x_2 + 1)\Big) \end{aligned}$$

$$\begin{aligned} n_3 = \beta\Big(&2x_2(1 - x_1) - 3\alpha\Big(x_1(2 + x_2) - x_2\Big) - 2\alpha^2(x_1 - 1)(x_2 + 1)\Big) \\ &- 2\beta^3(1 + \alpha)\Big(x_1(2 + x_2) - x_2 + \alpha(x_1 - 1)(x_2 + 1)\Big) \end{aligned}$$

$$\begin{aligned} n_4 = (x_1 - 1)\Big(&\beta^4 + 2\alpha\beta^2(3 + \beta^2) + \alpha^2\Big(1 + \beta^2(4 + \beta^2)\Big) \\ &+ x_2\Big((1 + \alpha^2)(1 + \beta^2(4 + \beta^2)) + 2\alpha\beta^2(3 + \beta^2)\Big)\Big) \end{aligned}$$

$$\begin{aligned} n_5 = -\beta\Big(&2x_2(x1 - 1) - 3\alpha(x_2(1 - x_1) + 2) + 2\alpha^2(x_1 - 1)(x_2 + 1) \\ &+ \beta^2\Big(2x_2(x_1 - 1) - 4 + 2\alpha(2x_2(x_1 - 1) + x_1 - 3) + 2\alpha^2(x_1 - 1)(x_2 + 1)\Big)\Big) \end{aligned}$$

$$n_6 = \alpha\Big(x_2(x_1 - 1) - 2\Big)$$
$$+ \beta^2\Big(x_2(x_1 - 1) - 6 + 3\alpha\Big(x_2(x_1 - 1) - 2\Big) + \alpha^2(x_1 - 1)(x_2 + 1)\Big)$$
$$n_7 = \beta\Big(4 + \alpha\Big(2 - x_2(x_1 - 1)\Big)\Big)$$

Overall transfer function :-

$$H(z) = \frac{B_i}{A_i} = \frac{zt_1}{zt_2}$$

Group delay parameter :-

$$\frac{1}{H(z)} \cdot \frac{dH(z)}{d\omega} = j\,z^{-1}\Big(x_1{}^2 - 1\Big)\Big(\beta - 2z^{-1} + \beta z^{-2}\Big)$$
$$\Big((1 + z^{-4})\alpha - 2\beta z^{-1}(1 + z^{-2})(1 + \alpha)$$
$$+ 2z^{-2}(1 + \beta^2(1 + \alpha))\Big)\Big(zt_1\ zt_2\Big)^{-1}$$

Gain/Phase coefficient sensitivity parameters :-

$$\frac{1}{H(z)} \cdot \frac{dH(z)}{dx_1} = \Big(z^{-2} - 1\Big)\Big(1 - 2\beta z^{-1} + z^{-2}\Big)\Big(zt_1\ zt_2\Big)^{-1}$$

$$\Big((1 + z^{-4}) - 2\beta z^{-1}(1 + z^{-2})(1 + \alpha) + 2z^{-2}(\alpha + \beta^2(1 + \alpha))\Big)$$
$$\Big((1 + z^{-8}) - 2\beta z^{-1}(1 + z^{-6})\Big(2 + \alpha(1 + x_2)\Big)$$
$$+ 2z^{-2}(1 + z^{-4})\Big(\alpha(1 + x_2) + \beta^2(3 + x_2 + \alpha(1 + x_2)(3 + 2\alpha))\Big)$$
$$- 2\beta z^{-3}(1 + z^{-2})\Big(2x_2 + \alpha(1 + x_2)(3 + 2\alpha) + 2\beta^2(1 + x_2)(1 + \alpha)2\Big)$$
$$+ 2z^{-4}\Big(x_2 + \alpha 2(1+x_2) + 2\beta^2(2x_2 + a(1+x_2)(3+2\alpha)) + \beta^4(1+x_2)(1+\alpha)^2\Big)\Big)$$

$$\frac{1}{H(z)} \cdot \frac{dH(z)}{dx_2} = \Big(x_1{}^2 - 1\Big)\,z^{-1}\Big(\beta z^{-1} - 1\Big)\Big(z^{-2} - 1\Big)\Big(1 - 2\beta z^{-1} + z^{-2}\Big)$$
$$\Big(\beta - z^{-1}\Big)\Big(\alpha - \beta z^{-1}(1 + \alpha) + z^{-2}\Big)\Big(1 - \beta z^{-1}(1 + \alpha) + \alpha z^{-2}\Big)$$
$$\Big((1 + z^{-4}) - 2\beta z^{-1}(1 + z^{-2})(1 + \alpha) + 2z^{-2}(\alpha + \beta^2(1 + \alpha))\Big)\Big(zt_1\ zt_2\Big)^{-1}$$

$$\frac{1}{H(z)} \cdot \frac{dH(z)}{d\alpha} = \Big(x_1{}^2 - 1\Big)\Big(\beta - z^{-1}\Big)\,z^{-1}\Big(z^{-2} - 1\Big)\Big(\beta z^{-1} - 1\Big)\Big(1 - 2\beta z^{-1} + z^{-2}\Big)$$

$$\Big(zt_1\ zt_2\Big)^{-1}\Big(x_2(1 + z^{-8})$$
$$- 2\beta z^{-1}(1 + z^{-6})\Big(\alpha + x_2(2 + \alpha)\Big)$$
$$+ 2z^{-2}(1 + z^{-4})\Big(\alpha(1 + x_2) + \beta^2(1 + 3x_2 + \alpha(3 + \alpha)(1 + x_2))\Big)$$
$$- 2\beta z^{-3}(1 + z^{-2})\Big(2 + \alpha(3 + 2\alpha)(1 + x_2) + 2\beta^2(1 + x_2)(1 + \alpha)^2\Big)$$
$$+ 2z^{-4}\Big(1 + \alpha^2(1+x_2) + 2\beta^2(2 + \alpha(3+2\alpha)(1+x_2)) + \beta^4(1+x_2)(1+\alpha)^2\Big)\Big)$$

$$\frac{1}{H(z)} \cdot \frac{dH(z)}{d\beta} = -z^{-1}\left(z^{-2} - 1\right)\left(x_1{}^2 - 1\right)\left(zt_1\, zt_2\right)^{-1}$$

$$\left(\alpha(1 + z^{-4}) - 2\beta z^{-1}(1 + z^{-2})(1 + \alpha) + 2z^{-2}(1 + \beta^2(1 + \alpha))\right)$$

$$\Big(x_2(1 + z^{-8}) - 2\beta z^{-1}(1 + z^{-6})\left(\alpha + x_2(2 + \alpha)\right)$$

$$+ 2z^{-2}(1 + z^{-4})\left(\alpha(1 + x_2) + \beta^2(1 + 3x_2 + \alpha(3 + \alpha)(1 + x_2))\right)$$

$$- 2\beta z^{-3}(1 + z^{-2})\left(2 + \alpha(3 + 2\alpha)(1 + x_2) + 2\beta^2(1 + x_2)(1 + \alpha)^2\right)$$

$$+ 2z^{-4}\left(1 + \alpha^2(1+x_2) + 2\beta^2(2 + \alpha(3+2\alpha)(1+x_2)) + \beta^4(1+x_2)(1+\alpha)^2\right)\Big)$$

Group delay coefficient sensitivity parameters :-

$$\frac{d\left(\frac{1}{H(z)} \cdot \frac{dH(z)}{d\omega}\right)}{dx_1}, \quad \frac{d\left(\frac{1}{H(z)} \cdot \frac{dH(z)}{d\omega}\right)}{dx_2}, \quad \frac{d\left(\frac{1}{H(z)} \cdot \frac{dH(z)}{d\omega}\right)}{d\alpha} \quad \text{and} \quad \frac{d\left(\frac{1}{H(z)} \cdot \frac{dH(z)}{d\omega}\right)}{d\beta}$$

have not been included within this Appendix due to their very large length and complexity. If the equations for these parameters is required please contact the author who will supply the Mathematica or Fortran code listings.

C5 Dual Bandstop APS Models

C5.1 4th order Dual Bandstop APS

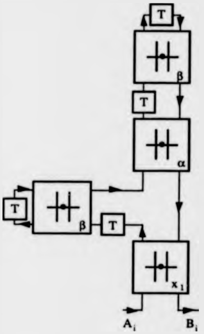

Limits :-

$-1 < x_1 < 1$

$-1 < \alpha < 1$

$-1 < \beta < 1$

$$n_1 = \beta\,(\alpha(x_1 - 1) - 2x_1)\ ,\ n_2 = -(x_1 - 1)(\alpha + \beta^2(\alpha - 1))\ ,\ n_3 = \beta\,(2 + \alpha(x_1 - 1))$$

$$zt_1 = x_1 + n_1 z^{-1} + n_2 z^{-2} + n_3 z^{-3} - z^{-4}\ ,\ zt_2 = -1 + n_3 z^{-1} + n_2 z^{-2} + n_1 z^{-3} + x_1 z^{-4}$$

Overall transfer function :-

$$H(z) = \frac{B_i}{A_i} = \frac{zt_1}{zt_2}$$

Group delay parameter :-

$$\begin{aligned}\frac{1}{H(z)} \cdot \frac{dH(z)}{d\omega} = \ & j\,z^{-1}\left(x_1{}^2 - 1\right)\left(\beta - 2z^{-1} + \beta z^{-2}\right)\\ & \Big((1 + z^{-4})\alpha + 2\beta z^{-1}(1 + z^{-2})(1 - \alpha)\\ & - 2z^{-2}(1 - \beta^2(\alpha - 1))\Big)\left(zt_1\, zt_2\right)^{-1}\end{aligned}$$

Gain/Phase coefficient sensitivity parameters :-

$$\begin{aligned}\frac{1}{H(z)} \cdot \frac{dH(z)}{dx_1} = \ & \left(z^{-2} - 1\right)\left(1 - 2\beta z^{-1} + z^{-2}\right)\\ & \Big((1 + z^{-4}) + 2\beta z^{-1}(1 + z^{-2})\\ & - 2z^{-2}(\alpha + \beta^2(\alpha - 1))\Big)\left(zt_1\, zt_2\right)^{-1}\end{aligned}$$

$$\begin{aligned}\frac{1}{H(z)} \cdot \frac{dH(z)}{d\alpha} = \ & z^{-1}\left(z^{-2} - 1\right)\left(1 - 2\beta z^{-1} + z^{-2}\right)\\ & \left(z^{-1} - \beta\right)\left(\beta z^{-1} - 1\right)\left(x_1{}^2 - 1\right)\left(zt_1\, zt_2\right)^{-1}\end{aligned}$$

$$
\begin{aligned}
\frac{1}{H(z)}\cdot\frac{dH(z)}{d\beta} = {} & z^{-1}\Big(z^{-2}-1\Big)\Big(x_1{}^2-1\Big) \\
& \Big((1+z^{-4})\alpha - 2\beta z^{-1}(1+z^{-2})(\alpha-1) \\
& \quad - 2z^{-2}(1-\beta^2(\alpha-1))\Big)\Big(zt_1\, zt_2\Big)^{-1}
\end{aligned}
$$

Group delay coefficient sensitivity parameters :-

$$
\frac{d\left(\frac{1}{H(z)}\cdot\frac{dH(z)}{d\omega}\right)}{dx_1} = -j\, z^{-1}\Big(\beta - 2z^{-1} + \beta z^{-2}\Big)\Big(zt_1\, zt_2\Big)^{-2}
$$

$$
\begin{aligned}
&\Big((1+z^{-4})\alpha - 2\beta z^{-1}(1+z^{-2})(\alpha-1) - 2z^{-2}(1-\beta^2(\alpha-1))\Big) \\
&\Big((1+z^{-8})\Big(1+x_1{}^2\Big) \\
&\quad - 2\beta z^{-1}(1+z^{-6})\Big(2(1+x_1{}^2) - \alpha(x_1-1)^2\Big) \\
&\quad - 2z^{-2}(1+z^{-4})\Big(\alpha(x_1-1)^2 - \beta^2\Big(3 - x_1(2-3x_1) - \alpha(3-\alpha)(x_1-1)^2\Big)\Big) \\
&\quad + 2\beta z^{-3}(1+z^{-2})\Big(4x_1 + \alpha(3-2\alpha)(x_1-1)^2 - 2\beta^2(x_1-1)^2(\alpha-1)^2\Big) \\
&\quad + 2z^{-4}\Big(\alpha^2(x_1-1)^2 - 2x_1 - 2\beta^2\Big(\alpha(3-2\alpha)(x_1-1)^2 + 4x_1\Big) \\
&\qquad\quad + \beta^4(x_1-1)^2(\alpha-1)^2\Big) \quad \Big)
\end{aligned}
$$

$$
\frac{d\left(\frac{1}{H(z)}\cdot\frac{dH(z)}{d\omega}\right)}{d\alpha} = j\, z^{-1}\Big(x_1{}^2-1\Big)\Big(\beta - 2z^{-1} + \beta z^{-2}\Big)\Big(zt_1\, zt_2\Big)^{-2}
$$

$$
\begin{aligned}
&\Big((1+z^{-12})x_1 - 6\beta z^{-1}(1+z^{-10})x_1 \\
&\quad + \beta^2 z^{-2}(1+z^{-8})\Big(1 + x_1(12+x_1) + \alpha^2(x_1-1)^2\Big) \\
&\quad - 2\beta z^{-3}(1+z^{-6})\Big(1 - x_1(3-x_1) + \alpha^2(x_1-1)^2 \\
&\qquad\qquad + 2\beta^2\Big((1+x_1)^2 + \alpha(\alpha-1)(x_1-1)^2\Big)\ \Big) \\
&\quad + z^{-4}(1+z^{-4})\Big(1 - x_1(3-x_1) + \alpha^2(x_1-1)^2 \\
&\qquad\qquad + 4\beta^2\Big(2(1-x_1(3-x_1)) - \alpha(3-2\alpha)(x_1-1)^2\Big) \\
&\qquad\qquad + \beta^4\Big(7 - x_1(6-7x_1) - \alpha(12-7\alpha)(x_1-1)^2\Big)\ \Big) \\
&\quad - 2\beta z^{-5}(1+z^{-2})\Big(2(1-x_1(3-x_1)) - \alpha(3-2\alpha)(x_1-1)^2 \\
&\qquad\qquad + 2\beta^2\Big(4(1-x_1(3-x_1)) - \alpha(9-4\alpha)(x_1-1)^2\Big) \\
&\qquad\qquad + 3\beta^4(x_1-1)^2(\alpha-1)^2\Big) \\
&\quad + 2z^{-6}\Big(-2\alpha(x_1-1)^2 \\
&\qquad\qquad + 6\beta^2\Big(1 - x_1(3-x_1) - \alpha(3-\alpha)(x_1-1)^2\Big) \\
&\qquad\qquad + 2\beta^4\Big(4(1-x_1(3-x_1)) - \alpha(9-4\alpha)(x_1-1)^2\Big) \\
&\qquad\qquad + \beta^6(x_1-1)^2(\alpha-1)^2\Big) \quad \Big)
\end{aligned}
$$

$$\frac{d\left(\frac{1}{H(z)}\cdot\frac{dH(z)}{d\omega}\right)}{d\beta} = j\,z^{-1}\left(x_1{}^2 - 1\right)\left(zt_1\;zt_2\right)^{-2}$$

$$\Big((1 + z^{-14})x_1\alpha - 4\beta z^{-1}(1 + z^{-12})x_1(\alpha - 1)$$

$$- z^{-2}(1 + z^{-10})\Big(3x_1(2 + \alpha) + \alpha^2(x_1 - 1)^2$$

$$+ \beta^2\Big(14x_1 + \alpha(1 - x_1(12 - x_1)) - \alpha^2(\alpha - 1)(x_1 - 1)^2\Big)\ \Big)$$

$$+ 4\beta z^{-3}(1 + z^{-8})\Big(4x_1 + \alpha^2(2 - \alpha)(x_1 - 1)^2$$

$$- \beta^2(\alpha - 1)\Big(4x_1 + \alpha^2(x_1 - 1)^2\Big)\ \Big)$$

$$+ z^{-4}(1 + z^{-6})\Big(10x_1 + \alpha(1 + x_1(9 + x_1)) - \alpha^2(1 - 3\alpha)(x_1 - 1)^2$$

$$- \beta^2\Big(2(1+x_1(1+x_1)) - 3\alpha(5-x_1(4-5x_1)) + \alpha^2(27-17\alpha)(x_1-1)^2\Big)$$

$$+ \beta^4(\alpha - 1)\Big(2(1+x_1)^2 + 5\alpha(\alpha - 1)(x_1-1)^2\Big)\ \Big)$$

$$- 4\beta z^{-5}(1 + z^{-4})\Big(1-x_1(11-x_1) - \alpha(5-x_1(3-5x_1)) - 3\alpha^2(\alpha - 1)(x_1-1)^2$$

$$+ 2\beta^2(\alpha - 1)^2(2 - 3\alpha)(x_1 - 1)^2)$$

$$- \beta^4(x_1 - 1)^2(\alpha - 1)^3\ \Big)$$

$$+ z^{-6}(1 + z^{-2})\Big(-2(1+x_1{}^2) + \alpha(5-x_1(19-5x_1)) - \alpha^2(4+\alpha)(x_1-1)^2$$

$$+ 2\beta^2\Big(-2(7-x_1(19-7x_1)) + 2\alpha(19-x_1(45-19x_1)) - \alpha^2(31-6\alpha)(x_1-1)^2\Big)$$

$$+ \beta^4(\alpha - 1)\Big(4(7 - x_1(16 - 7x_1)) - 5\alpha(11 - 5\alpha)(x_1 - 1)^2\Big)$$

$$+ 2\beta^6(x_1 - 1)^2(\alpha - 1)^3\ \Big)$$

$$+ 8\beta z^{-7}\Big(2(1 + x_1{}^2) - 4\alpha(1 - x_1(4 - x_1)) + \alpha^2(4 - \alpha)(x_1 - 1)^2$$

$$- \beta^2(\alpha - 1)\Big(2(3 - x_1(8 - 3x_1)) - \alpha(10 - 3\alpha)(x_1 - 1)^2\Big)$$

$$- 2\beta^4(x_1 - 1)^2(\alpha - 1)^2\Big)\qquad\Big)$$

C5.2 8th order Dual Bandstop APS

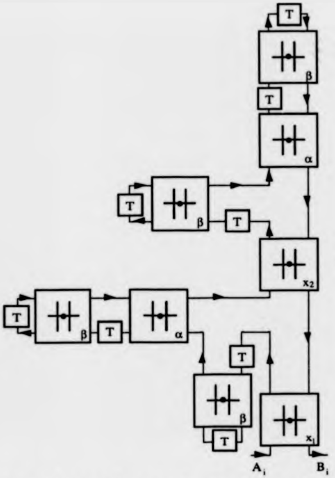

Limits :-

$-1 < x_1 < 0$

$-1 < x_2 < 1$

$-1 < \alpha < 1$

$-1 < \beta < 1$

$$zt_1 = x_1 + n_1 z^{-1} + n_2 z^{-2} + n_3 z^{-3} + n_4 z^{-4} + n_5 z^{-5} + n_6 z^{-6} + n_7 z^{-7} - z^{-8}$$

$$zt_2 = -1 + n_7 z^{-1} + n_6 z^{-2} + n_5 z^{-3} + n_4 z^{-4} + n_3 z^{-5} + n_2 z^{-6} + n_1 z^{-7} + x_1 z^{-8}$$

$$n_1 = -\beta\Big(4x_1 + \alpha(x_1(2 + x_2) - x_2)\Big)$$

$$n_2 = \alpha\Big(x_1(2 + x_2) - x_2\Big) + \beta^2\Big(x_1(6 + x_2) - x_2 \\ + 3\alpha\Big(x_1(2 + x_2) - x_2\Big) + \alpha^2(x_1 - 1)(x_2 + 1)\Big)$$

$$n_3 = \beta\Big(2x_2(1 - x_1) - 3\alpha\Big(x_1(2 + x_2) - x_2\Big) - 2\alpha^2(x_1 - 1)(x_2 + 1)\Big) \\ - 2\beta^3(1 + \alpha)\Big(x_1(2 + x_2) - x_2 + \alpha(x_1 - 1)(x_2 + 1)\Big)$$

$$n_4 = (x_1 - 1)\Big(\beta^4 + 2\alpha\beta^2(3 + \beta^2) + \alpha^2\Big(1 + \beta^2(4 + \beta^2)\Big) \\ + x_2\Big((1 + \alpha^2)(1 + \beta^2(4 + \beta^2)) + 2\alpha\beta^2(3 + \beta^2)\Big)\Big)$$

$$n_5 = -\beta\Big(2x_2(x1 - 1) - 3\alpha(x_2(1 - x_1) + 2) + 2\alpha^2(x_1 - 1)(x_2 + 1) \\ + \beta^2\Big(2x_2(x_1-1) - 4 + 2\alpha(2x_2(x_1-1) + x_1 - 3) + 2\alpha^2(x_1-1)(x_2+1)\Big)\Big)$$

$$
\begin{aligned}
n_6 = {} & \alpha\Big(x_2(x_1 - 1) - 2\Big) \\
& + \beta^2\Big(x_2(x_1 - 1) - 6 + 3\alpha\Big(x_2(x_1 - 1) - 2\Big) + \alpha^2(x_1 - 1)(x_2 + 1)\Big) \\
n_7 = {} & \beta\Big(4 + \alpha\Big(2 - x_2(x_1 - 1)\Big)\Big)
\end{aligned}
$$

Overall transfer function :-

$$H(z) = \frac{B_i}{A_i} = \frac{zt_1}{zt_2}$$

Group delay parameter :-

$$
\begin{aligned}
\frac{1}{H(z)} \cdot \frac{dH(z)}{d\omega} = {} & j\, z^{-1}\Big(x_1{}^2 - 1\Big)\Big(\beta - 2z^{-1} + \beta z^{-2}\Big) \\
& \Big((1 + z^{-4})\alpha - 2\beta z^{-1}(1 + z^{-2})(1 + \alpha) \\
& + 2z^{-2}(1 + \beta^2(1 + \alpha))\Big)\Big(zt_1\, zt_2\Big)^{-1}
\end{aligned}
$$

Gain/Phase coefficient sensitivity parameters :-

$$
\begin{aligned}
\frac{1}{H(z)} \cdot \frac{dH(z)}{dx_1} = {} & \Big(z^{-2} - 1\Big)\Big(1 - 2\beta z^{-1} + z^{-2}\Big)\Big(zt_1\, zt_2\Big)^{-1} \\
& \Big((1 + z^{-4}) - 2\beta z^{-1}(1 + z^{-2})(1 + \alpha) + 2z^{-2}(\alpha + \beta^2(1 + \alpha))\Big) \\
& \Big((1 + z^{-8}) - 2\beta z^{-1}(1 + z^{-6})\Big(2 + \alpha(1 + x_2)\Big) \\
& + 2z^{-2}(1 + z^{-4})\Big(\alpha(1 + x_2) + \beta^2(3 + x_2 + \alpha(1 + x_2)(3 + 2\alpha))\Big) \\
& - 2\beta z^{-3}(1 + z^{-2})\Big(2x_2 + \alpha(1 + x_2)(3 + 2\alpha) + 2\beta^2(1 + x_2)(1 + \alpha)2\Big) \\
& + 2z^{-4}\Big(x_2 + \alpha 2(1+x_2) + 2\beta^2(2x_2 + a(1+x_2)(3+2\alpha)) + \beta^4(1+x_2)(1+\alpha)^2\Big)\Big)
\end{aligned}
$$

$$
\begin{aligned}
\frac{1}{H(z)} \cdot \frac{dH(z)}{dx_2} = {} & \Big(x_1{}^2 - 1\Big) z^{-1}\Big(\beta z^{-1} - 1\Big)\Big(z^{-2} - 1\Big)\Big(1 - 2\beta z^{-1} + z^{-2}\Big) \\
& \Big(\beta - z^{-1}\Big)\Big(\alpha - \beta z^{-1}(1 + \alpha) + z^{-2}\Big)\Big(1 - \beta z^{-1}(1 + \alpha) + \alpha z^{-2}\Big) \\
& \Big((1 + z^{-4}) - 2\beta z^{-1}(1 + z^{-2})(1 + \alpha) + 2z^{-2}(\alpha + \beta^2(1 + \alpha))\Big)\Big(zt_1\, zt_2\Big)^{-1}
\end{aligned}
$$

$$
\begin{aligned}
\frac{1}{H(z)} \cdot \frac{dH(z)}{d\alpha} = {} & \Big(x_1{}^2 - 1\Big)\Big(\beta - z^{-1}\Big) z^{-1}\Big(z^{-2} - 1\Big)\Big(\beta z^{-1} - 1\Big)\Big(1 - 2\beta z^{-1} + z^{-2}\Big) \\
& \Big(zt_1\, zt_2\Big)^{-1}\Big(x_2(1 + z^{-8}) \\
& - 2\beta z^{-1}(1 + z^{-6})\Big(\alpha + x_2(2 + \alpha)\Big) \\
& + 2z^{-2}(1 + z^{-4})\Big(\alpha(1 + x_2) + \beta^2(1 + 3x_2 + \alpha(3 + \alpha)(1 + x_2))\Big) \\
& - 2\beta z^{-3}(1 + z^{-2})\Big(2 + \alpha(3 + 2\alpha)(1 + x_2) + 2\beta^2(1 + x_2)(1 + \alpha)^2\Big) \\
& + 2z^{-4}\Big(1 + \alpha^2(1+x_2) + 2\beta^2(2 + \alpha(3+2\alpha)(1+x_2)) + \beta^4(1+x_2)(1+\alpha)^2\Big)\Big)
\end{aligned}
$$

$$\frac{1}{H(z)} \cdot \frac{dH(z)}{d\beta} = -z^{-1}\left(z^{-2} - 1\right)\left(x_1{}^2 - 1\right)\left(zt_1\ zt_2\right)^{-1}$$

$$\begin{aligned}&\left(\alpha(1 + z^{-4}) - 2\beta z^{-1}(1 + z^{-2})(1 + \alpha) + 2z^{-2}(1 + \beta^2(1 + \alpha))\right)\\
&\Big(x_2(1 + z^{-8}) - 2\beta z^{-1}(1 + z^{-6})\left(\alpha + x_2(2 + \alpha)\right)\\
&\quad + 2z^{-2}(1 + z^{-4})\left(\alpha(1 + x_2) + \beta^2(1 + 3x_2 + \alpha(3 + \alpha)(1 + x_2))\right)\\
&\quad - 2\beta z^{-3}(1 + z^{-2})\left(2 + \alpha(3 + 2\alpha)(1 + x_2) + 2\beta^2(1 + x_2)(1 + \alpha)^2\right)\\
&\quad + 2z^{-4}\left(1 + \alpha^2(1+x_2) + 2\beta^2(2 + \alpha(3+2\alpha)(1+x_2)) + \beta^4(1+x_2)(1+\alpha)^2\right)\Big)\end{aligned}$$

Group delay coefficient sensitivity parameters :-

$$\frac{d\left(\frac{1}{H(z)} \cdot \frac{dH(z)}{d\omega}\right)}{dx_1}, \quad \frac{d\left(\frac{1}{H(z)} \cdot \frac{dH(z)}{d\omega}\right)}{dx_2}, \quad \frac{d\left(\frac{1}{H(z)} \cdot \frac{dH(z)}{d\omega}\right)}{d\alpha} \quad \text{and} \quad \frac{d\left(\frac{1}{H(z)} \cdot \frac{dH(z)}{d\omega}\right)}{d\beta}$$

have not been included within this Appendix due to their very large length and complexity. If the equations for these parameters is required please contact the author who will supply the Mathematica or Fortran code listings

Appendix D

Lattice WDF APS Models
(Time domain)

This Appendix details the various time domain software models for the APS's created for the design and analysis of the lattice WDF. Each APS is illustrated and provided with a fortran listing of its software model along with the model for the two-port adaptor upon which each APS is based. The time domain software models contained in this Appendix are :-

D1 Two-port Adaptor Model

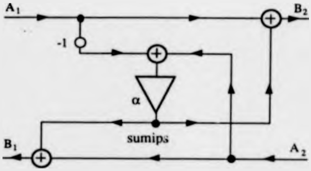

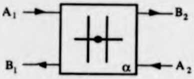

The source code for the two-port adaptor routine and the overflow and quantization routines called within that routine are detailed within this section. Global parameters for the internal signal length, overflow and quantization strategies are defined within the supervisor program which calls the APS routines in order to determine the time response.

```
      subroutine twoport(A1,A2,coeff,B1,B2)

C This routine mimics the action of a two-port adaptor. It accepts two input
C signals, A1 and A2 and a multiplier value, coeff, and then generates the
C corresponding outputs, B1 and B2.

C define common variables
C lensig is the signed bit length of all internal signals within the model
      integer lensig
      COMMON/gen3/ lensig

C define external variables
      double precision A1, A2, coeff, B1, B2

C define local variables
      double precision sumips

C Step 1, subtract the two input wave parameters, check for overflow,
C multiply by the coefficient and then quantize to the value to lensig.
      sumips = A2 - A1
      call overflow(sumips,lensig)
      sumips = sumips*coeff
      call quantize(sumips,lensig)

C Step 2, generate B2 and then check for overflows
      B2 = A1 + sumips
      call overflow(B2,lensig)

C Step 3, generate B1 and then check for overflows
      B1 = A2 + sumips
      call overflow(B1,lensig)

      return
      end
      subroutine overflow(sigvalue,bitlen)

C This routine mimics of overflow in a finite wordlength system by limiting
C the signal level passed into the routine according to the overflow strategy
C defined and then returning this value.

C define common variables
C oflimit is the value above which an overflow is considered to have
C occurred, while the variable offlag is used to indicate if an overflow
C has occurred. The parameter oftype is the overflow strategy desired,
C selected from the options :-
C      1 = no precautions.
C      2 = saturation arithmetic.
C      3 = zeroing arithmetic.
C      4 = 2's complement arithmetic.

      integer oftype, offlag
      double precision oflimit
      COMMON/gen2/ oftype, offlag, oflimit

C define external variables
      integer bitlen
      double precision sigvalue

C define local variables
      integer range

C Step 1, bitlen includes one bit for the sign so it must be removed for overflow
C calculations and the actual range stored in the parameter range.
      range = bitlen - 1

C Step 2, compare input signal value level with overflow limit.
      if( abs(sigvalue) .lt. abs(oflimit) ) then

C Step 3a, signal is within limit, return the original signal value.

        else

C Step 3b, signal is outside or on overflow limits, check if the signal is negative
          if((abs(sigvalue).eq.abs(oflimit)) .and. (sigvalue.lt.0)) then

C Step 4a, signal is within limit, return the original signal value.

            else

C Step 4b, signal has overflowed, apply the desired overflow strategy
              if( oftype .eq. 1 ) then

C Step 5a, no precautions, return original signal value and set overflow flag.
                  offlag = 1

                elseif( oftype .eq. 2 ) then

C Step 5b, saturation arithmetic, alter signal value and set overflow flag.
                  if( sigvalue .gt. 0 ) then
                    sigvalue = sigvalue - 0.5**range
                  endif
                  offlag = 1
                  elseif( oftype .eq. 3 ) then

C Step 5c, zeroing arithmetic, alter signal value and set overflow flag.
                    sigvalue = 0
                    offlag = 1

                  elseif( oftype .eq. 4 ) then

C Step 5d, 2's complement arithmetic, alter signal value and set overflow flag.
                    sigvalue = mod(sigvalue,oflimit)
                    offlag = 1

                  else
                    write(*,*)'ERROR - no overflow type selected!'
                endif
           endif
      endif

      return
      end


      subroutine quantize(datavalue,datalen)

C This routine mimics of quantization in a finite wordlength system by
C quantizing the value passed into the routine to the bit length passed
C into the routine with the specified quantization procedure. The
C resulting quantized value is then returned by this routine.

C define common variables
C qtype is the type of quantization required. The possible quantizing procedures
C are :-
C     1 = rounding
C     2 = magnitude truncation
C     3 = value truncation
      integer qtype
      COMMON/gen1/ qtype

C define external variables
      integer datalen
      double precision datavalue

C define local variables
      double precision range

C Step 1, check bit length is not zero
      if( datalen .le. 0 ) then
           write(*,*)'ERROR - data wordlength must be > 0'

        else

C Step 2, since the bit length includes a sign bit it must be removed
C to calculate the maximum number range
           range = 2.0**(datalen - 1)

C Step 3, switch to the desired quantization procedure
           if( qtype .eq. 1 ) then

C Step 4a, rounding
                datavalue = sign(1.0,datavalue)
     *                    *aint(abs(datavalue)*range + 0.50001)/range
```

```
             elseif( qtype .eq. 2 ) then

C Step 4b, magnitude truncation
                datavalue = sign(1.0,datavalue)
 #                *aint(abs(datavalue)*range)/range

             elseif( qtype .eq. 3 ) then

C Step 4c, value truncation
                datavalue = -aint(-datavalue*range + 0.9999)/range

             else
                write(*,*)'ERROR - no quantization type selected!'
           endif
      endif

      return
      end
```

D2 Lowpass APS Models

D2.1 1st order Lowpass APS Model.

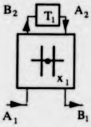

```
      subroutine tLPsec1(valin,valout,delay,coeff)

      integer MAXSIZEAPS, WAVESEC1
      parameter(MAXSIZEAPS = 8, WAVESEC1 = 2)

C define external variables
      double precision valin, valout, coeff(MAXSIZEAPS), delay(MAXSIZEAPS)

C define internal variables
      double precision a(WAVESEC1), b(WAVESEC1)

C Step 1. assign values from delay stack and valin to 'a' parameters
      a(1) = valin
      a(2) = delay(1)

C Step 2. call twoport routine to determine 'b' for the two-port adaptor
C containing the multiplier x1 held in coeff(1)
      call twoport(a(1),a(2),coeff(1),b(1),b(2))

C Step 3. assign output values to delay stack and valout parameters
      delay(1) = b(2)
      valout   = b(1)

      return
      end
```

D2.2 2nd order Lowpass APS Model.

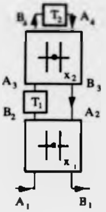

```
      subroutine tLPsec2(valin,valout,delay,coeff)

      integer MAXSIZEAPS, WAVESEC2
      parameter(MAXSIZEAPS = 8, WAVESEC2 = 4)

C define external variables
      double precision valin, valout, coeff(MAXSIZEAPS), delay(MAXSIZEAPS)

C define internal variables
      double precision a(WAVESEC2), b(WAVESEC2)

C Step 1, assign values from delay stack 'a' parameters
      a(3) = delay(1)
      a(4) = delay(2)

C Step 2, call twoport routine to determine 'b' values for the two-port adaptor
C containing the multiplier x2 held in coeff(2)
      call twoport(a(3),a(4),coeff(2),b(3),b(4))

C Step 3, assign values from new 'b' and valin parameters
      a(1) = valin
      a(2) = b(3)

C Step 4, call twoport routine to determine 'b' values for the two-port adaptor
C containing the multiplier x1 or coeff(1)
      call twoport(a(1),a(2),coeff(1),b(1),b(2))

C Step 5, assign output values to delay stack and valout parameters
      delay(1) = b(2)
      delay(2) = b(4)
      valout   = b(1)

      return
      end
```

D3 Highpass APS Models

D3.1 1st order Highpass APS Model

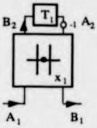

```
      subroutine tHPsec1(valin,valout,delay,coeff)

      integer MAXSIZEAPS, WAVESEC1
      parameter(MAXSIZEAPS = 8, WAVESEC1 = 2)

C define external variables
      double precision valin, valout, coeff(MAXSIZEAPS), delay(MAXSIZEAPS)

C define internal variables
      double precision a(WAVESEC1), b(WAVESEC1)

C Step 1, assign values from delay stack and valin to 'a' parameters
      a(1) = valin
      a(2) = -delay(1)

C Step 2, call twoport routine to determine 'b' values for the two-port adaptor
C containing the multiplier x1 held in coeff(1)
      call twoport(a(1),a(2),coeff(1),b(1),b(2))

C Step 3, assign output values to delay stack and valout parameters
      delay(1) = b(2)
      valout   = b(1)

      return
      end
```

D3.2 2^{nd} order Highpass APS Model

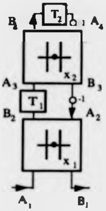

```
      subroutine tHPsec2(valin,valout,delay,coeff)

      integer MAXSIZEAPS, WAVESEC2
      parameter(MAXSIZEAPS = 8, WAVESEC2 = 4)

C define external variables
      double precision valin, valout, coeff(MAXSIZEAPS), delay(MAXSIZEAPS)

C define internal variables
      double precision a(WAVESEC2), b(WAVESEC2)

C Step 1, assign values from delay stack to 'a' parameters
      a(3) = delay(1)
      a(4) = -delay(2)

C Step 2, call twoport routine to determine 'b' values for the two-port adaptor
C containing the multiplier x2 held in coeff(2)
      call twoport(a(3),a(4),coeff(2),b(3),b(4))

C Step 3, assign values from new 'b' and valin parameters
      a(1) = valin
      a(2) = -b(3)

C Step 4, call twoport routine to determine 'b' values for the two-port adaptor
C containing the multiplier x1 held in coeff(1)
      call twoport(a(1),a(2),coeff(1),b(1),b(2))

C Step 5, assign output values to delay stack and valout parameters
      delay(1) = b(2)
      delay(2) = b(4)
      valout   = b(1)

      return
      end
```

D4 Single Bandpass APS Models

D4.1 2nd order Single Bandpass APS Model.

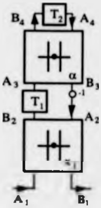

```
      subroutine tBP1sec1(valin,valout,delay,coeff)

      integer MAXSIZEAPS, WAVESEC2
      parameter(MAXSIZEAPS = 8, WAVESEC2 = 4)

C define external variables
      double precision valin, valout, coeff(MAXSIZEAPS), delay(MAXSIZEAPS)

C define internal variables
      double precision a(WAVESEC2), b(WAVESEC2)

C Step 1, assign values from delay stack 'a' parameters
      a(3) = delay(1)
      a(4) = -delay(2)

C Step 2, call twoport routine to determine 'b' values for the two-port adaptor
C containing the multiplier α held in coeff(2)
      call twoport(a(3),a(4),coeff(2),b(3),b(4))

C Step 3, assign values from new 'b' and valin parameters
      a(1) = valin
      a(2) = b(3)

C Step 4, call twoport routine to determine 'b' values for the two-port adaptor
C containing the multiplier x1 held in coeff(1)
      call twoport(a(1),a(2),coeff(1),b(1),b(2))

C Step 5, assign output values to delay stack and valout parameters
      delay(1) = b(2)
      delay(2) = b(4)
      valout   = b(1)

      return
      end
```

D4.2 4th order Single Bandpass APS Model.

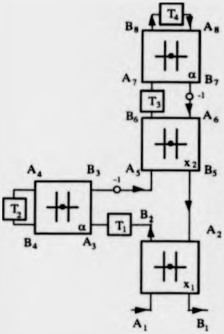

```
      subroutine tBP1sec2(valin,valout,delay,coeff)

      integer MAXSIZEAPS, WAVESEC4
      parameter(MAXSIZEAPS = 8, WAVESEC4 = 8)

C define external variables
      double precision valin, valout, coeff(MAXSIZEAPS), delay(MAXSIZEAPS)

C define internal variables
      double precision a(WAVESEC4), b(WAVESEC4)

C Step 1, assign values from delay stack 'a' parameters
      a(7) = delay(3)
      a(8) = delay(4)

C Step 2, call twoport routine to determine 'b' values for the two-port adaptor
C containing the multiplier α held in coeff(4)
      call twoport(a(7),a(8),coeff(4),b(7),b(8))

C Step 3, assign values from new 'b' and valin parameters
      a(3) = delay(1)
      a(4) = delay(2)

C Step 4, call twoport routine to determine 'b' values for the two-port adaptor
C containing themultiplier α held in coeff(3)
      call twoport(a(3),a(4),coeff(3),b(3),b(4))

C Step 5, assign values from new 'b' and valin parameters
      a(5) = -b(3)
      a(6) = -b(7)
```

```
C Step 6, call twoport routine to determine 'b' values for the two-port adaptor
C containing the multiplier x2 held in coeff(2)
      call twoport(a(5),a(6),coeff(2),b(5),b(6))

C Step 7, assign values from new 'b' and valin parameters
      a(1) = valin
      a(2) = b(5)

C Step 8, call twoport routine to determine 'b' values for the two-port adaptor
C containing the multiplier x1 held in coeff(1)
      call twoport(a(1),a(2),coeff(1),b(1),b(2))

C Step 9, assign output values to delay stack and valout parameters
      delay(1) = b(2)
      delay(2) = b(4)
      delay(3) = b(6)
      delay(4) = b(8)
      valout   = b(1)

      return
      end
```

D5 Single Bandstop APS Models

D5.1 2^nd order Single Bandstop APS Model.

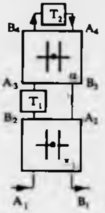

```
      subroutine tBS1sec1(valin,valout,delay,coeff)

      integer MAXSIZEAPS, WAVESEC2
      parameter(MAXSIZEAPS = 8, WAVESEC2 = 4)

C define external variables
      double precision valin, valout, coeff(MAXSIZEAPS), delay(MAXSIZEAPS)

C define internal variables
      double precision a(WAVESEC2), b(WAVESEC2)

C Step 1, assign values from delay stack 'a' parameters
      a(3) = delay(1)
      a(4) = delay(2)

C Step 2, call twoport routine to determine 'b' values for the two-port adaptor
C containing the multiplier α held in coeff(2)
      call twoport(a(3),a(4),coeff(2),b(3),b(4))

C Step 3, assign values from new 'b' and valin parameters
      a(1) = valin
      a(2) = b(3)

C Step 4, call twoport routine to determine 'b' values for the two-port adaptor
C containing the multiplier x1 held in coeff(1)
      call twoport(a(1),a(2),coeff(1),b(1),b(2))

C Step 5, assign output values to delay stack and valout parameters
      delay(1) = b(2)
      delay(2) = b(4)
      valout   = b(1)

      return
      end
```

D5.2 4th order Single Bandstop APS Model

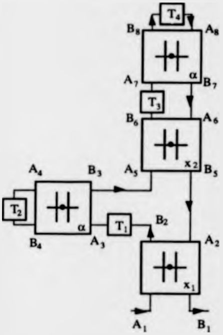

```
      subroutine tBP1sec2(valin,valout,delay,coeff)

      integer MAXSIZEAPS, WAVESEC4
      parameter(MAXSIZEAPS = 8, WAVESEC4 = 8)

C define external variables
      double precision valin, valout, coeff(MAXSIZEAPS), delay(MAXSIZEAPS)

C define internal variables
      double precision a(WAVESEC4), b(WAVESEC4)

C Step 1, assign values from delay stack to 'a' parameters
      a(7) = delay(3)
      a(8) = delay(4)

C Step 2, call twoport routine to determine 'b' values for the two-port adaptor
C containing the multiplier α held in coeff(4)
      call twoport(a(7),a(8),coeff(4),b(7),b(8))

C Step 3, assign values from new 'b' and valin parameters
      a(3) = delay(1)
      a(4) = delay(2)

C Step 4, call twoport routine to determine 'b' values for the two-port adaptor
C containing the multiplier α held in coeff(3)
      call twoport(a(3),a(4),coeff(3),b(3),b(4))

C Step 5, assign values from new 'b' and valin parameters
      a(5) = b(3)
      a(6) = b(7)
```

```
C Step 6. call twoport routine to determine 'b' values for the two-port adaptor
C containing the multiplier x2 held in coeff(2)
      call twoport(a(5),a(6),coeff(2),b(5),b(6))

C Step 7. assign values from new 'b' and valin parameters
      a(1) = valin
      a(2) = b(5)

C Step 8. call twoport routine to determine 'b' values for the two-port adaptor
C containing the multiplier x1 held in coeff(1)
      call twoport(a(1),a(2),coeff(1),b(1),b(2))

C Step 9. assign output values to delay stack and valout parameters
      delay(1) = b(2)
      delay(2) = b(4)
      delay(3) = b(6)
      delay(4) = b(8)
      valout   = b(1)

      return
      end
```

D6 Dual Bandpass APS Models

D6.1 4th order Dual Bandpass APS Model.

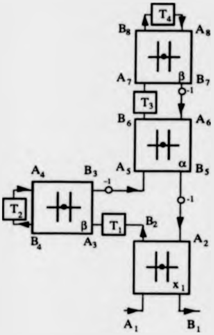

```
      subroutine tBP2sec1(valin,valout,delay,coeff)

      integer MAXSIZEAPS, WAVESEC4
      parameter(MAXSIZEAPS = 8, WAVESEC4 = 8)

C define external variables
      double precision valin, valout, coeff(MAXSIZEAPS), delay(MAXSIZEAPS)

C define internal variables
      double precision a(WAVESEC4), b(WAVESEC4)

C Step 1, assign values from delay stack to 'a' parameters
      a(7) = delay(3)
      a(8) = delay(4)

C Step 2, call twoport routine to determine 'b' values for the two-port adaptor
C containing the multiplier β held in coeff(4)
      call twoport(a(7),a(8),coeff(4),b(7),b(8))

C Step 3, assign values from new 'b' and valin parameters
      a(3) = delay(1)
      a(4) = delay(2)

C Step 4, call twoport routine to determine 'b' values for the two-port adaptor
C containing the multiplier β held in coeff(3)
      call twoport(a(3),a(4),coeff(3),b(3),b(4))
```

```
C Step 5, assign values from new 'b' and valin parameters
      a(5) = -b(3)
      a(6) = -b(7)

C Step 6, call twoport routine to determine 'b' values for the two-port adaptor
C containing the multiplier α held in coeff(2)
      call twoport(a(5),a(6),coeff(2),b(5),b(6))

C Step 7, assign values from new 'b' and valin parameters
      a(1) = valin
      a(2) = -b(5)

C Step 8, call twoport routine to determine 'b' values for the two-port adaptor
C containing the multiplier x1 held in coeff(1)
      call twoport(a(1),a(2),coeff(1),b(1),b(2))

C Step 9, assign output values to delay stack and valout parameters
      delay(1) = b(2)
      delay(2) = b(4)
      delay(3) = b(6)
      delay(4) = b(8)
      valout   = b(1)

      return
      end
```

D6.2 8th order Dual Bandpass APS Model.

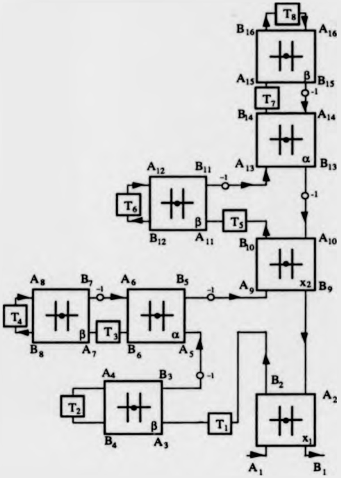

```
      subroutine tBP2sec2(valin,valout,delay,coeff)

      integer MAXSIZEAPS, WAVESEC8
      parameter(MAXSIZEAPS = 8, WAVESEC8 = 16)

C define external variables
      double precision valin, valout, coeff(MAXSIZEAPS), delay(MAXSIZEAPS)

C define internal variables
      double precision a(WAVESEC8), b(WAVESEC8)

C Step 1. assign values from delay stack to 'a' parameters
      a(15) = delay(7)
      a(16) = delay(8)

C Step 2. call twoport routine to determine 'b' values for the two-port adaptor
C containing the multiplier β held in coeff(8)
      call twoport(a(15),a(16),coeff(8),b(15),b(16))
```

```
C Step 3, assign values from delay stack to 'a' parameters
      a(11) = delay(5)
      a(12) = delay(6)

C Step 4, call twoport routine to determine 'b' values for the two-port adaptor
C containing the multiplier β held in coeff(7)
      call twoport(a(11),a(12),coeff(7),b(11),b(12))

C Step 5, assign values from delay stack to 'a' parameters
      a(7) = delay(3)
      a(8) = delay(4)

C Step 6, call twoport routine to determine 'b' values for the two-port adaptor
C containing the multiplier β held in coeff(6)
      call twoport(a(7),a(8),coeff(6),b(7),b(8))

C Step 7, assign values from delay stack to 'a' parameters
      a(3) = delay(1)
      a(4) = delay(2)

C Step 8, call twoport routine to determine 'b' values for the two-port adaptor
C containing the multiplier β held in coeff(5)
      call twoport(a(3),a(4),coeff(5),b(3),b(4))

C Step 9, assign values from new 'b' parameters
      a(13) = -b(11)
      a(14) = -b(15)

C Step 10, call twoport routine to determine 'b' values for the two-port adaptor
C containing the multiplier α held in coeff(4)
      call twoport(a(13),a(14),coeff(4),b(13),b(14))

C Step 11, assign values from new 'b' parameters
      a(5) = -b(3)
      a(6) = -b(7)

C Step 12, call twoport routine to determine 'b' values for the two-port adaptor
C containing the multiplier α held in coeff(3)
      call twoport(a(5),a(6),coeff(3),b(5),b(6))

C Step 13, assign values from new 'b' parameters
      a(9) = -b(5)
      a(10) = -b(13)

C Step 14, call twoport routine to determine 'b' values for the two-port adaptor
C containing the multiplier x2 held in coeff(2)
      call twoport(a(9),a(10),coeff(2),b(9),b(10))

C Step 15, assign values from new 'b' and valin parameters
      a(1) = valin
      a(2) = b(9)

C Step 16, call twoport routine to determine 'b' values for the two-port adaptor
C containing the multiplier x1 held in coeff(1)
      call twoport(a(1),a(2),coeff(1),b(1),b(2))
```

```
C Step 17, assign output values to delay stack and valout  parameters
      delay(1) = b(2)
      delay(2) = b(4)
      delay(3) = b(6)
      delay(4) = b(8)
      delay(5) = b(10)
      delay(6) = b(12)
      delay(7) = b(14)
      delay(8) = b(16)
      valout   = b(1)

      return
      end
```

D7 Dual Bandstop APS Models

D7.1 4th order Dual Bandstop APS Model.

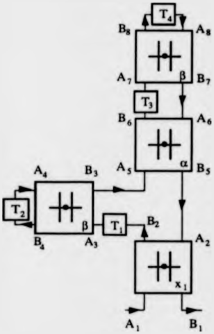

```
      subroutine tBS2sec1(valin,valout,delay,coeff)

      integer MAXSIZEAPS, WAVESEC4
      parameter(MAXSIZEAPS = 8, WAVESEC4 = 8)

C define external variables
      double precision valin, valout, coeff(MAXSIZEAPS), delay(MAXSIZEAPS)

C define internal variables
      double precision a(WAVESEC4), b(WAVESEC4)

C Step 1, assign values from delay stack to 'a' parameters
      a(7) = delay(3)
      a(8) = delay(4)

C Step 2, call twoport routine to determine 'b' values for the two-port adaptor
C containing the multiplier β held in coeff(4)
      call twoport(a(7),a(8),coeff(4),b(7),b(8))

C Step 3, assign values from new 'b' and valin parameters
      a(3) = delay(1)
      a(4) = delay(2)

C Step 4, call twoport routine to determine 'b' values for the two-port adaptor
C containing the multiplier β held in coeff(3)
      call twoport(a(3),a(4),coeff(3),b(3),b(4))
```

```
C Step 5, assign values from new 'b' and valin  parameters
      a(5) = b(3)
      a(6) = b(7)

C Step 6, call twoport routine to determine 'b' values for the two-port adaptor
C containing the multiplier α held in coeff(2)
      call twoport(a(5),a(6),coeff(2),b(5),b(6))

C Step 7, assign values from new 'b' and valin  parameters
      a(1) = valin
      a(2) = b(5)

C Step 8, call twoport routine to determine 'b' values for the two-port adaptor
C containing the multiplier x1 held in coeff(1)
      call twoport(a(1),a(2),coeff(1),b(1),b(2))

C Step 9, assign output values to delay stack and valout  parameters
      delay(1) = b(2)
      delay(2) = b(4)
      delay(3) = b(6)
      delay(4) = b(8)
      valout   = b(1)

      return
      end
```

D7.2 8th order Dual Bandstop APS Model.

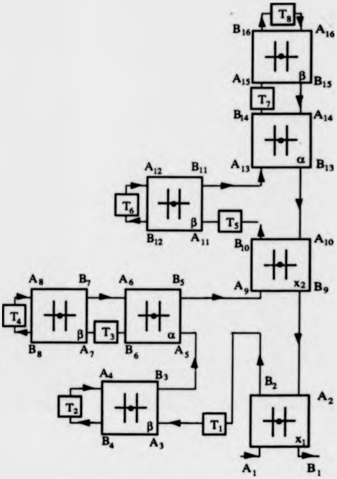

```
      subroutine tBS2sec2(valin,valout,delay,coeff)

      integer MAXSIZEAPS, WAVESEC8
      parameter(MAXSIZEAPS = 8, WAVESEC8 = 16)

C define external variables
      double precision valin, valout, coeff(MAXSIZEAPS), delay(MAXSIZEAPS)

C define internal variables
      double precision a(WAVESEC8), b(WAVESEC8)

C Step 1, assign values from delay stack to 'a' parameters
      a(15) = delay(7)
      a(16) = delay(8)

C Step 2, call twoport routine to determine 'b' values for the two-port adaptor
C containing the multiplier β held in coeff(8)
      call twoport(a(15),a(16),coeff(8),b(15),b(16))
```

```
C Step 3, assign values from delay stack to 'a' parameters
      a(11) = delay(5)
      a(12) = delay(6)

C Step 4, call twoport routine to determine 'b' values for the two-port adaptor
C containing the multiplier β held in coeff(7)
      call twoport(a(11),a(12),coeff(7),b(11),b(12))

C Step 5, assign values from delay stack to 'a' parameters
      a(7) = delay(3)
      a(8) = delay(4)

C Step 6, call twoport routine to determine 'b' values for the two-port adaptor
C containing the multiplier β held in coeff(6)
      call twoport(a(7),a(8),coeff(6),b(7),b(8))

C Step 7, assign values from delay stack to 'a' parameters
      a(3) = delay(1)
      a(4) = delay(2)

C Step 8, call twoport routine to determine 'b' values for the two-port adaptor
C containing the multiplier β held in coeff(5)
      call twoport(a(3),a(4),coeff(5),b(3),b(4))

C Step 9, assign values from new 'b' parameters
      a(13) = b(11)
      a(14) = b(15)

C Step 10, call twoport routine to determine 'b' values for the two-port adaptor
C containing the multiplier α held in coeff(4)
      call twoport(a(13),a(14),coeff(4),b(13),b(14))

C Step 11, assign values from new 'b' parameters
      a(5) = b(3)
      a(6) = b(7)

C Step 12, call twoport routine to determine 'b' values for the two-port adaptor
C containing the multiplier α held in coeff(3)
      call twoport(a(5),a(6),coeff(3),b(5),b(6))

C Step 13, assign values from new 'b' parameters
      a(9) = b(5)
      a(10) = b(13)

C Step 14, call twoport routine to determine 'b' values for the two-port adaptor
C containing the multiplier x2 held in coeff(2)
      call twoport(a(9),a(10),coeff(2),b(9),b(10))

C Step 15, assign values from new 'b' and valin parameters
      a(1) = valin
      a(2) = b(9)

C Step 16, call twoport routine to determine 'b' values for the two-port adaptor
C containing the multiplier x1 held in coeff(1)
      call twoport(a(1),a(2),coeff(1),b(1),b(2))
```

```
C Step 17, assign output values to delay stack and valout parameters
      delay(1) = b(2)
      delay(2) = b(4)
      delay(3) = b(6)
      delay(4) = b(8)
      delay(5) = b(10)
      delay(6) = b(12)
      delay(7) = b(14)
      delay(8) = b(16)
      valout   = b(1)

      return
      end
```